

**DETTRITAL ZIRCON GEOCHRONOLGY OF CAMBRO-ORDOVICIAN
SILICICLASTIC UNITS OF THE HUMBER ARM ALLOCHTHON,
NEWFOUNDLAND, CANADA**

A Thesis

Presented to

the Faculty of the Department of Earth and Atmospheric Sciences

University of Houston

In Partial Fulfillment

of the Requirements for the Degree

Master of Science

By

Adrian Stephen Gittens

August, 2012

**DETrital ZIRCON GEOCHRONOLoGY OF CAMBRO-ORDOVICIAN
SiLICiCLASTiC UNiT(S) OF THE HUMBER ARM ALLOCHTHON,
NEWFOUNDLAND, CANADA**

Adrian Stephen Gittens

APPROVED:

Dr. John F. Casey, Chairman

Dr. Thomas J. Lapen

Dr. John F. Dewey

Dr. Doug A. Reid

Dean, College of Natural Sciences and
Mathematics

ACKNOWLEDGEMENTS

I would like to specially thank Dr. John F. Casey for presenting me the opportunity and for his continued support, guidance and patience throughout this project. My sincerest gratitude goes to Mr. Barry J. Shaulis for taking the time to teach me the relevant techniques required for zircon processing and analysis and general suggestions and conversation. I would also like to thank Dr. T. Lapen and Dr. Yongjun Gao for their technical assistance and insights, especially when things went wrong. Finally, I would like to thank my mother for her continued support and encouragement, without which I would never have begun my academic career and certainly would not have seen it to the end.

**DETrital Zircon Geochronology of Cambro-OrdoVician
Siliciclastic Units of the Humber Arm Allochthon,
Newfoundland, Canada**

An Abstraction of a Thesis

Presented to

the Faculty of the Department of Earth and Atmospheric Sciences

University of Houston

In Partial Fulfillment

of the Requirements for the Degree

Master of Science

By

Adrian Stephen Gittens

August, 2012

ABSTRACT

Paleogeographic reconstruction of the Newfoundland area suggests that various arc terranes developed during the opening of the Iapetus Ocean and development of the Cambro-Ordovician Laurentian stable continental margin. These terranes were then accereted to the continental passive-margin upon initial closure of the ocean basin in the Ordovician. The origin and age of these terranes are still questionable as they may contain older Precambrian basement according to some workers, and if so, they could be interpreted as originating from Laurentia or any other bordering landmass to the Iapetus Ocean at that time. Newfoundland is the northernmost extent of the Appalachian Orogenic Belt which first developed during the Taconian Orogeny, a product of Iapetus Ocean closure in the Ordovician. The sedimentary packages of the Humber Arm allochthon were thrust upon the autochthonous sediment of the Laurentian passive-margin and deformed during Taconic Orogeny. Measurement of ages based on U-Pb isotope ratios of detrital zircons found in the syn- and post-rift siliciclastic strata coupled with correlation to known source region ages has provided the following determinations: (1) there is a predominantly Laurentian derived contribution to detrital sediment deposited along the passive margin and foreland basin units during the early Cambrian to middle Ordovician, with relative age contributions ranging from the Archean (3070 Ma) to the Paleozoic (551 Ma) which agrees with previous interpretations and provides a better constraint on the second phase of rifting (591 – 551 Ma); (2) further constraint on the age

and nature of the Taconic Arc, based on the method, used remains insufficient, as only two grains yielded ages consistent with an arc age (482 Ma and 480 Ma); (3) a biased analysis of young zircons yielded an arc-age range of 464 – 510 Ma and a peak age of 466 Ma (3 grains), better constraining the detritus from the arc system; (4) the North Atlantic craton and adjacent terranes in the Labrador region (Makkovik Province, Torngat Arc Province, and New Quebec Province) may possibly provide a more local source for sediments derivation; and (5) development and aggradation of an accretionary wedge in front of the advancing arc may have acted as a sediment barrier to arc-derived sediment (e.g. the modern-day Sunda-Banda and Barbados Arcs).

TABLE OF CONTENTS

Chapter 1:	INTRODUCTION	1
1.1	GEOLOGIC BACKGROUND	2
1.1.1	Rifting and the Formation of the Iapetus Ocean	2
1.1.2	The Taconic Orogeny	5
1.2	STRATIGRAPHY OF THE HUMBER ARM	
	ALLOCHTHON	10
1.2.1	Bradore Formation (LAB): Shelf	12
1.2.2	Blow Me Down Brook Formation (BMDB): Slope-rise	12
1.2.3	The Curling Group: Slope-rise	13
1.2.4	Lower Head Formation (LH): Foreland	14
1.2.5	Goose Tickle Formation (GT): Foreland	14
Chapter 2:	METHODS	15
2.1	SAMPLE PREPARATION	15
2.2	DATA ANALYSIS	17
2.2.1	Isotope Systems	17
2.2.2	Laser Ablation Inductively Coupled Mass Spectrometry (LA-ICPMS)	17
2.2.3	Zircon Standards	18
2.2.4	Data Acquisition and Reduction	18
Chapter 3:	RESULTS	23
3.1	SAMPLE DATA	23
3.1.1	Bradore Formation	23

Table of Contents (continued)

3.1.2	Blow Me Down Brook Formation	25
3.1.3	Summerside Formation	25
3.1.4	Irishtown Formation	26
3.1.5	Lower Head Formation	27
3.1.6	Goose Tickle Formation	28
Chapter 4:	DISCUSSION	29
4.1	POTENTIAL SOURCES	29
4.1.1	Grenville Normalization	29
4.1.2	Archean and Paleoproterozoic Zircons	32
4.1.3	Mesoproterozoic and Neoproterozoic Zircons	35
4.2	ARC-DERIVED SEDIMENT	37
4.3	TECTONIC MODEL	40
4.4	MODERN ANALOGUES	48
Chapter 5:	CONCLUSION	53
References Cited		55
Appendix 1:	Zircon Data Tables	64
Appendix 2:	Relative Age Distribution Plots for Individual Samples	135

CHAPTER 1

1. INTRODUCTION

The Humber Arm Allochthon has been extensively researched because of the well preserved ophiolite packages and associated igneous and sedimentary sequences. The study of these outcrops by previous workers has greatly contributed to the understanding of arc-continent collisions as well as orogenic processes. Although sedimentary packages have been correlated and classified by their depositional environment (e.g. Lindholm and Casey, 1989; Schwab, 1991; Palmer et al., 2001; and others), dating of detrital zircons using U-Pb geochronology can contribute and enhance the understanding of source contributions to the deposition of the Cambro-Ordovician siliciclastic units that make up the allochthon. Previous work on these siliciclastic units utilizing ID-TIMS and SHRIMP II analytical techniques (e.g. Cawood et al, 2001; Cawood and Nemchin, 2001) and, on time equivalent units in Ireland on the opposite side of the Iapetus Ocean suture (Clift et al, 2009 – LA-ICPMS) have indicated a predominantly Laurentian source.

This paper presents U-Pb age data for detrital zircons using LA-ICPMS, derived from the upper PreCambrian to middle Ordovician siliciclastic units that range from rift- and drift-related stable continental margin units to foreland basin units as ocean closure culminated. The purposes of this study are to (1) determine the source region contributions of the units analyzed, and compare rift, drift, and foreland basin flysch units (the Goose Tickle and Lower Head Formations); (2) determine the age of the colliding arc and the nature of its basement that was part of the pre-terminal collision which

resulted in obduction of the ophiolite allochthon; and (3) test the hypothesis that the foreland basin units were, in part, oceanic arc derived.

1.1 GEOLOGIC BACKGROUND

1.1.1 Rifting and the Formation of the Iapetus Ocean

The Iapetus Ocean formed in the Late Neoproterozoic around 600 – 550 Ma, when initial rifting of the supercontinent Rodinia began. Rifting caused separation into Laurentian, Baltica and Gondwanan plates (Dalla Salda et al., 1992; Niocaill et al., 1997; Cawood et al., 2001; Murphy and Nance, 2008). Iapetus was bound to the north by Laurentia, to the south then to the east by Baltica, and to the south by Gondwana. Paleomagnetic and faunal data suggest that the evolution of the Iapetus Ocean was dynamic and did not just result in the three separate plates mentioned above, but resulted in the formation of at least three major arc systems within the ocean basin in the Early to Middle Ordovician (Niocaill et al., 1997; Murphy and Nance, 2008). Paleolatitudes for these arcs were derived from paleomagnetic data (Niocaill et al., 1997) and they are as follows: an arc system dividing the Iapetus in two, referred to as a peri-Laurentian arc at approx. 10°-20°S, an intra-Iapetan arc separating the Iapetus Ocean from the Rheic ocean to the south, called the Exploits arc, at approx. 30°S, and a peri-Avalonian arc at approx. 50°S. The development of the peri-Laurentian arc was due to the formation of a then southward-dipping (presently eastward) subduction zone, south of the southern Laurentian passive margin, and it was this arc that eventually collided with the Laurentian passive margin in a pre-terminal collision, that resulted in the Taconic orogeny. Faunal evidence for the paleogeographic locations of these arcs are less

convincing and highly debated, but when combined with the paleomagnetic data, they provide a reasonable argument for multiple arcs rather than more simple continental plates alone (Niocaill et al., 1997). The differences in Celtic brachiopod fauna from localities on the eastern margin of Laurentia are more pronounced in the Early to Middle Ordovician than in the Late Ordovician, suggesting more isolated habitats in the Early to Middle Ordovician which indicates an origin within an island arc environment isolated from the Laurentian margin (Neuman, 1984; Niocaill et al., 1997).

The preferential subduction of the younger Iapetus and Rheic Oceanic crust (introversion – whereby the continents surrounding the oceanic basins assemble by consuming the younger oceanic crust) v. consumption of the older paleo-Pacific crusts (extroversion – whereby the continents reassemble by consuming the older oceanic crust) (Murphy and Nance, 2008), poses an interesting dynamic (Fig. 1). During this time, it prompted the closure of these Iapetus and Rheic Oceans and led to the eventual assembly of the Pangean supercontinent. Subduction of the older denser oceanic crust would be expected but was not the case and the previous mechanisms of subduction initiation could not account for sufficient slab to pull to promote the assembly of Pangea (Murphy and Nance, 2008). Therefore, it was proposed that superplume activity in the paleo-Pacific, due to hot mantle ponding resulting from insulation by the peripheral subducting slabs, would cause the geoid low to invert and become a geoid high while producing the inverse reaction in the Iapetus and Rheic Oceans (Murphy and Nance, 2008). This would have the favorable result of introversion, allowing for the assembly of Pangea and the collision of the peri-Laurentian arc with the Laurentian passive margin. This hypothesis was

further substantiated by sea-level rise indicators and lower $^{87}\text{Sr}/^{86}\text{Sr}$ values for the paleo-

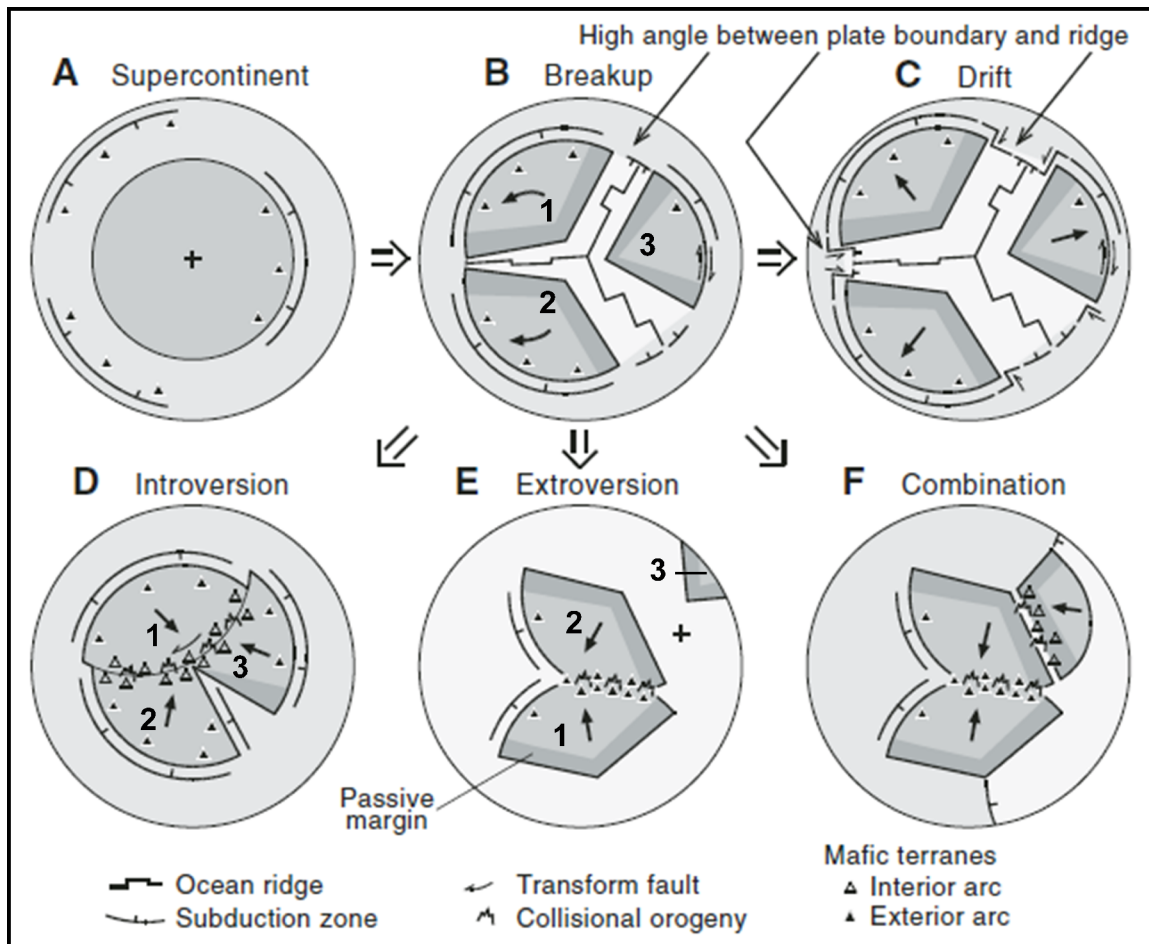


Figure 1. Simple models showing stages of open closure from stable to rift to drift (A-C); Closure via introversion (D); Closure via extroversion (E); and a combination of events ending in closure (F). Light gray ocean = new oceanic crust; dark gray ocean = old oceanic crust. Numbers 1, 2, and 3 (B, D, AND F) represent the same plates for all three stages.

Modified after Murphy and Nance, 2008

Pacific ocean, indicating increased seafloor spreading rates, which was then compensated for by subduction in the younger Iapetan and Rheic Ocean basins in the Middle to Late Ordovician (Murphy and Nance, 2008). A Wilson Cycle model would require the

reverse mechanism and would predict the opposite, resulting in continental assembly via extroversion and the closing of the older paleo-Pacific (Dewey and Burke, 1974).

1.1.2 The Taconic Orogeny

The Taconic orogeny extends the length of the eastern continental margin of North America, from Newfoundland to Alabama, a distance of 1600 miles. It is generally regarded as a result of the attempted subduction of the present-day easterly-facing (then southerly-facing) passive margin of Laurentia, as it entered an “east” dipping subduction zone with an overriding plate consisting of Late Cambrian to Early-Middle Ordovician oceanic crust (Nelson and Casey, 1979; Casey and Dewey, 1984; Pinet and Tremblay, 1995; Cawood et al., 2001; Murphy and Nance, 2008) and an island arc terrane of Middle to Late Ordovician age (Nelson and Casey, 1979; Casey and Dewey, 1984; van der Pluijm, 1987; Whitehead et al., 1996; Ratcliffe et al., 1998; Karabinos et al., 1998), forming the orogen. The orogenic belt can be divided into several regions of study: Newfoundland, Quebec and eastern Canada, New England, Pennsylvania and the Central and South Appalachians (Wise and Ganis, 2009). The arc-continent collision was diachronous (Bradley and Kusky, 1986; Bradley, 1989; Garver et al., 1996; Waldron and van Staal, 2001; Wise and Ganis, 2009) probably due to the formation of an irregular passive continental margin after rifting (Dewey and Burke, 1974), and an arc orientation that was relatively parallel to the general strike of the passive margin but perpendicular to the collision direction (Bradley, 1989). Because of this diachronous nature, it should be expected that different regions would experience

collision and orogeny for roughly the same protracted duration but at different times depending on their geometry.

After the rifting event that initiated breakup of Rodinia in the Neoproterozoic and subsequent thermal subsidence of the rifted margin synchronous with predominantly Grenville basement, rift-related siliciclastics were deposited unconformably on the Grenville Basement, e.g. the Bradore Formation in Newfoundland and the Potsdam Sandstone in New York, in the Pre-cambrian to Early Cambrian (Bradley and Kusky, 1986; Lindholm and Casey, 1989). Cambrian shelf carbonates developed conformably above the shelf siliciclastic units e.g. Forteau Formation deposited in the Early Cambrian to deposition of the Early Ordovician St. George's Formation in Newfoundland (Lindholm and Casey, 1989) and the Late Cambrian to Middle Ordovician Beekmantown Group of Pennsylvania ((Wise and Ganis, 2009). There was simultaneous deposition of distal continental slope and rise siliciclastic deposits, e.g. the Blow Me Down Brook Formation and two members of the Curling Group in Newfoundland (Lindholm and Casey, 1989). All of these distally transported units would be later incorporated into thrust slices of the Humber Arm Allochthon (Fig. 2), as the Taconic orogeny progressed toward the Laurentian passive margin shelf (Lindholm and Casey, 1989; Bradley, 1989; Wise and Ganis, 2009).

The onset of the Taconic orogeny on the shelf was signaled by the uplift and erosion of the carbonate deposits as the forebulge migrated toward the Laurentian passive margin due to flexure of the continental-oceanic transition lithosphere (Nelson and Casey, 1979; Bradley and Kusky, 1986; van der Pluijm, 1987; Bradley, 1989; Ettensohn

and Brett, 2002). This resulted in a disconformity across the top of the Ordovician carbonate sequences (e.g St. George – Table Head Formations, Fig. 3) which may have occurred at different times along the margin (Bradley, 1989). As the forebulge migrated

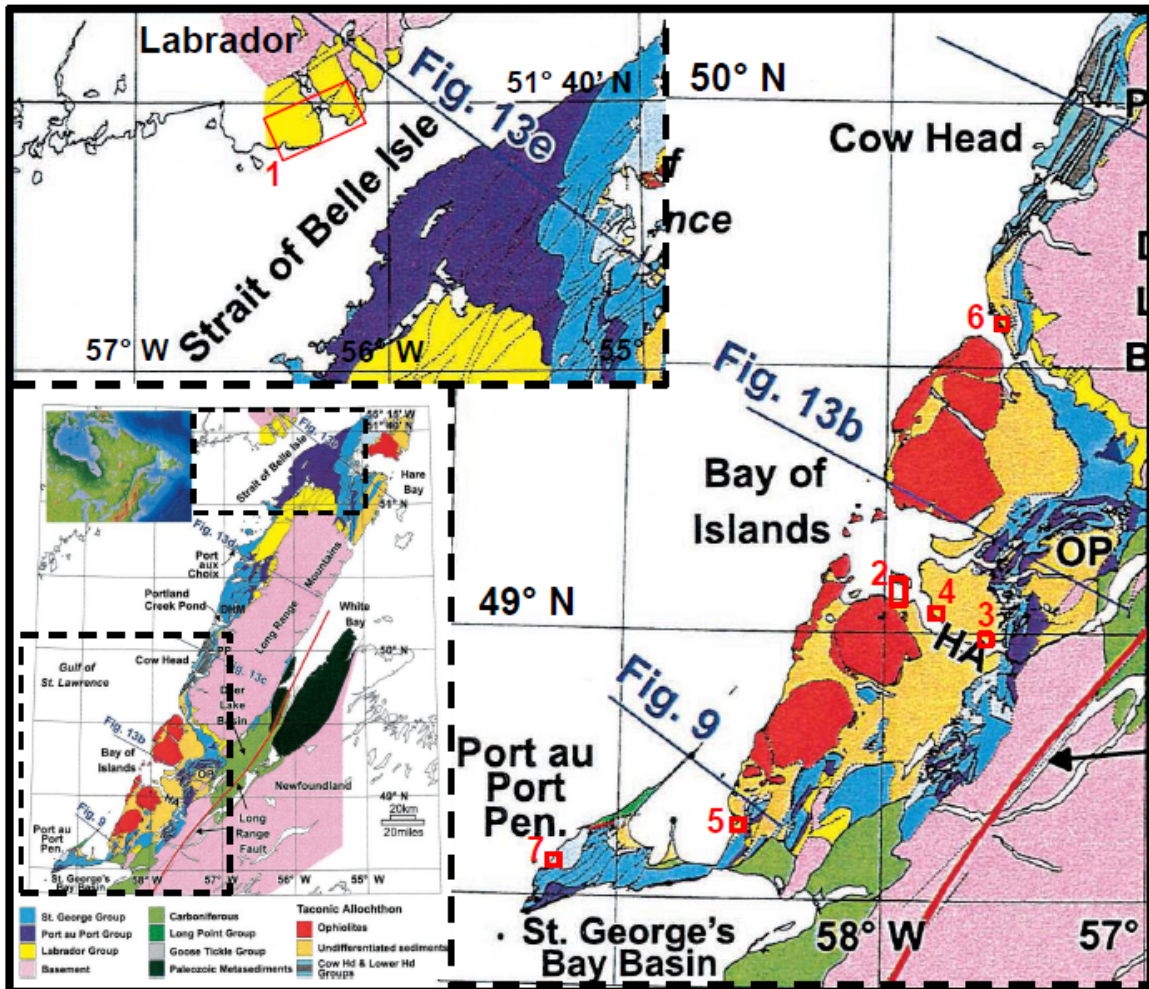


Figure 2. Geologic map of The Humber Arm Allochthon, Newfoundland, and Eastern Labrador, Canada. Dashed boxes represent highlight the areas studied by R. Lindholm (PhD Dissertation, 1987-1989) and numbered red boxes indicate sample locations for this study. Sample locations are also listed in Table 1. Units labeled as undifferentiated sediments refer to the Blow Me Down Brook, Summerside, and Irishtown Formations. Modified after Cooper et al, 2001.

further landward, there was rapid subsidence of the foreland basin that resulted in the diachronous deposition of condensed sections of black muds overlying the unconformity

above the now drowned carbonate shelf. These deposits were a product of very slow sedimentation, as there was not yet any major clastic sediment influx (Bradley, 1989; Ettensohn and Brett, 2002) on what is considered the outer trench wall. Initiation of foreland development began in Newfoundland (Bradley, 1989) with the influx of turbiditic flysch into the foreland basin, and the initial development of the fold and thrust belt associated with the overriding ophiolitic forearc plate (and a subaccreted metamorphic sole), accretionary prism consisting of mélanges, and detached slices of the continental slope and rise deposits. As the collision proceeded, substantial relief probably produced in the accretionary allochthon by the mass from stacked thrust sheets loaded the down going slab which caused the subsidence of the foreland basin. This allochthon assembly provided the uplifted material to be subsequently eroded (Bradley, 1989; Ettensohn and Brett, 2002). Thus the deposition of “easterly derived” flysch began onto the continental slope and rise deposits as a conformable sequence (Dewey, 1976; Bradley and Kusky, 1986; Bradley, 1989; Ettensohn and Brett, 2002). These flysch deposits are reported to contain ophiolitic detritus, reflected by the chrome spinel and high concentrations of chromium and nickel, suggesting a source derived from the advancing ophiolitic thrust wedge (Nelson and Casey, 1979; Lindholm and Casey, 1989; Schwab, 1991; Garver et al., 1996). These allochthonous flysch units are the Lower Head Formation of Newfoundland (Lindholm and Casey, 1989; Bradley, 1989), the Tourelle Formation of Quebec, the Pawlet Formation of New York and the Windsor/Township Formations of Pennsylvania (Bradley, 1989). These units may also consist of recycled sediments derived from slope and rise deposits and could therefore have mixed sources, although some authors argue that the foreland basin sediments have an increased

influence from juvenile sources based on Nd isotopic data (Andersen and Samson, 1995). But this may also be a local variation and may not apply across the entire orogenic belt or may be a part of the distal mud matrix. The orogen advanced further toward Laurentia with the now mobile deep-water allochthon consisting of slope deposits, overlain by rise deposits, and conformably overlain by “westerly derived” flysch, which were then thrusted onto the autochthonous carbonate and siliciclastic units forming the Humber Arm Allochton of Newfoundland in the Middle Ordovician (Dewey, 1976; Bradley, 1989; Ettensohn and Brett, 2002) (Fig. 2). As the Laurentian passive margin entered the trench, the subduction of the lighter continental crust was prevented by buoyancy forces and resulted in the obduction of the oceanic lithosphere of the overriding plate onto the passive margin during the Middle to Late Ordovician, where it sits at the structurally highest position (Dewey, 1976; Lindholm and Casey, 1989). Simultaneously, autochthonous “westerly derived” flysch was deposited onto the mutually emplaced allochthonous thrust slices e.g. the Late Ordovician Goose Tickle Formation of Newfoundland, the Austin Glen and the Schenectady Formations of New York and Pennsylvania, and the Cloridome Formation of Quebec (Bradley, 1989). The failure of the Laurentian continental crust to subduct caused convergence to be taken up by a subduction polarity flip as a “westward” dipping subduction zone (Dewey, 1976; Anderson and Moecher, 2009) behind the colliding arc, ending the Taconic orogeny to the west.

The metamorphic sole of the Bay of Islands ophiolite has an age of 469 Ma (Lindholm and Casey, 1989) and grades quickly from granulites and garnet-amphibolite to amphibolites above to greenschist facies below (Dewey, 1976), suggesting rapid

formation in a subduction zone setting below a young forearc lithosphere in an oceanic setting during the Late Middle Ordovician. In Quebec, age constraints for the moderate pressure metamorphism of Grenville basement and continental margin sediment associated with attempted subduction of the continental margin, place it at 463 Ma. This is based on $^{40}\text{Ar}/^{39}\text{Ar}$ dating of muscovite, hornblende and orthoclase, most of which were collected along the Baie Verte-Brompton Line which separates the Humber zone from the Dunnage zone (Whitehead et al., 1996). The age of Taconian metamorphism due to uplift in New England is estimated at 450 to 445 Ma based on $^{40}\text{Ar}/^{39}\text{Ar}$ analysis of prograde hornblende (Ratcliffe et al., 1998). Metamorphic dating of granulite facies rocks caused by igneous events in the Southern Appalachians is estimated at 460 to 458 Ma, based on thermal-ionization mass spectrometry (458 Ma) and ion microprobe (460 Ma) analysis on zircons taken from leucosomes of the Blue Ridge area (Moecher et al., 2004; Anderson and Moecher, 2009). The narrow range of ages of metamorphism is probably due to the diachronous nature of the Taconian orogeny or age of uplift and exhumation of deep-seated metamorphic rocks.

1.2 STRATIGRAPHY OF THE HUMBER ARM ALLOCHTHON

The focus of this study will be detrital zircon analysis of the Cambro-Ordovician siliciclastic units that make up the allochthonous and autochthonous sedimentary packages in the Humber Arm allochthon (Fig. 3). This was done to better understand the provenance of the components of the rift-suture system. These allochthonous sedimentary packages are predominantly deep-water sequences. All of these formations, with the exception of the autochthonous Goose Tickle Formation, are correlative to the

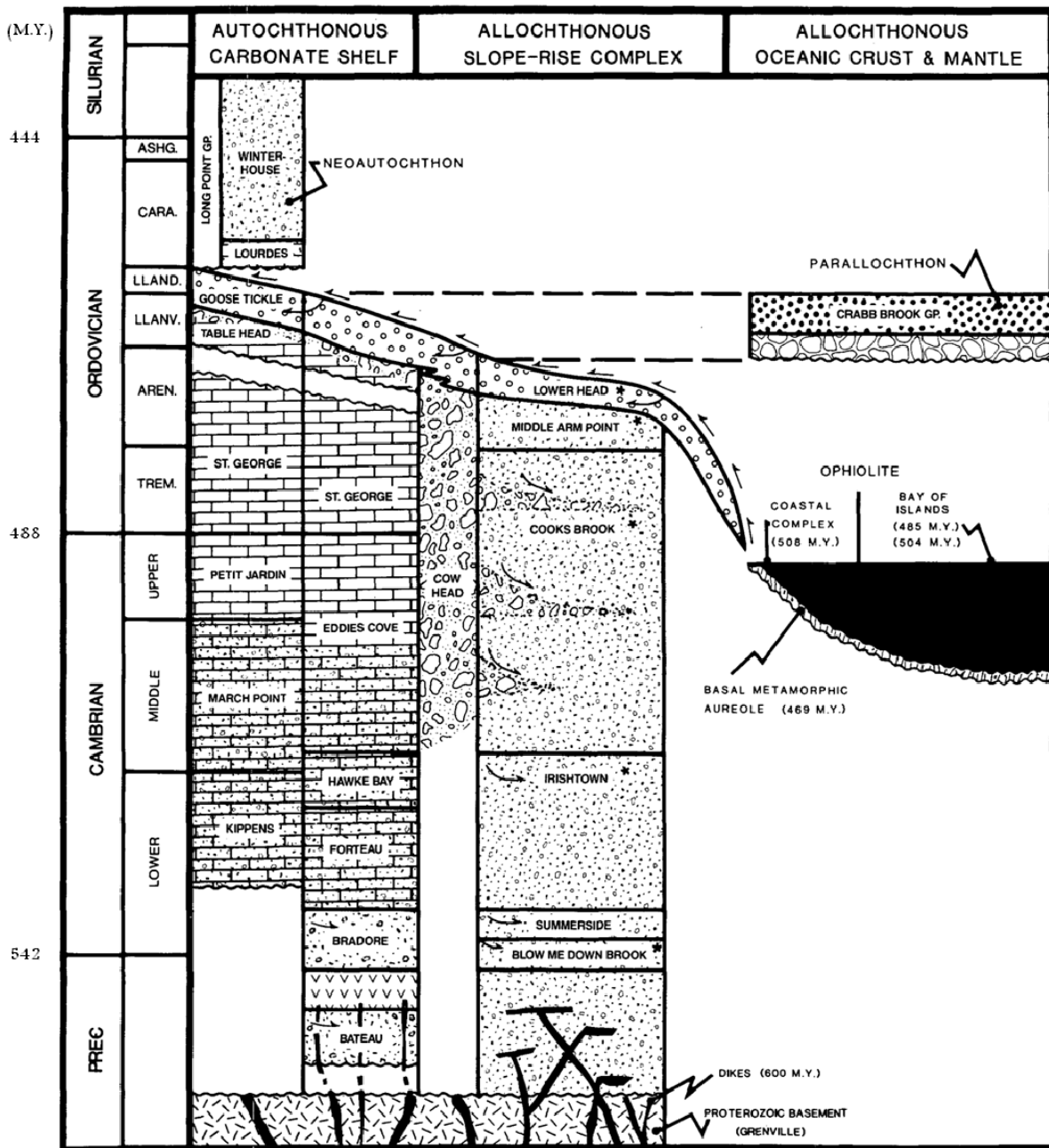


Figure 3. Stratigraphic column of the Humber Arm Allochthon showing tectonic relationships. Small arrows indicate transport direction. Modified after Lindholm and Casey, 1989

allochthonous Lower Head sandstone (Lindholm and Casey, 1989). The entire interval is referred to as the Humber Arm Supergroup (Lindholm and Casey, 1989; Schwab, 1991; Palmer et al., 2001). The Humber Arm Supergroup's major components consists of the time equivalent distal Curling Group and proximal Cow Head Group.

The Curling Group is comprised of the Cambrian units of Summerside, Irishtown, Middle Arm, and Cooks Brook Formations. The Cow Head Group is comprised of the Mid-Cambrian to Mid-Ordovician shelf carbonate sequences. The Lower Cambrian Bradore Formation of the Labrador Group is the proximal shelf equivalent to the distal continental slope Blow Me Down Brook Formation (Schwab, 1991; Lindholm and Casey, 1989). The Bradore, Blow Me Down Brook, Summerside, and Irishtown Formations were deposited in a passive margin environment while the Lower Head and Goose Tickle Formations were deposited from an easterly (formerly southerly) derived source terrane in an active margin setting.

1.2.1 Bradore Formation (LAB): Shelf

The Bradore Formation is Pre-cambrian to Cambrian in age and is the proximal time-equivalent of the Blow Me Down Brook Formation. It consists of coarse-grained, arkosic sandstones (Lindholm, 1990; Schwab, 1991) and conglomerates that have a fluvial to marine signature, indicating a more terrestrial to shallow-marine derivation (Lindholm and Casey, 1989).

1.2.2 Blow Me Down Brook Formation (BMDDB): Slope-Rise

This formation is Pre-cambrian to Cambrian age and is the stratigraphically lowest distal deposit, overlying Pre-cambrian basement, and is characterized as a coarse-grained, arkosic sandstone (Schwab, 1991) or a quartz-rich to quartz-intermediate sandstone (Lindholm, 1990). The formation can be considered compositionally and texturally immature but possesses evidence of reworking (Palmer et al., 2001). Higher

feldspar content is believed to reflect earlier stages of rifting and was prior to the development of the passive margin (Schwab, 1991). It was originally thought to be of Early to Middle Ordovician age as lack of fossils in the formation prevented the certain recognition of its age at its type locality. Stevens (1970) had contended that the formation contained ophiolitic detritus, shed from the Bay of Islands Ophiolite and as such, was placed stratigraphically higher than its present position (Lindholm and Casey, 1989). However, the discovery of the trace fossil *Oldhamia* in localities outside of its type locality (Lindholm and Casey, 1989), the lack of ophiolitic detritus, and mineralogy have placed it in its present stratigraphic location and as a “westerly derived” sandstone (Lindholm and Casey, 1989; Schwab, 1991).

1.2.3 Curling Group: Slope-Rise

The Curling Group units consist of the Summerside (SS), Irishtown (IT), Middle Arm, and Cooks Brook Formations. The Summerside and Irishtown Formations are predominantly Cambrian in age, whereas the upper Cooks Brook and Middle Arm are Lower Ordovician in age. Only the lower Cambrian Summerside and Irishtown Formations were sampled for this study. They are predominantly coarse- to fine-grained turbiditic deposits of cratonic origin (Palmer et al., 2001). Interbeds of shales and slate (due to mélange forming processes) are found in these turbidite deposits, with increasing shale content higher stratigraphically. These were “westerly derived” and deposited distally, possibly on the base of the continental rise (Lindholm and Casey, 1989; Schwab, 1991). However, these units are highly disrupted by faults and deformation zones in the allochthon and are of uncertain origin.

1.2.4 Lower Head Formation (LH): Foreland

The Lower Head Formation is the youngest (middle Ordovician in age) transported allochthonous unit. It consists of shales and fine- to medium-grained sandstones which are poorly sorted, consistent with a turbidite origin and commonly associated with mélange zones (Lindholm and Casey, 1989). The derivation of this unit is suggested to be “easterly” derived as it contains ophiolitic detritus identified by detrital chromite (Lindholm and Casey, 1989).

1.2.5 Goose Tickle Formation (GT): Foreland

The Goose Tickle Formation is autochthonous (middle Ordovician in age) and its lower boundary demarcates the sedimentation transition from “westerly derived” passive-margin to condensed black shale (outer wall) sequences to that of “easterly derived” foreland basin sequences. This reflects the uplift of the Taconic orogen further to the east (Schwab, 1991). The cratonic, quartz-rich mineralogy of the sandstone, predominantly flysch deposits, may imply that its source is that of a recycled orogen cannibalized from the telescoped Laurentian continental slope-rise complex caught up in the advancing accretionary prism in advance of the colliding arc (Schwab, 1991). These deposits also contain ophiolitic detritus (detrital chromite and high Ni and Cr as common trace element components) which is indicative of an “eastern derivation” with ophiolitic sources.

CHAPTER 2

2. METHODS

2.1 SAMPLE PREPARATION

The detrital zircons required for this study were extracted from siliciclastic samples collected by Dr. Rosanne M. Lindholm during her PhD research at the University of Houston in 1987-1989. Sample locations are shown in Fig. 2, and sample descriptions and nomenclature are shown in Table 1. Two (2) samples were taken from each of the lower Ordovician and Cambrian units (Summerside, Irishtown, and Bradore Formations), one (1) sample from the Blow Me Down Brook Formation, and five (5) samples each from the Goose Tickle and Lower Head Formations. Samples were approximately 1 – 2 kg in weight. Zircon separation, mounting, and polishing was performed according to standard techniques on $250\mu\text{m} - 500\mu\text{m}$ (larger) and $< 250\mu\text{m}$ (smaller) fractions. Heavy liquid separation was done using Methylene Iodide (MI) at a specific gravity range of 3.26-3.31 (variations due to the reclamation process).

Zircon grains were handpicked using a binocular microscope. To determine the relative proportions, picking was done randomly with no preference to grain shape or color, in order to not exclude any age range or to not bias the sample toward a particular age range. Grains were approximately $100\mu\text{m}$ in the longest dimension although some grains from coarser samples (e.g. Bradore) were commonly $300 - 400\mu\text{m}$.

Table 1. . Formations and associated sample names with their map locations. Samples and sample locations from Lindholm, 1989.

Formation Name	Sample Reference	Location
Goose Tickle Fm. (GT)	NNP-4-86	Neddy Harbor, Bonne Bay
	NNP-5-86	
	NNP-7-86	
	NML-11B-86	Cape Cormorant, Port au Port
	NML-11F-86	
Lower Head Fm. (LH)	NPM-1D-86	Black Point, East Port au Port
	NPM-4D-86	
	NRH-1-86	Rocky Harbor, Bonne Bay
	NRH-2-86	
	NRH-15-86	
Irishtown Fm. (IT)	IT-1-89	Humber Arm
	IT-2-89	
Summerside Fm. (SS)	SS-3-89	Humber Arm
	SS-4-89	
Blow Me Down Brook Fm. (BMDB)	BW-1-88	Woods Island/Blow Me Down Massif
Bradore Fm. (LAB)	LAB-5C-88	Labrador
	LAB-7B-88	

Map Locations

1 - Labrador

5 - Black Point, E. Port au Port

2 - Woods Island, Blow Me Down Massif

6 - Bonne Bay

3, 4 - Humber Arm

7 - Port au Port

2.2 DATA ANALYSIS

2.2.1 Isotope Systems

To determine sandstone provenance, ages attained from zircon analysis will be correlated to the age of possible sources. Age dates will be determined by analyzing the U/Pb and Th/Pb ratios of the zircon samples, specifically, $^{238}\text{U}/^{206}\text{Pb}$, $^{235}\text{U}/^{207}\text{Pb}$, and $^{232}\text{Th}/^{208}\text{Pb}$. These isotope systems are particularly suitable as U/Th and subsequently Pb are strongly incorporated into the zircon crystal lattice because of their similar behavior and are readily retained. The half lives of these isotopes allow for suitable measurements relative to earth time, 4.468 Gy., 0.7038 Gy., and 14.01 Gy. for ^{238}U , ^{235}U , and ^{232}Th respectively (Steiger and Jäger, 1977). Because analytical precision varies depending on which isotope system is used, reported concordant ages are determined by the more precise isotopic system. The $^{206}\text{Pb}/^{238}\text{U}$ age is more precise for younger ages (<1.5 Ga) and the $^{206}\text{Pb}/^{207}\text{Pb}$ is being more precise for older ages (>1.5 Ga). Although the poorest resolution is around 1.4 Ga (Gehrels, 2008; 2010), 1.5 Ga is a more viable threshold based on the acquired data. The U/Th ratio can also be used to determine the nature of crystallization of zircons whereby, a U/Th ratio < 1 indicates a mafic origin, U/Th ratio < 10 indicates an igneous source and a U/Th ratio > 10 indicates metamorphism generally (Gehrels, 2010).

2.2.2 Laser Ablation Inductively Coupled Mass Spectrometry (LA-ICPMS)

Zircon mounts were polished and measured in situ using LA-ICPMS. The ICPMS system is a Varian 810 Quadrupole ICPMS system with an argon-plasma. Two

laser ablation systems were used for analysis, a CETAC LSX – 213 nm system and an Analyte 193 Ultra-Short Pulse Excimer system. Both systems use Helium as the carrier gas. The spot size used for laser ablation was 25 μm (usually at 10Hz) for all analyses with the exception of one Bradore sample, in which a 50 μm spot size was used as those samples contained coarser grain-sizes.

2.2.3 Zircon Standards

In order to determine the ages of unknown samples, the isotopic ratios of each unknown was correlated with the ratios of standards of known ages. Four standards were used for analyses and they are as follows: FC5z, reported ID-TIMS age of 1096.2 ± 1 Ma (Shaulis, 2010); Plesovice, reported TIMS age of 337.13 ± 0.37 Ma (Slama, 2008); Peixe, reported ID-TIMS age of 564 ± 4 Ma (Dickinson and Gehrels, 2003); and Stettin, reported age of 1565 ± 8 Ma (Shaulis, 2010). For the first six samples analyzed (1 sample from each target unit), FC5z was used as the target standard in conjunction with Peixe and Stettin to account for drift. The target standard was switched to Plesovice (used in conjunction with FC5z) for the rest of the analyses (11 samples) as it was more homogenous in composition and thus provided more consistent concentrations. Target standards were analyzed twice after every 5 unknown analyses, and auxiliary standards (used in conjunction with target) were analyzed twice after every 10 unknown analyses. NIST 612 glass (Pearce et al., 1997) was used to determine U and Th concentrations and to correct for depth-dependent fractionation and instrumental mass bias. The NIST 612 glass was analyzed 3 times at the end of sample analysis.

2.2.4 Data Acquisition and Reduction

Data was acquired across 1-minute intervals for each sample. During the first 16 seconds, the laser was not fired to allow for measurement of background intensities. This was followed by 20 seconds of laser ablation and then 24 seconds of no ablation to allow the system to be purged and to return to background values. The signal intensities are imported as raw data into Wavemetrics Igor ProTM (v. 6.2.0.0) software, with Iolite v. 2.11 (Hellstrom et al, 2008) as an add-in, where integration lengths were automatically selected for all ablation as well as baseline intensities to avoid bias. For the ablation period (20 seconds) approximately 16 seconds were selected so that the first 2 seconds of ablation time were excluded as this interval usually contained ²⁰⁴Pb spikes commonly caused by surface contamination of the sample. The iteration length of signals could be adjusted where age zoning or inclusions/cracks were detected that could be sources for high common Pb.

Analysis of signal selection was initially performed using GLITTER software (van Achterberg et al. 1999) on the Bradore Formation sample 7B-88, but Igor ProTM, was used for all other samples. The software was changed because the external errors associated with isotope data exported with GLITTER could not be resolved effectively as the ages were calculated within the software and not separately. The fact that the resultant ages in GLITTER were visible during the signal selection process also introduced a possible source of bias as the ages could be seen in real-time with corresponding changes to location and length of iterations along the signal intensities. Therefore, ages could be “tweaked” to a particular age across all isotope systems for each

analysis in GLITTER. This problem does not exist in Igor ProTM since ages are not calculated within the program. The baseline-subtracted data for ^{202}Hg , ^{204}Hg , ^{204}Pb , ^{206}Pb , ^{207}Pb , ^{208}Pb , ^{232}Th , and ^{238}U are exported with error uncertainties at 2σ as a comma delimited file into a reduction spreadsheet (personal communication with T. Lapen and B. Shaulis, 2009). Here internal errors exported from Igor ProTM, systematic and random errors were assessed, and elemental and instrumental mass fractionation was calculated, as well as potential common Pb error corrections. External standards were used to correct for instrumental drift by applying a fractionation factor of true ratio/measured ratio (Shaulis et al., 2010) determined from the standards, to the unknown measurements. Discordance was filtered at <30% in order to yield the maximum range of ages for each sample (Gehrels, 2010).

Analytical precision of standards was determined for each standard by comparison of the mean values with mean standard weighted deviations (MSWD), individually and combined for the analyses of each unit shown at 2σ uncertainties, to the known standard ages (Fig. 4). For target standard Plesovice, the mean values of subordinate standard FC5z (known age of 1096.2 ± 1 Ma) was determined. All combined mean values for each set of analyzed samples and the total combined mean values (1101 ± 2.4 Ma, MSWD = 0.79) were within < 1% uncertainty of known standard age. However, only the mean value for the Irishtown samples was within standard uncertainty as well as analytical uncertainty at 1096.8 ± 5.6 Ma. The mean value of the Bradore samples was not within standard uncertainty but was within analytical uncertainty at 1099

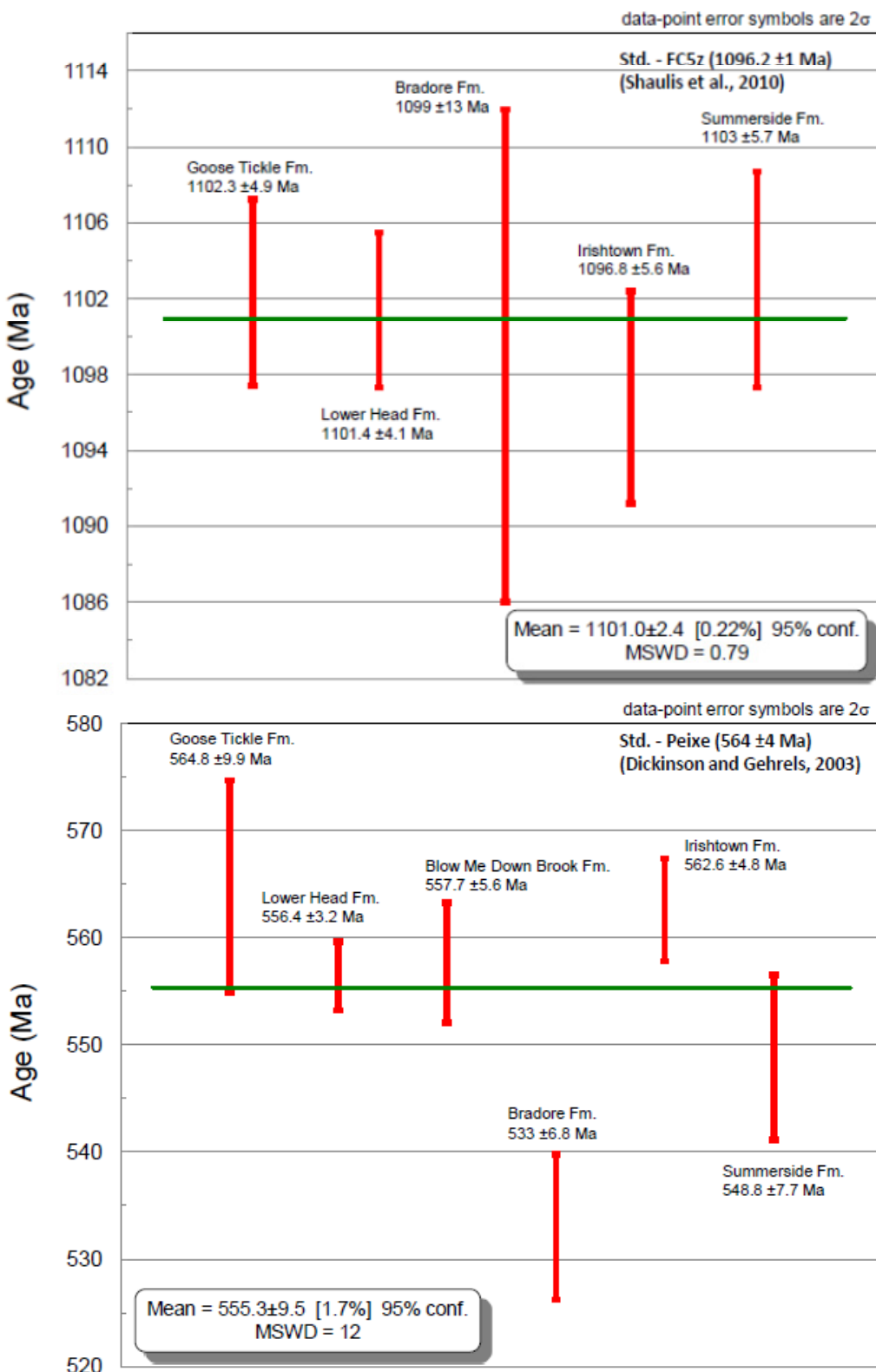


Figure 4. Mean values with Mean Standard Weighted Deviations (MSWD) for combined values of sample sets for each unit. Errors are at 2σ .

± 13 Ma. The Blow Me Down Brook Formation did not have an analysis for this subordinate standard as only one sample was analyzed using Peixe as the subordinate. For target standard FC5z, subordinate standard Peixe (known age of 564 ± 4 Ma) was used. The mean results were not as favorable for these analyses as for FC5z possibly due to lower signal intensity analytical conditions for those values well outside of the uncertainty range for the known standard ages, i.e. for Bradore Formation (533 ± 6.8 Ma) and Summerside Formation (548 ± 7.7 Ma). Both mean sample values from the Goose Tickle Formation (564.8 ± 9.9 Ma) and the Irishtown Formation (562.6 ± 4.8 Ma) were within standard and analytical uncertainty. The mean values for the Lower Head and Blow Me Down Brook Formations were within $< 2\%$ analytical uncertainty at 556.4 ± 3.2 Ma and 557.7 ± 5.6 Ma respectively but fell outside standard uncertainty. The overall mean values for all samples using Peixe as a subordinate was also within $< 2\%$ of analytical uncertainty at 555.3 ± 9.5 Ma and fell outside the standard uncertainty. The actual MSWD value of 12 is representative of the great variation due to the Bradore and Summerside Formations.

CHAPTER 3

3. RESULTS

3.1 SAMPLE DATA

Analysis of 17 samples from 6 siliciclastic units of the Humber Arm Allochthon in Newfoundland yielded 1829 detrital zircon grains. These units represent different stages of passive margin development in eastern Laurentia from late Neoproterozoic to middle Ordovician time. The U-Pb ages of the detrital zircons range from 3744 ± 25 Ma – 481 ± 15 Ma. All analytical results are presented in Supplementary - Tables 1 – 6 (1 – Goose Tickle Fm.; 2 – Lower Head Fm.; 3 – Irishtown Fm.; 4 – Summerside Fm.; 5 – Blow Me Down Brook Fm.; and 6 – Bradore Fm.) in the Appendix – 1. The concordant ages for each formation were combined and are represented on probability density plots (Fig. 5) using DZ Age Pick (Gehrels, 2007) in which 3 or more ages that overlap within uncertainty contribute to an age peak and all age ranges stated refer to combined data and errors are at 2σ uncertainty. A $25\mu\text{m}$ spot size was used for all samples except LAB-7B-88. Relative age probability distribution plots for individual samples are presented in Appendix – 2.

3.1.1 Bradore Formation

This formation yielded the coarsest grain sizes. The fraction analyzed of predominantly subrounded – rounded zircon grains was between $250\mu\text{m} – 500\mu\text{m}$ with a spot size of $50\mu\text{m}$ (LAB-7B-88) and $25\mu\text{m}$ (LAB-5C-88). The dated grains yielded ages ranging from 1466 ± 30 Ma to 513 ± 14 Ma with defined age peaks at 582 Ma (40 grains),

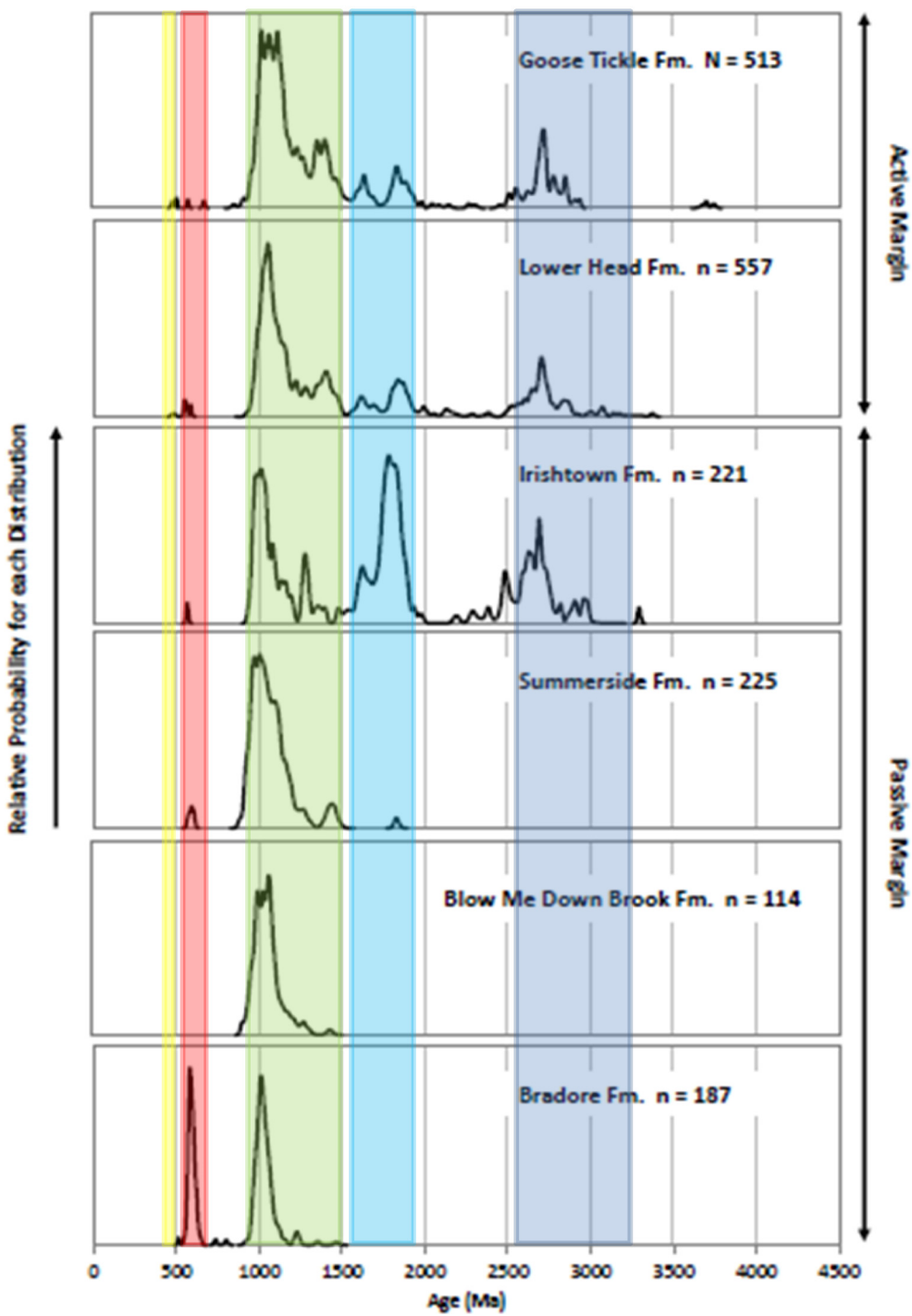


Figure 5. Relative age probability distribution plots of U-Pb ages determined for detrital zircons of the siliciclastic units analyzed. Only concordant age data was used, discordance = 30%. n = total number of grains analyzed. D. blue = North Atlantic Craton; L. blue = Torngat Arc/Makkovik Province; Green = Grenville and Pre-Grenville, Granite/Rhyolite; Red = Laurentian Rift-related; Yellow = Taconic Arc

1011 Ma (62 grains), and 1226 (4 grains) Ma. A total of 221 zircon grains were analyzed with 72 grains from LAB-7B-88 (3 discordant) and 119 grains from LAB-5C-88 (4 discordant). Age peaks were not uniform between both samples however, as LAB-7B-88 only had two age peaks, 583 Ma (25 grains) and 1005 Ma (24 grains) whereas LAB-5C-88 had four age peaks, 580 Ma (13 grains), 619 Ma (10 grains), 1020 Ma (45 grains), and 1226 Ma (4 grains). The lack of population similarity could be due to a smaller sample population for LAB-7B-88.

3.1.2 Blow Me Down Brook Formation

Only one sample was analyzed for this formation which yielded 119 angular to subrounded grains (5 discordant) and a grain size fraction of $< 250\mu\text{m}$. Age ranges are from 1428 ± 36 Ma to 898 ± 18 Ma with age peaks at 994 Ma, 1029 Ma, 1061 Ma, and 1269 Ma. The apparent lack of variability may be due to a very restricted source region of Grenville age or could be due to heterogeneity of zircon populations within the unit.

3.1.3 Summerside Formation

For this unit 237 grains were analyzed, 119 from SS-3-89 (1 discordant) and 118 from SS-4-89 (9 discordant). Both samples contained about 30% angular grains. SS-4-89 tended to have more rounded grains with the remainder being rounded to well rounded grains compared to the remaining grains of SS-3-89 which were subrounded to rounded. Dated ages ranged from 1831 ± 33.7 Ma to 570.3 ± 17.1 Ma. Peak ages for this unit were 591 Ma, 968 Ma, 1002 Ma, 1091 Ma, 1265 Ma, and 1439 Ma. There is an apparent shift in the quantity of grains that contribute to the c. 968 Ma age peak and 1002 Ma to 1091

Ma peaks in the two samples analyzed. In the SS-3-89 sample, only 3 grains contributed to an age peak of 919 Ma whereas 65 grains contributed to age peaks of 1012 Ma (33 grains) and 1016 Ma (32 grains). This is in contrast to 30 grains contributing to a 959 Ma age peak and 25 grains for an age peak of 1042 Ma for SS-4-89. The 591 Ma peak age only appears with the combined data as there were 3 or more grains contributing to that age within error when both sets of sample data were combined. This change could represent a shift in sources contributing to the deposition of this unit. Three grains had U/Th ratios > 10 (all Grenville-aged) which may indicate a metamorphic origin.

3.1.4 Irishtown Formation

Analysis of the 2 samples of this unit yielded 239 grains, 119 grains from IT-1-89 (17 discordant) and 120 grains from IT-2-89 (1 discordant). The grains were mostly subrounded to rounded and ages ranged from 3292 ± 18.1 Ma to 565.5 ± 14.7 Ma forming clusters at 2959 – 2905 Ma, 2628 – 2382 Ma, 1933 – 1781 Ma, 1621 – 1353 Ma, and 1276 – 981 Ma. Peak ages of individual samples were mostly consistent with the combined data; however, some peak ages were not common between samples. There were 2 peak ages (1767 Ma and 1353 Ma) which were unique to IT-1-89 and there were 4 peak ages (2954 Ma, 1933 Ma, 1829 Ma, and 1536 Ma) unique to IT-1-89. Also, there were 2 peak ages, 1 from each sample that were not present in the combined data; 2689 Ma (9 grains) from IT-1-89 and 2731 (6 grains) from IT-2-89. These ages may have been excluded due to overlap of applied uncertainties in the age peak calculation. Conversely, 2 age peaks (2905 Ma and 1478 Ma) are only evident upon combination of

the data, possibly for the same reason. Six grains analyzed had U/Th ratios > 10 suggesting a metamorphic origin for these grains.

3.1.5 Lower Head Formation

For this unit, 5 samples were analyzed yielding 579 grains, 117 grains (4 discordant) from NPM-1D-86, 105 grains (0 discordant) from NPM-4D-86, 118 grains (12 discordant) from NRH-1-86, 124 grains (1 discordant) from NRH-2-86, and 115 grains (5 discordant) from NRH-15-86. The dated ages of these samples ranged from 3373.9 ± 221 Ma to 482.2 ± 22.1 Ma. Most of the grains were subrounded in each sample. The quantity of angular grains in each sample ranged from 1 grain (NRH-1-86) to 56 grains (NRH-2-86) with 2 samples (NPM-1D-86 and NPM-4D-86) having approximately 30 angular grains. Major age peak groupings occurred at 3070 – 3001 Ma, 2838 – 2523 Ma, 2129 – 1838 Ma, 1688 – 1403 Ma, 1279 – 1052 Ma, and at 551 Ma. Individual samples show strong agreement with these ranges although there is some variability across samples. NPM-4D-86 only had 1 age peak at 2725 Ma (4 grains) greater than 2000 Ma. NRH-15-86 had no age peak around 2600 Ma and was the only sample to have and age peak at 2129 Ma (3 grains) and the youngest age peak at 556 Ma (3 grains). The 2 age peaks above 3000 Ma, 3070 Ma (5 grains) and 3001 Ma (3 grains) only occurred when the data was combined. This variability could indicate heterogeneity within the samples or different source contributions. Fourteen grains had U/Th ratios > 10 suggesting a metamorphic origin, and 5 grains from NRH-1-86 and 1 grain from NRH-15-86, had ratios > 1000 (23973.72, 5822.05, 8412.91, -6412.23, 1897.47, and 15273.37 respectively). This suggests that these grains (6) were affected by a high-grade

metamorphic event between 1835 – 1785 Ma (5 grains) and during the Grenville period (1032 Ma – 1 grain).

3.1.6 Goose Tickle Formation

Five samples were analyzed for this unit yielding 537 grains, 120 grains from NNP-4-86 (1 discordant), 95 grains from NNP-5-86 (3 discordant), 115 grains from NNP-7-86 (9 discordant), 107 grains from NML-11B-86 (1 discordant), and 100 grains from NML-11F-86 (8 discordant). Angular grains constituted approximately 40% of each sample with the exception of NNP-7-86 which only had 12% angular grains. The remainder of grains in each sample was subrounded. Grain ages ranged from 3744.4 ± 24.8 Ma to 480.5 ± 15.4 Ma with age peak clusters at 2909 – 2511 Ma, 1981 – 1832 Ma, 1635 Ma, 1462 – 1353 Ma, and 1267 – 911 Ma. Age peaks between 1600 – 1500 Ma were common in 2 samples, NNP-4-86 (6 grains) and NNP-5-86 (3 grains); but this age range did not occur in the combined data. Further variability between individual samples included no age peaks around 1900 Ma and 1200 Ma for NNP-5-86; 1900 Ma, 1600 Ma, and 1500 Ma for NNP-7-86; 1800 Ma and 1500 Ma for NML-11B-86; and none around 1900 Ma and 1500 Ma for NML-11F-86. Two age peaks at 2511 Ma (4 grains) and 2551 Ma (6 grains) occurred in the combined data only. Eleven grains had U/Th ratios > 10 suggesting a metamorphic origin for these grains and a high grade metamorphic event for one of these grains ($U/Th = -8604.16$). All of these grains were of Grenville age (912 – 1287 Ma) except one grain dated at 2626 Ma.

CHAPTER 4

4. DISCUSSION OF RESULTS

4.1 POTENTIAL SOURCES

Analyzed samples produce age peaks that fall into defined age groupings that can be more generally grouped into Archean (> 2500 Ma), Paleoproterozoic (2500 Ma – 1600 Ma), Mesoproterozoic (1600 Ma – 1000 Ma), Neoproterozoic (1000 Ma – 542 Ma), and early Paleozoic (< 542 Ma). Each unit contained varying quantities (represented as percentages) of ages falling under these broader ranges (Fig. 5). Early Paleozoic grains are subdivided into Cambrian and Ordovician age ranges. These ages can then be correlated to sources of known age (Fig. 8 for Laurentia) to determine possible provenance contributions to the Cambro-Ordovician siliciclastic units of the Humber Arm Allochthon (Fig. 6).

4.1.1 Grenville Normalization

The combined age peaks for each sample were grouped into smaller age groupings that were common to all samples in an attempt to further discriminate the age relationships of the sampled units (Fig. 6; horizontal axis, Fig. 7). These age groupings were then normalized to the Grenville-age group. Normalization in this case means that for each sample, the number of grains that contributed to each age peak was determined, and then each contribution was divided by the number of grains that contributed to the Grenville age range of that particular sample, yielding a ratio (vertical axis, Fig. 7). The

actual Grenville contribution (1.00) is included for better visualization since some samples have very restricted age ranges (e.g. Bradore, Blow Me Down Brook, and

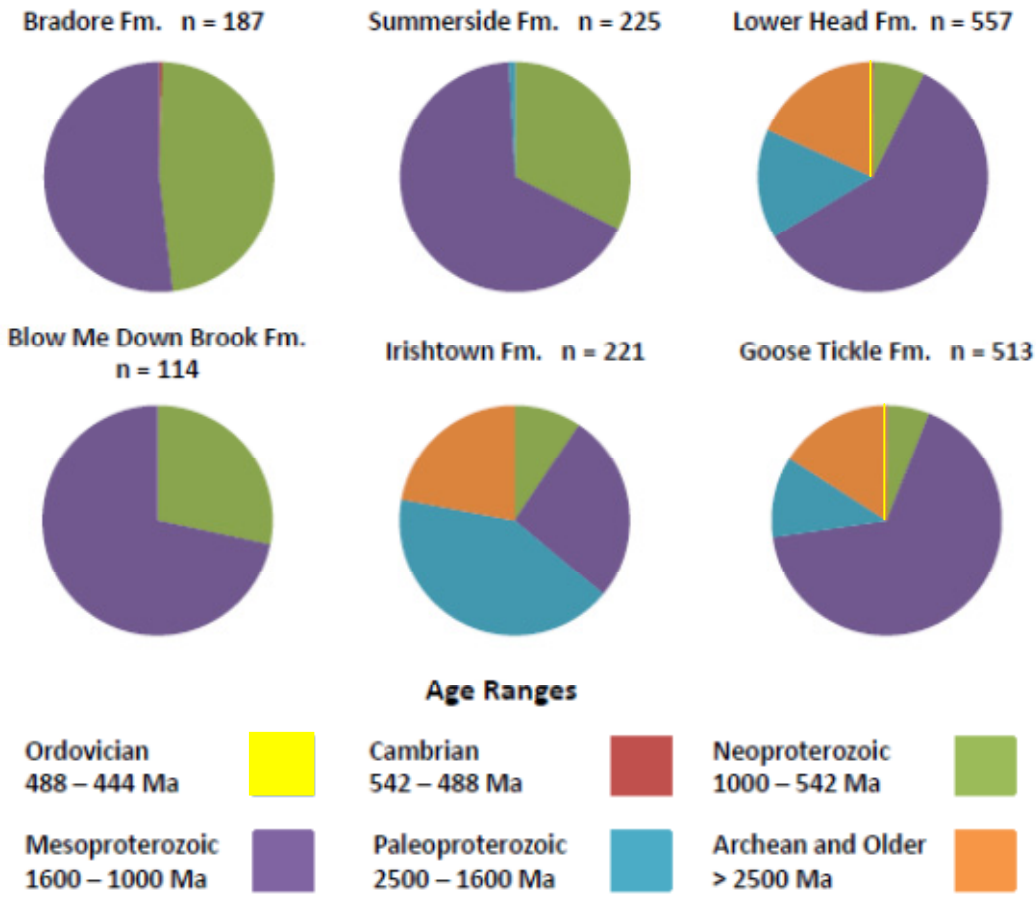


Figure 6. Pie charts showing the age ranges for the relative contribution of grains for each sample. n = number of concordant grains. The Ordovician contribution to the Goose Tickle and Lower Head Fms. is <1%

Summerside Formations) and they would not have been well represented graphically. Grenville age range is taken as 1350 -950 Ma (Davidson, 1998) and is represented by the age range of 1353 – 963 Ma. The slightly higher (3 Ma) upper limit for the Grenville age range was chosen because both the Goose Tickle Formation (30 grains) and the Irishtown Formation (3 grains) had an age peak of 1353 Ma (Fig. 5), but this is not meant to redefine said boundary. The Lower Head Formation has an age peak at 1350 Ma (25

grains). This normalization “removes” the Grenville signature from the analyses as it can overwhelm the other age signatures significantly and is common to all samples in varying quantities (Fig. 6), and therefore the other age contributions can be better highlighted and compared since a Grenville signature is common to all samples and trends can be determined. Grenville components can be analyzed separately.

Based on figure 7, a few trends can be seen. There is a general increase in the relative contribution of grains from a 1538 – 1398 Ma range from the Summerside Formation to the Goose Tickle Formation with a decrease in formation age. At age ranges 1690 – 1617 Ma, 1884 – 1781 Ma, 2688 – 2605 Ma, and 3070 – 2905 Ma, the Irishtown Formation had a greater relative contribution of grains than both the Lower Head and Goose Tickle Formations. The relative grain contributions at ranges 1884 – 1781 Ma and 2688 – 2605 Ma are significantly higher in the Irishtown than the other two formations. The Irishtown formation was also the only unit sampled to contain an age range of 2482 – 2382 Ma and 1538 Ma. It should also be noted that this formation has the least (36.6%, 75 grains) population of Grenville-aged grains (Fig. 6). The Lower Head and Goose Tickle Formations show very similar age contribution patterns, with the Lower Head having the greater quantity in each range and both have contributions from age ranges 2778 – 2703 Ma and 2848 – 2838 Ma. These ranges are missing in the Irishtown Formation.

Age Range Comparison Normalized To Grenville

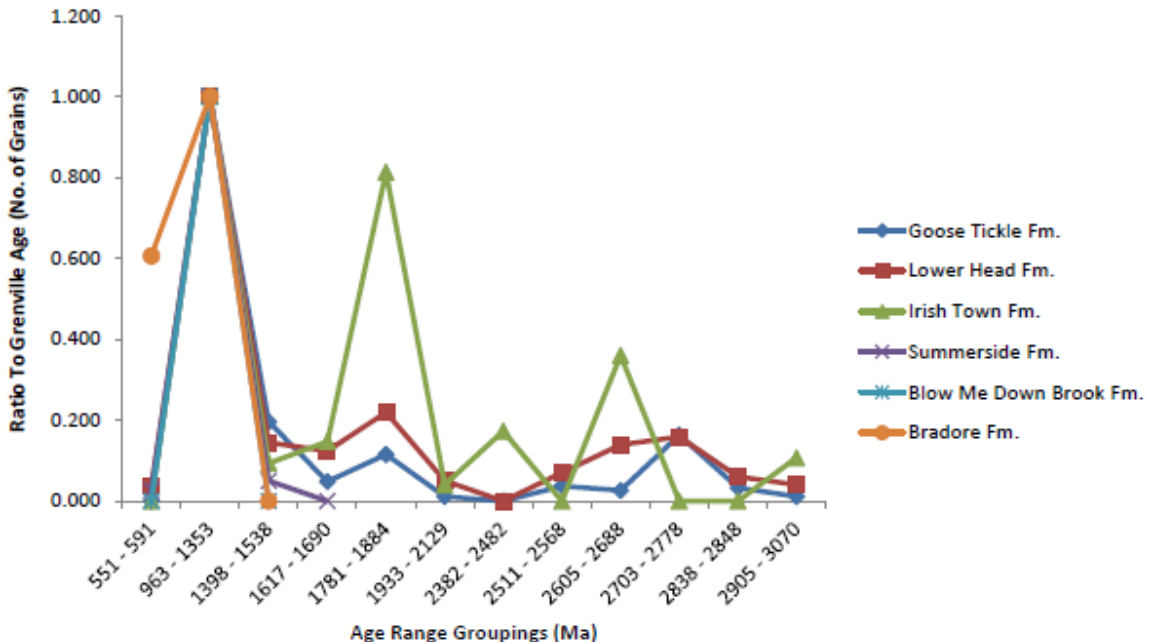


Figure 7. The graph shows the Grenville-age normalized ratio of each unit vs. the age ranges. Units are listed on the right from youngest at the top.

4.1.2 Archean and Paleoproterozoic Zircons

The Irishtown, Lower Head, and Goose Tickle Formations were the only units to contain detrital zircon grains older than the Neoproterozoic. The Archean age peaks ranged from 3070 – 2511 Ma, however, only the Lower Head and Goose Tickle Formations contained age peaks between 2600 – 2500 Ma, and only the Lower Head contained age peaks older than 3000 Ma. The oldest detrital zircon dated was derived from the Goose Tickle Formation and it yielded a $^{206}\text{Pb}/^{207}\text{Pb}$ age of 3744.4 ± 24.8 Ma (2σ uncertainty). A possible source for a grain of this age could be the 3750 - 3700 Ma igneous and metamorphic rocks of the northeastern margin of Laurentia (Saglek Block) (Krogh and Kamo, 2006), (Fig. 8). The North Atlantic craton is also expected to show age clusters at 3200 – 2900 Ma and 2800 – 2700 Ma (Cawood and Nemchin, 2001),

consistent with the age peaks of 3070 – 2905 Ma, 2848 – 2838 Ma, and 2778 – 2703 Ma derived from all three units. The northern region of the North Atlantic craton also contains metamorphic rocks where zircon growth is dated at 2770 – 2700 Ma (Lucas et al., 1998) which can be represented by the 2778 – 2703 Ma age peak range. Another possible source would be from metamorphic rocks of the Superior province dated at 2750 – 2700 Ma (Cawood and Nemchin, 2001). Alternatively, granite-greenstone terrane has been dated at 2700 – 2650 Ma for the Kaminak Block, Rae and Hearne province could be represented by the lower age range (age peaks at 2716 Ma, 2703 Ma, 2688 Ma, and 2652 Ma); however the proximity of the North Atlantic craton gives it the better probability for greater contributions. Granitoid intrusions associated with post-tectonic activity in the southern region (Hopedale Block) of the North Atlantic craton with dated ages at 2580 – 2550 Ma (Lucas et al., 1998) could correlate to age peaks at 2568 Ma (Lower Head) and 2551 Ma (Goose Tickle). The southern granitoid intrusions could also be a possible source for the lower age peaks of 2523 Ma (Lower Head) and 2511 Ma (Goose Tickle) within error.

The Paleoproterozoic is represented by an age peak range of 2482 – 1617 Ma. Loosely defined groupings are recognized at 2482 – 2382 Ma, 2129 – 1933 Ma, 1884 – 1781 Ma, and 1690 – 1617 Ma. The best source region for the age range 2482 – 2382 Ma would either be the Huronian Supergroup in the Superior province dated at 2490 – 2450 Ma and associated granitic intrusion dated at 2400 Ma (Davidson, 1998) or the Wopmay orogen located over 2000 miles to the west, where Nd isotopes suggest that 1900 Ma arcs were formed on 2400 – 2200 Ma crust (Whitmeyer and Karlstrom, 2007).

Detrital zircons from the Tasiuyak paragneiss dated at 2200 – 1900 Ma (Lucas et al.,

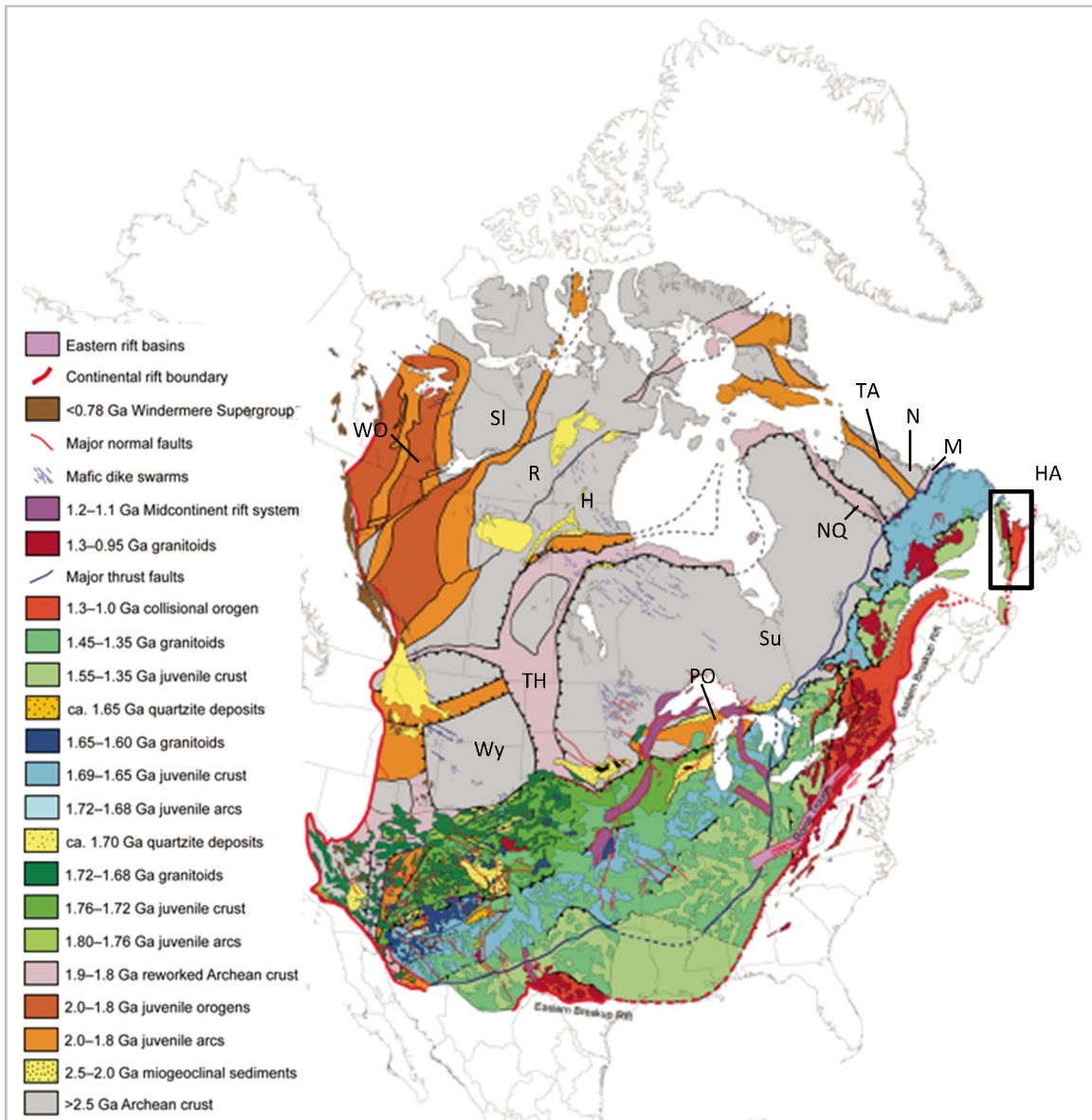


Figure 8. Geologic map of Archean to Mesoproterozoic rocks overlain on a map of North America in its present orientation. The black rectangle outlines the Humber Arm Allochthon. Abbreviations are as follows: H = Hearne Province; HA = Humber Arm Allochthon; M = Makkovik Province; N = North Atlantic Craton/ Nain Province; NQ = New Quebec Orogen; PO = Penokean Orogen; R = Rae Province; SI = Slave Craton; Su = Superior Province; TA = Torngat Orogen; TH = Trans Hudson Orogen; WO = Wopmay Orogen; Wy = Wyoming Craton. Modified after Whitmeyer and Karlstrom, 2007

1998) could account for the age peaks of 2129 – 1933 Ma, suggesting a metamorphic origin. The Makkovik province of eastern Labrador contains rock units from both the Ketilidian (1900 – 1800 Ma) and Labradoran orogenies (1700 – 1650 Ma) (Davidson, 1998), and seems a likely source for detrital zircons characterized by age ranges of 1933 – 1690 Ma and possibly the lower age peak of 1617 Ma, within error. The Torngat orogeny can also be a potential source for detrital zircons of igneous origin with age ranges from 1933 – 1884 Ma as these can be possibly correlated to the Burwell intrusive suite dated at 1910 – 1870 Ma. The Penokean orogen dated from 1900 – 1830 Ma (Davidson, 1998; Cawood and Nemchin, 2001) can also be considered a contributor for this age range; however, it would require a much longer transport distance and quite possibly more reworking.

4.1.3 Mesoproterozoic and Neoproterozoic Zircons

Mesoproterozoic age spectrum can be divided into a pre-Grenville age range of 1538 – 1398 Ma and a Grenville age range which continues into the early Neoproterozoic at 1353 – 963 Ma. The pre-Grenville ages can be correlated to the 1550 – 1400 Ma juvenile crustal blocks thought to have collided with the Laurentian margin (Whitmeyer and Karlstrom, 2007) and the Pinware terrane in northeastern Canada that occurred at 1500 – 1470 Ma (Davidson, 1998). Other possible sources include the Granite-Rhyolite province dated at 1550 – 1300 Ma, as well as rocks in eastern Laurentia dated at the same age, bounded to the north by Mazatzal basement (Whitmeyer and Karlstrom, 2007). The Granite – Rhyolite province also yields ages of 1480 – 1350 Ma of dated intrusive (Whitmeyer and Karlstrom, 2007). The Grenville period is characterized by global

continent – continent collisions that led up to the formation of Rodinia in the mid – late Neoproterozoic. Grenville age ranges are most likely derived from reworking of Grenvillian terranes that are very prolific along the eastern margin of Laurentia. The broad age range can be correlated to different events within the Grenville province such as 1360 – 1230 Ma inferred Grenvillian arc magmatism (Cawood and Nemchin, 2001) followed by the Elzevirian orogeny at 1300 – 1200 Ma (Mclelland et al., 1996; Whitmeyer and Karlstrom, 2007). The anorthosite-mangerite+charnockite-granites (AMCG) associated with the Wakeham Supergroup have reported ages at 1080 Ma (Davidson, 1998), 1165 – 1090 Ma (Cawood and Nemchin, 2001), and 1190 – 1110 Ma (Whitmeyer and Karlstrom, 2007). Renewed activity in the southeastern region of Canada has been reported at 1090 – 980 Ma (Whitmeyer and Karlstrom, 2007).

Neoproterozoic ages for combined data ranged from 591 – 551 Ma and only occurred in 3 analyzed units. These are the Bradore Formation (582 Ma), Summerside Formation (591 Ma and 573 Ma), and Lower Head Formation (551 Ma). These ages can be correlated to rift-related magmatism (dikes), related to the breakup of Rodinia in the mid to late Neoproterozoic. The ranges represent the main pulse of rifting that occurred at 620 – 550 Ma (Cawood et al., 2001; Whitmeyer and Karlstrom, 2007). There are no age peaks that represent the first pulse of rifting from 760 – 700 Ma. Both the Summerside and Goose Tickle units had an age peak close to 900 Ma, 919 Ma (3 grains) and 911 Ma (3 grains) respectively, and these may represent the lower range of uplift and or metamorphism that occurred at the end of the Grenville orogeny (Davidson, 1998).

4.2 ARC-DERIVED SEDIMENT

One aim of this study was to attempt to constrain the age range of the colliding arc and its basement involved in the pre-terminal collision at the beginning of the Taconic orogeny. The age of the colliding arc is suggested to be middle to late Ordovician in age (Casey and Dewey, 1984, and others). A constraint on the upper limit of the age of the arc would also help constrain the age of sedimentation of the allochthonous (Lower Head) and autochthonous (Goose Tickle) foreland basin units. The only concordant early Paleozoic ages were derived from 2 grains, one each from the Lower Head and Goose Tickle Formations, yielding $^{206}\text{Pb}/^{238}\text{U}$ ages of 482.2 ± 22.1 Ma and 480.5 ± 15.4 Ma with 2σ uncertainty. Both of these grains had U/Th ratios less than 10 (1.09 and 1.75 respectively) suggesting an igneous origin. It is quite possible that these ages represent an arc age which is somewhat constrained to be equal to or younger than the age of the Bay of Islands ophiolite dated at 485 Ma (Lindholm and Casey, 1989). Unfortunately, based on the technique used to calculate the age peaks, one dated grain is seen as an unreliable representation of a particular population since at least 3 grains are needed to determine a reliable age peak. The lack of more arc-aged grains could be due to one or a combination of several factors: (1) arc-derived sediment was not sufficiently incorporated into the accretionary wedge or recycled sources as they were lost to the trench (Clift et al., 2009); (2) the arc signature could have been totally overwhelmed by detrital grains from Laurentian (particularly Grenville-aged) source rocks, due to the difference in zircon fertility of the contributing sources (Moecher and Sampson, 2006; Dickinson, 2008), that they are not well represented. This is further supported by the fact that these young ages are only detected with sample quantities far above the suggested statistical

limit necessary for 95% confidence that no more than 5% of the populations contributing to a particular unit is missed (Vermeesch, 2004); (3) there was some obstruction to the delivery of arc material to the trench, such as an uplifted and/or subaerial accretionary wedge (Fig. 10). Also, further isotopic discrimination (e.g. Hf or Nd isotopic data) is necessary to possibly determine the nature of the basement due to the high probability of reworking and/or recycling of Grenville-aged sediment.

Subsequently, a biased analysis was performed to determine, with certainty, the presence of arc-aged zircons, based on the evidence listed above. The Lower Head Formation was chosen for this analysis. It is the first foreland basin deposit (allochthonous) and would record initial zircon contributions derived from the arc that

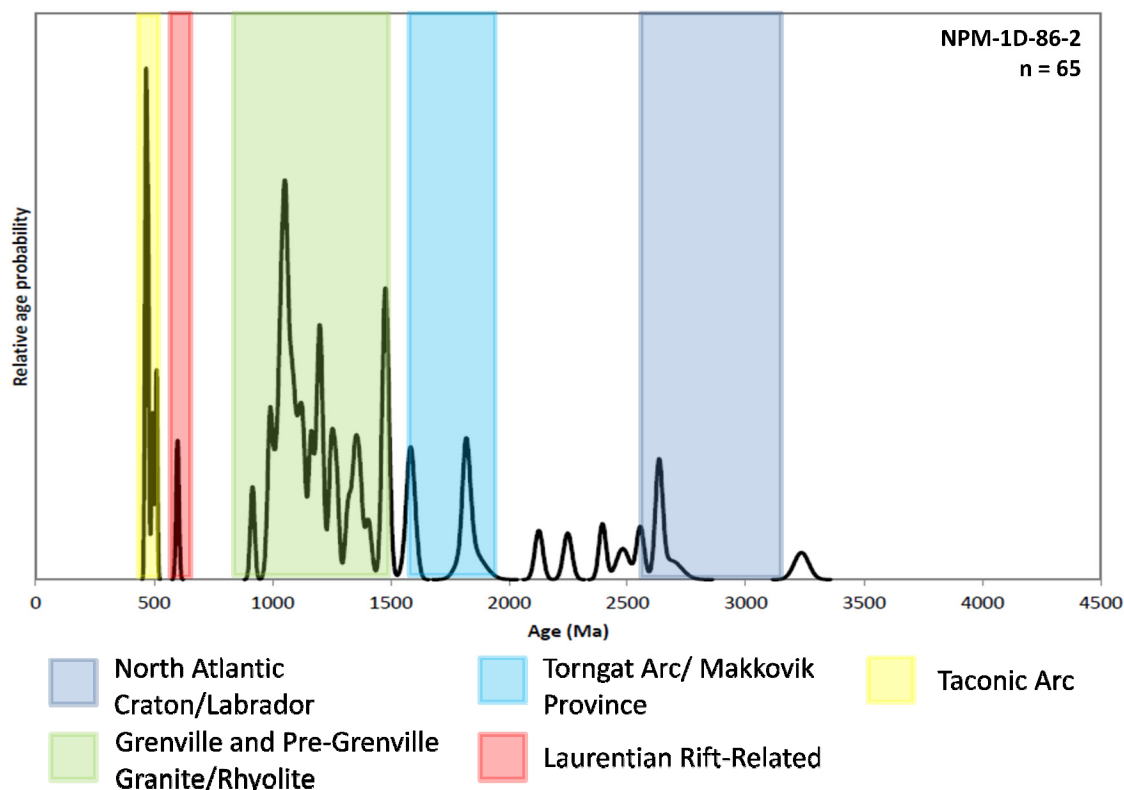


Figure 9. Relative age probability distribution for Lower Head Formation sample NPM-1D-86-2 biased analysis. n = Number of concordant grains

were not lost to the trench. The arc-related age of 482.2 ± 22.1 Ma was derived from sample NPM-1D-86 and for this analysis the name was amended to NPM-1D-86-2. Sixty-five (65) zircon grains were chosen with grain sizes ranging from $50\mu\text{m}$ - $100\mu\text{m}$. These grains were specifically selected based on their clear color, euhedral grain shape and smaller grain size as they could possibly represent young, arc-aged zircons derived from arc lithosphere or basement, or from ash fall. Colored and rounded zircons were excluded as these usually represent older aged zircons. A spot size of $25\mu\text{m}$ was used and discordance parameters etc. are the same as for all other samples. Only the arc-aged zircons will be addressed here. The analysis yielded 6 concordant zircon ages that can be correlated to an arc age: 464.2 ± 9.4 Ma, 467 ± 9.9 Ma, 471.2 ± 11.2 Ma, 475.2 ± 9.6 Ma, 494.9 ± 11.9 Ma, and 510.1 ± 9.3 Ma at 2σ uncertainty (Table 2, Appendix – 1), and a peak age of 466 Ma (3 grains) (Fig. 9). The 510 – 464 Ma age range probably encompasses the time from the formation of the Coastal Complex at 508 Ma (Mattinson, 1975; Casey et al., 1985) and initiation of subduction to the development of the basal metamorphic aureole, dated at 469 Ma (Casey et al., 1985). The Bay of Islands Ophiolite Complex is dated at 485 Ma (Casey et al., 1985) and slightly older at 504 Ma (Mattinson, 1976; Casey et al., 1985). Therefore, these ages can represent the duration of arc activity, with the peak age of 466 Ma representing the younger age limit for the arc since the aureole was formed while still in an oceanic arc setting (Dewey and Casey, 2011), or they can be representative of more than one element of the arc/ophiolite system. In either case, it constrains the age of arc activity and correlates well with previously published data for the Coastal Complex and basal metamorphic aureole.

4.3. TECTONIC MODEL

The Cambro-Ordovician siliciclastic units of the Humber Arm Allochthon record the evolution of the Laurentian margin from the late Neoproterozoic rifting of Rodinia, to the formation of the Iapetus Ocean, to the eventual closure of the Iapetus culminating in the Taconic orogeny in the late Ordovician. From the U-Pb age data determined for these samples a sequence of evolution can be inferred and is partly illustrated in a simple tectonic model (Fig. 10). The three oldest formations, the Bradore, Blow Me Down Brook, and Summerside Formations, each show restricted source regions for their detrital sediment. The most restricted of these three is the Blow Me Down Brook Formation.

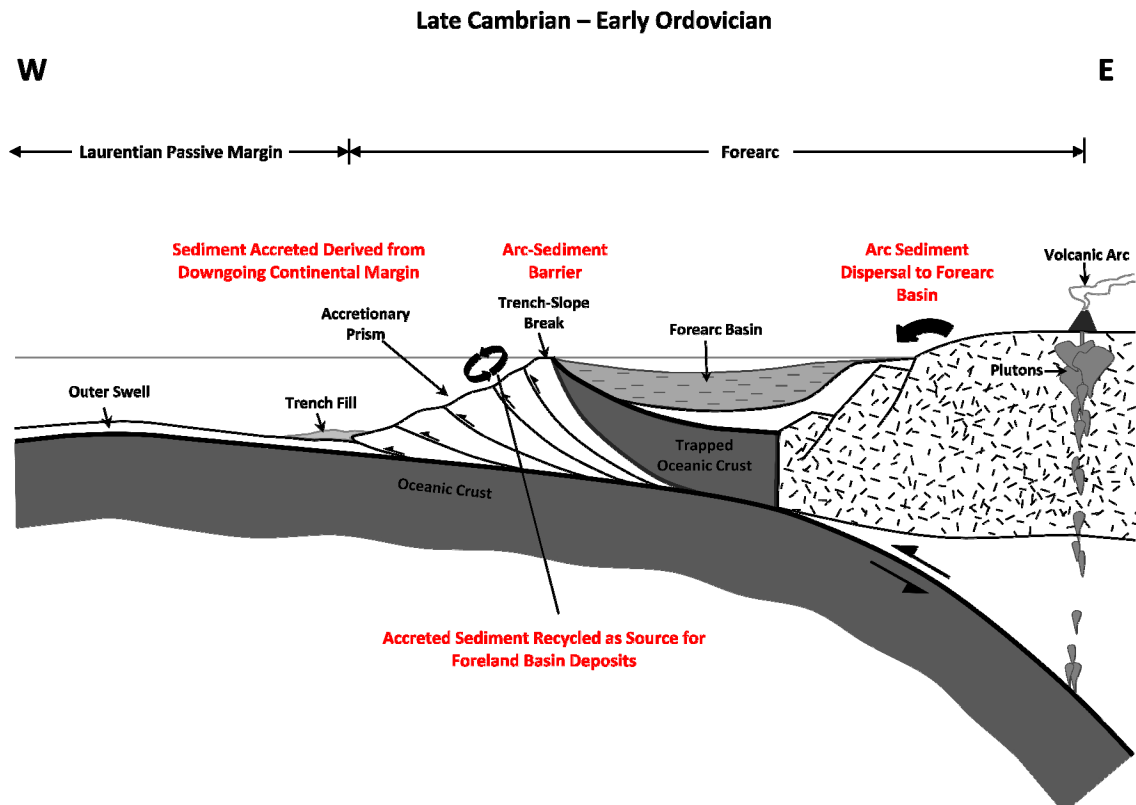


Figure 10. Simple tectonic model showing the formation and aggradation of the accretionary wedge until it becomes a source for subsequent foreland basin deposition. Dashed pattern = forearc basin sediments

The bimodal age distribution of the Bradore Formation can be interpreted as deposition within a restricted rift basin on the Laurentian shelf (Fig. 12). The existence of a prominent rift shoulder consisting of mafic dikes associated with late stage rifting (570 – 550 Ma) and Grenville basement could have restricted flow into the basin and served as the source for bimodal rift age (582 Ma) and Grenville ages (1226 Ma and 1011 Ma). The enhanced topography at the elevated rift shoulder would prohibit block drainage from Laurentia thereby restricting the available sources to be derived from erosion of the rift shoulder. The Red Sea can be considered a modern example of this depositional environment (Fig. 12), where the rift shoulders represented by the Red Sea Hills for example. The Blow Me Down Brook Formation is considered the distal equivalent of the Bradore (Lindholm and Casey, 1989) but it has a very restricted age peak range (Grenville) from 1269 – 994 Ma, although there was one grain dated at 1428 ± 36 Ma. This may be the result of heterogeneity in the unit or a product of only one sample being analysed as much as an even more restricted source and site of deposition. The Summerside formation is almost equivalent in depositional age as the Blow Me Down Brook and shares a much more similar age distribution profile to the Bradore with an almost bimodal distribution mirroring the Bradore although the relative contributions are different (Fig. 6). The Summerside Formation also has an age peak at 1439 Ma (10 grains) which would indicate the introduction of an older source. Both the Blow Me Down and Summerside formations are thought to be slope deposits.

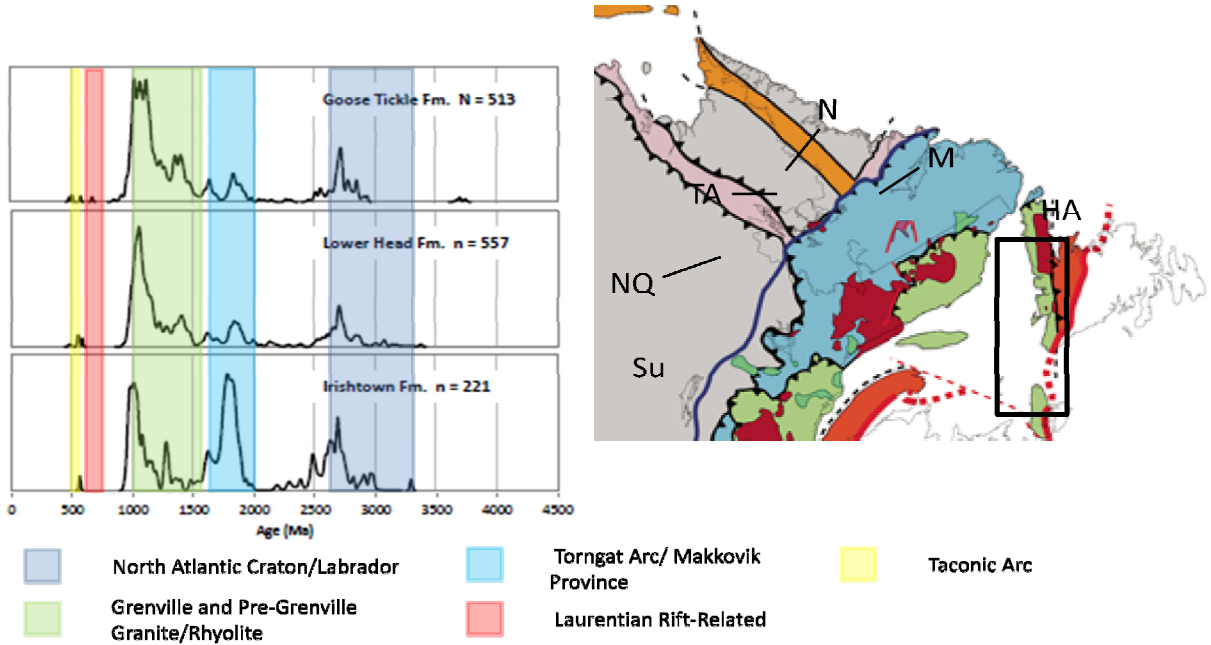


Figure 11. Relative Age Probability Plots for Irishtown, Lower Head and Goose Tickle Fms. on the left. On the right is a zoomed in image of the Labrador and North Atlantic Craton (N) region. The black rectangle represents the Humber Arm Allochthon (HA). NQ = New Quebec Orogen, M = Makkovik Province, Su = Superior Province, TA = Torngat Arc

There is a sharp contrast between the contributions of the Summerside and the Irishtown Formations. The Irishtown Formation contains the greatest contribution of Archean to early Neoproterozoic-aged detritus (Fig. 7). It can be interpreted that at the time of deposition a new and fairly proximal source region became exposed and/or began to contribute to the deposition of the unit. The region of the North Atlantic craton and adjacent tectonic terranes could serve as the proximal source for most if not all of the age spectra of the unit (Fig. 11), assuming the relative spatial relationship of source and sink remained the same. An unroofing event or exposure of this region could be related to the arc-continent collision that occurred at an earlier time. The similarity of peak ages between the Lower Head, Goose Tickle, and Irishtown Formations suggest a common

source. The degree of relative contributions older than Grenville age, decreases with formation age, while the Grenville contribution behaves inversely to this, increasing with a corresponding decrease of formation age (Fig. 7). In the model presented in figure 9, assuming that the Irishtown Formation was included in the aggrading accretionary wedge along with the other slope sequences, it could serve as a source for recycled material to the foreland basin units at that time. The consistent decrease of older age contributions would be consistent with this scenario, as well as continued Grenville-age contributions from Laurentia, if the supply from the North Atlantic craton was only temporary and probably ended during deposition of the Lower Head Formation where the older material (3070 Ma and 3011 Ma) was contributed. The suggested metamorphic origin of 5 grains analyzed from the Lower Head Formation ranging from 1835 – 1785 Ma, could be correlated to rocks associated with the Ketilidian (1900 – 1800 Ma) and Labradorian (1700 – 1650 Ma) orogenic events of the Labrador region, which may have been exposed during this time (Fig. 11). By the time the Goose Tickle Formation was deposited in the late Ordovician, the Irishtown Formation may have been the only source for older sediment. Older units (Summerside and Blow Me Down Brook) may have also contributed sediment as recycled material, increasing the Grenville age signature relative to the older signatures. This interpretation is also consistent with “westerly” derived foreland basin units (e.g Lindholm and Casey, 1989; Schwab, 1991) but with a predominance of recycled material as opposed to arc-derived sediment. It is also consistent with interpretations suggesting a predominantly Laurentian source for

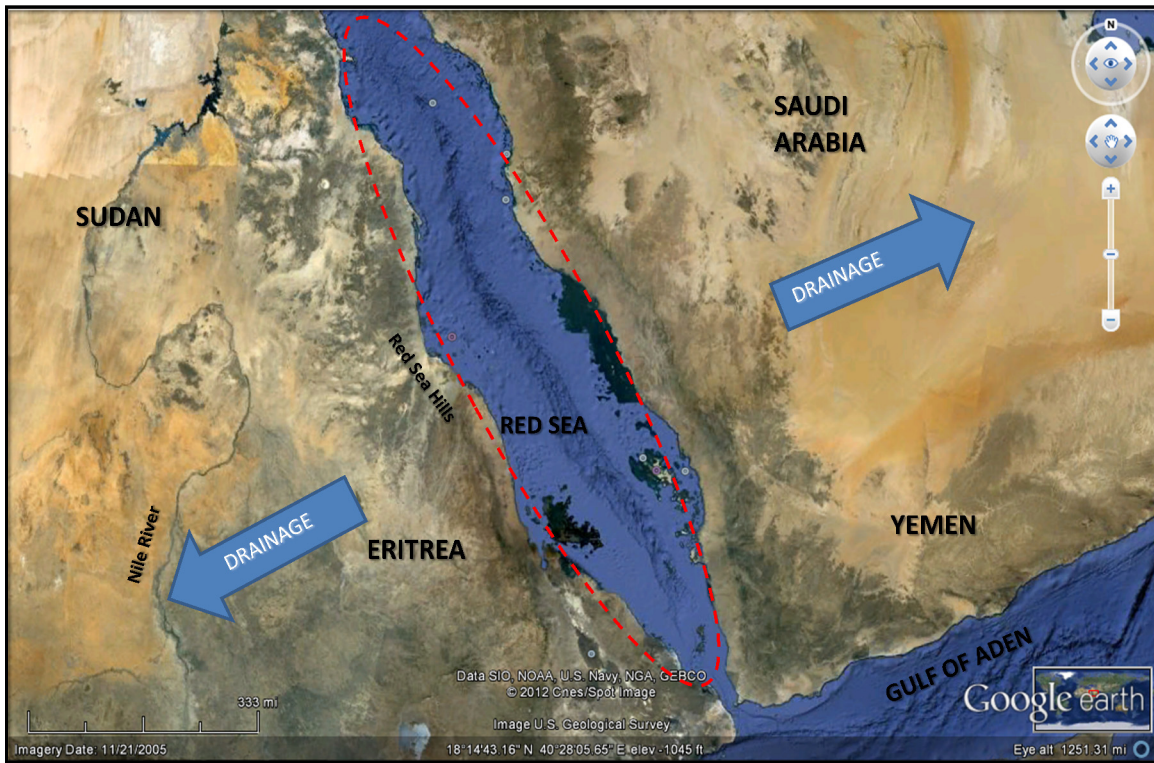


Figure 12. Google Earth image of the Red Sea rifted area. Elevated topography at the rift shoulder blocks drainage from the mainland on both sides of the Red Sea. The red outline represents the restricted depositional area.

analyzed units (e.g. Cawood and Nemchin, 2001; Clift et al., 2009). However, there are some differences with this study compared to the ID-TIMS/SHRIMP II study done by Cawood and Nemchin (2001). There are four units sampled that are common to both studies; the Goose Tickle, Summerside, Blow Me Down Brook, and Bradore Formations. Of the 4 units, only 2 shared similar relative age probability distribution profiles; the Goose Tickle and Summerside Formations. The 582 Ma age peak reported for the Bradore Formation in this study was correlated to the timing of late-stage rifting of Rodinia, was not identified by Cawood and Nemchin, 2001 however, the Grenville-age peaks of both studies are consistent for this formation. The age spectra for the Blow Me Down Brook Formation are completely different in the two studies; a very restricted,

Grenvillian age range (this study) compared to a very diverse, age peak distribution ranging from >3500 Ma – 1000 Ma. This may suggest heterogeneity in the detrital population distribution for the unit or different and/or restricted sources for the unit due to compartmentalization of depositional areas. The latter was suggested as a mechanism for the restricted age peak range of the Bradore Formation (Cawood and Nemchin, 2001), and resembles the age spectrum for the Blow Me Down Brook Formation in this study.

Results from mineralogical discrimination are presented as ternary diagrams in Fig. 13. This analysis was done using the Gazzi-Dickinson method of point counting (Lindholm, 1990). Both ternary diagrams (Qt-F-L, Qm-F-Lt) are divided into three provenance types – Continental Block, Magmatic Arc, and Recycled Orogen. The Continental Block provenance region is further divided into Craton Interior, Transitional Continental, and Basement Uplift (Fig. 13A). The Magmatic Arc provenance region is divided into Dissected Arc, Transitional Arc and Undissected Arc (Fig. 13B). There is also a Mixed Region in Figure 13B. Twenty-one (21) samples from all 6 siliciclastic units analysed in this study are represented in the ternary diagrams. The Passive Margin Mean plotted in the Continental Block region (Fig. 13A) and in the upper limit of the Transitional Continental region (Fig. 13B). This is probably due to the predominantly Grenville-aged contribution to these samples. The Active Margin Mean plotted in the Recycled Orogen region, approaching the lower limit (Fig. 13A), and in the Mixed Region (Fig. 13B). This indicates recycling of the passive margin units as they are accreted, as well as lesser components from Laurentia and the approaching island arc and has good agreement with the zircon age data. Unfortunately only 2 Goose Tickle units were analyzed compared to 11 Lower Head samples. Analysis of an equal quantity from

both samples may have reflected the similarity of contributions between the two formations seen in relative age distribution data. The results indicate a provenance type that is consistent with interpretations made for the passive and active margin units in this study, and also highlights the more restricted sources for the passive margin units compared to more diverse sources for active margin units.

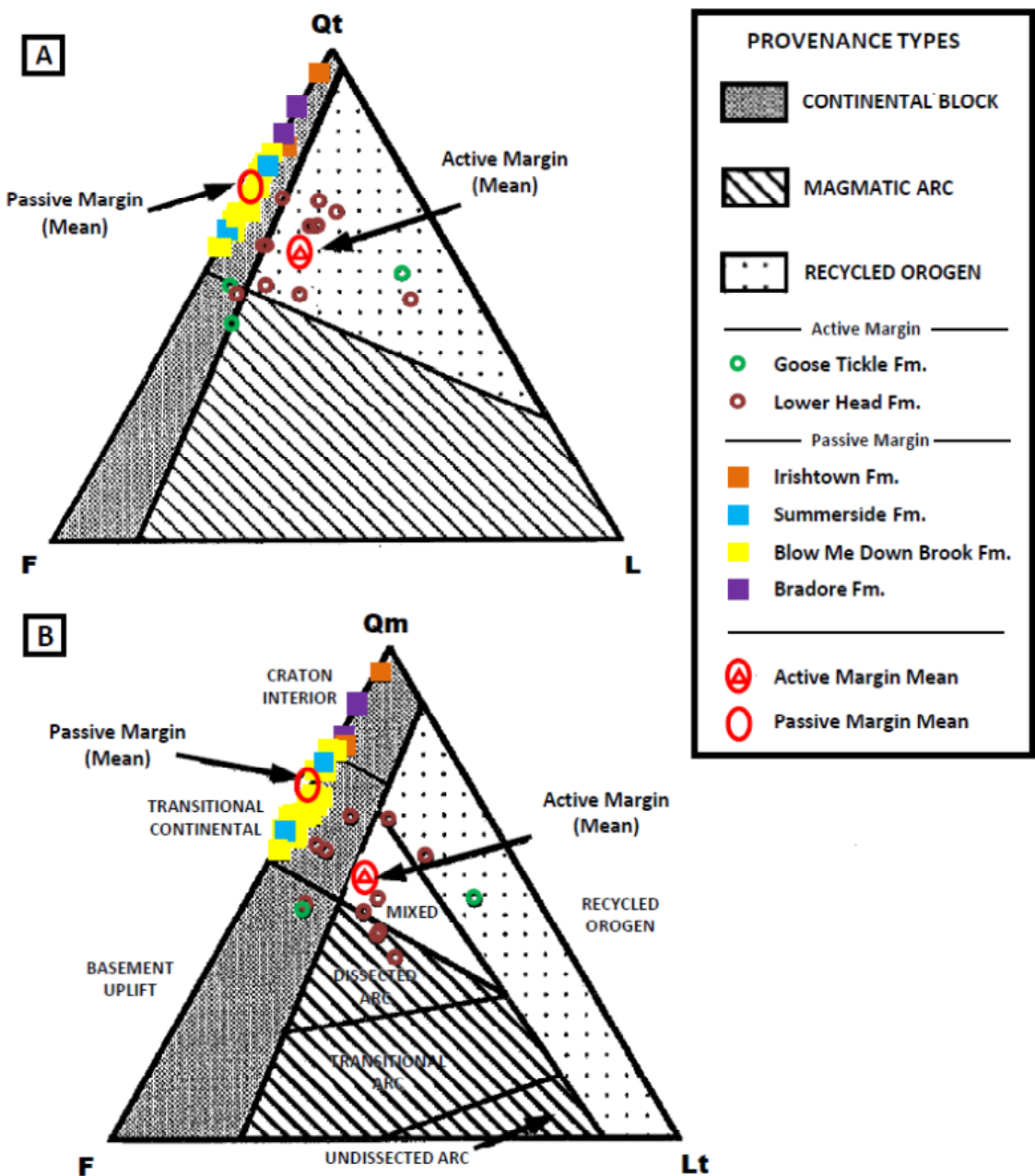


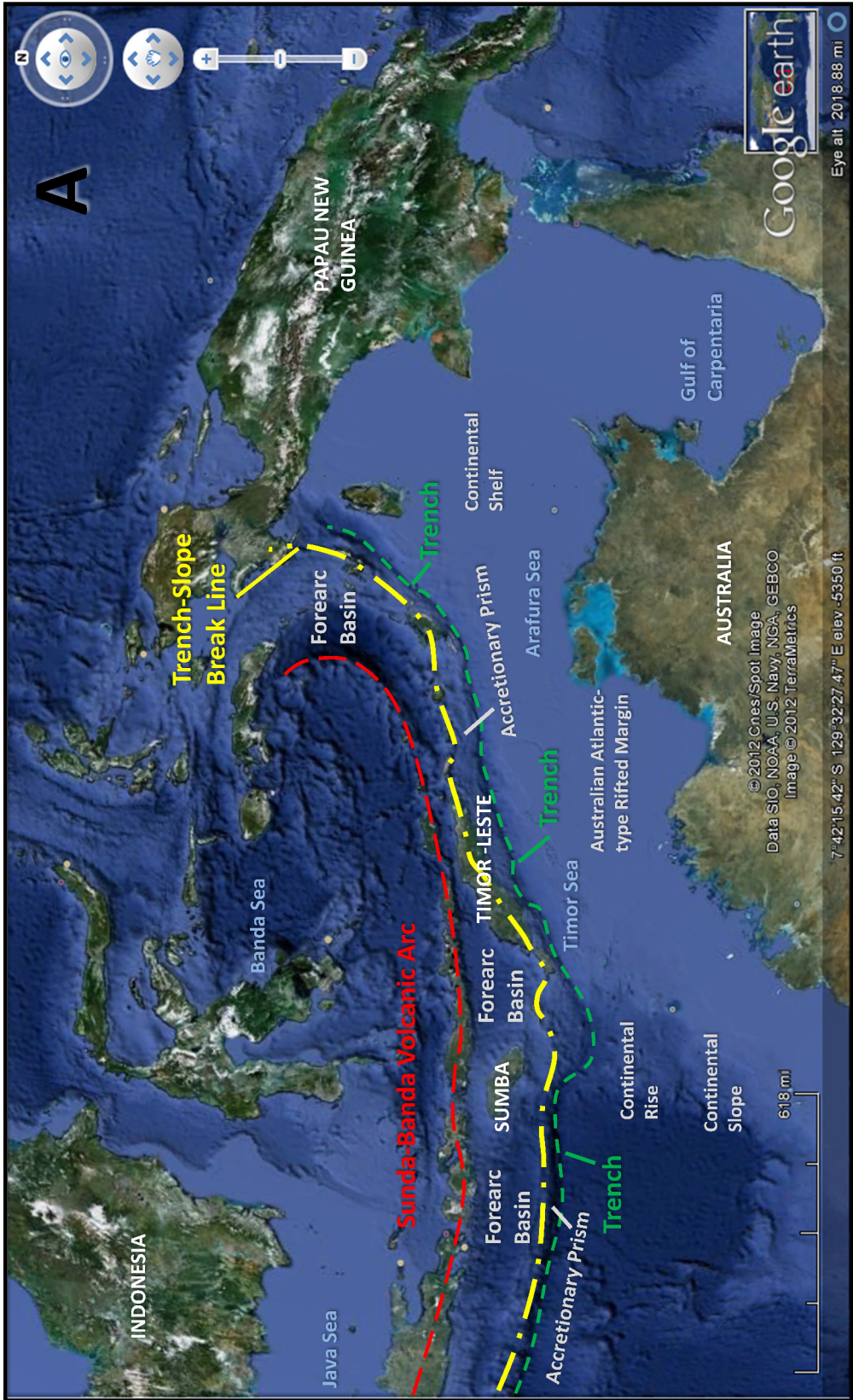
Figure 13. (A) Qt-F-L Ternary Diagram showing 3 general provenance types for the units analyzed. (B) Qm-F-Lt Ternary Diagram showing the further division of those provenance types. Qt = Total quartzose grains; Qm = Monocrystalline quartz grains; F = Total feldspar grains; L = Total unstable aphanitic lithic fragments; Lt = Total aphinitic lithic fragments (including) quartzose and carbonate varieties). Modified after Lindholm, 1990.

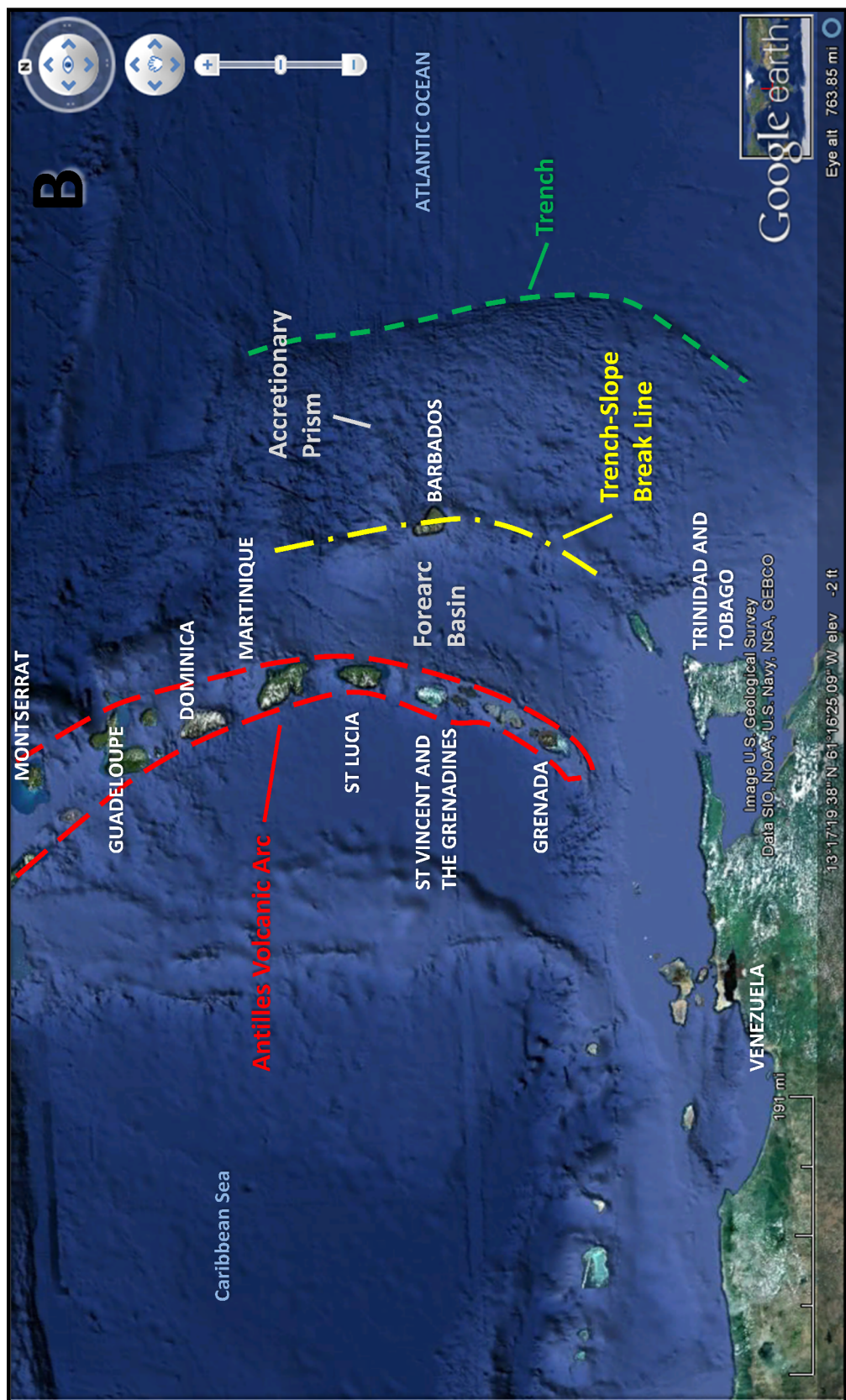
4.4 MODERN ANALOGUES

Modern arc-continent collisional settings give insight into the evolution of comparable terranes preserved in the rock record and tectonic province of source terranes involved in sediment delivery to the trench when it is tectonically underlain by the continental margin. The Sunda-Banda volcanic arc (Fig. 14A) and the Antilles Arc (Fig. 14B) systems provide good analogues to the evolution of the Taconic arc system during the early – middle Ordovician, as it was approaching Laurentia. Both modern systems show an aggrading accretionary wedge that has elevated topography and in some places, it is exposed above sea level. Examples of these include Barbados (Speed, 1983; Larue and Speed, 1984; Torrini et al., 1985), Timor-Leste (Karig et al., 1987), and south of Sumba Island (Breen et al., 1986). The enhanced topography produced at the trench-slope break line forms a significant barrier to sediment shed off the approaching arc. Sediment is subsequently trapped in the forearc basin (Torrini et al., 1985), much like Timor-Leste and Barbados today. This can be an analogous mechanism for preventing the transport of arc-aged detrital zircons to the foreland basin in Newfoundland in the Ordovician. The arrival of the trench to the margin and sudden accretion of thick continental slope and rise sedimentary sequences would allow for significant growth of the accretionary prism and presumable uplift of the trench-slope break analogous to, for example, the Barbados Ridge (Fig. 14B). The initial development of the accretionary wedge in the late Cambrian – early Ordovician and its enhancement as it engulfed the continental margin sequences, would have mitigated direct transport of arc sediments to the trench considerably and this transportation path would eventually be completely blocked with increased accretion of sediments and elevation of the accretionary prism

(Fig. 10). More importantly, the accretion of continental margin sediments and their tectonic rotation, uplift, and exposure during transport within the accretionary prism, would result in recycled Laurentian sources that would be preferentially delivered to the trench and flysch basins in the foreland region of the Taconic orogeny.

Figure 14. Google Earth images of the Sunda-Banda Volcanic Arc, South East Asia (A) and the Antilles Arc, the Caribbean (B). The yellow dashed and dotted line represents the Trench-Slope Break Line. The red dashed line represents the volcanic arc and the green dashed line the trench. Note the sediment trap formed by the Trench-Slope Break.





CHAPTER 5

5. CONCLUSION

U-Pb geochronology of detrital zircons from the Cambro-Ordovician siliciclastic units of the Humber Arm Allochthon provide further discrimination of an already well studied area, allowing enhancement to current source and depositional interpretations of the units as well as re-interpretation of the tectonic evolution of the Laurentian passive margin during the arc-continent collision that culminated in the late Ordovician in the Taconic orogeny.

The age data derived from this analysis agree with existing interpretations of predominantly Laurentian sources for the passive margin units with relative age contributions ranging from the Archean (3070 Ma) to the Paleozoic (551 Ma). Rift-related peak ages of 591 Ma, 582 Ma, 573 Ma, and 551 Ma provide more constraint to the duration of the second pulse of rifting in the Neoproterozoic. Unfortunately, the method used in this study did not provide sufficient resolution to the age, timing of collision, and basement of the arc that collided with the Laurentian passive margin, as only two grains yielded ages consistent with an arc age (482 Ma and 480 Ma). A biased analysis of only young zircons was done which yielded a peak age of 466 Ma (3 grains) and ages from 464 – 510 Ma which represent arc- and ophiolite-related detritus. These results better constrain the components of the arc system and agree with previously published data. The suggestion by other authors that the relative age contributions to the passive margin sediment has been re-interpreted to show that a more local source, the North Atlantic craton and adjacent terranes, could be the potential source for the analyzed

units. This is still consistent with a predominantly Laurentian derivation. The aggradation of the accretionary wedge in front of the approaching Taconic Arc probably acted as a sediment barrier to the arc derived sediment, thereby greatly lessening the contribution of detrital zircons to the foreland basin. The settings of the Sunda-Banda volcanic arc and Antilles Arc systems provide good examples for the mechanism to block arc derived sediment transport to the foreland basin of the Laurentian passive margin during the early to middle Ordovician. This resulted in preferential delivery of recycled accretionary prism sediments to the trench and flysch basins in the foreland region of the Taconic orogeny and a very minor or very diluted arc derived component.

REFERENCES CITED

- Andersen, C.B., and Samson, S.D., 1995; Temporal changes in Nd isotopic composition of sedimentary rocks in the Sevier and Taconic foreland basins: Increasing influence of Juvenile sources. *Geology*, v. 23, p. 983-986
- Anderson, E.D., and Moehler, D.P., 2009; Formation of high-pressure metabasites in the southern Appalachian Blue Ridge via Taconic continental subduction beneath the Laurentian margin. *Tectonics*, v. 28, TC5012
- Bradley, D.C., 1989; Taconic plate kinematics as revealed by foredeep stratigraphy, Appalachian Orogen. *Tectonics* v. 8, p. 1037-1049
- Bradley, D.C., and Kusky, T.M., 1986; Geologic evidence for rate of plate convergence during the Taconic Arc-continent collision. *The Journal of Geology*, v. 94, p. 667-681
- Breen, N.A., Silver, E.A., and Hussong, D.M., 1986. Structural styles of an accretionary wedge south of the island of Sumba, Indonesia, revealed by SeaMARC II side scan sonar. *Geological Society of America Bulletin*, v. 10, p. 1250-1261
- Casey, J.F., and Dewey, J.F., 1984; Initiation of subduction zones along transform and accreting plate boundaries, triple junction evolution and spreading centres - implications for ophiolitic geology and obduction. in: *Ophiolites and Oceanic Lithosphere*, ed. I.G. Gass, S.J. Lippard and A.W. Shelton, Geol. Soc. London Spec. Publ. pp.413, p.269-290

Casey, J.F., Elthon, D.L., Siroky, F.X., Karson, J.A., and Suliivan, J., 1985; Geochemical and geological evidence bearing on the origin of the Bay of Islands and Coastal Complex ophiolites of Western Newfoundland. *Tectonophysics*, v. 116, p. 1-40

Cawood, P. A., McCausland, P. J. A., and Dunning, G. R., 2001,; Opening Iapetus: Constraints from the Laurentian margin in Newfoundland. *GSA Bulletin*, v. 113, p. 443-453

Cawood, P.A., and Nemchin, A. A., 2001; Paleogeographic development of the east Laurentian margin: Constraints form U-Pb dating on detrital zircons in the Newfoundland Appalachians. *Geological Society of America Bulletin*, v. 113, p. 1234-1246

Clift, P.D., Carter, A., Draut, A.E., Long, H.V., Chew, D.M., and Shouten, H.A., 2009; Detrital U-Pb zircon dating of lower Ordovician syn-arc-continent collision conglomerates in the Irish Caledonides. *Tectonophysics*, v. 479, p. 165-174

Dalla Salda, L.H., Dalziel, I.W.D., Cingolani, C.A., and Varela, R., 1992; Did the Taconic Appalachians continue into southern South America. *Geology*, v. 20, p. 1059-1062

Davidson, A., 1998; An overview of Grenville Province geology, Canadian Shield; Chapter 3, in: *Geology of the Precambrian Superior and Grenville Provinces and Precambrian Fossils in North America*, (co-ord.) S.B. Lucas and M.R. St-Onge; Geological Survey of Canada, *Geology of Canada*, no. 7, p. 205-270

Dewey, J.F., 1976; Ophiolite obduction. *Tectonophysics*, v. 31, p. 93-120

Dewey, J.F., and Burke, K., 1974; Hot spots and continental break-up: Implications for collisional orogeny. *Geology*, v. 2, p. 57-60

Dewey, J.F., and Casey, J.F., 2011; The origin of obducted large-slab ophiolite complexes, arc-continent collision, *Frontiers in Earth Sciences*, p. 431-444. DOI 10.1007/978-3-540-88558-0_15

Dickinson, W.R., 2008; Impact of differential zircon fertility of granitoid basement rocks in North America on age populations of detrital zircons and implications for granite petrogenesis. *Earth and Planetary Science Letters*, v. 275, p. 80-92

Dickinson, W.R., and Gehrels, G.E., 2003; U-Pb ages of detrital zircons from Permian and Jurassic eolianite sandstones of the Colorado Plateau, USA: Paleogeographic implications: *Sedimentary Geology*, v. 163, p. 29-66.

Ettensohn, F.R., and Brett, C.E., 2002; Stratigraphic evidence from the Appalachian Basin for continuation of the Taconian orogeny into early Silurian time. *Physics and Chemistry of the Earth*, v. 27, p. 279-288

Garver, J.I., Royce, P.R., and Smick, T.A., 1996; Chromium and nickel in shale of the Taconic foreland: A case study for the provenance of fine-grained sediments with an ultramafic source. *Journal of Sedimentary Research*, v. 66, p. 100-106

Gehrels, G.E., 2007; AgePick, <https://sites.google.com/a/laserchrn.org/laserchron/home>

Gehrels, G. E., Valencia, V. A., and Ruiz, J., 2008, Enhanced precision, accuracy, efficiency, and spatial resolution of U-Pb ages by laser ablation – multicollector –

inductively coupled plasma – mass spectrometry. *Geochemistry, Geophysics, Geosystems*, v. 9, p. 1-13

Gehrels, G., 2010; Detrital zircon U-Pb geochronology: Current methods and new opportunities, in: *Recent Advances in Tectonics of Sedimentary Basins*, C. Busby and A. Azor, editors, Blackwell Publishing.

Hellstrom, J., et al., 2008; Iolite: software for spatially resolved LA-(quad and MC) ICPMS analysis, in *Laser Ablation ICPMS in Earth Sciences: Current Practices and Outstanding Issues*, edited by P. Sylvester. Mineralogical Association of Canada, Vancouver, B.C., Canada, p. 343-348

Karabinos, P., Samson, S.D., Hepburn, J.C., and Stoll, H.M., 1998; Taconian orogeny in the New England Appalachians: Collision between Laurentia and the Shelburne Falls arc. *Geology*, v. 26, p. 215-218

Karig, D.E., Barber, A.J., Charlton, T.R., Klemperer, S., and Hussong, D.M., 1987; Nature and distribution of deformation across the Banda Arc-Australian collision zone at Timor. *Geological Society of America Bulletin*, v. 1, p. 18-32

Krogh, T.E., and Kamo, S.L., 2006; Precise U-Pb zircon ID-TIMS ages provide an alternative interpretation to early ion microprobe ages and new insights into Archean crustal process, northern Labrador. *Geological Society of America Special Papers*, v. 405, p. 91-103

Larue, D.K., and Speed, R.C., 1984; Structure of the accretionary complex of Barbados, II: Bissex Hill. *Geological Society of America Bulletin*, v. 11, p. 1360-1372

Lindholm, R.M., and Casey, J.F., 1989, Regional significance of the Blow Me Down Brook Formation, western Newfoundland: New fossil evidence for an Early Cambrian age: Geological Society of America Bulletin, v. 101, p. 1-13

Lindholm, R.M., 1990; Regional Correlation, Age, Provenance, and Tectonic Significance of Sandstone-Mudstone Sequences in the Humber Arm Allochthon, Western Newfoundland, Canada. PhD Dissertation, University of Houston.

Lucas, S.B., St-Onge, M.R., and Percival, J.A., 1998; Introduction; Chapter 1 in: Geology of the Precambrian Superior and Grenville Provinces and Precambrian Fossils in North America, (co-ord.) S.B. Lucas and M.R. St-Onge; Geological Survey of Canada, Geology of Canada, no. 7, p. 1-12

Mattinson, J.M., 1975; Early Paleozoic ophiolite complexes of Newfoundland: isotopic ages of zircons. Geology, v. 3, p. 181-183

Mattinson, J.M., 1976; Ages of zircons from the Bay of Islands Ophiolite Complex, western Newfoundland. Geology, v. 4, p. 393-394

McLlland, J., Daly, J.S., and McLlland, J.M., 1996; The Grenville orogenic cycle (ca. 1350 – 1000 Ma): an Adirondack perspective. Tectonophysics, v. 265, p. 1-28

Moecher, D.P., Samson, S.D., and Miller, C.F., 2004; Precise time and conditions of peak Taconian granulite facies metamorphism in the Southern Appalachian Orogen, U.S.A., with Implications for zircon behavior during crustal melting events. Journal of Geology, v. 112, p. 289-304

Moecher, D.P., and Samson, S.D., 2006; Differential zircon fertility of source terranes and natural bias in the detrital zircon record: Implications for sedimentary provenance analysis. *Earth and Planetary Science Letters*, v. 247, p. 252-266

Murphy, J.B., and Nance, R.D., 2008; The Pangea conundrum. *Geology*, v. 36, p. 703-706

Nelson, K. D., and Casey, J. F., 1979, Ophiolitic detritus in the Upper Ordovician flysch of Notre Dame Bay and its bearing on the tectonic evolution of western Newfoundland: v. 7, p. 27-31

Neuman, R.B., 1984: Geology and paleobiology of the islands in the Ordovician Iapetus ocean: Review and implications. *Geological Society of America Bulletin*, v. 95, p. 1188 – 1201

Niocaill, C.M., Van der Pluijm, B.A., and Van der Voo, R., 1997; Ordovician paleogeography and the evolution of the Iapetus ocean. *Geology*, v. 25, p. 159-162

Palmer, S.E., Burden, E., and Waldron, J.W.F., 2001, Stratigraphy of the Curling Group (Cambrian) Humber Arm Allochthon, Bay of Islands: Current Research, Newfoundland Department of Mines and Energy Geological Survey, Report 2001-1, p. 105-112

Pearce, N.J.G., Perkins, T.W., Westgate, J.A., Gorton, M.P., Jackson, S.E., Neal, C.R., and Chinery, S.P., 1997; A compilation of new and published major and trace element data for NIST SRM 610 and NIST SRM 612 glass reference materials.

Geostandards Newsletter, Journal of Geostandards and Geoanalysis, v. 21, p. 115-144

Pinet, N., and Tremblay, A., 1995; Is the Taconian orogeny of southern Quebec the result of an Oman-type obduction? *Geology*, v. 23, p. 121-124

Ratcliffe, N.M., Hames, W.E., and Stanley, R.S., 1998; Interpretation of ages of arc magmatism, metamorphism, and collisional tectonics in the Taconian orogen of western New England. *American Journal of Science*, v. 298, p. 791-797

Schwab, F. L., 1991; Detrital modes of late Precambrian – early Paleozoic sandstones across Newfoundland: Do they constrain Appalachian tectonic models?: *Geological Society of America Bulletin*, v. 103, p. 1317-1323

Shaulis, B., Lapen, T.J., and Toms, A., 2010; Signal linearity of an extended range pulse counting detector. Applications to accurate and precise U-Pb dating of zircon by laser ablation quadrupole ICP-MS. *Geochemistry, Geophysics, Geosystems*, v. 11, Q0AA11, doi:10.1029/2010GC003198.

Sláma, J., Dunkley, D.L., Kachlik, V., and Kusiak, M.A., 2008; Transition from island-arc to passive setting on the continental margin of Gondwana: U–Pb zircon dating of Neoproterozoic metaconglomerates from the SE margin of the Teplá–Barrandian Unit, Bohemian Massif. *Tectonophysics*, v. 461, p. 44-59

Speed, R.C., 1983; Structure of the accretionary complex of Barbados, I: Chalky Mount. *Geological Society of America Bulletin*, v. 1, p. 92-116

Steiger, R. H., and Jäger, E., 1977; Subcommission on Geochronology: Convention on the use of decay constants in geo- and cosmochronology. Earth and Planetary Science Letters, v. 36, p. 359-362

Stevens, R.K., 1970; Cambro-Ordovician flysch sedimentation and tectonics in west Newfoundland and their possible bearing on a proto-Atlantic Ocean, *in* Lajoie, J., ed., Flysch Sedimentology of North America: Geological Association of Canada Special Paper 7, p. 165-177

Torrini, Jr., R., Speed, R.C., and Mattioli, G.S., 1985; Tectonic relationships between forearc-basin strata and the accretionary complex at Bath, Barbados. Geological Society of America Bulletin, v. 7, p. 861-874

Van Achterberg, E., Ryan, C.G., and Griffin, W.L., 1999, Glitter: on line intesity reduction for the laser ablation inductively coupled mass spectrometry: 9th Goldschmidt Conference, p. 305.

van der Pluijm, B.A., 1987; Timing and spatial distribution of deformation in the Newfoundland Appalachians: a “multi-stage collision” history. Tectonophysics, v. 135, p. 15-24

Vermeesch, P., 2004; How many grains are needed for a provenance study?: Earth and Planetary Science Letters, v. 224, p. 441-451

Waldron, J.W.F., and van Staal, C.R., 2001; Taconian orogeny and the accretion of the Dashwoods block: A peri-Laurentian microcontinent in the Iapetus Ocean. Geology, v. 29, p. 811-814

Whitehead, J., Reynolds, P.H., and Spray, J.G., 1996; $^{40}\text{Ar}/^{39}\text{Ar}$ age constraints on Taconian and Acadian events in the Quebec Appalachians. *Geology*, v. 24, p. 359-362

Whitmeyer, S.J., and Karlstrom, K.E., 2007; Tectonic model for the Proterozoic growth of North America. *Geosphere*, v. 3, p. 220-259

Wise, D.U., and Ganis, G.R., 2008; Taconic Orogeny in Pennsylvania: A ~15-20 m.y. Apennine-style Ordovician event viewed from its Martic hinterland. *Journal of Structural Geology*, v. 31, p. 887-899

APPENDIX 1 – Zircon Data Tables

Table 1 – Goose Tickle Formation

Spot	[U]	[Th]	U/Th	Conc. (ppm)			Ratios			Ages			%			
				$^{206}\text{Pb}/^{238}\text{U}$	$\pm 2\sigma$	$^{207}\text{Pb}/^{235}\text{U}$	$\pm 2\sigma$	$^{207}\text{Pb}/^{206}\text{Pb}$	$\pm 2\sigma$	$^{206}\text{Pb}/^{238}\text{U}$	$\pm 2\sigma$	$^{207}\text{Pb}/^{235}\text{U}$	$\pm 2\sigma$	Disc		
<i>NML-1IB-86 (25 μm)</i>																
1	60	22	2.77	0.53347	0.01533	14.24086	0.42210	0.19361	0.00461	2756.1	64.4	2765.9	28.1	2773.1	39.0	0.6
2	52	45	1.17	0.17901	0.00414	1.87113	0.05656	0.07581	0.00220	1061.6	22.6	1070.9	20.0	1090.1	58.3	2.7
3	223	90	2.48	0.17121	0.00370	1.77733	0.04313	0.07529	0.00148	1018.8	20.4	1037.2	15.8	1076.2	39.4	5.6
4	86	78	1.10	0.25596	0.00673	3.16079	0.08394	0.08956	0.00192	1469.2	34.5	1447.6	20.5	1416.2	41.0	-3.6
5	49	24	2.08	0.17769	0.00492	1.82887	0.05867	0.07465	0.00171	1054.4	26.9	1055.9	21.1	1059.0	46.0	0.4
6	201	78	2.59	0.19444	0.00460	2.13186	0.05888	0.07952	0.00130	1145.4	24.8	1159.2	19.1	1185.1	32.3	3.5
7	134	80	1.68	0.16885	0.00457	1.70298	0.05428	0.07315	0.00147	1005.8	25.2	1009.7	20.4	1018.1	40.6	1.2
8	67	48	1.38	0.54940	0.01403	15.35755	0.47860	0.20273	0.00294	2822.7	58.4	2837.7	29.7	2848.3	23.6	0.9
9	477	205	2.33	0.50257	0.01294	12.15888	0.39226	0.17547	0.00274	2624.8	55.5	2616.7	30.3	2610.5	26.0	-0.5
10	22	24	0.92	0.17947	0.00518	1.91431	0.06789	0.07736	0.00228	1064.1	28.3	1086.1	23.7	1130.5	58.7	6.2
11	147	86	1.71	0.77155	0.01804	38.16103	1.05528	0.35872	0.00585	3686.4	65.6	3724.1	27.4	3744.4	24.8	1.6
12	107	93	1.15	0.17149	0.00477	1.80149	0.05886	0.07619	0.00176	1020.3	26.2	1046.0	21.3	1100.0	46.3	7.8
13	53	33	1.62	0.24497	0.00640	2.93495	0.07921	0.08689	0.00183	1412.5	33.2	1391.0	20.4	1358.2	40.6	-3.8
14	23	0	-8604	0.16874	0.00537	1.64638	0.06859	0.07076	0.00245	1005.2	29.6	988.2	26.3	950.5	70.8	-5.4
15	104	125	0.83	0.23319	0.00800	2.72509	0.09045	0.08475	0.00147	1351.2	41.8	1335.3	24.7	1309.9	33.8	-3.1
16	111	113	0.98	0.14118	0.00519	1.38198	0.05561	0.07100	0.00193	851.3	29.3	881.3	23.7	957.3	55.5	12.4
17	80	29	2.75	0.20192	0.00599	2.18863	0.06210	0.07861	0.00175	1185.6	32.1	1177.4	19.8	1162.4	44.2	-2.0
18	22	12	1.78	0.16917	0.00594	1.72658	0.05966	0.07402	0.00248	1007.5	32.7	1018.5	22.2	1042.1	67.6	3.4
19	54	71	0.76	0.16975	0.00545	1.72406	0.05526	0.07366	0.00178	1010.7	30.0	1017.5	20.6	1032.2	48.9	2.1
20	159	92	1.73	0.17863	0.00489	1.87195	0.04968	0.07601	0.00142	1059.5	26.7	1071.2	17.6	1095.2	37.3	3.4
21	33	38	0.87	0.17399	0.00483	1.86306	0.05873	0.07766	0.00190	1034.0	26.5	1068.1	20.8	1138.2	48.6	10.1
22	252	231	1.09	0.16978	0.00508	1.77288	0.05206	0.07573	0.00128	1010.9	28.0	1035.6	19.1	1088.0	33.8	7.6
23	70	45	1.55	0.24153	0.00580	3.02161	0.07506	0.09073	0.00158	1394.6	30.1	1413.1	19.0	1441.0	33.2	3.3
24	133	65	2.03	0.54380	0.01315	14.88377	0.36005	0.19851	0.00301	2799.3	54.9	2807.8	23.0	2814.0	24.8	0.5
25	126	25	5.09	0.17212	0.00415	1.77212	0.04654	0.07467	0.00135	1023.8	22.8	1035.3	17.0	1059.7	36.4	3.5

Spot	Conc. (ppm)	Ratios						Ages				% Disc				
		[U]	[Th]	$^{206}\text{Pb}/^{238}\text{U}$	$^{207}\text{Pb}/^{235}\text{U}$	$\pm 2\sigma$	$^{207}\text{Pb}/^{206}\text{Pb}$	$\pm 2\sigma$	$^{206}\text{Pb}/^{238}\text{U}$	$\pm 2\sigma$	$^{207}\text{Pb}/^{235}\text{U} \pm 2\sigma$	$^{207}\text{Pb}/^{206}\text{Pb} \pm 2\sigma$				
26	541	408	1.33	0.39200	0.01238	7.91294	0.28563	0.14640	0.00269	2132.1	57.4	2221.2	32.6	2304.3	31.5	8.1
27	32	28	1.17	0.13766	0.00330	1.54489	0.06117	0.08139	0.00315	831.4	18.7	948.5	24.4	1231.0	76.1	48.1
28	140	77	1.81	0.38345	0.00845	7.06184	0.15132	0.13357	0.00256	2092.4	39.4	2119.2	19.1	2145.4	33.5	2.5
29	35	82	0.43	0.15771	0.00428	1.59460	0.06280	0.07333	0.00263	944.0	23.8	968.1	24.6	1023.1	72.5	8.4
30	148	100	1.49	0.28213	0.00572	3.94233	0.08770	0.10135	0.00175	1602.1	28.8	1622.4	18.0	1648.9	32.0	2.9
31	893	18	48.38	0.17260	0.00433	1.79051	0.04594	0.07524	0.00125	1026.4	23.8	1042.0	16.7	1074.8	33.3	4.7
32	28	26	1.10	0.20798	0.00521	2.49679	0.08165	0.08707	0.00257	1218.1	27.8	1271.1	23.7	1362.0	56.9	11.8
33	94	59	1.60	0.28665	0.00587	3.96409	0.09526	0.10030	0.00192	1624.7	29.4	1626.9	19.5	1629.6	35.5	0.3
34	73	71	1.03	0.21237	0.00524	2.54534	0.07906	0.08693	0.00189	1241.4	27.9	1285.1	22.6	1358.9	41.9	9.5
35	116	55	2.11	0.17864	0.00377	1.84267	0.04131	0.07481	0.00139	1059.5	20.6	1060.8	14.8	1063.4	37.3	0.4
36	36	19	1.93	0.18739	0.00477	1.99241	0.04817	0.07711	0.00257	1107.2	25.9	1112.9	16.3	1124.1	66.4	1.5
37	127	75	1.69	0.34771	0.00898	5.49878	0.12403	0.11470	0.00180	1923.7	43.0	1900.4	19.4	1875.1	28.3	-2.5
38	319	17	18.62	0.20078	0.00489	2.18693	0.04759	0.07900	0.00117	1179.5	26.3	1176.9	15.2	1172.1	29.3	-0.6
39	134	110	1.22	0.23092	0.00635	2.59612	0.06473	0.08154	0.00146	1339.3	33.2	1299.5	18.3	1234.5	35.2	-7.8
40	225	60	3.75	0.17627	0.00464	1.78990	0.04271	0.07364	0.00126	1046.6	25.4	1041.8	15.5	1031.8	34.5	-1.4
41	37	20	1.80	0.27942	0.00738	3.90393	0.09669	0.10133	0.00210	1588.4	37.2	1614.5	20.0	1648.6	38.4	3.8
42	212	96	2.20	0.53929	0.01264	15.17664	0.32869	0.20410	0.00338	2780.5	53.0	2826.4	20.6	2859.3	26.9	2.8
43	182	79	2.30	0.30392	0.00617	4.62056	0.07279	0.11026	0.00200	1710.7	30.5	1753.0	13.2	1803.8	32.9	5.4
44	36	33	1.09	0.17608	0.00450	1.85626	0.05070	0.07646	0.00189	1045.5	24.6	1065.7	18.0	1107.1	49.5	5.9
45	153	60	2.56	0.17910	0.00379	1.85402	0.04026	0.07508	0.00131	1062.0	20.7	1064.9	14.3	1070.7	35.1	0.8
46	28	16	1.71	0.49305	0.01091	12.68843	0.26535	0.18664	0.00280	2583.9	47.1	2656.8	19.7	2712.8	24.7	5.0
47	82	96	0.85	0.46457	0.01093	10.54753	0.20637	0.16466	0.00253	2459.7	48.1	2484.1	18.1	2504.1	25.8	1.8
48	105	74	1.43	0.23197	0.00529	2.77507	0.06152	0.08677	0.00143	1344.8	27.7	1348.9	16.5	1355.3	31.8	0.8
49	68	42	1.61	0.17033	0.00370	1.77189	0.04102	0.07545	0.00149	1013.9	20.4	1035.2	15.0	1080.5	39.7	6.6
50	380	111	3.41	0.25791	0.00649	3.36636	0.08611	0.09467	0.00150	1479.1	33.3	1496.6	20.0	1521.4	29.9	2.9
51	49	41	1.20	0.17401	0.00381	1.80977	0.04762	0.07543	0.00186	1034.1	20.9	1049.0	17.2	1080.0	49.6	4.4
52	180	100	1.81	0.23769	0.00859	3.00722	0.12165	0.09176	0.00146	1374.7	44.7	1409.5	30.8	1462.4	30.2	6.4
53	474	176	2.69	0.17715	0.00377	1.79893	0.03845	0.07365	0.00130	1051.4	20.7	1045.1	13.9	1031.8	35.7	-1.9
54	28	13	2.08	0.20243	0.00548	2.11607	0.08780	0.07581	0.00278	1188.4	29.4	1154.1	28.6	1090.2	73.6	-8.3
55	167	137	1.22	0.18256	0.00381	1.87199	0.04387	0.07437	0.00180	1081.0	20.8	1071.2	15.5	1051.5	48.8	-2.7
56	88	43	2.06	0.45598	0.00891	10.35487	0.20824	0.16470	0.00293	2421.8	39.4	2467.0	18.6	2504.5	29.9	3.4

Spot	Conc. (ppm)	[Th]	U/Th	Ratios				Age			
				$^{206}\text{Pb}/^{238}\text{U}$	$^{207}\text{Pb}/^{235}\text{U}$	$\pm 2\sigma$	$^{207}\text{Pb}/^{206}\text{Pb}$	$\pm 2\sigma$	$^{206}\text{Pb}/^{238}\text{U} \pm 2\sigma$	$^{207}\text{Pb}/^{235}\text{U} \pm 2\sigma$	$^{207}\text{Pb}/^{206}\text{Pb} \pm 2\sigma$
57	85	93	0.92	0.51662	0.01192	13.14297	0.34486	0.18451	0.00349	2684.8	50.7
58	38	37	1.03	0.17396	0.00411	1.88833	0.05334	0.07873	0.00236	1033.9	22.6
59	35	19	1.86	0.16635	0.00428	1.73475	0.05469	0.07563	0.00243	992.0	23.6
61	81	35	2.28	0.17065	0.00388	1.76840	0.04781	0.07516	0.00165	1015.7	21.3
62	83	31	2.73	0.19471	0.00433	2.09597	0.05075	0.07807	0.00164	1146.9	23.4
63	23	26	0.87	0.16972	0.00464	1.68747	0.05659	0.07211	0.00276	1010.5	25.6
64	70	80	0.87	0.16968	0.00379	1.76941	0.04491	0.07563	0.00158	1010.3	20.9
65	235	198	1.19	0.23352	0.00534	2.77777	0.06256	0.08627	0.00164	1352.9	27.9
66	278	124	2.23	0.32377	0.00815	5.22338	0.14765	0.11701	0.00254	1808.1	39.7
67	241	94	2.57	0.17050	0.00413	1.69344	0.03725	0.07204	0.00138	1014.9	22.7
68	77	29	2.64	0.19009	0.00563	1.98067	0.05355	0.07557	0.00163	1121.9	30.5
69	60	34	1.76	0.18653	0.00413	2.06961	0.05268	0.08047	0.00199	1102.6	22.4
70	56	82	0.68	0.52687	0.01190	13.57670	0.28053	0.18689	0.00345	2728.2	50.3
71	171	166	1.03	0.21467	0.00516	2.46747	0.05700	0.08336	0.00163	1253.7	27.4
72	104	83	1.25	0.18894	0.00518	1.96786	0.07794	0.07554	0.00191	1115.6	28.1
73	80	76	1.05	0.49531	0.01005	11.55014	0.23465	0.16912	0.00262	2593.6	43.3
74	145	44	3.33	0.16212	0.00454	1.63295	0.03709	0.07305	0.00163	968.5	25.2
75	95	73	1.29	0.20901	0.00444	2.35930	0.04787	0.08187	0.00163	1223.5	23.7
76	208	81	2.56	0.20609	0.00546	2.44600	0.06315	0.08608	0.00154	1207.9	29.2
77	80	69	1.15	0.24165	0.00575	3.02387	0.05865	0.09076	0.00147	1395.2	29.8
78	46	31	1.48	0.53440	0.01375	13.41951	0.27127	0.18212	0.00321	2760.0	57.7
79	79	77	1.59	0.17380	0.00435	1.78702	0.04238	0.07457	0.00123	1033.0	23.9
80	131	146	0.90	0.17804	0.00408	1.84104	0.03622	0.07500	0.00120	1056.2	22.3
81	37	52	0.72	0.26823	0.00839	3.83829	0.12212	0.10379	0.00274	1531.8	42.6
82	186	80	2.33	0.24716	0.00653	3.13788	0.06764	0.09208	0.00152	1423.8	33.7
83	191	60	3.21	0.25982	0.00671	3.15673	0.08142	0.08812	0.00166	1488.9	34.4
84	92	57	1.63	0.18818	0.00523	2.05223	0.05482	0.07909	0.00171	1111.5	28.3
85	38	23	1.66	0.39896	0.01002	6.54132	0.14959	0.11892	0.00265	2164.2	46.2
86	32	31	1.02	0.18018	0.00529	1.97711	0.07301	0.07958	0.00263	1068.0	28.9
87	202	65	3.09	0.23364	0.00584	2.77933	0.05833	0.08628	0.00161	1353.6	30.5
88	284	117	2.43	0.17984	0.00468	1.85142	0.04927	0.07467	0.00157	1066.1	25.6

Conc. (ppm)	Ratios										Ages				
	[Th]	U/Th	$^{206}\text{Pb}/^{238}\text{U}$	$\pm 2\sigma$	$^{207}\text{Pb}/^{235}\text{U}$	$\pm 2\sigma$	$^{206}\text{Pb}/^{206}\text{Pb}$	$\pm 2\sigma$	$^{206}\text{Pb}/^{238}\text{U} \pm 2\sigma$	$^{207}\text{Pb}/^{235}\text{U} \pm 2\sigma$	$^{207}\text{Pb}/^{206}\text{Pb} \pm 2\sigma$	% Disc			
89	134	61	2.20	0.19959	0.00560	2.17859	0.05156	0.07917	0.00142	1173.1	30.1	1174.2	16.5	35.4	0.3
90	89	197	0.45	0.52456	0.01216	13.67259	0.24891	0.18904	0.00326	2718.5	51.4	2727.3	17.2	2733.8	28.4
91	288	118	2.45	0.23186	0.00660	2.76832	0.06698	0.08659	0.00159	1344.2	34.5	1347.0	18.1	1351.5	35.4
92	60	53	1.13	0.17964	0.00593	1.92479	0.06676	0.07771	0.00193	1065.0	32.4	1089.7	23.2	1139.5	49.5
93	259	104	2.49	0.17576	0.00461	1.78373	0.03800	0.07360	0.00140	1043.8	25.3	1039.5	13.9	1030.6	38.4
94	42	45	0.94	0.17229	0.00478	1.87295	0.04921	0.07884	0.00164	1024.7	26.3	1071.6	17.4	1168.2	41.1
95	382	257	1.48	0.17675	0.00516	1.82891	0.05027	0.07505	0.00130	1049.2	28.3	1055.9	18.0	1069.8	34.8
96	146	45	3.24	0.21048	0.00645	2.24938	0.05436	0.07751	0.00155	1231.4	34.4	1196.6	17.0	1134.3	39.8
97	111	68	1.63	0.20284	0.00680	2.19723	0.06353	0.07856	0.00176	1190.5	36.5	1180.2	20.2	1161.2	44.4
98	36	32	1.10	0.17835	0.00572	1.90109	0.06406	0.07731	0.00224	1057.9	31.3	1081.5	22.4	1129.2	57.8
99	108	49	2.18	0.17879	0.00582	1.81468	0.05553	0.07361	0.00164	1060.4	31.9	1050.8	20.0	1030.9	45.0
100	172	100	1.72	0.18199	0.00544	1.88897	0.04947	0.07528	0.00158	1077.8	29.7	1077.2	17.4	1076.0	42.1
101	55	43	1.29	0.24877	0.00661	3.13628	0.08356	0.09143	0.00147	1432.1	34.1	1441.6	20.5	1455.7	30.5
102	33	49	0.68	0.18444	0.00629	1.94171	0.06727	0.07635	0.00229	1091.2	34.2	1095.6	23.2	1104.3	60.0
103	182	60	3.04	0.23376	0.00749	2.84405	0.07537	0.08813	0.00158	1354.2	39.2	1366.3	19.9	1385.3	34.4
104	20	28	0.71	0.17676	0.00631	1.80994	0.07327	0.07427	0.00245	1049.2	34.6	1049.1	26.5	1048.7	66.6
105	174	74	2.36	0.18414	0.00619	1.90080	0.05757	0.07487	0.00129	1089.6	33.7	1081.4	20.2	1064.9	34.5
106	149	72	2.08	0.35036	0.01205	5.67876	0.16983	0.11755	0.00172	1936.3	57.5	1928.1	25.8	1919.4	26.2
107	87	91	0.95	0.24692	0.01016	3.04084	0.10384	0.08932	0.00186	1422.6	52.5	1417.9	26.1	1410.9	39.9
108	110	90	1.22	0.27554	0.01189	3.48436	0.12518	0.09171	0.00173	1568.9	60.1	1523.7	28.4	1461.5	35.8
<i>NML-1IF-86 (25 μm)</i>															
1	101	104	0.97	0.31110	0.00806	4.82401	0.13124	0.11246	0.00207	1746.1	39.6	1789.1	22.9	1839.6	33.3
2	45	36	1.26	0.17396	0.00415	1.88234	0.05701	0.07848	0.00239	1033.9	22.8	1074.9	20.1	1159.1	60.3
3	391	222	1.76	0.52397	0.01255	14.05268	0.33508	0.19451	0.00343	2716.0	53.1	2753.3	22.6	2780.7	28.9
4	308	118	2.61	0.15939	0.00329	1.53192	0.03172	0.06971	0.00127	953.4	18.3	943.3	12.7	919.7	37.5
5	57	37	1.55	0.17844	0.00411	1.90592	0.04810	0.07747	0.00200	1058.4	22.5	1083.2	16.8	1133.2	51.5
6	696	113	6.17	0.18076	0.00489	1.85744	0.04680	0.07453	0.00137	1071.1	26.7	1066.1	16.6	1055.8	37.2
7	128	98	1.31	0.17052	0.00448	1.78157	0.05076	0.07578	0.00197	1015.0	24.7	1038.8	18.5	1089.1	52.0
8	116	3	40.75	0.17068	0.00428	1.74484	0.04872	0.07414	0.00181	1015.8	23.6	1025.3	18.0	1045.4	49.1
9	97	54	1.78	0.23520	0.00593	3.43083	0.12589	0.10580	0.00407	1361.7	30.9	1511.5	28.9	1728.2	70.6
10	118	84	1.40	0.52661	0.01321	13.60003	0.31689	0.18731	0.00345	2727.1	55.8	2722.3	22.0	2718.6	-0.3

Spot	Conc. (ppm)	Ratios										Ages				
		[Th]	U/Th	$^{206}\text{Pb}/^{238}\text{U}$	$\pm 2\sigma$	$^{207}\text{Pb}/^{235}\text{U}$	$\pm 2\sigma$	$^{207}\text{Pb}/^{206}\text{Pb}$	$\pm 2\sigma$	$^{206}\text{Pb}/^{238}\text{U} \pm 2\sigma$	$^{207}\text{Pb}/^{235}\text{U} \pm 2\sigma$	$^{207}\text{Pb}/^{206}\text{Pb} \pm 2\sigma$	% Disc			
11	86	42	2.02	0.21316	0.00644	2.47032	0.13606	0.08405	0.00364	1245.6	34.2	1263.4	39.8	1293.7	84.3	3.9
12	74	73	1.01	0.47398	0.01262	11.19591	0.28937	0.17132	0.00282	2501.0	55.2	2539.6	24.1	2570.5	27.6	2.8
13	109	113	0.97	0.16537	0.00478	1.67629	0.05258	0.07352	0.00151	986.5	26.4	999.6	19.9	1028.3	41.7	4.2
14	78	54	1.46	0.17548	0.00494	1.76777	0.05144	0.07306	0.00149	1042.2	27.1	1033.7	18.9	1015.7	41.3	-2.5
15	56	21	2.69	0.18079	0.00531	1.97698	0.05465	0.07931	0.00178	1071.3	29.0	1107.7	18.6	1179.8	44.3	10.1
16	256	149	1.72	0.19402	0.00578	2.08921	0.05757	0.07810	0.00140	1143.1	31.2	1145.3	18.9	1149.4	35.5	0.5
17	186	113	1.65	0.20479	0.00815	2.38963	0.08680	0.08463	0.00210	1201.0	43.6	1239.5	26.0	1307.1	48.1	8.8
18	23	26	0.87	0.16935	0.00576	1.73343	0.05709	0.07424	0.00145	1008.5	31.8	1021.0	21.2	1047.9	39.5	3.9
19	70	80	0.87	0.24358	0.00815	2.91128	0.09322	0.08668	0.00153	1405.3	42.3	1384.8	24.2	1353.5	34.1	-3.7
20	235	198	1.19	0.21790	0.00762	2.29439	0.07347	0.07637	0.00198	1270.8	40.3	1210.6	22.6	1104.7	51.8	-13.1
21	278	124	2.23	0.17237	0.00488	1.83405	0.06790	0.07717	0.00301	1025.2	26.8	1057.7	24.3	1125.5	77.9	9.8
22	241	94	2.57	0.20270	0.00731	2.27580	0.08135	0.08143	0.00205	1189.8	39.2	1204.8	25.2	1231.8	49.3	3.5
23	77	29	2.64	0.16454	0.00390	1.64906	0.06667	0.07269	0.00262	982.0	21.6	989.2	25.6	1005.2	73.2	2.4
24	60	34	1.76	0.50740	0.01138	12.81136	0.24722	0.18312	0.00303	2645.5	48.7	2665.9	18.2	2681.4	27.4	1.4
25	56	82	0.68	0.24471	0.00602	2.95808	0.06815	0.08767	0.00162	1411.1	31.2	1396.9	17.5	1375.3	35.5	-2.5
26	171	166	1.03	0.17031	0.00375	1.71336	0.03800	0.07296	0.00133	1013.8	20.7	1013.5	14.2	1013.0	37.1	-0.1
27	104	83	1.25	0.16960	0.00428	1.72593	0.05290	0.07381	0.00186	1009.9	23.6	1018.2	19.7	1036.1	50.8	2.6
28	80	76	1.05	0.17084	0.00406	1.72057	0.04251	0.07304	0.00160	1016.7	22.4	1016.2	15.9	1015.2	44.3	-0.2
29	145	44	3.33	0.17495	0.00412	1.77333	0.03538	0.07351	0.00142	1039.3	22.6	1035.7	13.0	1028.2	39.1	-1.1
30	95	73	1.29	0.16815	0.00428	1.72307	0.03766	0.07432	0.00144	1001.9	23.6	1017.2	14.0	1050.2	39.1	4.8
31	208	81	2.56	0.34524	0.00865	5.47013	0.10769	0.11492	0.00165	1911.8	41.4	1895.9	16.9	1878.6	25.9	-1.7
32	80	69	1.15	0.51656	0.01480	13.13420	0.28103	0.18441	0.00309	2684.6	62.9	2689.3	20.2	2692.9	27.6	0.3
33	46	31	1.48	0.09283	0.00226	0.78944	0.03084	0.06168	0.00253	572.2	13.4	590.9	17.5	663.0	88.0	15.9
34	123	77	1.59	0.27063	0.00726	3.74388	0.11922	0.10033	0.00348	1544.0	36.8	1580.8	25.5	1630.3	64.4	5.6
35	131	146	0.90	0.32292	0.00868	5.07998	0.12786	0.11409	0.00332	1804.0	42.3	1832.8	21.4	1865.6	52.5	3.4
36	37	52	0.72	0.17305	0.00477	1.75826	0.03699	0.07369	0.00125	1028.9	26.2	1030.2	13.6	1033.0	34.2	0.4
37	186	80	2.33	0.18630	0.00344	2.03442	0.04214	0.07920	0.00155	1101.3	18.7	1127.1	14.1	1177.1	38.6	6.9
38	191	60	3.21	0.17067	0.00411	1.74953	0.06452	0.07435	0.00255	1015.8	22.6	1027.0	23.8	1051.0	69.0	3.5
39	92	57	1.63	0.20570	0.00440	2.33445	0.05328	0.08231	0.00141	1205.9	23.5	1222.8	16.2	1252.8	33.4	3.9
40	38	23	1.66	0.18549	0.00443	1.99157	0.06368	0.07787	0.00280	1096.9	24.1	1112.7	21.6	1143.6	71.4	4.3
41	32	31	1.02	0.21832	0.00458	2.50296	0.05718	0.08315	0.00135	1273.0	24.2	1272.9	16.6	1272.8	31.6	0.0

Spot	Conc. (ppm)	Ratios										Ages			
		[U]	[Th]	$^{206}\text{Pb}/^{238}\text{U}$	$\pm 2\sigma$	$^{207}\text{Pb}/^{235}\text{U}$	$\pm 2\sigma$	$^{207}\text{Pb}/^{206}\text{Pb}$	$\pm 2\sigma$	$^{206}\text{Pb}/^{238}\text{U} \pm 2\sigma$	$^{207}\text{Pb}/^{235}\text{U} \pm 2\sigma$	$^{207}\text{Pb}/^{206}\text{Pb} \pm 2\sigma$	% Disc		
42	202	65	3.09	0.19594	0.00403	2.15426	0.05524	0.07974	0.00167	1153.5	21.7	1166.4	17.8	1190.5	41.4
43	284	117	2.43	0.25597	0.00689	3.37301	0.11747	0.09557	0.00210	1469.2	35.4	1498.1	27.3	1539.4	41.4
44	134	61	2.20	0.29089	0.00697	4.03655	0.09997	0.10064	0.00167	1646.0	34.8	1641.6	20.2	1636.0	30.7
45	89	197	0.45	0.53543	0.01230	14.80780	0.31118	0.20058	0.00301	2764.3	51.6	2803.0	20.0	2830.9	24.5
46	288	118	2.45	0.24827	0.00672	3.00845	0.08660	0.08789	0.00231	1429.5	34.7	1409.8	21.9	1380.0	50.5
47	60	53	1.13	0.19503	0.00551	2.03369	0.06849	0.07563	0.00214	1148.6	29.7	1126.9	22.9	1085.3	56.7
48	259	104	2.49	0.22935	0.00656	2.74082	0.07132	0.08667	0.00149	1331.1	34.4	1339.6	19.4	1353.2	33.1
49	42	45	0.94	0.22381	0.00647	2.66751	0.07715	0.08644	0.00142	1302.0	34.1	1319.5	21.4	1348.1	31.8
50	57	42	1.34	0.19312	0.00480	2.08996	0.06037	0.07849	0.00203	1138.2	26.0	1145.5	19.8	1159.3	51.4
51	144	90	1.59	0.18271	0.00455	1.88671	0.05138	0.07489	0.00152	1081.8	24.8	1076.4	18.1	1065.6	40.9
52	45	48	0.94	0.18000	0.00523	1.85916	0.06823	0.07491	0.00237	1067.0	28.6	1066.7	24.2	1066.1	63.6
53	142	43	3.29	0.23210	0.00609	2.80859	0.07836	0.08776	0.00183	1345.5	31.8	1357.8	20.9	1377.3	40.1
54	140	61	2.31	0.46324	0.00987	11.97478	0.25407	0.18748	0.00288	2453.8	43.5	2602.4	19.9	2720.2	25.3
55	127	48	2.63	0.33778	0.00817	5.36766	0.12799	0.11525	0.00219	1876.0	39.4	1879.7	20.4	1883.8	34.2
56	119	59	2.01	0.20356	0.00490	2.17701	0.05885	0.07757	0.00178	1194.4	26.2	1173.7	18.8	1135.8	45.7
57	111	54	2.04	0.19325	0.00453	2.11569	0.05987	0.07940	0.00171	1139.0	24.4	1153.9	19.5	1182.1	42.6
58	102	70	1.46	0.19346	0.00471	2.12969	0.05633	0.07984	0.00197	1140.1	25.5	1158.5	18.3	1193.0	48.6
59	60	34	1.76	0.21244	0.00573	2.40174	0.07649	0.08200	0.00218	1241.8	30.5	1243.1	22.8	1245.4	52.1
60	35	26	1.38	0.19636	0.00536	2.20204	0.08731	0.08133	0.00282	1155.7	28.9	1181.7	27.7	1229.5	68.2
61	55	12	4.54	0.18958	0.00493	2.07990	0.06283	0.07957	0.00223	1119.1	26.7	1142.2	20.7	1186.4	55.3
62	409	204	2.00	0.24332	0.00717	2.96330	0.09274	0.08833	0.00200	1404.0	37.2	1398.3	23.8	1389.6	43.5
63	115	71	1.62	0.57398	0.01122	16.74985	0.34504	0.21165	0.00349	2924.1	45.9	2920.6	19.7	2918.2	26.7
64	938	184	5.10	0.29786	0.00689	4.50771	0.10585	0.10976	0.00157	1680.7	34.2	1732.4	19.5	1795.4	26.1
65	26	11	2.42	0.16546	0.00448	1.73703	0.07347	0.07614	0.00312	987.0	24.8	1022.4	27.3	1098.8	81.9
66	120	254	0.47	0.50575	0.01158	12.33237	0.31270	0.17685	0.00300	2638.5	49.6	2630.0	23.8	2623.6	28.2
67	176	161	1.10	0.19156	0.00501	2.09982	0.09644	0.07950	0.00258	1129.8	27.1	1148.7	31.6	1184.7	64.1
68	176	64	2.74	0.24436	0.00589	2.94123	0.07673	0.08730	0.00188	1409.3	30.5	1392.6	19.8	1367.0	41.6
69	41	58	0.70	0.17958	0.00489	1.90232	0.06051	0.07683	0.00264	1064.7	26.7	1081.9	21.2	1116.8	68.5
70	103	51	2.03	0.56319	0.01368	16.14729	0.43840	0.20794	0.00392	2879.8	56.4	2885.6	26.0	2889.6	30.6
71	88	67	1.31	0.56484	0.01230	15.86683	0.33371	0.20373	0.00297	2886.6	50.7	2868.8	20.1	2856.3	23.7
72	103	40	2.56	0.23438	0.00412	2.88695	0.06551	0.08933	0.00183	1357.4	21.5	1378.5	17.1	1411.3	39.3

Spot	Conc. (ppm)	Ratios										Ages			
		[U]	[Th]	U/Th	$^{206}\text{Pb}/^{238}\text{U}$	$\pm 2\sigma$	$^{207}\text{Pb}/^{235}\text{U}$	$\pm 2\sigma$	$^{207}\text{Pb}/^{206}\text{Pb}$	$\pm 2\sigma$	$^{206}\text{Pb}/^{238}\text{U} \pm 2\sigma$	$^{207}\text{Pb}/^{235}\text{U} \pm 2\sigma$	$^{207}\text{Pb}/^{206}\text{Pb} \pm 2\sigma$	% Disc	
73	152	61	2.49	0.16432	0.00351	1.60942	0.03740	0.07104	0.00145	980.7	19.4	973.9	14.6	958.5	-2.3
74	394	70	5.66	0.36177	0.00697	5.77944	0.12529	0.11586	0.00178	1990.6	33.0	1943.3	18.8	1893.4	-4.9
75	68	49	1.38	0.18155	0.00390	1.87150	0.04020	0.07477	0.00183	1075.4	21.3	1071.1	14.2	1062.2	-1.2
76	202	76	2.65	0.17501	0.00298	1.76229	0.03524	0.07303	0.00149	1039.7	16.3	1031.7	13.0	1014.8	-2.4
77	56	65	0.87	0.22136	0.00516	2.58821	0.06960	0.08480	0.00245	1289.0	27.2	1297.3	19.7	1311.0	1.7
78	146	109	1.33	0.28339	0.00583	3.91377	0.08655	0.10016	0.00222	1608.4	29.3	1616.5	17.9	1627.1	41.2
79	106	44	2.44	0.18944	0.00524	1.92785	0.05648	0.07381	0.00194	1118.4	28.4	1090.8	19.6	1036.2	-7.4
80	408	487	0.84	0.32256	0.00633	4.99573	0.10747	0.11233	0.00187	1802.2	30.9	1818.6	18.2	1837.4	30.2
81	159	64	2.49	0.17741	0.00411	1.77636	0.04404	0.07262	0.00147	1052.8	22.5	1036.8	16.1	1003.3	-4.7
82	233	197	1.18	0.16782	0.00353	1.71850	0.03271	0.07427	0.00126	1000.1	19.5	1015.5	12.2	1048.8	34.2
83	92	66	1.40	0.21468	0.00501	2.48789	0.06486	0.08405	0.00198	1253.7	26.6	1268.5	18.9	1293.7	45.9
84	156	60	2.59	0.55761	0.01232	15.02730	0.31318	0.19546	0.00365	2856.7	51.0	2817.0	19.8	2788.6	30.6
85	96	19	5.05	0.19536	0.00453	2.19398	0.04933	0.08145	0.00180	1150.3	24.4	1179.1	15.7	1232.3	43.4
86	231	297	0.78	0.27459	0.00620	3.87091	0.07345	0.10224	0.00223	1564.1	31.4	1607.6	15.3	1665.2	40.4
87	118	136	0.86	0.27272	0.00589	3.74164	0.07365	0.09950	0.00255	1554.6	29.8	1580.3	15.8	1614.8	47.7
88	76	43	1.79	0.17736	0.00429	1.79251	0.04579	0.07330	0.00207	1052.5	23.5	1042.7	16.6	1022.3	-2.9
89	54	61	0.89	0.20151	0.00527	2.13814	0.05460	0.07696	0.00278	1183.4	28.3	1161.2	17.7	1120.0	-72.1
90	51	40	1.26	0.19291	0.00523	2.00897	0.06025	0.07553	0.00243	1137.1	28.3	1118.5	20.3	1082.7	-64.4
91	142	58	2.46	0.24005	0.00554	2.82638	0.10731	0.08539	0.00301	1387.0	28.8	1362.6	28.5	1324.5	-4.5
92	104	39	2.67	0.19385	0.00511	2.11561	0.10596	0.07915	0.00358	1142.2	27.6	1153.9	34.5	1175.9	89.5
93	66	62	1.07	0.18310	0.00490	2.13071	0.11781	0.08440	0.00394	1083.9	26.7	1158.8	38.2	1301.8	90.7
94	279	94	2.96	0.17171	0.00370	1.71337	0.05799	0.07237	0.00224	1021.5	20.4	1013.5	21.7	996.3	62.8
95	283	233	1.22	0.23167	0.00449	2.94732	0.09499	0.09227	0.00274	1343.2	23.5	1394.2	24.4	1472.9	56.3
96	75	24	3.11	0.23995	0.00575	3.01649	0.12383	0.09118	0.00339	1386.4	29.9	1411.8	31.3	1450.3	70.8
97	364	149	2.45	0.23029	0.00468	2.79533	0.11611	0.08803	0.00336	1336.0	24.5	1354.3	31.1	1383.2	73.4
98	131	74	1.78	0.20002	0.00531	2.25741	0.12775	0.08185	0.00391	1175.4	28.5	1199.1	39.8	1242.0	93.6
99	445	1	548.98	0.16962	0.00323	1.75799	0.07398	0.07517	0.00290	1010.0	17.8	1030.1	27.2	1073.0	77.5
100	149	60	2.48	0.19330	0.00397	2.08133	0.08506	0.07809	0.00297	1139.2	21.4	1142.7	28.0	1149.2	75.6
										<i>NNP-4-86 (25 μm)</i>					
1	259	85	3.03	0.19725	0.00426	2.10563	0.04789	0.07742	0.00120	1160.5	22.9	1150.7	15.7	1132.1	30.9
2	254	86	2.94	0.24243	0.00574	2.89573	0.06935	0.08663	0.00141	1399.3	29.8	1380.8	18.1	1352.3	31.4

Spot	Conc. (ppm)	Ratios						Ages					
		[U]	[Th]	$^{206}\text{Pb}/^{238}\text{U}$	$\pm 2\sigma$	$^{207}\text{Pb}/^{235}\text{U}$	$\pm 2\sigma$	$^{207}\text{Pb}/^{206}\text{Pb}$	$\pm 2\sigma$	$^{206}\text{Pb}/^{238}\text{U} \pm 2\sigma$	$^{207}\text{Pb}/^{235}\text{U} \pm 2\sigma$	$^{207}\text{Pb}/^{206}\text{Pb} \pm 2\sigma$	$\pm 2\sigma$
3	42	35	1.21	0.17615	0.00398	1.82848	0.05050	0.07529	0.00187	1045.9	21.8	1055.7	18.1
4	16	17	0.95	0.17437	0.00466	1.78202	0.06935	0.07412	0.00277	1036.1	25.6	1038.9	25.3
5	191	104	1.82	0.54052	0.01324	13.64480	0.31124	0.18309	0.00249	2785.6	55.4	2725.4	21.6
6	117	176	0.67	0.24103	0.00572	2.95276	0.07588	0.08885	0.00157	1392.0	29.7	1395.6	19.5
7	413	265	1.56	0.35203	0.01029	5.53418	0.16361	0.11402	0.00175	1944.3	49.0	1905.9	25.4
8	102	61	1.66	0.52640	0.01487	12.58964	0.33364	0.17346	0.00293	2726.3	62.8	2649.4	24.9
9	69	33	2.09	0.17943	0.00500	1.85600	0.04944	0.07502	0.00175	1063.9	27.3	1065.6	17.6
10	63	36	1.76	0.19429	0.00522	2.02692	0.06170	0.07566	0.00180	1144.6	28.2	1124.6	20.7
11	142	83	1.71	0.18557	0.00417	1.94611	0.05114	0.07606	0.00146	1097.3	22.7	1097.1	17.6
12	14	6	2.40	0.18829	0.00618	2.14201	0.08678	0.08251	0.00317	1112.1	33.5	1162.5	28.1
13	152	54	2.82	0.20977	0.00527	2.33995	0.06771	0.08090	0.00113	1227.6	28.1	1224.5	20.6
14	66	102	0.65	0.23862	0.00601	2.84999	0.09257	0.08663	0.00172	1379.5	31.3	1368.8	24.4
15	58	63	0.92	0.53958	0.01309	13.99479	0.36464	0.18811	0.00236	2781.7	54.8	2749.4	24.7
16	116	58	1.99	0.31872	0.00785	4.56380	0.13025	0.10385	0.00150	1783.5	38.4	1742.7	23.8
17	87	72	1.21	0.18960	0.00500	1.98228	0.06188	0.07583	0.00111	1119.2	27.1	1109.5	21.1
18	252	143	1.76	0.21816	0.00498	2.45305	0.07204	0.08155	0.00127	1272.2	26.4	1258.3	21.2
19	36	25	1.44	0.21143	0.00519	2.29017	0.07667	0.07856	0.00184	1236.4	27.6	1209.3	23.7
20	42	31	1.38	0.22329	0.00890	2.30983	0.09759	0.07502	0.00204	1299.2	46.9	1215.3	29.9
21	1132	196	5.77	0.18108	0.00427	1.82123	0.04320	0.07295	0.00105	1072.9	23.3	1053.1	15.6
22	145	48	3.04	0.20007	0.00434	2.14013	0.04464	0.07758	0.00132	1175.7	23.3	1161.9	14.4
23	98	35	2.82	0.19022	0.00446	1.99102	0.04395	0.07591	0.00156	1122.5	24.2	1112.5	14.9
24	299	108	2.78	0.27777	0.01177	3.33157	0.14348	0.08699	0.00121	1580.1	59.4	1488.5	33.6
25	206	162	1.28	0.18933	0.00364	1.98509	0.03489	0.07604	0.00121	1117.7	19.7	1110.5	11.9
26	196	74	0.74	0.34803	0.00684	5.35666	0.08593	0.11163	0.00171	1925.2	32.7	1878.0	13.7
27	93	132	0.71	0.55378	0.00992	14.83319	0.26851	0.19427	0.00318	2840.9	41.1	2804.6	17.2
28	158	157	1.00	0.28047	0.00648	3.80207	0.08879	0.09832	0.00163	1593.7	32.6	1593.2	18.8
29	8	6	1.28	0.33458	0.00879	5.47725	0.18586	0.11873	0.00429	1860.6	42.5	1897.0	29.1
30	384	401	0.96	0.18917	0.00363	1.96535	0.03589	0.07535	0.00098	1116.9	19.7	1103.7	12.3
31	50	25	1.96	0.21180	0.00507	2.74353	0.13129	0.09395	0.00338	1238.4	26.9	1340.3	35.6
32	120	54	2.21	0.19355	0.00434	2.02804	0.05252	0.07599	0.00141	1140.6	23.5	1125.0	17.6
33	196	100	1.97	0.21083	0.00466	2.27666	0.04413	0.07832	0.00135	1233.2	24.8	1205.1	13.7

Spot	Conc. (ppm)	Ratios						Ages					
		[U]	[Th]	$^{206}\text{Pb}/^{238}\text{U}$	$^{207}\text{Pb}/^{235}\text{U}$	$\pm 2\sigma$	$^{207}\text{Pb}/^{206}\text{Pb}$	$\pm 2\sigma$	$^{206}\text{Pb}/^{238}\text{U} \pm 2\sigma$	$^{207}\text{Pb}/^{235}\text{U} \pm 2\sigma$	$^{207}\text{Pb}/^{206}\text{Pb} \pm 2\sigma$	% Disc	
34	362	150	2.42	0.19168	0.00452	1.96263	0.04100	0.07426	0.00125	1130.4	24.5	1102.8	14.1
35	140	174	0.80	0.58244	0.01163	16.89172	0.28082	0.21034	0.00324	2958.7	47.4	2928.7	15.9
36	85	61	1.39	0.22351	0.00526	2.51787	0.04459	0.0870	0.00171	1300.4	27.7	1277.2	12.9
37	138	119	1.15	0.53378	0.01377	13.79152	0.21398	0.18739	0.00382	2757.4	57.9	2735.5	14.7
38	9	11	0.81	0.24055	0.00803	2.98201	0.11120	0.08991	0.00372	1389.6	41.7	1403.0	28.4
39	101	79	1.28	0.19433	0.00480	2.06312	0.04297	0.07700	0.00182	1144.8	25.9	1136.7	14.2
40	38	34	1.11	0.53802	0.01285	13.70885	0.26719	0.18480	0.00377	2775.2	53.8	2729.8	18.4
41	506	287	1.76	0.33913	0.00766	5.40826	0.10269	0.11566	0.00193	1882.5	36.9	1886.2	16.3
42	530	181	2.93	0.48925	0.01311	11.46307	0.27595	0.16993	0.00330	2567.4	56.8	2561.6	22.5
43	110	82	1.35	0.19072	0.00478	2.00329	0.04825	0.07618	0.00173	1125.2	25.9	1116.6	16.3
44	134	78	1.72	0.18686	0.00462	1.89068	0.04638	0.07338	0.00157	1104.3	25.1	1077.8	16.3
45	156	71	2.20	0.24157	0.00517	2.85398	0.06409	0.08569	0.00162	1394.9	26.8	1369.9	16.9
46	203	72	2.82	0.22986	0.00489	2.73341	0.05398	0.08625	0.00149	1333.8	25.6	1337.6	14.7
47	76	34	2.20	0.19994	0.00403	2.12248	0.04874	0.07699	0.00150	1175.0	21.6	1156.1	15.9
48	87	101	0.86	0.18426	0.00312	1.90244	0.04033	0.07488	0.00164	1090.2	17.0	1081.9	14.1
49	361	21	17.16	0.18926	0.00417	1.92554	0.04679	0.07379	0.00134	1117.3	22.6	1090.0	16.2
50	158	107	1.48	0.18127	0.00379	1.88284	0.03630	0.07533	0.00113	1073.9	20.7	1075.1	12.8
51	219	88	2.49	0.18207	0.00478	1.84266	0.04826	0.07340	0.00126	1078.3	26.0	1060.8	17.2
52	186	192	0.97	0.10944	0.00265	0.91167	0.02443	0.06042	0.00146	669.5	15.4	657.9	13.0
53	382	298	1.28	0.19205	0.00422	1.98231	0.04494	0.07486	0.00121	1132.5	22.8	1109.5	15.3
54	152	161	0.95	0.34115	0.00711	5.21216	0.11426	0.11081	0.00179	1892.2	34.2	1854.6	18.7
55	186	238	0.78	0.33055	0.00803	4.68653	0.11617	0.10283	0.00186	1841.0	38.9	1764.8	20.7
56	43	26	1.67	0.20719	0.00540	2.33826	0.06966	0.08185	0.00186	1213.8	28.8	1224.0	21.2
57	81	89	0.91	0.18916	0.00462	1.96264	0.05793	0.07525	0.00155	1116.8	25.0	1102.8	19.9
58	130	109	1.19	0.18736	0.00386	1.94791	0.05131	0.07540	0.00131	1107.0	20.9	1097.7	17.7
59	61	68	0.90	0.19028	0.00420	1.98263	0.05342	0.07557	0.00161	1122.9	22.8	1109.6	18.2
60	157	124	1.27	0.19311	0.00438	2.06115	0.05607	0.07741	0.00131	1138.2	23.7	1136.0	18.6
61	790	47	16.92	0.50590	0.02212	12.35706	0.61295	0.17715	0.00324	2639.1	94.7	2631.9	46.6
62	203	74	2.75	0.18960	0.00449	1.94344	0.05079	0.07434	0.00116	1119.2	24.3	1096.2	17.5
63	37	22	1.71	0.18843	0.00431	1.98235	0.05865	0.07630	0.00198	1112.9	23.4	1109.5	20.0
64	291	282	1.03	0.52673	0.01227	13.62916	0.34316	0.18766	0.00250	2727.7	51.8	2724.3	23.8

Spot	Conc. (ppm)	Ratios										Ages			
		[U]	[Th]	$^{206}\text{Pb}/^{238}\text{U}$	$\pm 2\sigma$	$^{207}\text{Pb}/^{235}\text{U}$	$\pm 2\sigma$	$^{207}\text{Pb}/^{206}\text{Pb}$	$\pm 2\sigma$	$^{206}\text{Pb}/^{238}\text{U} \pm 2\sigma$	$^{207}\text{Pb}/^{235}\text{U} \pm 2\sigma$	$^{207}\text{Pb}/^{206}\text{Pb} \pm 2\sigma$	$\pm 2\sigma$	% Disc	
65	168	250	0.67	0.36015	0.00782	5.85637	0.12828	0.11794	0.00169	1982.9	37.1	1954.8	19.0	1925.2	25.7
66	68	34	2.01	0.19106	0.00502	2.01441	0.05322	0.07647	0.00154	1127.1	27.2	1120.4	17.9	1107.3	40.1
67	151	212	0.71	0.51038	0.01263	12.62349	0.26140	0.17938	0.00259	2658.3	53.9	2652.0	19.5	2647.2	23.9
68	177	193	0.92	0.26339	0.00660	3.49501	0.08790	0.09624	0.00155	1507.2	33.7	1526.1	19.9	1552.4	30.2
69	42	22	1.95	0.17580	0.00454	1.77800	0.05133	0.07335	0.00196	1044.0	24.9	1037.4	18.8	1023.6	54.1
70	39	27	1.46	0.18594	0.00501	1.96336	0.06033	0.07658	0.00218	1099.3	27.2	1103.0	20.7	1110.3	56.8
71	88	73	1.21	0.26077	0.00639	3.22012	0.07502	0.08956	0.00157	1493.8	32.7	1462.0	18.1	1416.1	33.5
72	406	268	1.51	0.24119	0.00719	2.74785	0.07531	0.08263	0.00156	1392.9	37.4	1341.5	20.4	1260.5	36.8
73	295	142	2.08	0.18660	0.00448	1.94267	0.05133	0.07551	0.00118	1102.9	24.4	1095.9	17.7	1082.0	31.4
74	174	108	1.62	0.28016	0.00668	3.51936	0.08896	0.09111	0.00141	1592.2	33.6	1531.6	20.0	1448.9	29.4
75	53	40	1.31	0.19678	0.00415	2.05104	0.05520	0.07559	0.00179	1158.0	22.4	1132.6	18.4	1084.3	47.5
76	136	41	3.29	0.55244	0.01152	14.67940	0.34280	0.19272	0.00291	2835.3	47.8	2794.7	22.2	2765.5	24.8
77	133	129	1.03	0.18214	0.00369	1.83029	0.04647	0.07288	0.00152	1078.7	20.1	1056.4	16.7	1010.6	42.2
78	71	66	1.07	0.18288	0.00395	1.89911	0.04946	0.07531	0.00152	1082.7	21.5	1080.8	17.3	1076.9	40.5
79	97	77	1.25	0.18597	0.00467	1.87436	0.05018	0.07310	0.00163	1099.5	25.4	1072.1	17.7	1016.7	45.3
80	154	132	1.17	0.54344	0.01030	13.96060	0.27903	0.18632	0.00285	2797.8	43.0	2747.0	18.9	2709.9	25.2
81	60	36	1.66	0.21264	0.00533	2.35030	0.10886	0.08016	0.00286	1242.9	28.3	1227.6	33.0	1201.0	70.3
82	126	36	3.52	0.33362	0.00712	5.10292	0.27246	0.11093	0.00447	1855.9	34.4	1836.6	45.4	1814.8	73.1
83	366	67	5.47	0.35556	0.00817	5.71274	0.50333	0.11653	0.00907	1961.1	38.8	1933.3	76.3	1903.6	139.8
84	190	155	1.22	0.29157	0.00605	4.05459	0.29994	0.10086	0.00674	1649.4	30.2	1645.2	60.3	1640.0	124.1
85	322	259	1.24	0.25757	0.00611	3.14015	0.23284	0.08842	0.00585	1477.4	31.3	1442.6	57.2	1391.7	127.0
86	108	43	2.53	0.20129	0.00370	2.19348	0.17914	0.07903	0.00623	1182.3	19.9	1179.0	57.0	1173.0	156.0
87	96	62	1.56	0.18409	0.00368	1.88193	0.18851	0.07414	0.00725	1089.3	20.0	1074.7	66.5	1045.4	197.2
88	221	157	1.41	0.08157	0.00196	0.65609	0.06631	0.05834	0.00569	505.5	11.7	512.2	40.7	542.5	213.1
89	160	80	1.99	0.19429	0.00485	1.96292	0.19799	0.07327	0.00713	1144.6	26.2	1102.9	68.0	1021.6	197.1
90	55	33	1.66	0.19713	0.00517	2.06630	0.17354	0.07602	0.00604	1159.9	27.8	1137.7	57.5	1095.7	159.0
91	284	100	2.84	0.17523	0.00428	1.79709	0.14373	0.07438	0.00582	1040.8	23.5	1044.4	52.2	1051.9	157.5
92	107	39	2.76	0.18930	0.00550	1.89415	0.19047	0.07257	0.00726	1117.6	29.8	1079.0	66.9	1002.0	203.1
93	363	240	1.51	0.55191	0.01525	14.10911	1.13768	0.18541	0.01436	2833.1	63.4	2757.1	76.6	2701.9	127.9
94	713	153	4.65	0.43753	0.01643	11.51957	0.86879	0.19095	0.01225	2339.6	73.7	2566.2	70.6	2750.4	105.5
95	80	51	1.59	0.24175	0.00570	2.91443	0.20143	0.08744	0.00566	1395.8	29.6	1385.7	52.3	1370.1	124.6

Spot	Conc. (ppm)	Ratios						Ages					
		[U]	[Th]	$^{206}\text{Pb}/^{238}\text{U}$	$\pm 2\sigma$	$^{207}\text{Pb}/^{235}\text{U}$	$\pm 2\sigma$	$^{207}\text{Pb}/^{206}\text{Pb}$	$\pm 2\sigma$	$^{206}\text{Pb}/^{238}\text{U} \pm 2\sigma$	$^{207}\text{Pb}/^{235}\text{U} \pm 2\sigma$	$^{207}\text{Pb}/^{206}\text{Pb} \pm 2\sigma$	$\pm 2\sigma$
96	44	49	0.90	0.18138	0.00473	1.84158	0.04654	0.07364	0.00176	1074.5	25.8	1060.4	16.6
97	278	154	1.80	0.49109	0.01197	11.24190	0.21117	0.16603	0.00227	2575.4	51.7	2543.4	17.5
98	321	171	1.88	0.54521	0.01489	13.92065	0.31829	0.18518	0.00280	2805.2	62.1	2744.3	21.7
99	745	367	2.03	0.18377	0.00457	1.89685	0.03582	0.07486	0.00101	1087.5	24.9	1080.0	12.6
100	143	110	1.30	0.18924	0.00493	2.11778	0.05056	0.08116	0.00128	1117.3	26.7	1154.6	16.5
101	100	74	1.35	0.19867	0.00499	2.03491	0.04514	0.07429	0.00147	1168.2	26.8	1127.3	15.1
102	53	21	2.54	0.17925	0.00501	1.77784	0.04965	0.07193	0.00177	1062.9	27.4	1037.4	18.1
103	158	64	2.48	0.24527	0.00700	2.94225	0.07950	0.08700	0.00133	1414.1	36.3	1392.9	20.5
104	89	87	1.03	0.19021	0.00599	1.97514	0.06113	0.07531	0.00154	1122.5	32.5	1107.1	20.9
105	423	140	3.03	0.32532	0.01151	7.95513	0.28454	0.17735	0.00259	1815.7	56.0	2225.9	32.3
106	252	91	2.78	0.24732	0.00811	3.00460	0.09551	0.08811	0.00139	1424.7	41.9	1408.8	24.2
107	20	9	2.31	0.24236	0.01016	2.99388	0.14432	0.08959	0.00331	1399.0	52.7	1406.1	36.7
108	161	232	0.69	0.53906	0.02117	13.99391	0.53870	0.18828	0.00291	2779.5	88.7	2749.3	36.5
109	397	197	2.01	0.19070	0.00791	2.00174	0.08417	0.07613	0.00122	1125.2	42.8	1116.1	28.5
110	245	134	1.84	0.18980	0.00634	1.95638	0.06544	0.07476	0.00105	1120.3	34.3	1100.6	22.5
111	44	54	0.80	0.17618	0.00554	1.80452	0.06736	0.07429	0.00206	1046.1	30.4	1047.1	24.4
112	107	71	1.52	0.20547	0.00741	2.20029	0.08453	0.07766	0.00151	1204.7	39.6	1181.1	26.8
113	65	70	0.93	0.36319	0.01332	5.57607	0.20395	0.11135	0.00194	1997.3	63.0	1912.4	31.5
114	19	23	0.83	0.19493	0.00698	2.40698	0.14039	0.08956	0.00448	1148.0	37.6	1244.7	41.9
115	97	96	1.00	0.34932	0.01086	5.53035	0.18218	0.11482	0.00207	1931.3	51.9	1905.3	28.3
116	38	24	1.54	0.19588	0.00619	2.21639	0.07285	0.08206	0.00311	1153.1	33.4	1186.2	23.0
117	114	83	1.37	0.18665	0.00462	1.93945	0.03753	0.07536	0.00146	1103.2	25.1	1094.8	13.0
118	226	66	3.40	0.24797	0.00645	2.95032	0.06552	0.08629	0.00163	1428.0	33.3	1394.9	16.8
119	85	75	1.13	0.18221	0.00469	1.84620	0.04546	0.07349	0.00179	1079.0	25.6	1062.1	16.2
120	114	143	0.80	0.17310	0.00414	1.70525	0.03493	0.07145	0.00147	1029.2	22.8	1010.5	13.1
<i>NNP-5-86 (25 μm)</i>													
1	43	12	3.64	0.16782	0.00919	1.71943	0.10454	0.07431	0.00127	1000.1	50.7	1015.8	39.1
2	192	77	2.49	0.23236	0.01346	3.03171	0.18502	0.09463	0.00166	1346.9	70.4	1415.6	46.6
3	305	204	1.49	0.45517	0.01240	10.40067	0.28441	0.16572	0.00265	2418.2	54.9	2471.1	25.3
4	177	60	2.95	0.50315	0.01675	11.73725	0.42855	0.16919	0.00247	2627.3	71.8	2583.7	34.2
5	91	107	0.86	0.29452	0.00870	4.07494	0.13555	0.10035	0.00167	1664.1	43.3	1649.3	27.1

Spot	Conc. (ppm)		Ratios						Ages					
	[U]	[Th]	$^{206}\text{Pb}/^{238}\text{U}$	$\pm 2\sigma$	$^{207}\text{Pb}/^{235}\text{U}$	$\pm 2\sigma$	$^{206}\text{Pb}/^{206}\text{Pb}$	$\pm 2\sigma$	$^{206}\text{Pb}/^{238}\text{U}$	$\pm 2\sigma$	$^{207}\text{Pb}/^{235}\text{U} \pm 2\sigma$	$^{207}\text{Pb}/^{206}\text{Pb} \pm 2\sigma$	% Disc	
6	159	151	1.05	0.51917	0.01533	12.64991	0.40843	0.17671	0.00257	2695.7	65.1	2653.9	30.4	2622.3
7	300	85	3.54	0.19626	0.00807	2.11096	0.08681	0.07801	0.00228	1155.2	43.5	1152.4	28.3	1147.1
8	141	101	1.39	0.17877	0.00632	1.83117	0.07572	0.07429	0.00117	1060.2	34.6	1056.7	27.2	1049.4
9	348	216	1.61	0.18693	0.00562	2.02967	0.08987	0.07875	0.00140	1104.7	30.5	1125.5	30.1	1165.9
10	163	93	1.75	0.52059	0.01649	13.37368	0.57516	0.18632	0.00332	2701.7	69.9	2706.4	40.7	2709.9
11	143	68	2.10	0.17740	0.00710	1.83228	0.05966	0.07491	0.00121	1052.7	38.9	1057.1	21.4	1066.1
12	791	315	2.51	0.18545	0.00985	3.82793	0.50537	0.14970	0.01510	1096.7	53.6	1598.6	106.7	2342.6
13	32	30	1.05	0.27298	0.01173	3.76564	0.14583	0.10005	0.00163	1555.9	59.4	1585.5	31.1	1624.9
14	625	384	1.63	0.53375	0.02102	13.59469	0.42875	0.18473	0.00306	2757.2	88.4	2721.9	29.8	2695.8
15	108	67	1.60	0.50343	0.01838	13.54549	0.44220	0.19514	0.00317	2628.5	78.8	2718.5	30.9	2786.0
16	314	205	1.53	0.34092	0.01021	5.14692	0.15570	0.10949	0.00165	1891.1	49.1	1843.9	25.7	1791.0
17	244	230	1.06	0.18900	0.00581	1.94035	0.06089	0.07446	0.00115	1115.9	31.5	1095.1	21.0	1053.9
18	306	193	1.58	0.27849	0.00962	3.75639	0.13890	0.09783	0.00170	1583.8	48.5	1583.5	29.7	1583.1
19	522	103	5.08	0.33538	0.01017	5.20158	0.16063	0.11249	0.00198	1864.4	49.1	1852.9	26.3	1840.0
20	95	159	0.60	0.53516	0.01634	13.84003	0.41418	0.18757	0.00255	2763.1	68.6	2738.8	28.3	2720.9
21	120	56	2.13	0.64970	0.02792	30.74702	1.04866	0.34323	0.00785	3227.0	109.1	3511.0	33.6	3677.2
22	38	18	2.11	0.28347	0.01165	4.21655	0.13841	0.10788	0.00195	1608.8	58.5	1677.2	26.9	1764.0
23	362	212	1.71	0.21795	0.00833	2.56555	0.08882	0.08537	0.00129	1271.0	44.1	1290.9	25.3	1324.0
24	663	487	1.36	0.52474	0.01675	13.60068	0.37014	0.18798	0.00327	2719.2	70.8	2722.3	25.7	2724.6
25	110	216	0.51	0.18397	0.00564	1.93884	0.05399	0.07643	0.00147	1088.6	30.7	1094.6	18.7	1106.4
26	337	203	1.66	0.19867	0.00651	2.25449	0.06812	0.08230	0.00166	1168.2	35.0	1198.2	21.3	1252.8
27	152	103	1.48	0.23097	0.00865	2.76273	0.10048	0.08675	0.00165	1339.6	45.3	1345.5	27.1	1355.0
28	323	122	2.65	0.17919	0.00616	1.88891	0.06681	0.07645	0.00176	1062.6	33.7	1077.2	23.5	1107.0
29	99	43	2.29	0.16802	0.00608	1.81290	0.05998	0.07826	0.00177	1001.2	33.6	1050.1	21.7	1153.4
30	125	68	1.85	0.16273	0.00553	1.72214	0.05499	0.07675	0.00145	971.9	30.7	1016.8	20.5	1114.8
31	126	61	2.06	0.20873	0.00884	2.41866	0.09802	0.08404	0.00174	1222.0	47.2	1248.2	29.1	1293.5
32	165	96	1.72	0.19310	0.00773	2.08637	0.07707	0.07836	0.00118	1138.2	41.8	1144.3	25.4	1156.1
33	1122	146	7.70	0.17937	0.00676	2.79792	0.17026	0.11313	0.00472	1063.5	37.0	1355.0	45.5	1850.3
34	93	64	1.45	0.18933	0.00642	2.08134	0.07107	0.07973	0.00157	1117.8	34.8	1142.7	23.4	1190.3
35	237	136	1.75	0.18837	0.00782	2.31948	0.10495	0.08930	0.00289	1112.6	42.4	1218.3	32.1	1410.7
36	332	189	1.75	0.26177	0.00941	3.39317	0.11645	0.09401	0.00213	1498.9	48.1	1502.8	26.9	1508.4

Spot	Conc. (ppm)	Ratios						Ages						% Disc		
		[U]	[Th]	$^{206}\text{Pb}/^{238}\text{U}$	$\pm 2\sigma$	$^{207}\text{Pb}/^{235}\text{U}$	$\pm 2\sigma$	$^{206}\text{Pb}/^{206}\text{Pb}$	$\pm 2\sigma$	$^{206}\text{Pb}/^{238}\text{U}$	$\pm 2\sigma$	$^{207}\text{Pb}/^{235}\text{U}$	$\pm 2\sigma$			
37	52	52	0.99	0.30131	0.01013	4.64284	0.13330	0.111176	0.00173	1697.8	50.2	1757.0	24.0	1828.2	28.1	7.7
38	766	381	2.01	0.28067	0.00840	3.81430	0.09904	0.09856	0.00152	1594.8	42.3	1595.8	20.9	1597.1	28.7	0.1
39	171	103	1.65	0.17765	0.00569	1.84884	0.05420	0.07548	0.00112	1054.1	31.2	1063.0	19.3	1081.3	29.7	2.6
40	416	177	2.35	0.19646	0.00658	2.12933	0.06628	0.07861	0.00185	1156.3	35.5	1158.4	21.5	1162.3	46.7	0.5
41	126	59	2.14	0.17174	0.00809	1.99328	0.09788	0.08418	0.00222	1021.7	44.5	1113.2	33.2	1296.6	51.2	26.9
42	517	273	1.89	0.24979	0.01161	3.16292	0.14345	0.09183	0.00206	1437.4	59.9	1448.2	35.0	1464.0	42.7	1.8
43	49	42	1.17	0.23522	0.00975	2.80113	0.11861	0.08637	0.00170	1361.8	50.9	1355.8	31.7	1346.4	37.9	-1.1
44	212	173	1.23	0.24149	0.00892	3.05577	0.10986	0.09178	0.00143	1394.4	46.3	1421.7	27.5	1462.7	29.7	4.9
45	781	422	1.85	0.49234	0.02183	12.57628	0.53301	0.18526	0.00358	2580.8	94.3	2648.4	39.9	2700.6	31.9	4.6
46	328	201	1.63	0.30121	0.01531	4.64303	0.24475	0.11180	0.00183	1697.3	75.8	1757.0	44.1	1828.8	29.7	7.7
47	665	409	1.63	0.24385	0.01237	2.91284	0.15172	0.08663	0.00140	1406.7	64.1	1385.2	39.4	1352.4	31.2	-3.9
48	250	91	2.75	0.17078	0.00902	1.80760	0.10334	0.07676	0.00179	1016.4	49.7	1048.2	37.4	1115.1	46.6	9.7
49	125	73	1.71	0.51505	0.02581	13.20210	0.72163	0.18591	0.00380	2678.1	109.8	2694.2	51.6	2706.3	33.7	1.1
50	134	244	0.55	0.19301	0.00968	2.19927	0.12865	0.08264	0.00245	1137.6	52.3	1180.8	40.9	1260.8	58.0	10.8
51	125	62	2.02	0.18064	0.00493	1.98761	0.06477	0.07980	0.00183	1070.4	26.9	1111.3	22.0	1192.2	45.2	11.4
52	121	83	1.46	0.18819	0.00516	2.09515	0.06061	0.08075	0.00172	1111.5	28.0	1147.2	19.9	1215.3	41.9	9.3
53	174	84	2.09	0.46833	0.01438	11.81964	0.33214	0.18304	0.00306	2476.2	63.1	2590.2	26.3	2680.6	27.7	8.3
54	208	317	0.65	0.53022	0.01394	14.14539	0.35254	0.19349	0.00323	2742.4	58.7	2759.5	23.6	2772.0	27.4	1.1
55	248	147	1.68	0.53422	0.01394	13.26386	0.32625	0.18007	0.00332	2759.2	58.6	2698.6	23.2	2653.5	30.5	-3.8
56	472	270	1.75	0.07738	0.00257	0.62637	0.02104	0.05871	0.00148	480.5	15.4	493.8	13.1	556.3	55.0	15.8
57	463	122	3.78	0.35167	0.01799	8.27848	0.40192	0.17073	0.00339	1942.6	85.8	2262.0	44.0	2564.8	33.2	32.0
58	902	792	1.14	0.43691	0.01527	9.63821	0.26045	0.15999	0.00312	2336.8	68.5	2400.8	24.9	2455.6	33.0	5.1
59	487	350	1.39	0.18913	0.00616	1.93163	0.05901	0.07407	0.00134	1116.7	33.4	1092.1	20.4	1043.4	36.6	-6.6
60	470	22	21.07	0.16085	0.00593	1.65851	0.05702	0.07478	0.00204	961.5	32.9	992.8	21.8	1062.6	54.9	10.5
71	438	255	1.72	0.32789	0.01983	5.03940	0.29917	0.11147	0.00176	1828.1	96.3	1826.0	50.3	1823.5	28.7	-0.3
72	305	144	2.12	0.18216	0.01096	2.22325	0.14944	0.08852	0.00391	1078.7	59.8	1188.4	47.1	1393.8	84.7	29.2
73	49	51	0.95	0.24014	0.01057	2.83833	0.13385	0.08572	0.00157	1387.4	55.0	1365.7	35.4	1331.9	35.4	-4.0
74	172	135	1.27	0.51277	0.02776	12.61488	0.59789	0.17843	0.00399	2668.4	118.3	2651.3	44.6	2638.3	37.2	-1.1
75	247	179	1.38	0.17923	0.00845	1.94443	0.07821	0.07868	0.00175	1062.8	46.2	1096.5	27.0	1164.2	44.1	9.5
76	337	210	1.60	0.25795	0.01189	3.10879	0.13274	0.08741	0.00180	1479.3	60.9	1434.9	32.8	1369.6	39.6	-7.4
77	146	123	1.19	0.18371	0.00865	1.91041	0.07758	0.07542	0.00133	1087.2	47.1	1084.7	27.1	1079.7	35.3	-0.7

Spot	Conc. (ppm)	Ratios						Ages					
		[U]	[Th]	$^{206}\text{Pb}/^{238}\text{U}$	$\pm 2\sigma$	$^{207}\text{Pb}/^{235}\text{U}$	$\pm 2\sigma$	$^{206}\text{Pb}/^{204}\text{Pb}$	$\pm 2\sigma$	$^{207}\text{Pb}/^{238}\text{U} \pm 2\sigma$	$^{207}\text{Pb}/^{235}\text{U} \pm 2\sigma$	$^{207}\text{Pb}/^{206}\text{Pb} \pm 2\sigma$	$\pm 2\sigma$
78	395	187	2.12	0.18463	0.00850	1.96167	0.08988	0.07706	0.00219	1092.2	46.2	1102.5	30.8
79	42	37	1.15	0.19962	0.01008	2.07174	0.09332	0.07527	0.00142	1173.3	54.2	1139.5	30.9
80	206	128	1.61	0.17430	0.00841	1.77390	0.08044	0.07381	0.00180	1035.7	46.2	1035.9	29.5
81	132	67	1.97	0.20446	0.00741	2.09464	0.07384	0.07430	0.00193	1199.2	39.7	1147.0	24.2
82	181	64	2.85	0.43747	0.01393	11.29892	0.30004	0.18732	0.00340	2339.3	62.5	2548.1	24.8
83	303	175	1.73	0.55895	0.01895	15.06879	0.44525	0.19553	0.00413	2862.3	78.4	2819.6	28.1
84	48	76	0.63	0.18450	0.00580	2.09130	0.06156	0.08221	0.00235	1091.5	31.6	1146.0	20.2
85	124	65	1.91	0.18427	0.00617	1.89878	0.06393	0.07473	0.00191	1090.3	33.6	1080.7	22.4
86	49	51	0.95	0.16011	0.00459	1.62854	0.05390	0.07377	0.00194	957.4	25.5	981.3	20.8
87	172	135	1.27	0.17410	0.00503	1.81129	0.06035	0.07546	0.00218	1034.6	27.6	1049.5	21.8
88	247	179	1.38	0.52137	0.01346	13.69032	0.39572	0.19044	0.00377	2705.0	57.1	2728.5	27.4
89	251	24	10.49	0.22103	0.00585	2.52992	0.06788	0.08301	0.00145	1287.3	30.9	1280.7	19.5
90	288	198	1.45	0.52160	0.01509	13.55684	0.34481	0.18850	0.00295	2706.0	64.0	2719.3	24.1
91	80	39	2.04	0.18500	0.00462	1.95138	0.05921	0.07650	0.00156	1094.2	25.1	1098.9	20.4
92	327	207	1.58	0.26810	0.00680	3.43614	0.09310	0.09296	0.00176	1531.1	34.6	1512.7	21.3
93	300	157	1.91	0.20762	0.00746	2.31818	0.11937	0.08098	0.00253	1216.1	39.8	1217.9	36.5
94	308	60	5.15	0.22510	0.00503	2.61323	0.06121	0.08420	0.00133	1308.8	26.5	1304.4	17.2
95	310	60	5.18	0.25447	0.00627	3.22467	0.09767	0.09191	0.00234	1461.5	32.2	1463.1	23.5
NVP-7-86 (25 μm)													
1	35	49	0.72	0.30644	0.00585	4.68968	0.12251	0.11099	0.00210	1723.2	28.9	1765.4	21.9
2	171	252	0.68	0.16986	0.00250	1.71855	0.03525	0.07338	0.00096	1011.3	13.8	1015.5	13.2
3	314	192	1.63	0.18168	0.00381	1.88964	0.04106	0.07543	0.00090	1076.2	20.8	1077.5	14.4
4	329	220	1.49	0.18626	0.00449	1.92157	0.04838	0.07482	0.00095	1101.1	24.4	1088.6	16.8
5	290	153	1.89	0.16149	0.00376	1.611765	0.04006	0.07265	0.00103	965.0	20.9	977.1	15.5
6	77	48	1.61	0.25410	0.00397	3.27918	0.05760	0.09360	0.00130	1459.6	20.4	1476.1	13.7
7	37	26	1.43	0.18556	0.00506	1.95172	0.05926	0.07628	0.00192	1097.3	27.5	1099.0	20.4
8	69	58	1.20	0.17920	0.00332	1.90800	0.04525	0.07722	0.00143	1062.6	18.2	1083.9	15.8
9	65	34	1.90	0.18753	0.00354	2.01382	0.04549	0.07789	0.00146	1108.0	19.2	1120.2	15.3
10	100	76	1.31	0.20981	0.00414	2.40275	0.05347	0.08306	0.00137	1227.8	22.0	1243.4	16.0
11	334	170	1.96	0.50833	0.01243	11.99195	0.26125	0.17110	0.00302	2649.5	53.1	2603.8	20.4
12	429	42	10.17	0.18712	0.00432	2.03137	0.04258	0.07874	0.00111	1105.7	23.5	1126.1	14.3

Spot	Conc. (ppm)	Ratios										% Disc
		[U]	[Th]	$^{206}\text{Pb}/^{238}\text{U}$	$^{207}\text{Pb}/^{238}\text{U} \pm 2\sigma$	$^{207}\text{Pb}/^{235}\text{U} \pm 2\sigma$	$^{206}\text{Pb}/^{207}\text{Pb} \pm 2\sigma$	$^{206}\text{Pb}/^{238}\text{U} \pm 2\sigma$	$^{207}\text{Pb}/^{235}\text{U} \pm 2\sigma$	$^{207}\text{Pb}/^{206}\text{Pb} \pm 2\sigma$		
13	44	58	0.76	0.20311	0.00398	2.26366	0.05512	0.08083	0.00192	1192.0	21.3	1201.0
14	179	265	0.68	0.15869	0.00296	1.61713	0.02650	0.07391	0.00126	949.5	16.5	976.9
15	69	52	1.32	0.48484	0.00939	12.47217	0.23416	0.18657	0.00271	2548.3	40.8	2640.6
16	88	57	1.55	0.15169	0.00339	1.66170	0.05861	0.07945	0.00299	910.4	19.0	994.0
17	93	117	0.80	0.51875	0.01110	14.02097	0.22833	0.19603	0.00317	2693.9	47.1	2751.1
18	66	39	1.69	0.20720	0.00728	3.14459	0.23028	0.11007	0.00547	1213.9	38.9	1443.7
19	87	80	1.09	0.16531	0.00366	1.68951	0.03780	0.07413	0.00156	986.2	20.3	1004.6
20	169	177	0.95	0.16582	0.00385	1.79134	0.05426	0.07835	0.00141	989.0	21.3	1042.3
21	167	81	2.06	0.35902	0.00674	6.24338	0.10947	0.12612	0.00167	1977.5	32.0	2010.5
22	186	154	1.21	0.16907	0.00402	1.77191	0.03839	0.07601	0.00128	1007.0	22.2	1035.2
23	585	270	2.16	0.20631	0.00585	2.48064	0.07108	0.08721	0.00156	1209.1	31.3	1266.4
24	7	0	44.35	0.15213	0.00464	1.73640	0.10264	0.08278	0.00455	912.9	26.0	1022.1
25	184	93	1.99	0.22033	0.00389	2.65444	0.04638	0.08738	0.00125	1283.6	20.6	1315.9
26	171	101	1.69	0.23356	0.00449	2.87682	0.05340	0.08933	0.00125	1353.1	23.5	1375.9
27	45	38	1.19	0.16566	0.00331	1.70190	0.05057	0.07451	0.00202	988.2	18.3	1009.2
28	55	57	0.97	0.21609	0.00472	2.52033	0.06945	0.08459	0.00207	1261.2	25.0	1277.9
29	145	64	2.26	0.52505	0.00817	14.41260	0.26012	0.19908	0.00250	2720.6	34.5	2777.3
30	190	91	2.08	0.16622	0.00367	1.70033	0.03524	0.07419	0.00113	991.2	20.3	1008.7
31	152	83	1.84	0.45356	0.00919	10.57538	0.21541	0.16910	0.00200	2411.1	40.7	2486.6
32	785	211	3.72	0.32498	0.00676	5.20241	0.09960	0.11610	0.00140	1814.0	32.9	1853.0
33	195	90	2.17	0.21841	0.00506	2.60090	0.05554	0.08637	0.00125	1273.5	26.8	1300.9
34	150	62	2.42	0.21720	0.00428	2.55899	0.04949	0.08545	0.00134	1267.0	22.7	1289.0
35	432	530	0.81	0.15976	0.00309	1.58748	0.02808	0.07207	0.00098	955.4	17.2	965.3
36	148	40	3.70	0.54166	0.01140	15.19194	0.28266	0.20341	0.00294	2790.4	47.7	2827.3
37	357	141	2.53	0.14151	0.00302	1.60991	0.04299	0.08251	0.00178	853.2	17.1	974.1
38	225	184	1.22	0.22843	0.00550	2.57464	0.06688	0.08174	0.00129	1326.3	28.9	1329.5
39	140	126	1.11	0.49442	0.00968	12.61296	0.25915	0.18502	0.00271	2589.8	41.8	2651.2
40	639	97	6.56	0.23092	0.00606	3.08684	0.06862	0.09695	0.00201	1339.3	31.7	1429.4
41	306	227	1.35	0.24249	0.00483	3.23142	0.06796	0.09665	0.00139	1399.6	25.1	1464.7
42	351	150	2.34	0.17208	0.00428	1.75586	0.04626	0.07401	0.00131	1023.5	23.5	1029.3
43	290	411	0.71	0.45265	0.00884	11.60217	0.22194	0.18590	0.00276	2407.0	39.2	2572.8

Spot	Conc. (ppm)	Ratios						Ages					
		[U]	[Th]	$^{206}\text{Pb}/^{238}\text{U}$	$^{207}\text{Pb}/^{235}\text{U}$	$\pm 2\sigma$	$^{207}\text{Pb}/^{206}\text{Pb}$	$\pm 2\sigma$	$^{206}\text{Pb}/^{238}\text{U} \pm 2\sigma$	$^{207}\text{Pb}/^{235}\text{U} \pm 2\sigma$	$^{207}\text{Pb}/^{206}\text{Pb} \pm 2\sigma$	$\pm 2\sigma$	
44	166	76	2.18	0.21141	0.00391	2.50867	0.04374	0.08606	0.00152	1236.3	20.8	1274.5	12.7
45	524	594	0.88	0.26365	0.00629	3.65824	0.07620	0.10063	0.00136	1508.5	32.1	1562.3	16.6
46	303	122	2.49	0.32131	0.00565	5.00304	0.09009	0.11293	0.00133	1796.1	27.6	1819.8	15.2
47	146	61	2.38	0.16387	0.00340	1.64566	0.03433	0.07284	0.00113	978.2	18.8	987.9	13.2
48	1587	1326	1.20	0.13168	0.01269	3.19249	0.39241	0.17584	0.00676	797.4	72.3	1455.3	95.3
49	36	32	1.11	0.16789	0.00357	1.78023	0.05350	0.07691	0.00197	1000.5	19.7	1038.3	19.5
50	54	39	1.41	0.16686	0.00346	2.01020	0.05386	0.08737	0.00185	994.8	19.1	1119.0	18.2
51	48	59	0.81	0.21470	0.00441	2.57172	0.06137	0.08687	0.00173	1253.8	23.4	1292.6	17.4
52	146	70	2.07	0.53469	0.00943	14.88946	0.32275	0.20196	0.00256	2761.2	39.6	2808.2	20.6
53	515	329	1.57	0.23628	0.00594	2.88366	0.06498	0.08851	0.00104	1367.3	31.0	1377.6	17.0
54	132	117	1.13	0.22465	0.00478	2.81036	0.05725	0.09073	0.00135	1306.4	25.2	1358.3	15.3
55	324	255	1.27	0.17073	0.00402	1.75452	0.04108	0.07453	0.00125	1016.2	22.1	1028.8	15.1
56	235	366	0.64	0.48633	0.00950	12.29992	0.21148	0.18343	0.00207	2554.8	41.2	2627.6	16.1
57	145	93	1.55	0.16785	0.00336	1.75615	0.03345	0.07588	0.00108	1000.3	18.5	1029.4	12.3
58	58	12	4.66	0.33022	0.00701	5.16539	0.10949	0.11345	0.00175	1839.5	34.0	1846.9	18.0
59	309	225	1.37	0.21708	0.00468	2.66524	0.04891	0.08905	0.00122	1266.4	24.8	1318.9	13.5
60	344	270	1.28	0.17085	0.00329	1.77616	0.03171	0.07540	0.00104	1016.8	18.1	1036.8	11.6
61	446	201	2.22	0.222251	0.00514	2.67425	0.06553	0.08717	0.00104	1295.1	27.1	1321.4	18.1
62	175	85	2.05	0.17084	0.00345	1.77204	0.04162	0.07523	0.00105	1016.7	19.0	1035.3	15.2
63	129	85	1.53	0.49613	0.01032	12.71862	0.27676	0.18593	0.00241	2597.1	44.5	2659.0	20.5
64	161	69	2.33	0.70797	0.01609	34.00361	0.68109	0.34835	0.00444	3450.8	60.7	3610.1	19.8
65	42	28	1.48	0.16373	0.00321	1.74732	0.04270	0.07740	0.00177	977.5	17.8	1026.2	15.8
66	109	21	5.17	0.31417	0.00655	4.85318	0.10335	0.11204	0.00158	1761.2	32.1	1794.2	17.9
67	194	108	1.80	0.24843	0.00532	3.10357	0.07365	0.09061	0.00121	1430.4	27.5	1433.6	18.2
68	179	188	0.95	0.55192	0.01063	15.43096	0.33978	0.20277	0.00220	2833.2	44.2	2842.2	21.0
69	232	83	2.79	0.17994	0.00451	1.83073	0.04890	0.07379	0.00107	1066.7	24.6	1056.5	17.5
70	123	29	4.23	0.353387	0.00874	6.30342	0.15203	0.12919	0.00246	1953.0	41.6	2018.9	21.1
71	148	75	1.98	0.17882	0.00429	1.82431	0.04566	0.07399	0.00133	1060.5	23.4	1054.2	16.4
72	291	121	2.40	0.23359	0.00512	2.80743	0.06448	0.08717	0.00131	1353.3	26.8	1357.5	17.2
73	476	270	1.76	0.18895	0.00561	2.06220	0.05184	0.07916	0.00096	1115.7	30.4	1136.4	17.2
74	112	141	0.79	0.16330	0.00448	1.61165	0.03857	0.07158	0.00126	975.1	24.9	974.7	15.0

Spot	Conc. (ppm)	Ratios						Ages					
		[U]	[Th]	$^{206}\text{Pb}/^{238}\text{U}$	$^{207}\text{Pb}/^{235}\text{U}$	$\pm 2\sigma$	$^{207}\text{Pb}/^{206}\text{Pb}$	$\pm 2\sigma$	$^{206}\text{Pb}/^{238}\text{U} \pm 2\sigma$	$^{207}\text{Pb}/^{235}\text{U} \pm 2\sigma$	$^{207}\text{Pb}/^{206}\text{Pb} \pm 2\sigma$	% Disc	
75	179	305	0.59	0.14975	0.00431	1.53790	0.05156	0.07448	0.00152	899.6	24.1	945.7	20.6
76	10	5	1.80	0.16684	0.00498	1.81107	0.07531	0.07873	0.00328	994.7	27.5	1049.5	27.2
77	127	90	1.42	0.17255	0.00464	1.77268	0.04034	0.07451	0.00128	1026.1	25.5	1035.5	14.8
78	124	40	3.07	0.52600	0.01530	14.03444	0.30176	0.19351	0.00306	2724.6	64.6	2752.0	20.4
79	67	44	1.53	0.19017	0.00585	1.94289	0.05763	0.07410	0.00169	1122.3	31.7	1096.0	19.9
80	24	41	0.59	0.15412	0.00435	1.57585	0.05359	0.07416	0.00249	924.0	24.3	960.7	21.1
81	200	148	1.35	0.15834	0.00380	2.02268	0.06220	0.09265	0.00212	947.6	21.1	1123.2	20.9
82	183	97	1.88	0.17838	0.00412	1.84042	0.03788	0.07483	0.00096	1058.1	22.6	1060.0	13.5
83	320	419	0.76	0.26931	0.00652	3.73601	0.08212	0.10061	0.00117	1537.3	33.1	1579.1	17.6
84	46	24	1.88	0.18335	0.00362	1.91250	0.04356	0.07565	0.00150	1085.2	19.7	1085.5	15.2
85	259	173	1.50	0.17803	0.00511	1.77339	0.04439	0.07225	0.00101	1056.2	28.0	1035.8	16.3
86	35	39	0.88	0.22691	0.00509	2.76335	0.07572	0.08832	0.00183	1318.3	26.7	1345.7	20.4
87	138	74	1.86	0.17187	0.00275	1.78670	0.03368	0.07540	0.00117	1022.4	15.1	1040.6	12.3
88	402	59	6.80	0.50113	0.00941	12.57991	0.18450	0.18207	0.00236	2618.6	40.4	2648.7	13.8
89	137	64	2.15	0.17175	0.00318	1.75576	0.03019	0.07414	0.00116	1021.7	17.5	1029.3	11.1
90	85	117	0.72	0.23547	0.00418	2.97612	0.07262	0.09167	0.00187	1363.1	21.8	1401.5	18.5
91	109	139	0.78	0.50515	0.01004	13.16591	0.19657	0.18903	0.00235	2635.9	43.0	2691.6	14.1
92	265	199	1.33	0.36517	0.00762	9.40302	0.20389	0.18675	0.00221	2006.7	36.0	2378.1	19.9
93	110	149	0.74	0.18991	0.00388	2.17754	0.04606	0.08316	0.00146	1120.9	21.0	1173.9	14.7
94	135	84	1.60	0.17453	0.00360	1.79807	0.03776	0.07472	0.00102	1037.0	19.8	1044.8	13.7
95	75	75	1.01	0.18873	0.00365	2.06025	0.04421	0.07917	0.00109	1114.5	19.8	1135.7	14.7
96	135	92	1.46	0.16810	0.00270	1.76030	0.02630	0.07595	0.00117	1001.6	14.9	1031.0	9.7
97	159	84	1.90	0.21796	0.00335	2.58364	0.03968	0.08597	0.00105	1271.1	17.7	1296.0	11.2
98	245	135	1.82	0.20900	0.00497	2.48663	0.05873	0.08629	0.00114	1223.5	26.5	1268.1	17.1
99	137	97	1.42	0.17939	0.00426	1.87153	0.05161	0.07567	0.00118	1063.6	23.3	1071.1	18.2
100	325	260	1.25	0.47395	0.01423	12.10463	0.31646	0.18523	0.00232	2500.9	62.2	2612.5	24.5
101	166	139	1.20	0.54909	0.01269	16.22627	0.33188	0.21433	0.00211	2821.4	52.8	2890.2	19.6
102	244	140	1.74	0.17163	0.00357	1.73939	0.03203	0.07350	0.00092	1021.1	19.6	1023.2	11.9
103	119	69	1.72	0.25457	0.00577	3.29139	0.06868	0.09377	0.00117	1462.0	29.6	1479.0	16.3
104	49	37	1.32	0.60546	0.01104	16.89096	0.32674	0.20233	0.00251	3051.8	44.3	2928.7	18.5
105	201	162	1.24	0.34967	0.00701	5.86951	0.10707	0.12174	0.00139	1933.0	33.5	1956.7	15.8

Spot	Conc. (ppm)	Ratios										Ages				
		[U]	[Th]	U/Th	$^{206}\text{Pb}/^{238}\text{U}$	$\pm 2\sigma$	$^{207}\text{Pb}/^{235}\text{U}$	$\pm 2\sigma$	$^{207}\text{Pb}/^{206}\text{Pb}$	$\pm 2\sigma$	$^{206}\text{Pb}/^{238}\text{U} \pm 2\sigma$	$^{207}\text{Pb}/^{235}\text{U} \pm 2\sigma$	$^{207}\text{Pb}/^{206}\text{Pb} \pm 2\sigma$	% Disc		
106	158	102	1.54	0.48778	0.00973	12.64611	0.21666	0.18803	0.00190	2561.1	42.1	2653.7	16.1	2725.0	16.7	6.4
107	98	155	0.63	0.20350	0.00603	2.41443	0.06949	0.08605	0.00196	1194.1	32.3	1246.9	20.7	1339.3	44.1	12.2
108	232	201	1.15	0.24667	0.00592	3.16127	0.06882	0.09295	0.00120	1421.3	30.6	1447.8	16.8	1486.8	24.4	4.6
109	271	173	1.56	0.24858	0.00620	3.11754	0.06787	0.09096	0.00107	1431.1	32.0	1437.0	16.7	1445.8	22.4	1.0
110	331	276	1.20	0.16660	0.00447	1.69968	0.04448	0.07399	0.00097	993.3	24.7	1008.4	16.7	1041.3	26.6	4.8
111	395	234	1.69	0.39658	0.01048	7.83026	0.19768	0.14320	0.00196	2153.3	48.4	2211.7	22.7	2266.3	23.6	5.2
112	131	80	1.64	0.19712	0.00529	2.27835	0.06159	0.08383	0.00143	1159.8	28.5	1205.6	19.1	1288.6	33.3	11.1
113	813	524	1.55	0.32755	0.00739	5.08072	0.11472	0.11250	0.00150	1826.5	35.9	1832.9	19.2	1840.1	24.2	0.7
114	122	64	1.92	0.19397	0.00443	2.04043	0.05535	0.07629	0.00143	1142.8	23.9	1129.1	18.5	1102.8	37.6	-3.5
115	145	106	1.36	0.19903	0.00472	2.76060	0.06769	0.10060	0.00259	1170.1	25.4	1345.0	18.3	1635.2	47.7	39.7

Table 2 – Lower Head Formation

Spot	Conc. (ppm)	Ratios						Ages					
		[U]	[Th]	U/Th	$^{206}\text{Pb}/^{238}\text{U}$	$\pm 2\sigma$	$^{207}\text{Pb}/^{235}\text{U}$	$\pm 2\sigma$	$^{207}\text{Pb}/^{206}\text{Pb}$	$\pm 2\sigma$	$^{207}\text{Pb}/^{235}\text{U} \pm 2\sigma$	$^{207}\text{Pb}/^{206}\text{Pb} \pm 2\sigma$	% Disc
NPM-ID-86 (25 μm)													
1	68	38	1.79	0.17122	0.00424	1.79275	0.05417	0.07594	0.00205	1018.8	23.3	1042.8	19.7
2	71	48	1.48	0.27460	0.00597	3.71873	0.08994	0.09822	0.00190	1564.1	30.2	1575.4	19.4
3	66	29	2.28	0.28789	0.00673	4.01438	0.09451	0.10113	0.00187	1631.0	33.7	1637.1	19.1
4	28	56	0.51	0.16045	0.00400	1.66033	0.06479	0.07505	0.00281	959.3	22.2	993.5	24.7
5	40	29	1.37	0.17762	0.00452	1.85609	0.06384	0.07579	0.00246	1053.9	24.7	1065.6	22.7
6	152	234	0.65	0.52393	0.01157	13.73819	0.30349	0.19017	0.00273	2715.8	48.9	2731.8	20.9
7	74	31	2.37	0.21259	0.00599	2.62295	0.08917	0.08949	0.00267	1242.6	31.9	1307.1	25.0
8	28	17	1.65	0.18127	0.00783	1.82202	0.10163	0.07290	0.00396	1073.9	42.7	1053.4	36.6
9	54	33	1.63	0.20777	0.00567	2.38822	0.08313	0.08337	0.00259	1216.9	30.3	1239.1	24.9
10	69	59	1.17	0.17703	0.00430	1.82167	0.05461	0.07463	0.00184	1050.7	23.5	1053.3	19.7
11	21	19	1.06	0.24280	0.00731	3.26335	0.14435	0.09748	0.00411	1401.3	37.9	1472.4	34.4
12	191	77	2.47	0.18665	0.00404	1.97512	0.04997	0.07675	0.00148	1103.2	22.0	1107.1	17.1
13	196	113	1.73	0.21712	0.00609	2.65455	0.07535	0.08867	0.00215	1266.6	32.2	1315.9	20.9
14	60	47	1.27	0.15897	0.00397	1.58357	0.05360	0.07225	0.00223	951.0	22.1	963.8	21.1
15	164	70	2.34	0.17471	0.00402	1.80183	0.04553	0.07480	0.00154	1038.0	22.1	1046.1	16.5
16	171	68	2.51	0.17049	0.00463	1.76648	0.07536	0.07515	0.00232	1014.8	25.5	1033.2	27.7
17	132	91	1.44	0.16423	0.00410	1.67638	0.05385	0.07403	0.00187	980.2	22.7	999.6	20.4
18	417	244	1.71	0.17860	0.00381	1.87277	0.04825	0.07605	0.00155	1059.3	20.8	1071.5	17.1
19	89	96	0.93	0.24499	0.00715	3.02825	0.11285	0.08965	0.00283	1412.6	37.0	1414.8	28.5
20	210	87	2.41	0.48397	0.01138	12.53209	0.32219	0.18780	0.00325	2544.5	49.5	2645.1	24.2
21	51	29	1.78	0.55659	0.01475	15.46762	0.46570	0.20155	0.00392	2852.5	61.1	2844.5	28.7
22	454	430	1.05	0.13500	0.00545	1.39376	0.05683	0.07488	0.00154	816.3	31.0	886.3	24.1
23	223	80	2.80	0.23139	0.00815	2.73919	0.09039	0.08586	0.00145	1341.8	42.7	1339.2	24.6
24	450	126	3.57	0.32585	0.00926	5.06854	0.13541	0.11281	0.00175	1818.2	45.0	1830.9	22.7
25	846	406	2.08	0.33693	0.01156	5.69893	0.20241	0.12268	0.00193	1871.9	55.7	1931.2	30.7
26	575	24	23.97	0.17591	0.00568	1.80622	0.05752	0.07447	0.00126	1044.6	31.2	1047.7	20.8
27	66	72	0.92	0.24096	0.00783	3.03433	0.08477	0.09133	0.00218	1391.7	40.7	1416.3	21.3
28	84	42	2.00	0.22608	0.00824	2.81244	0.09106	0.09022	0.00225	1313.9	43.3	1358.9	24.3

Spot	Conc. (ppm)	Ratios						Ages				
		[U]	[Th]	$^{206}\text{Pb}/^{238}\text{U}$	$\pm 2\sigma$	$^{207}\text{Pb}/^{235}\text{U}$	$\pm 2\sigma$	$^{206}\text{Pb}/^{207}\text{Pb}$	$\pm 2\sigma$	$^{207}\text{Pb}/^{235}\text{U} \pm 2\sigma$	$^{207}\text{Pb}/^{206}\text{Pb} \pm 2\sigma$	
29	83	73	1.13	0.44506	0.01547	11.12394	0.29493	0.18128	0.00318	2373.3	69.0	
30	176	83	2.12	0.17189	0.00501	1.83398	0.05110	0.07738	0.00192	1022.5	27.6	
31	73	76	0.96	0.48373	0.01282	11.38255	0.28727	0.17066	0.00283	2543.5	55.7	
32	127	141	0.90	0.17313	0.00525	1.78081	0.05942	0.07460	0.00146	1029.3	28.9	
33	68	63	1.07	0.18156	0.00529	2.42241	0.15419	0.09677	0.00449	1075.5	28.9	
34	113	148	0.76	0.51780	0.01123	13.19521	0.28825	0.18482	0.00225	2689.8	47.7	
35	160	85	1.89	0.18065	0.00502	1.91245	0.05432	0.07678	0.00129	1070.5	27.4	
36	296	197	1.50	0.17335	0.00436	1.80733	0.04529	0.07562	0.00122	1030.6	24.0	
37	59	94	0.62	0.17764	0.00492	1.88272	0.06638	0.07687	0.00195	1054.1	27.0	
38	198	72	2.74	0.29784	0.00727	4.39562	0.10645	0.10704	0.00154	1680.6	36.1	
39	143	53	2.69	0.25615	0.00604	3.34244	0.09389	0.09464	0.00175	1470.1	31.0	
40	81	56	1.45	0.18465	0.00425	2.02444	0.05685	0.07952	0.00183	1092.3	23.2	
83	41	44	24	1.80	0.20739	0.00552	2.35805	0.08191	0.08246	0.00235	1214.9	29.5
42	72	47	1.53	0.16366	0.00388	1.62044	0.04311	0.07181	0.00188	977.1	21.5	
43	1422	824	1.73	0.10574	0.00238	2.90049	0.09502	0.19894	0.00443	648.0	13.8	
44	146	46	3.17	0.32760	0.00660	5.28550	0.13773	0.11701	0.00224	1826.7	32.1	
45	11	23	0.47	0.47788	0.01315	11.19947	0.41422	0.16997	0.00542	2518.0	57.4	
46	37	30	1.22	0.16446	0.00341	1.75976	0.06856	0.07761	0.00276	981.5	18.9	
47	95	47	2.02	0.50305	0.00925	16.05959	0.511121	0.23154	0.00614	2626.9	39.7	
48	782	57	13.80	0.40191	0.01023	9.14747	0.33094	0.16507	0.00417	2177.8	47.0	
49	51	47	1.10	0.50696	0.01157	13.08642	0.44356	0.18722	0.00492	2643.6	49.5	
50	92	37	2.49	0.17093	0.00404	1.77516	0.05938	0.07532	0.00216	1017.2	22.3	
51	88	22	4.07	0.17960	0.00436	1.85040	0.06528	0.07472	0.00212	1064.8	23.9	
52	133	126	1.06	0.17305	0.00555	1.76016	0.08030	0.07377	0.00237	1028.9	30.5	
53	90	72	1.25	0.19510	0.00490	2.08891	0.07501	0.07765	0.00216	1148.9	26.4	
54	31	15	2.12	0.18983	0.00617	2.68361	0.20577	0.10253	0.00598	1120.4	33.4	
55	20	8	2.55	0.20265	0.00557	2.45493	0.10311	0.08786	0.00370	1189.5	29.8	
56	24	17	1.44	0.16337	0.00495	1.69881	0.08095	0.07542	0.00345	975.5	27.4	
57	64	171	0.37	0.50637	0.01315	13.33993	0.42257	0.19107	0.00318	2641.1	56.3	
58	281	89	3.17	0.17705	0.00404	1.82472	0.04840	0.07475	0.00108	1050.8	22.1	
59	108	121	0.90	0.50328	0.01238	12.93037	0.36869	0.18634	0.00245	2627.9	53.1	

Spot	Conc. (ppm)	Ratios						Ages					
		[Th]	U/Th	$^{206}\text{Pb}/^{238}\text{U}$	$\pm 2\sigma$	$^{207}\text{Pb}/^{235}\text{U}$	$\pm 2\sigma$	$^{206}\text{Pb}/^{207}\text{Pb}$	$\pm 2\sigma$	$^{207}\text{Pb}/^{235}\text{U} \pm 2\sigma$	$^{207}\text{Pb}/^{206}\text{Pb}$	$\pm 2\sigma$	
60	162	122	1.32	0.66807	0.01570	25.97441	0.61431	0.28198	0.00399	3298.4	60.7	3345.6	23.1
61	129	94	1.37	0.18780	0.00413	2.06362	0.09625	0.07969	0.00299	1109.5	22.4	1136.8	31.9
62	112	86	1.30	0.43766	0.00916	10.48483	0.55609	0.17375	0.00798	2340.2	41.1	2478.6	49.2
63	237	87	2.73	0.33520	0.00725	5.37284	0.24329	0.11625	0.00446	1863.5	35.0	1880.5	38.8
64	346	117	2.95	0.17651	0.00322	1.83141	0.06765	0.07525	0.00249	1047.9	17.6	1056.8	24.3
65	219	101	2.18	0.55543	0.01423	15.42645	0.61252	0.20144	0.00698	2847.7	59.0	2841.9	37.9
66	13	4	3.12	0.24490	0.00621	2.96642	0.15416	0.08785	0.00456	1412.1	32.2	1399.1	39.5
67	63	58	1.09	0.58818	0.01391	20.56771	1.08405	0.25362	0.01253	2982.0	56.5	3118.4	51.1
69	34	19	1.78	0.17120	0.00451	1.77466	0.10136	0.07518	0.00432	1018.7	24.8	1036.2	37.1
71	56	30	1.89	0.62296	0.01582	22.88063	1.10283	0.26638	0.01059	3121.7	62.8	3221.9	46.9
72	72	61	1.19	0.17649	0.00425	1.83877	0.05578	0.07556	0.00214	1047.8	23.3	1059.4	20.0
73	83	47	1.75	0.17175	0.00390	1.81832	0.05026	0.07678	0.00156	1021.8	21.5	1052.1	18.1
74	70	51	1.38	0.19599	0.00471	2.08855	0.06103	0.07729	0.00196	1153.7	25.4	1145.0	20.1
75	128	118	1.09	0.17409	0.00356	1.84371	0.04287	0.07681	0.00140	1034.6	19.5	1061.2	15.3
76	133	75	1.78	0.16618	0.00321	1.69387	0.04585	0.07393	0.00162	991.0	17.7	1006.2	17.3
77	82	59	1.38	0.23119	0.00443	2.78745	0.06980	0.08745	0.00208	1340.7	23.2	1352.2	18.7
78	12	6	1.91	0.16604	0.00652	1.67765	0.10420	0.07328	0.00453	990.3	36.1	1000.1	39.5
79	48	31	1.56	0.33451	0.00784	5.25788	0.14424	0.11400	0.00218	1860.2	37.9	1862.1	23.4
80	135	96	1.41	0.18064	0.00466	1.87900	0.06628	0.07544	0.00274	1070.5	25.5	1073.7	23.4
81	138	193	0.71	0.27885	0.00687	3.91666	0.13422	0.10187	0.00369	1585.6	34.7	1617.1	27.7
82	250	549	0.46	0.52362	0.01323	13.55019	0.47963	0.18769	0.00822	2714.5	56.0	2718.8	33.5
83	59	37	1.58	0.33003	0.00791	5.16350	0.20041	0.11347	0.00532	1838.5	38.4	1846.6	33.0
84	79	64	1.24	0.24411	0.00652	2.98007	0.16931	0.08854	0.00483	1408.0	33.8	1402.5	43.2
85	71	60	1.18	0.57077	0.01547	17.48495	0.98009	0.22218	0.01149	2911.0	63.5	2961.8	53.9
86	803	343	2.34	0.52079	0.01452	13.73261	0.85618	0.19124	0.01076	2702.5	61.5	2731.4	59.1
87	66	27	2.46	0.22723	0.00718	2.83829	0.21264	0.09059	0.00621	1319.9	37.7	1365.7	56.3
88	86	32	2.72	0.23076	0.00704	2.75817	0.20584	0.08669	0.00581	1338.5	36.9	1344.3	55.7
89	38	25	1.51	0.17155	0.00493	1.85453	0.14565	0.07841	0.00569	1020.6	27.1	1065.0	51.9
90	25	7	3.44	0.20282	0.01025	2.18219	0.17503	0.07803	0.00475	1190.5	54.9	1175.4	55.9
91	620	567	1.09	0.07768	0.00369	0.61298	0.04404	0.05723	0.00330	482.2	22.1	485.4	27.7
92	123	58	2.11	0.19126	0.01127	2.06988	0.17933	0.07849	0.00471	1128.2	61.0	1138.9	59.4

Conc. (ppm)	Spot	[U]	[Th]	Ratios						Ages							
				$^{206}\text{Pb}/^{238}\text{U}$	$\pm 2\sigma$	$^{207}\text{Pb}/^{235}\text{U}$	$\pm 2\sigma$	$^{207}\text{Pb}/^{206}\text{Pb}$	$\pm 2\sigma$	$^{206}\text{Pb}/^{238}\text{U}$	$\pm 2\sigma$	$^{207}\text{Pb}/^{235}\text{U}$	$\pm 2\sigma$	$^{207}\text{Pb}/^{206}\text{Pb}$	$\pm 2\sigma$		
93	95	103	0.92	0.18607	0.00913	2.03395	0.14546	0.07928	0.00435	1100.1	49.6	1126.9	48.7	1179.1	108.5	7.2	
94	72	36	1.99	0.18578	0.00813	1.98277	0.12539	0.07740	0.00394	1098.5	44.2	1109.7	42.7	1131.6	101.4	3.0	
95	61	26	2.38	0.19476	0.00840	2.08033	0.12913	0.07747	0.00400	1147.1	45.3	1142.3	42.6	1133.3	102.9	-1.2	
96	310	542	0.57	0.23469	0.01195	2.92138	0.20353	0.09028	0.00489	1359.0	62.4	1387.5	52.7	1431.5	103.4	5.3	
97	49	38	1.31	0.16620	0.00977	1.73817	0.07996	0.07585	0.00316	991.1	54.0	1022.8	29.7	1091.2	83.4	10.1	
98	200	103	1.93	0.20051	0.01252	2.12482	0.09591	0.07686	0.00265	1178.1	67.2	1156.9	31.2	1117.5	68.8	-5.1	
99	46	32	1.43	0.16206	0.01013	1.72632	0.09959	0.07726	0.00384	968.2	56.2	1018.4	37.1	1127.9	99.1	16.5	
100	80	121	0.66	0.17545	0.00869	1.85452	0.07251	0.07666	0.00255	1042.1	47.7	1065.0	25.8	1112.4	66.5	6.8	
101	152	64	2.39	0.18805	0.00720	1.90863	0.12173	0.07361	0.00594	1110.8	39.1	1084.1	42.5	1030.8	163.2	-7.2	
102	689	4	181.50	0.18416	0.00739	1.87428	0.14136	0.07381	0.00724	1089.7	40.2	1072.0	50.0	1036.4	198.2	-4.9	
103	75	48	1.57	0.17455	0.00718	1.83170	0.13234	0.07611	0.00623	1037.1	39.4	1056.9	47.5	1097.9	163.8	5.9	
104	56	27	2.04	0.23551	0.00849	2.81866	0.17388	0.08680	0.00593	1363.3	44.3	1360.5	46.3	1356.1	131.8	-0.5	
85	105	122	45	2.72	0.19520	0.00606	2.15769	0.13005	0.08017	0.00530	1149.5	32.7	1167.5	41.8	1201.2	130.3	4.5
106	377	300	1.26	0.28463	0.01036	4.01496	0.27834	0.10231	0.00784	1614.6	52.0	1637.2	56.4	1666.4	141.8	3.2	
107	56	33	1.67	0.29026	0.00911	3.97403	0.34846	0.09930	0.00919	1642.8	45.5	1628.9	71.3	1611.0	172.5	-1.9	
108	96	65	1.48	0.16291	0.00513	1.63386	0.14473	0.07274	0.00679	972.9	28.4	983.3	55.8	1006.6	189.3	3.5	
109	181	185	0.98	0.24476	0.00745	3.00589	0.25963	0.08907	0.00822	1411.4	38.6	1409.1	65.9	1405.7	176.8	-0.4	
110	9	11	0.81	0.39215	0.01364	7.27623	0.57211	0.13457	0.01171	2132.8	63.2	2145.9	70.3	2158.5	151.8	1.2	
111	40	17	2.35	0.17398	0.00501	1.80262	0.14205	0.07514	0.00627	1034.0	27.5	1046.4	51.5	1072.4	167.5	3.7	
112	133	58	2.28	0.23503	0.00544	2.77190	0.06896	0.08554	0.00176	1360.8	28.4	1348.0	18.6	1327.7	39.7	-2.4	
114	250	98	2.53	0.23368	0.00504	2.85118	0.06248	0.08849	0.00155	1353.7	26.3	1369.1	16.5	1393.2	33.6	2.9	
115	106	42	2.55	0.18600	0.00505	1.87779	0.05903	0.07322	0.00166	1099.7	27.4	1073.3	20.8	1020.0	45.9	-7.2	
116	53	30	1.79	0.17685	0.00475	1.82165	0.05947	0.07471	0.00222	1049.7	26.0	1053.3	21.4	1060.6	59.7	1.0	
117	167	97	1.73	0.18192	0.00433	1.97858	0.07678	0.07888	0.00209	1077.5	23.6	1108.2	26.2	1169.2	52.5	8.5	
118	94	71	1.32	0.16880	0.00503	1.73594	0.07123	0.07459	0.00217	1005.5	27.7	1022.0	26.4	1057.4	58.5	5.2	
119	203	77	2.62	0.17991	0.00347	1.85370	0.04194	0.07473	0.00139	1066.5	18.9	1064.7	14.9	1061.2	37.4	-0.5	
120	143	191	0.75	0.17747	0.00361	1.76505	0.04396	0.07213	0.00140	1053.1	19.7	1032.7	16.1	989.7	39.4	-6.0	
										NPM-4D-86 (25 μm)							
1	273	124	2.21	0.55888	0.01857	15.34142	0.51689	0.19909	0.00337	2862.0	76.8	2836.7	32.1	2818.7	27.6	-1.5	
2	1087	79095	0.01	0.27274	0.00888	4.09076	0.13612	0.10878	0.00175	1554.7	45.0	1652.5	27.2	1779.1	29.4	14.4	
3	122	65	1.89	0.18531	0.00658	1.92058	0.06692	0.07517	0.00144	1095.9	35.8	1088.3	23.3	1073.0	38.5	-2.1	

Spot	Conc. (ppm)	Ratios										% Disc				
		[U]	[Th]	U/Th	$^{206}\text{Pb}/^{238}\text{U}$	$\pm 2\sigma$	$^{207}\text{Pb}/^{235}\text{U}$	$\pm 2\sigma$	$^{207}\text{Pb}/^{206}\text{Pb}$	$\pm 2\sigma$	$^{206}\text{Pb}/^{238}\text{U}$	$\pm 2\sigma$	$^{207}\text{Pb}/^{235}\text{U} \pm 2\sigma$	$^{207}\text{Pb}/^{206}\text{Pb} \pm 2\sigma$		
4	224	181	1.24	0.30331	0.01059	4.31187	0.13234	0.10311	0.00186	1707.7	52.4	1695.6	25.3	1680.8	33.3	-1.6
5	175	281	0.62	0.32871	0.00965	5.04404	0.14432	0.11129	0.00195	1832.1	46.8	1826.7	24.2	1820.6	31.8	-0.6
6	299	87	3.44	0.17043	0.00528	1.71872	0.04784	0.07314	0.00130	1014.5	29.1	1015.5	17.9	1017.8	36.0	0.3
7	210	266	0.79	0.19055	0.00473	1.97519	0.05044	0.07518	0.00158	1124.4	25.6	1107.1	17.2	1073.2	42.2	-4.5
8	89	49	1.84	0.19262	0.00431	2.10752	0.04922	0.07936	0.00181	1135.5	23.3	1151.3	16.1	1181.0	45.1	4.0
9	113	176	0.64	0.17134	0.00393	1.98580	0.05390	0.08406	0.00204	1019.5	21.7	1110.7	18.3	1293.8	47.1	26.9
10	30	25	1.21	0.19904	0.00615	2.34899	0.07973	0.08559	0.00258	1170.2	33.0	1227.3	24.2	1329.0	58.3	13.6
11	173	145	1.19	0.51993	0.01287	13.21924	0.27986	0.18440	0.00268	2698.9	54.6	2695.4	20.0	2692.9	24.0	-0.2
12	35	31	1.14	0.25180	0.00782	2.97653	0.08964	0.08573	0.00249	1447.8	40.3	1401.6	22.9	1332.2	56.3	-8.0
13	23	38	0.60	0.18897	0.00451	2.15061	0.06428	0.08254	0.00240	1115.8	24.5	1165.3	20.7	1258.3	56.8	12.8
14	41	21	1.97	0.56975	0.01327	16.64041	0.31146	0.21183	0.00353	2906.8	54.5	2914.3	17.9	2919.6	27.0	0.4
15	325	196	1.66	0.17483	0.00341	1.80069	0.03674	0.07470	0.00125	1038.7	18.7	1045.7	13.3	1060.4	33.7	2.1
16	325	176	1.84	0.20874	0.00431	2.31983	0.04543	0.08060	0.00143	1222.1	23.0	1218.4	13.9	1211.7	34.8	-0.9
17	131	60	2.19	0.45683	0.00939	10.26404	0.18324	0.16295	0.00269	2425.5	41.5	2458.9	16.5	2486.5	27.9	2.5
18	52	53	0.99	0.59660	0.01307	18.14589	0.36438	0.22060	0.00391	3016.1	52.8	2997.5	19.3	2985.0	28.5	-1.0
19	131	115	1.14	0.32539	0.00771	4.95379	0.09137	0.11042	0.00197	1816.0	37.5	1811.5	15.6	1806.3	32.5	-0.5
20	744	189	3.95	0.16882	0.00721	1.72272	0.08012	0.07401	0.00128	1005.6	39.7	1017.0	29.9	1041.8	34.9	3.6
21	106	64	1.67	0.51363	0.02540	13.20511	0.73680	0.18646	0.00343	2672.1	108.2	2694.4	52.7	2711.2	30.3	1.5
22	87	63	1.39	0.24844	0.01401	3.05203	0.19946	0.08910	0.00215	1430.4	72.4	1420.7	50.0	1406.3	46.1	-1.7
23	147	66	2.22	0.18284	0.00864	1.85415	0.10282	0.07355	0.00174	1082.5	47.1	1064.9	36.6	1029.1	47.7	-4.9
24	11	24	0.48	0.27859	0.01208	4.09646	0.21446	0.10664	0.00367	1584.3	60.9	1653.6	42.8	1742.8	63.0	10.0
25	255	90	2.82	0.49191	0.01869	11.36634	0.48796	0.16759	0.00283	2578.9	80.7	2553.7	40.1	2533.7	28.4	-1.8
26	98	78	1.26	0.24126	0.01077	2.74268	0.13661	0.08245	0.00220	1393.2	55.9	1340.1	37.1	1256.3	52.1	-9.8
27	62	60	1.03	0.27071	0.01294	3.38514	0.18256	0.09069	0.00240	1544.4	65.7	1501.0	42.3	1440.2	50.4	-6.7
28	76	62	1.23	0.26680	0.01241	3.29131	0.16596	0.08947	0.00196	1524.5	63.1	1479.0	39.3	1414.3	41.9	-7.2
29	69	46	1.49	0.37705	0.02070	6.87535	0.40036	0.13225	0.00274	2062.5	96.9	2095.5	51.7	2128.1	36.2	3.2
30	240	94	2.54	0.19224	0.00818	1.98215	0.10982	0.07478	0.00169	1133.5	44.2	1109.5	37.4	1062.6	45.4	-6.3
31	93	59	1.57	0.19481	0.00705	2.13207	0.10064	0.07938	0.00205	1147.4	38.0	1159.3	32.6	1181.5	51.0	3.0
32	114	62	1.83	0.19311	0.00446	2.06785	0.06536	0.07766	0.00167	1138.2	24.1	1138.2	21.6	1138.3	42.8	0.0
33	229	113	2.03	0.19607	0.00455	2.12608	0.05801	0.07864	0.00151	1154.2	24.5	1157.3	18.8	1163.2	38.0	0.8
34	179	92	1.94	0.35514	0.00971	7.44447	0.37319	0.15203	0.00508	1959.1	46.2	2166.3	44.9	2368.9	57.0	20.9

Conc. (ppm)	Ratios						Ages									
	Spot	[Th]	U/Th	$^{206}\text{Pb}/^{238}\text{U}$	$\pm 2\sigma$	$^{207}\text{Pb}/^{235}\text{U}$	$\pm 2\sigma$	$^{207}\text{Pb}/^{206}\text{Pb}$	$\pm 2\sigma$	$^{206}\text{Pb}/^{238}\text{U} \pm 2\sigma$	$^{207}\text{Pb}/^{235}\text{U} \pm 2\sigma$	$^{207}\text{Pb}/^{206}\text{Pb} \pm 2\sigma$	% Disc			
35	19	1	14.72	0.21167	0.00671	2.26430	0.10182	0.07758	0.003322	1237.7	35.7	1201.2	31.7	1136.2	82.7	-8.2
36	166	64	2.58	0.56366	0.01200	15.69171	0.36271	0.20191	0.00351	2881.7	49.5	2858.2	22.1	2841.7	28.3	-1.4
37	65	57	1.13	0.17945	0.00446	1.88255	0.05683	0.07609	0.00196	1064.0	24.4	1075.0	20.0	1097.3	51.4	3.1
38	121	36	3.36	0.26078	0.00824	3.46333	0.15099	0.09632	0.00211	1493.9	42.1	1518.9	34.4	1554.0	41.2	4.0
39	106	136	0.78	0.17608	0.00380	1.82929	0.04533	0.07535	0.00161	1045.5	20.8	1056.0	16.3	1077.8	42.9	3.1
40	131	119	1.10	0.51566	0.01052	13.32060	0.28702	0.18735	0.00316	2680.7	44.7	2702.6	20.4	2719.1	27.8	1.4
41	61	42	1.44	0.17905	0.00452	1.84903	0.05447	0.07490	0.00199	1061.8	24.7	1063.1	19.4	1065.8	53.5	0.4
42	89	27	3.30	0.17911	0.00387	1.88193	0.04343	0.07621	0.00202	1062.1	21.2	1074.7	15.3	1100.5	53.0	3.6
43	3265	110953	0.03	0.28712	0.00745	4.40610	0.08616	0.11130	0.00195	1627.1	37.3	1713.5	16.2	1820.7	31.8	11.9
44	142	73	1.93	0.19508	0.00497	2.10934	0.04772	0.07842	0.00134	1148.8	26.8	1151.9	15.6	1157.6	33.9	0.8
45	82	39	2.11	0.16825	0.00414	1.71477	0.04666	0.07392	0.00162	1002.5	22.8	1014.1	17.5	1039.2	44.2	3.7
46	408	190	2.15	0.19672	0.00516	2.10245	0.04757	0.07751	0.00127	1157.7	27.8	1149.6	15.6	1134.4	32.7	-2.0
47	59	23	2.55	0.19441	0.00517	2.21114	0.05200	0.08249	0.00189	1145.2	27.9	1184.6	16.4	1257.2	44.9	9.8
48	196	165	1.19	0.56052	0.01350	17.31007	0.36736	0.22398	0.00365	2868.8	55.8	2952.2	20.4	3009.5	26.2	4.9
49	201	86	2.32	0.31400	0.00799	4.78912	0.10781	0.11062	0.00174	1760.4	39.2	1783.0	18.9	1809.6	28.6	2.8
50	103	73	1.41	0.22308	0.00535	2.57479	0.07015	0.08371	0.00171	1298.1	28.2	1293.5	19.9	1285.8	39.9	-0.9
51	13	6	2.14	0.18202	0.00567	2.00570	0.08537	0.07992	0.00339	1078.0	30.9	1117.4	28.8	1194.9	83.7	10.8
52	104	56	1.85	0.18031	0.00414	1.86843	0.05501	0.07515	0.00129	1068.7	22.6	1070.0	19.5	1072.6	34.5	0.4
53	63	28	2.23	0.17782	0.00331	1.87360	0.04749	0.07642	0.00183	1055.1	18.1	1071.8	16.8	1106.0	47.9	4.8
54	76	113	0.68	0.51605	0.01317	13.48267	0.34719	0.18949	0.00297	2682.4	56.0	2714.1	24.3	2737.7	25.8	2.1
55	258	110	2.34	0.17733	0.00420	1.76143	0.04106	0.07204	0.00128	1052.4	23.0	1031.4	15.1	987.1	36.3	-6.2
56	202	105	1.93	0.18487	0.00516	1.91505	0.05180	0.07513	0.00118	1093.5	28.1	1086.3	18.0	1072.0	31.4	-2.0
57	277	229	1.21	0.46452	0.01372	11.38215	0.31947	0.17771	0.00246	2459.5	60.4	2555.0	26.2	2631.6	23.0	7.0
58	122	101	1.20	0.22249	0.00584	2.61880	0.07412	0.08537	0.00146	1295.0	30.8	1305.9	20.8	1323.9	33.1	2.2
59	451	99	4.58	0.17224	0.00508	1.70568	0.04826	0.07182	0.00110	1024.5	28.0	1010.7	18.1	980.9	31.2	-4.3
60	65	45	1.46	0.24944	0.00697	3.12013	0.08967	0.09072	0.00187	1435.6	36.0	1437.7	22.1	1440.7	39.2	0.4
61	123	110	1.12	0.24214	0.00608	3.06869	0.07285	0.09191	0.00157	1397.8	31.5	1424.9	18.2	1465.6	32.4	4.9
62	73	43	1.70	0.47178	0.01224	10.74064	0.29530	0.16512	0.00294	2491.4	53.6	2500.9	25.5	2508.7	30.0	0.7
63	73	41	1.78	0.17216	0.00495	1.83563	0.05376	0.07733	0.00178	1024.0	27.2	1058.3	19.3	1129.7	45.9	10.3
64	64	24	2.71	0.18458	0.00526	1.92617	0.06150	0.07568	0.00169	1092.0	28.6	1090.2	21.3	1086.7	44.8	-0.5
65	349	280	1.24	0.18874	0.00656	1.91821	0.06012	0.07371	0.00156	1114.5	35.6	1087.4	20.9	1033.6	42.7	-7.3

Spot	Conc. (ppm)	Ratios										Ages				
		[U]	[Th]	$^{206}\text{Pb}/^{238}\text{U}$	$\pm 2\sigma$	$^{207}\text{Pb}/^{235}\text{U}$	$\pm 2\sigma$	$^{207}\text{Pb}/^{206}\text{Pb}$	$\pm 2\sigma$	$^{206}\text{Pb}/^{238}\text{U}$	$\pm 2\sigma$	$^{207}\text{Pb}/^{235}\text{U} \pm 2\sigma$	$^{207}\text{Pb}/^{206}\text{Pb} \pm 2\sigma$	% Disc		
66	558	336	1.66	0.31803	0.00898	5.16829	0.14550	0.11786	0.00180	1780.1	43.9	1847.4	24.0	1924.1	27.4	8.1
67	256	80	3.20	0.19836	0.00611	2.18086	0.06738	0.07974	0.00139	1166.5	32.9	1175.0	21.5	1190.6	34.3	2.1
68	19	6	2.97	0.21743	0.00751	2.64019	0.10905	0.0807	0.00320	1268.3	39.8	1311.9	30.4	1383.9	69.7	9.1
69	442	168	2.63	0.31766	0.00936	4.80416	0.14628	0.10969	0.00192	1778.3	45.8	1785.6	25.6	1794.2	31.9	0.9
70	44	21	2.04	0.20442	0.00533	2.32074	0.07219	0.08234	0.00171	1199.0	28.6	1218.7	22.1	1253.6	40.7	4.6
71	98	46	2.14	0.19405	0.00540	2.13955	0.05866	0.07997	0.00167	1143.3	29.2	1161.7	19.0	1196.1	41.2	4.6
72	89	42	2.12	0.20115	0.00635	2.22951	0.06355	0.08039	0.00143	1181.5	34.1	1190.4	20.0	1206.5	35.0	2.1
73	56	49	1.15	0.63865	0.02910	21.81807	0.94103	0.24777	0.00413	3183.7	114.5	3175.7	41.9	3170.6	26.4	-0.4
74	279	148	1.89	0.17837	0.00705	1.85413	0.07295	0.07539	0.00125	1058.1	38.6	1064.9	26.0	1078.9	33.2	2.0
75	151	96	1.57	0.27033	0.01021	3.61044	0.13952	0.09686	0.00161	1542.5	51.8	1551.8	30.7	1564.6	31.1	1.4
76	35	50	0.70	0.45796	0.01823	10.81897	0.46565	0.17134	0.00393	2430.5	80.6	2507.7	40.0	2570.8	38.3	5.8
77	148	61	2.40	0.21866	0.01078	2.67481	0.13136	0.08872	0.00151	1274.8	57.0	1321.5	36.3	1398.2	32.6	9.7
78	280	125	2.24	0.28977	0.01482	4.14451	0.20124	0.10373	0.00178	1640.4	74.1	1663.1	39.7	1692.0	31.6	3.1
79	125	54	2.29	0.19403	0.00995	2.10445	0.10515	0.07866	0.00143	1143.2	53.7	1150.3	34.4	1163.7	36.0	1.8
80	251	124	2.03	0.25683	0.01077	3.26765	0.13347	0.09228	0.00146	1473.6	55.2	1473.4	31.8	1473.1	30.1	0.0
81	42	53	0.79	0.18113	0.00793	1.90519	0.08761	0.07629	0.00240	1073.1	43.3	1082.9	30.6	1102.6	62.8	2.7
82	88	49	1.81	0.20520	0.00887	2.21852	0.09156	0.07841	0.00176	1203.2	47.4	1186.9	28.9	1157.4	44.6	-3.8
83	137	63	2.18	0.22424	0.00893	2.77332	0.09620	0.08970	0.00197	1304.2	47.0	1348.4	25.9	1419.1	42.1	8.8
84	56	33	1.69	0.16998	0.00559	1.82033	0.06035	0.07767	0.00189	1012.0	30.8	1052.8	21.7	1138.5	48.4	12.5
85	132	70	1.89	0.16942	0.00563	1.74572	0.05189	0.07473	0.00148	1008.9	31.0	1025.6	19.2	1061.4	39.9	5.2
86	17	8	2.10	0.17599	0.00523	2.01765	0.08472	0.08315	0.00352	1045.0	28.7	1121.5	28.5	1272.7	82.6	21.8
87	99	120	0.83	0.18639	0.00568	1.99523	0.05042	0.07764	0.00224	1101.8	30.9	1113.9	17.1	1137.6	57.4	3.3
88	31	16	1.97	0.17670	0.00526	1.90973	0.05825	0.07839	0.00248	1048.9	28.8	1084.5	20.3	1156.7	62.7	10.3
89	572	262	2.18	0.17752	0.00634	1.84101	0.04955	0.07522	0.00174	1053.4	34.7	1060.2	17.7	1074.3	46.4	2.0
90	264	266	0.99	0.27317	0.00743	3.70189	0.08587	0.09828	0.00227	1556.9	37.6	1571.8	18.5	1591.8	43.1	2.2
91	30	14	2.06	0.26885	0.00774	3.29257	0.12530	0.08882	0.00311	1534.9	39.3	1479.3	29.6	1400.4	67.1	-8.8
92	170	196	0.87	0.18319	0.00399	1.89880	0.04164	0.07518	0.00139	1084.4	21.8	1080.7	14.6	1073.2	37.2	-1.0
93	512	262	1.95	0.32101	0.00645	5.01910	0.12030	0.11340	0.00202	1794.7	31.5	1822.5	20.3	1854.6	32.1	3.3
94	188	158	1.19	0.34822	0.00770	5.74312	0.13155	0.11962	0.00216	1926.1	36.8	1937.9	19.8	1950.5	32.2	1.3
95	297	281	1.06	0.52302	0.01065	13.60494	0.27833	0.18866	0.00348	2712.0	45.1	2722.6	19.4	2730.5	30.4	0.7
96	663	423	1.57	0.32602	0.00677	5.06192	0.11634	0.11261	0.00195	1819.1	32.9	1829.7	19.5	1841.9	31.4	1.3

Spot	Conc. (ppm)		Ratios						Ages								
	[U]	[Th]	$^{206}\text{Pb}/^{238}\text{U}$	$\pm 2\sigma$	$^{207}\text{Pb}/^{235}\text{U}$	$\pm 2\sigma$	$^{207}\text{Pb}/^{206}\text{Pb}$	$\pm 2\sigma$	$^{206}\text{Pb}/^{238}\text{U}$	$\pm 2\sigma$	$^{207}\text{Pb}/^{235}\text{U} \pm 2\sigma$	$^{207}\text{Pb}/^{206}\text{Pb} \pm 2\sigma$	% Disc				
97	258	157	1.64	0.20196	0.00491	2.28238	0.06787	0.08197	0.00162	1185.8	26.3	1206.9	21.0	1244.7	38.8	5.0	
98	164	77	2.14	0.17776	0.00355	1.84322	0.04474	0.07520	0.00162	1054.7	19.4	1061.0	16.0	1074.0	43.3	1.8	
99	197	69	2.87	0.33244	0.00674	5.27239	0.13061	0.11503	0.00243	1850.2	32.6	1864.4	21.1	1880.3	38.1	1.6	
100	120	45	2.66	0.21403	0.00489	2.47835	0.07119	0.08398	0.00179	1250.2	25.9	1265.7	20.8	1292.1	41.5	3.4	
101	138	113	1.22	0.55712	0.01539	15.76304	0.47516	0.20521	0.00396	2854.7	63.7	2862.5	28.8	2868.1	31.4	0.5	
102	52	31	1.69	0.17177	0.00461	1.83548	0.06142	0.07750	0.00186	1021.9	25.4	1058.2	22.0	1134.1	47.9	11.0	
103	175	81	2.16	0.18608	0.00524	1.95341	0.06830	0.07614	0.00168	1100.1	28.5	1099.6	23.5	1098.7	44.3	-0.1	
104	202	271	0.74	0.23526	0.00702	2.73381	0.08856	0.08428	0.00164	1362.0	36.6	1337.7	24.1	1299.0	37.9	-4.6	
105	162	42	3.86	0.20546	0.00530	2.25483	0.07125	0.07959	0.00150	1204.6	28.4	1198.3	22.2	1187.0	37.1	-1.5	
NRH-1-86 (25 μm)																	
1	39	0	23973.72	0.34769	0.00831	5.34424	0.15940	0.11148	0.00302	1923.5	39.8	1876.0	25.5	1823.7	49.1	-5.2	
2	10	4	2.54	0.20791	0.00666	4.25514	0.23281	0.14844	0.00687	1217.6	35.6	1684.7	45.0	2328.0	79.2	91.2	
89	4	15	95	0.15	0.97571	0.04160	94.70397	4.30734	0.70396	0.01294	4389.5	135.8	4631.4	45.7	4738.8	26.4	8.0
5	18	36	0.50	0.17830	0.00547	2.74169	0.12698	0.11152	0.00408	1057.7	29.9	1339.8	34.5	1824.4	66.4	72.5	
6	87	49	1.76	0.18046	0.00532	2.19679	0.10254	0.08829	0.00257	1069.5	29.0	1180.0	32.6	1388.8	55.8	29.9	
7	12	5	2.44	0.35919	0.01419	9.66040	0.45797	0.19506	0.00656	1978.3	67.3	2402.9	43.6	2785.3	55.1	40.8	
8	41	0	5822.05	0.34389	0.01018	5.26899	0.19284	0.11112	0.00221	1905.4	48.8	1863.9	31.2	1817.9	36.1	-4.6	
9	144	91	1.59	0.32313	0.00845	5.09933	0.16589	0.11445	0.00189	1805.0	41.2	1836.0	27.6	1871.3	29.7	3.7	
10	12	1	9.74	0.23314	0.00743	4.97151	0.20413	0.15466	0.00450	1350.9	38.8	1814.5	34.7	2398.0	49.5	77.5	
11	88	117	0.75	0.28193	0.00636	4.01236	0.08938	0.10322	0.00172	1601.1	32.0	1636.7	18.1	1682.8	30.8	5.1	
12	162	167	0.97	0.20961	0.00389	2.56674	0.05251	0.08881	0.00143	1226.7	20.7	1291.2	14.9	1400.1	30.8	14.1	
13	57	113	0.51	0.17124	0.00438	1.98209	0.06802	0.08395	0.00214	1018.9	24.1	1109.4	23.2	1291.4	49.6	26.7	
14	8	8	0.99	0.18802	0.00741	4.28269	0.21294	0.16520	0.00818	1110.6	40.2	1690.0	41.0	2509.6	83.2	126.0	
15	228	92	2.48	0.16685	0.00369	1.83577	0.05322	0.07980	0.00162	994.7	20.4	1058.3	19.1	1192.0	40.1	19.8	
16	71	50	1.41	0.17904	0.00433	2.06926	0.06738	0.08382	0.00186	1061.7	23.7	1138.7	22.3	1288.4	43.1	21.3	
17	78	66	1.18	0.55065	0.01465	17.55725	0.37535	0.23125	0.00413	2827.9	60.9	2965.8	20.5	3060.7	28.6	8.2	
18	152	57	2.66	0.20715	0.00807	2.45909	0.11196	0.08610	0.00179	1213.6	43.1	1260.1	32.9	1340.3	40.3	10.4	
19	361	77	4.66	0.54604	0.01210	14.17141	0.31877	0.18823	0.00263	2808.7	50.4	2761.2	21.3	2726.7	23.0	-2.9	
20	84	73	1.14	0.52677	0.01189	13.07966	0.29065	0.18008	0.00222	2727.8	50.2	2685.4	21.0	2653.6	20.4	-2.7	
21	194	76	2.54	0.19534	0.00613	2.10376	0.06444	0.07811	0.00114	1150.2	33.1	1150.0	21.1	1149.7	28.9	0.0	
22	102	66	1.55	0.17140	0.00438	1.89227	0.05015	0.08007	0.00137	1019.8	24.1	1078.4	17.6	1198.7	33.8	17.5	

Spot	Conc. (ppm)	Ratios						Ages						%		
		[Th]	U/Th	$^{206}\text{Pb}/^{238}\text{U}$	$\pm 2\sigma$	$^{207}\text{Pb}/^{235}\text{U}$	$\pm 2\sigma$	$^{206}\text{Pb}/^{204}\text{Pb}$	$\pm 2\sigma$	$^{207}\text{Pb}/^{238}\text{U}$	$\pm 2\sigma$	$^{207}\text{Pb}/^{235}\text{U} \pm 2\sigma$	$^{207}\text{Pb}/^{206}\text{Pb}$	$\pm 2\sigma$	Disc	
23	140	50	2.80	0.30174	0.00823	4.30912	0.12663	0.10357	0.00164	1699.9	40.8	1695.1	24.2	1689.1	29.1	-0.6
24	49	18	2.76	0.24545	0.00598	3.07581	0.10232	0.09089	0.00230	1415.0	31.0	1426.7	25.5	1444.2	48.2	2.1
25	118	124	0.96	0.29473	0.00812	4.10896	0.11546	0.10111	0.00155	1665.1	40.4	1656.1	23.0	1644.7	28.5	-1.2
26	568	338	1.68	0.09490	0.00202	0.79418	0.01643	0.06070	0.00106	584.4	11.9	593.5	9.3	628.5	37.5	7.5
27	12	0	292.13	0.21964	0.00604	3.41979	0.14472	0.11293	0.00468	1280.0	31.9	1509.0	33.3	1847.0	75.0	44.3
28	80	118	0.68	0.42835	0.00920	9.05833	0.22339	0.15337	0.00250	2298.3	41.5	2343.9	22.6	2383.9	27.8	3.7
29	89	60	1.49	0.18199	0.00377	1.98495	0.04813	0.07910	0.00163	1077.8	20.6	1110.4	16.4	1174.7	40.9	9.0
30	304	345	0.88	0.35899	0.00818	5.57404	0.12768	0.11261	0.00166	1977.4	38.8	1912.1	19.7	1842.0	26.7	-6.8
31	43	64	0.67	0.33642	0.00820	5.41299	0.13379	0.11670	0.00199	1869.4	39.5	1886.9	21.2	1906.2	30.6	2.0
32	34	29	1.18	0.18585	0.00488	2.29604	0.07985	0.08960	0.00269	1098.8	26.5	1211.1	24.6	1417.1	57.5	29.0
33	88	61	1.43	0.16098	0.00327	1.76412	0.04275	0.07948	0.00167	962.2	18.2	1032.4	15.7	1184.1	41.6	23.1
34	81	30	2.72	0.23282	0.00556	2.86280	0.07171	0.08918	0.00139	1349.2	29.1	1372.2	18.9	1408.1	29.9	4.4
35	21	16	1.35	0.20362	0.00530	2.87549	0.10564	0.10242	0.00326	1194.8	28.4	1375.5	27.7	1668.4	58.9	39.6
36	633	376	1.68	0.19949	0.00936	2.95099	0.14166	0.10729	0.00140	1172.6	50.3	1395.1	36.4	1753.8	23.9	49.6
37	479	171	2.80	0.333301	0.00639	5.05172	0.10251	0.11002	0.00120	1853.0	30.9	1828.0	17.2	1799.8	19.8	-2.9
38	74	25	2.90	0.19932	0.00473	2.29382	0.06714	0.08346	0.00145	1171.7	25.4	1210.4	20.7	1280.1	33.8	9.3
39	54	37	1.46	0.17801	0.00416	2.09078	0.06595	0.08519	0.00184	1056.1	22.8	1145.8	21.7	1319.8	41.7	25.0
40	111	53	2.10	0.25578	0.00487	3.13689	0.06618	0.08895	0.00137	1468.2	25.0	1441.8	16.2	1403.0	29.5	-4.4
41	56	60	0.93	0.17710	0.00427	2.02000	0.05374	0.08272	0.00179	1051.1	23.4	1122.3	18.1	1262.7	42.3	20.1
42	92	30	3.09	0.19550	0.00533	2.18452	0.06182	0.08104	0.00147	1151.1	28.7	1176.1	19.7	1222.5	35.7	6.2
43	321	145	2.20	0.17944	0.00473	1.83640	0.04493	0.07423	0.00118	1063.9	25.9	1058.6	16.1	1047.6	32.0	-1.5
44	125	66	1.89	0.17888	0.00357	1.93716	0.04155	0.07854	0.00141	1060.9	19.5	1094.0	14.4	1160.6	35.5	9.4
45	1	0	6.63	0.50361	0.02766	21.45393	1.70427	0.30897	0.02435	2629.3	118.6	3159.3	77.2	3515.8	121.7	33.7
46	21	9	2.42	0.47583	0.01446	12.39450	0.36140	0.18892	0.00457	2509.1	63.1	2634.8	27.4	2732.8	39.9	8.9
47	220	174	1.26	0.43044	0.00882	10.94628	0.15582	0.18444	0.00273	2307.7	39.8	2518.6	13.2	2693.2	24.5	16.7
48	163	53	3.09	0.19105	0.00454	2.05839	0.04709	0.07814	0.00137	1127.1	24.6	1135.1	15.6	1150.5	34.8	2.1
49	16	4	3.68	0.34833	0.01040	6.55003	0.25026	0.13638	0.00332	1926.6	49.7	2052.6	33.7	2181.7	42.3	13.2
50	145	158	0.92	0.28952	0.00712	4.00006	0.08508	0.10020	0.00158	1639.1	35.6	1634.2	17.3	1627.9	29.4	-0.7
51	50	22	2.28	0.24460	0.00546	3.00660	0.08767	0.08915	0.00190	1410.6	28.3	1409.3	22.2	1407.4	40.8	-0.2
52	37788	0.01088	6.29815	0.19665	0.12088	0.00251	2066.4	50.9	2018.2	27.4	1969.3	37.0	40.8	-4.7		
53	16	3	4.72	0.38515	0.00820	9.08532	0.20453	0.17108	0.00212	2100.3	38.2	2346.6	20.6	2568.3	20.7	22.3

Spot	Conc. (ppm)	[Th]	U/Th	Ratios				Ages				% Disc				
				$^{206}\text{Pb}/^{238}\text{U}$	$\pm 2\sigma$	$^{207}\text{Pb}/^{235}\text{U}$	$\pm 2\sigma$	$^{207}\text{Pb}/^{206}\text{Pb}$	$\pm 2\sigma$	$^{206}\text{Pb}/^{238}\text{U}$	$\pm 2\sigma$	$^{207}\text{Pb}/^{235}\text{U}$	$\pm 2\sigma$			
55	1060	683	1.55	0.28010	0.01241	6.78628	0.31017	0.17572	0.00206	1591.9	62.5	2083.9	40.5	2612.9	19.5	64.1
56	124	42	2.93	0.19656	0.00477	2.16993	0.05957	0.08007	0.00136	1156.8	25.7	1171.5	19.1	1198.7	33.4	3.6
57	31	20	1.58	0.18470	0.00483	2.26168	0.07365	0.08881	0.00209	1092.6	26.3	1200.4	22.9	1400.1	45.2	28.1
58	20	0	8412.91	0.34417	0.01030	5.29100	0.17968	0.11150	0.00269	1906.7	49.4	1867.4	29.0	1824.0	43.7	-4.3
59	80	76	1.05	0.51390	0.01144	13.04192	0.28301	0.18406	0.00248	2673.3	48.7	2682.7	20.5	2689.8	22.3	0.6
60	221	140	1.58	0.23152	0.00528	2.79598	0.06463	0.08759	0.00119	1342.5	27.6	1354.5	17.3	1373.4	26.1	2.3
61	32	30	1.06	0.17443	0.00442	1.99776	0.06527	0.08307	0.00229	1036.5	24.3	1114.8	22.1	1270.8	53.9	22.6
62	474	202	2.35	0.38411	0.01708	9.52043	0.47989	0.17976	0.00301	2095.4	79.5	2389.5	46.3	2650.7	27.8	26.5
63	51	23	2.24	0.18906	0.00568	2.04538	0.07034	0.07847	0.00175	1116.3	30.8	1130.8	23.5	1158.7	44.2	3.8
64	109	226	0.48	0.52071	0.01288	13.21284	0.30847	0.18403	0.00232	2702.2	54.6	2695.0	22.0	2689.6	20.9	-0.5
65	208	122	1.71	0.34713	0.00841	5.46256	0.12699	0.11413	0.00181	1920.9	40.2	1894.7	20.0	1866.2	28.6	-2.8
66	99	36	2.76	0.54511	0.01264	13.28354	0.33152	0.17674	0.00330	2804.8	52.7	2700.0	23.6	2622.5	31.0	-6.5
67	125	102	1.23	0.28868	0.00650	3.93671	0.09139	0.09890	0.00175	1634.9	32.5	1621.3	18.8	1603.5	32.9	-1.9
68	13	0	-6412.2	0.34665	0.00921	5.36301	0.16723	0.11221	0.00284	1918.6	44.1	1879.0	26.7	1835.5	45.9	-4.3
69	338	292	1.16	0.49516	0.01217	12.36821	0.27600	0.18116	0.00264	2592.9	52.5	2632.8	21.0	2663.5	24.2	2.7
70	47	33	1.42	0.25932	0.00637	3.28299	0.08719	0.09182	0.00207	1486.4	32.6	1477.0	20.7	1463.7	42.9	-1.5
71	72	32	2.23	0.24054	0.00650	2.96981	0.09416	0.08955	0.00184	1389.5	33.8	1399.9	24.1	1415.9	39.3	1.9
72	280	102	2.75	0.49666	0.01427	11.97550	0.41820	0.17488	0.00227	2599.4	61.5	2602.5	32.7	2604.9	21.7	0.2
73	39	17	2.37	0.18790	0.00457	2.06758	0.07768	0.07980	0.00226	1110.0	24.8	1138.1	25.7	1192.2	56.0	7.4
74	199	258	0.77	0.52267	0.01253	12.83083	0.31525	0.17804	0.00259	2710.5	53.0	2667.3	23.1	2634.7	24.2	-2.8
75	14	0	1897.47	0.33842	0.01104	5.09391	0.21618	0.10917	0.00270	1879.1	53.2	1835.1	36.0	1785.5	45.1	-5.0
76	131	93	1.41	0.54565	0.01211	13.97141	0.38473	0.18570	0.00295	2807.1	50.5	2747.8	26.1	2704.5	26.2	-3.7
77	199	127	1.57	0.54601	0.01301	14.27178	0.40266	0.18957	0.00254	2808.5	54.3	2767.9	26.8	2738.5	22.0	-2.5
78	56	40	1.40	0.17060	0.00426	1.83111	0.06108	0.07784	0.00189	1015.4	23.4	1056.7	21.9	1142.9	48.2	12.6
79	167	58	2.86	0.26408	0.00661	3.37650	0.10084	0.09273	0.00157	1510.7	33.7	1499.0	23.4	1482.4	32.1	-1.9
80	395	190	2.08	0.19803	0.00451	2.12032	0.05672	0.07766	0.00107	1164.7	24.3	1155.4	18.5	1138.1	27.4	-2.3
81	127	44	2.87	0.23966	0.00539	2.92523	0.07672	0.08853	0.00142	1384.9	28.0	1388.5	19.8	1393.9	30.7	0.7
82	17	16	1.05	0.18640	0.00532	2.44054	0.12665	0.09496	0.00396	1101.9	28.9	1254.6	37.4	1527.2	78.5	38.6
83	21	18	1.18	0.18523	0.00594	2.21950	0.10465	0.08690	0.00353	1095.5	32.3	1187.2	33.0	1358.4	78.2	24.0
84	33	28	1.18	0.16106	0.00438	1.78262	0.06934	0.08027	0.00291	962.7	24.3	1039.1	25.3	1203.6	71.3	25.0
85	104	35	2.98	0.20059	0.00552	2.21766	0.06724	0.08018	0.00159	1178.5	29.7	1186.6	21.2	1201.5	39.0	2.0

Spot	Conc. (ppm)	Ratios						Ages						%		
		[Th]	U/Th	$^{206}\text{Pb}/^{238}\text{U}$	$^{207}\text{Pb}/^{235}\text{U}$	$\pm 2\sigma$	$^{207}\text{Pb}/^{206}\text{Pb}$	$\pm 2\sigma$	$^{206}\text{Pb}/^{238}\text{U}$	$\pm 2\sigma$	$^{207}\text{Pb}/^{235}\text{U}$	$\pm 2\sigma$	$^{207}\text{Pb}/^{206}\text{Pb}$	$\pm 2\sigma$	Disc	
86	35	60	0.57	0.16545	0.00535	1.98329	0.09430	0.08694	0.00371	987.0	29.6	1109.8	32.1	1359.2	82.3	37.7
87	20	17	1.14	0.23611	0.00665	3.18259	0.13437	0.09776	0.00317	1366.4	34.7	1452.9	32.6	1581.9	60.7	15.8
88	55	30	1.85	0.51729	0.01199	13.81153	0.31200	0.19365	0.00273	2687.7	51.0	2736.9	21.4	2773.4	23.2	3.2
89	55	13	4.19	0.53255	0.01476	14.18397	0.36898	0.19317	0.00288	2752.2	62.1	2762.1	24.7	2769.3	24.5	0.6
90	117	36	3.29	0.17053	0.00406	1.89861	0.05008	0.08075	0.00201	1015.0	22.4	1080.6	17.5	1215.3	48.9	19.7
91	40	37	1.07	0.18005	0.00406	1.95609	0.05962	0.07879	0.00194	1067.2	22.2	1100.5	20.5	1167.0	48.7	9.3
92	91	202	0.45	0.48743	0.01042	12.06961	0.25700	0.17959	0.00277	2559.6	45.2	2609.8	20.0	2649.1	25.6	3.5
93	224	97	2.31	0.09539	0.00241	0.81203	0.02010	0.06174	0.00111	587.3	14.2	603.6	11.3	665.2	38.5	13.3
94	49	49	1.01	0.18530	0.00422	2.00703	0.05734	0.07856	0.00201	1095.8	22.9	1117.9	19.4	1161.0	50.6	5.9
95	114	149	0.76	0.16515	0.00471	1.81001	0.06295	0.07949	0.00248	985.3	26.0	1049.1	22.8	1184.3	61.6	20.2
96	129	44	2.91	0.17335	0.00430	1.77499	0.04185	0.07426	0.00130	1030.6	23.6	1036.3	15.3	1048.6	35.2	1.7
97	46	39	1.19	0.23852	0.00543	3.01208	0.07699	0.09159	0.00191	1379.0	28.3	1410.7	19.5	1458.8	39.7	5.8
98	337	212	1.59	0.31920	0.00725	5.01484	0.11176	0.11394	0.00169	1785.8	35.4	1821.8	18.9	1863.2	26.8	4.3
99	45	38	1.20	0.30965	0.00674	4.67110	0.12531	0.10941	0.00191	1739.0	33.2	1762.1	22.4	1789.6	31.8	2.9
100	30	30	1.00	0.20588	0.00586	2.41626	0.09295	0.08512	0.00230	1206.8	31.3	1247.4	27.6	1318.3	52.3	9.2
101	140	162	0.87	0.46003	0.01053	11.08195	0.25992	0.17472	0.00224	2439.7	46.5	2530.0	21.8	2603.3	21.3	6.7
102	54	28	1.89	0.19942	0.00556	2.41645	0.10642	0.08788	0.00241	1172.2	29.9	1247.5	31.6	1380.0	52.7	17.7
103	84	54	1.56	0.17560	0.00392	1.88095	0.04829	0.07769	0.00143	1042.9	21.5	1074.4	17.0	1138.9	36.6	9.2
104	32	21	1.50	0.18167	0.00465	2.06054	0.07586	0.08226	0.00254	1076.1	25.3	1135.8	25.2	1251.7	60.5	16.3
105	81	42	1.95	0.62991	0.01316	21.04625	0.38212	0.24232	0.00342	3149.2	52.1	3140.7	17.6	3135.3	22.4	-0.4
106	104	13	7.83	0.32939	0.00713	5.06720	0.11405	0.11157	0.00189	1835.4	34.6	1830.6	19.1	1825.2	30.8	-0.6
107	92	55	1.68	0.17785	0.00420	1.86922	0.04593	0.07622	0.00167	1055.2	23.0	1070.3	16.3	1101.0	43.7	4.3
108	90	71	1.27	0.18306	0.00386	1.87470	0.04375	0.07427	0.00124	1083.7	21.1	1072.2	15.5	1048.9	33.8	-3.2
109	651	114	5.71	0.34650	0.00869	5.47893	0.12598	0.11468	0.00144	1917.9	41.6	1897.3	19.7	1874.9	22.7	-2.2
110	26	41	0.65	0.17184	0.00533	1.88083	0.07124	0.07938	0.00277	1022.2	29.3	1074.4	25.1	1181.7	69.0	15.6
111	178	188	0.94	0.17134	0.00365	1.71059	0.03783	0.07241	0.00110	1019.5	20.1	1012.5	14.2	997.4	31.0	-2.2
112	182	101	1.79	0.18953	0.00493	2.07770	0.07285	0.07951	0.00140	1118.8	26.7	1141.5	24.0	1184.8	34.8	5.9
113	269	87	3.08	0.18009	0.00390	1.81718	0.04042	0.07318	0.00107	1067.4	21.3	1051.7	14.6	1019.0	29.7	-4.5
114	80	69	1.16	0.52477	0.01144	13.29258	0.30670	0.18371	0.00240	2719.4	48.4	2700.7	21.8	2686.7	21.6	-1.2
115	192	95	2.02	0.18606	0.00419	1.95197	0.04730	0.07609	0.00107	1100.0	22.8	1099.1	16.3	1097.4	28.3	-0.2
116	121	29	4.16	0.18762	0.00414	1.98343	0.05170	0.07667	0.00135	1108.5	22.5	1109.9	17.6	1112.7	35.1	0.4

Spot	Conc. (ppm)	Ratios						Ages								
		[U]	[Th]	$^{206}\text{Pb}/^{238}\text{U}$	$\pm 2\sigma$	$^{207}\text{Pb}/^{206}\text{Pb}$	$\pm 2\sigma$	$^{207}\text{Pb}/^{235}\text{U}$	$\pm 2\sigma$	$^{206}\text{Pb}/^{238}\text{U}$	$\pm 2\sigma$	$^{207}\text{Pb}/^{235}\text{U} \pm 2\sigma$	$^{207}\text{Pb}/^{206}\text{Pb} \pm 2\sigma$	% Disc		
117	117	56	2.10	0.17171	0.00433	1.74978	0.04702	0.07391	0.00202	1021.5	23.8	1027.1	17.4	1039.0	55.2	1.7
118	36	17	2.16	0.18851	0.00511	2.07507	0.07208	0.07984	0.00237	1113.3	27.7	1140.6	23.8	1193.0	58.7	7.2
119	207	107	1.92	0.34618	0.00832	5.54941	0.12840	0.11626	0.00167	1916.3	39.9	1908.3	19.9	1899.5	25.8	-0.9
120	184	75	2.45	0.17566	0.00454	1.80144	0.05091	0.07438	0.00123	1043.2	24.9	1046.0	18.5	1051.8	33.2	0.8
NRH-2-86 (25 μm)																
1	71	65	1.08	0.18391	0.00600	1.89691	0.06296	0.07481	0.00154	1088.3	32.6	1080.0	22.1	1063.4	41.4	-2.3
2	129	56	2.32	0.26576	0.00940	3.18681	0.10488	0.08697	0.00157	1519.2	47.9	1454.0	25.4	1359.8	34.8	-10.5
3	280	105	2.68	0.21025	0.00641	2.33498	0.07406	0.08055	0.00132	1230.2	34.1	1223.0	22.6	1210.4	32.2	-1.6
4	79	28	2.85	0.17813	0.00577	1.96728	0.05879	0.08010	0.00159	1056.7	31.6	1104.4	20.1	1199.5	39.2	13.5
5	50	53	0.94	0.37748	0.01239	6.59990	0.18968	0.12681	0.00199	2064.5	58.0	2059.3	25.3	2054.2	27.7	-0.5
6	76	60	1.26	0.16816	0.00583	1.74711	0.06169	0.07535	0.00179	1001.9	32.2	1026.1	22.8	1078.0	47.7	7.6
7	111	45	2.50	0.16647	0.00505	1.70544	0.05206	0.07430	0.00151	992.6	27.9	1010.6	19.5	1049.7	41.0	5.8
8	91	92	0.99	0.17355	0.00538	1.80126	0.05405	0.07527	0.00139	1031.7	29.5	1045.9	19.6	1075.8	37.0	4.3
9	68	18	3.79	0.24223	0.00775	2.92146	0.09360	0.08747	0.00160	1398.3	40.2	1387.5	24.2	1370.9	35.2	-2.0
10	111	36	3.06	0.19260	0.00540	2.09724	0.06212	0.07897	0.00135	1135.5	29.2	1147.9	20.4	1171.5	33.9	3.2
11	272	178	1.52	0.50195	0.01311	12.43678	0.32070	0.17970	0.00258	2622.2	56.3	2638.0	24.2	2650.1	23.8	1.1
12	888	241	3.69	0.18249	0.00486	2.00142	0.04852	0.07954	0.00131	1080.6	26.5	1116.0	16.4	1185.7	32.6	9.7
13	80	46	1.75	0.24391	0.00588	2.94317	0.06194	0.08751	0.00158	1407.0	30.5	1393.1	16.0	1371.9	34.8	-2.5
14	119	65	1.83	0.36475	0.00954	6.14076	0.14654	0.12210	0.00146	2004.7	45.1	1996.1	20.8	1987.2	21.3	-0.9
15	170	106	1.60	0.35572	0.00950	5.65919	0.14134	0.11538	0.00157	1961.9	45.2	1925.2	21.6	1885.9	24.5	-3.9
16	144	73	1.97	0.17452	0.00369	1.75971	0.04093	0.07313	0.00116	1037.0	20.3	1030.7	15.1	1017.6	32.1	-1.9
17	59	37	1.59	0.18071	0.00441	1.85592	0.05182	0.07449	0.00147	1070.9	24.1	1065.5	18.4	1054.6	39.7	-1.5
18	433	154	2.81	0.17337	0.00441	1.75392	0.04612	0.07337	0.00086	1030.7	24.2	1028.6	17.0	1024.2	23.6	-0.6
19	95	41	2.30	0.22137	0.00509	2.60014	0.06830	0.08519	0.00131	1289.1	26.9	1300.7	19.3	1319.8	29.8	2.4
20	26	24	1.11	0.17746	0.00593	1.86433	0.07606	0.07619	0.00180	1053.1	32.5	1068.5	27.0	1100.1	47.4	4.5
21	109	59	1.85	0.23297	0.00651	2.77624	0.10105	0.08643	0.00135	1350.1	34.1	1349.2	27.2	1347.8	30.1	-0.2
22	43	22	1.93	0.16925	0.00490	1.75243	0.06675	0.07509	0.00180	1008.0	27.0	1028.1	24.6	1071.0	48.1	6.2
23	52	54	0.96	0.16875	0.00458	1.74483	0.06017	0.07499	0.00218	1005.2	25.3	1025.3	22.3	1068.2	58.6	6.3
24	157	59	2.65	0.17794	0.00486	1.81678	0.05861	0.07405	0.00105	1055.7	26.6	1051.5	21.1	1042.8	28.5	-1.2
25	152	99	1.53	0.24676	0.00589	3.09936	0.07945	0.09110	0.00131	1421.7	30.5	1432.5	19.7	1448.6	27.3	1.9
26	67	21	3.23	0.25539	0.00719	2.97818	0.09381	0.08457	0.00159	1466.2	36.9	1402.1	23.9	1305.8	36.6	10.9

Spot	Conc. (ppm)	Ratios										Ages		
		[U]	[Th]	$^{206}\text{Pb}/^{238}\text{U}$	$^{207}\text{Pb}/^{235}\text{U}$	$\pm 2\sigma$	$^{207}\text{Pb}/^{206}\text{Pb}$	$\pm 2\sigma$	$^{206}\text{Pb}/^{238}\text{U}$	$\pm 2\sigma$	$^{207}\text{Pb}/^{235}\text{U} \pm 2\sigma$	$^{207}\text{Pb}/^{206}\text{Pb} \pm 2\sigma$	% Disc	
27	147	63	2.33	0.18276	0.00526	1.91590	0.05934	0.07603	0.00149	1082.0	28.7	1086.6	20.7	39.1
28	64	92	0.70	0.15968	0.00465	1.59972	0.05194	0.07266	0.00148	955.0	25.8	970.1	20.3	41.3
29	28	19	1.48	0.25944	0.00869	3.25851	0.11344	0.09109	0.00193	1487.0	44.5	1471.2	27.1	1448.5
30	208	128	1.62	0.18299	0.00462	1.89218	0.05339	0.07499	0.00118	1083.3	25.2	1078.3	18.7	1068.4
31	89	104	0.85	0.53952	0.01191	15.21971	0.33955	0.20460	0.00322	2781.4	49.9	2829.1	21.3	25.6
32	39	34	1.14	0.21895	0.00489	2.58762	0.07028	0.08571	0.00205	1276.3	25.9	1297.1	19.9	1331.7
33	209	118	1.77	0.22448	0.00552	2.90044	0.07493	0.09371	0.00183	1305.5	29.1	1382.0	19.5	1502.3
34	33	56	0.58	0.49326	0.01126	11.84872	0.26530	0.17422	0.00297	2584.8	48.6	2592.5	21.0	2598.6
35	137	39	3.52	0.17056	0.00346	1.72283	0.03462	0.07326	0.00117	1015.2	19.1	1017.1	12.9	1021.2
36	46	21	2.19	0.46828	0.01048	11.49434	0.24122	0.17802	0.00326	2476.0	46.0	2564.1	19.6	2634.6
37	137	50	2.72	0.17664	0.00439	1.82337	0.04528	0.07487	0.00150	1048.6	24.0	1053.9	16.3	1064.9
38	30	46	0.66	0.22066	0.00545	2.69848	0.06882	0.08869	0.00210	1285.4	28.8	1328.0	18.9	1397.5
39	742	193	3.85	0.21902	0.00535	2.54004	0.06073	0.08411	0.00139	1276.7	28.3	1283.6	17.4	1295.2
40	73	33	2.18	0.19983	0.00549	2.26723	0.07826	0.08229	0.00198	1174.4	29.5	1202.2	24.3	1252.3
41	156	190	0.82	0.17458	0.00467	1.75191	0.04560	0.07278	0.00121	1037.3	25.6	1027.9	16.8	1007.8
42	57	50	1.15	0.16747	0.00477	1.70808	0.04964	0.07397	0.00167	998.2	26.3	1011.6	18.6	1040.7
43	256	98	2.62	0.17985	0.00460	1.89781	0.04300	0.07653	0.00110	1066.1	25.1	1080.3	15.1	1109.0
44	193	107	1.81	0.18304	0.00428	1.89560	0.04080	0.07511	0.00111	1083.5	23.3	1079.5	14.3	1071.5
45	613	241	2.55	0.32091	0.00785	4.97451	0.11564	0.11243	0.00153	1794.2	38.3	1815.0	19.7	1839.0
46	112	54	2.06	0.49936	0.01587	13.69581	0.36947	0.19892	0.00368	2611.0	68.2	2728.9	25.5	2817.3
47	144	55	2.62	0.18194	0.00455	1.89158	0.05103	0.07541	0.00117	1077.5	24.8	1078.1	17.9	1079.3
48	154	77	2.00	0.25106	0.00684	3.01257	0.08583	0.08703	0.00141	1444.0	35.3	1410.8	21.7	1361.1
49	146	125	1.17	0.17457	0.00443	1.78360	0.05207	0.07410	0.00131	1037.2	24.3	1039.5	19.0	1044.3
50	170	165	1.03	0.19558	0.00596	1.99728	0.05969	0.07414	0.00168	1150.4	32.1	1114.6	20.2	1045.3
51	115	66	1.73	0.51151	0.01505	12.24786	0.37011	0.17366	0.00210	2663.1	64.2	2623.6	28.4	2593.2
52	338	315	1.07	0.42642	0.02532	10.49183	0.64604	0.17845	0.00276	2289.6	114.4	2479.2	57.1	2638.5
53	169	61	2.75	0.24020	0.00713	2.89157	0.09565	0.08731	0.00122	1387.7	37.1	1379.7	25.0	1367.3
54	229	146	1.57	0.19048	0.00670	1.99354	0.07205	0.07591	0.00143	1124.0	36.3	1113.3	24.4	1092.6
55	40	34	1.17	0.22944	0.00609	2.72142	0.08695	0.08603	0.00189	1331.6	31.9	1334.3	23.7	1338.8
56	93	39	2.39	0.19736	0.00472	2.15630	0.05120	0.07924	0.00133	1161.1	25.4	1167.1	16.5	1178.1
57	65	36	1.81	0.17604	0.00523	1.93849	0.07638	0.07987	0.00262	1045.3	28.6	1094.5	26.4	1193.7

Spot	Conc. (ppm)	Ratios						Ages								
		[U]	[Th]	$^{206}\text{Pb}/^{238}\text{U}$	$\pm 2\sigma$	$^{207}\text{Pb}/^{235}\text{U}$	$\pm 2\sigma$	$^{207}\text{Pb}/^{206}\text{Pb}$	$\pm 2\sigma$	$^{206}\text{Pb}/^{238}\text{U} \pm 2\sigma$	$^{207}\text{Pb}/^{235}\text{U} \pm 2\sigma$	$^{207}\text{Pb}/^{206}\text{Pb} \pm 2\sigma$	$\pm 2\sigma$			
58	35	36	0.97	0.17788	0.00476	1.86948	0.05784	0.07623	0.00187	1055.4	26.1	1070.3	20.5	1101.0	49.2	4.3
59	181	50	3.60	0.21039	0.00482	2.40843	0.05165	0.08303	0.00118	1230.9	25.7	1245.1	15.4	1269.8	27.8	3.2
60	346	205	1.69	0.33093	0.01071	5.31145	0.16051	0.11640	0.00139	1842.9	51.9	1870.7	25.8	1901.7	21.4	3.2
61	97	38	2.56	0.19335	0.00613	2.03040	0.07659	0.07616	0.00174	1139.5	33.1	1125.7	25.7	1099.4	45.7	-3.5
62	370	231	1.60	0.19173	0.00621	1.95840	0.06255	0.07408	0.00109	1130.7	33.6	1101.3	21.5	1043.7	29.8	-7.7
63	73	48	1.51	0.24378	0.00567	3.01661	0.07101	0.08975	0.00161	1406.3	29.4	1411.8	18.0	1420.2	34.2	1.0
64	227	76	3.00	0.17520	0.00381	1.83700	0.03687	0.07605	0.00098	1040.7	20.9	1058.8	13.2	1096.3	25.9	5.3
65	1400	235	5.97	0.19011	0.00443	2.05544	0.04614	0.07842	0.00092	1122.0	24.0	1134.1	15.3	1157.4	23.3	3.2
66	774	295	2.63	0.18142	0.00480	1.86564	0.04744	0.07459	0.00103	1074.7	26.2	1069.0	16.8	1057.3	27.8	-1.6
67	167	120	1.40	0.18936	0.00405	2.02205	0.04680	0.07745	0.00108	1117.9	22.0	1122.9	15.7	1132.7	27.7	1.3
68	93	95	0.98	0.50265	0.01181	13.17357	0.34387	0.19008	0.00266	2625.2	50.7	2692.2	24.6	2742.9	23.0	4.5
69	195	88	2.22	0.19248	0.00449	2.07391	0.04677	0.07815	0.00111	1134.8	24.3	1140.2	15.4	1150.6	28.3	1.4
70	280	139	2.01	0.32741	0.00734	5.06078	0.10578	0.11210	0.00154	1825.8	35.6	1829.6	17.7	1833.8	24.9	0.4
71	170	68	2.48	0.23441	0.00553	2.81903	0.06720	0.08722	0.00125	1357.6	28.9	1360.6	17.9	1365.4	27.7	0.6
72	37	35	1.08	0.16454	0.00458	1.71032	0.05362	0.07539	0.00192	982.0	25.4	1012.4	20.1	1078.8	51.2	9.9
73	490	148	3.32	0.50218	0.01274	12.35488	0.32523	0.17843	0.00226	2623.2	54.7	2631.8	24.7	2638.4	21.1	0.6
74	107	47	2.30	0.17303	0.00398	1.74268	0.04795	0.07305	0.00127	1028.8	21.9	1024.5	17.8	1015.2	35.1	-1.3
75	214	99	2.15	0.28797	0.00625	3.95115	0.08877	0.09951	0.00157	1631.4	31.3	1624.2	18.2	1615.0	29.4	-1.0
76	41	12	3.38	0.16917	0.00483	1.75725	0.05891	0.07534	0.00171	1007.6	26.6	1029.8	21.7	1077.5	45.7	6.9
77	24	19	1.25	0.21820	0.00510	2.66089	0.07453	0.08844	0.00219	1272.4	27.0	1317.7	20.7	1392.1	47.5	9.4
78	246	304	0.81	0.33694	0.00753	5.23363	0.12150	0.11266	0.00168	1871.9	36.3	1858.1	19.8	1842.7	27.1	-1.6
79	185	178	1.04	0.19256	0.00439	2.10757	0.04981	0.07938	0.00119	1135.2	23.7	1151.3	16.3	1181.7	29.7	4.1
80	282	331	0.85	0.19055	0.00468	2.08503	0.04776	0.07936	0.00125	1124.4	25.3	1143.9	15.7	1181.1	31.1	5.0
81	129	43	3.01	0.16805	0.00390	1.72631	0.03768	0.07451	0.00135	1001.3	21.5	1018.4	14.0	1055.2	36.5	5.4
82	78	61	1.29	0.19596	0.00574	2.03159	0.06662	0.07519	0.00148	1153.6	31.0	1126.1	22.3	1073.6	39.6	-6.9
83	130	109	1.20	0.16727	0.00442	1.68729	0.04801	0.07316	0.00185	997.0	24.4	1003.7	18.1	1018.4	51.3	2.1
84	63	49	1.29	0.17316	0.00369	1.79004	0.04542	0.07498	0.00140	1029.5	20.3	1041.8	16.5	1067.8	37.6	3.7
85	64	71	0.90	0.28534	0.00589	4.12420	0.08330	0.10483	0.00170	1618.2	29.5	1659.1	16.5	1711.3	29.8	5.8
86	248	260	0.95	0.33607	0.00822	5.22610	0.11721	0.11278	0.00174	1867.7	39.7	1856.9	19.1	1844.8	28.0	-1.2
87	217	246	0.88	0.32917	0.00664	5.00888	0.10180	0.11036	0.00177	1834.4	32.2	1820.8	17.2	1805.4	29.2	-1.6
88	53	26	2.03	0.32680	0.00762	5.54991	0.17784	0.12317	0.00257	1822.9	37.0	1908.4	27.6	2002.6	37.1	9.9

Conc. (ppm)	Ratios						Ages						
	Spot	[Th]	$^{206}\text{Pb}/^{238}\text{U}$	$^{207}\text{Pb}/^{235}\text{U}$	$\pm 2\sigma$	$^{207}\text{Pb}/^{206}\text{Pb}$	$\pm 2\sigma$	$^{206}\text{Pb}/^{238}\text{U}$	$\pm 2\sigma$	$^{207}\text{Pb}/^{235}\text{U}$	$\pm 2\sigma$	$^{207}\text{Pb}/^{206}\text{Pb}$	$\pm 2\sigma$
89	162	212	0.77	0.32189	0.00663	4.90858	0.11712	0.11060	0.00180	1799.0	32.3	1803.7	20.1
90	106	131	0.81	0.28505	0.00693	3.89411	0.08611	0.09008	0.00174	1616.7	34.8	1612.5	17.9
91	755	262	2.88	0.46990	0.00992	10.84720	0.22868	0.16742	0.00285	2483.1	43.5	2510.1	19.6
92	489	287	1.70	0.24939	0.00544	3.14163	0.06545	0.09136	0.00138	1435.3	28.1	1443.0	16.0
93	126	56	2.26	0.17350	0.00381	1.81082	0.04447	0.07569	0.00124	1031.4	20.9	1049.4	16.1
94	45	37	1.20	0.52038	0.01197	13.39097	0.29708	0.18663	0.00261	2700.8	50.8	2707.6	21.0
95	1274	584	2.18	0.08893	0.00196	0.72731	0.01523	0.05931	0.00081	549.2	11.6	555.0	9.0
96	220	114	1.93	0.21947	0.00504	2.50836	0.05635	0.08289	0.00119	1279.1	26.7	1274.5	16.3
97	364	219	1.66	0.17195	0.00421	1.78948	0.04842	0.07548	0.00128	1022.8	23.1	1041.6	17.6
98	63	35	1.81	0.20971	0.00465	2.42439	0.05702	0.08385	0.00168	1227.3	24.8	1249.9	16.9
99	37	22	1.66	0.20787	0.00374	2.38429	0.06239	0.08319	0.00184	1217.5	19.9	1237.9	18.7
100	185	94	1.97	0.53354	0.01149	13.38946	0.26577	0.18201	0.00216	2756.4	48.3	2707.5	18.8
101	140	71	1.97	0.46727	0.01031	10.71379	0.25088	0.16629	0.00217	2471.6	45.3	2498.6	21.8
102	39	19	2.11	0.17982	0.00416	1.90643	0.05063	0.07689	0.00160	1066.0	22.7	1083.3	17.7
103	170	118	1.44	0.25144	0.00531	3.25263	0.06182	0.09382	0.00111	1445.9	27.4	1469.8	14.8
104	212	154	1.38	0.28234	0.00723	3.94052	0.10020	0.10122	0.00165	1603.2	36.3	1622.0	20.6
105	60	41	1.48	0.17605	0.00416	1.85260	0.05225	0.07632	0.00148	1045.4	22.8	1064.4	18.6
106	56	32	1.76	0.18881	0.00400	1.99429	0.05473	0.07661	0.00156	1114.9	21.7	1113.6	18.6
107	193	109	1.77	0.54675	0.01207	15.12349	0.30235	0.20061	0.00305	2811.6	50.3	2823.0	19.0
108	58	33	1.78	0.17749	0.00360	1.82943	0.04051	0.07476	0.00143	1053.2	19.7	1056.1	14.5
109	256	221	1.16	0.52946	0.01281	13.57908	0.30447	0.18601	0.00229	2739.2	54.0	2720.8	21.2
110	114	52	2.20	0.47362	0.01165	11.76813	0.27505	0.18021	0.00293	2499.4	51.0	2586.1	21.9
111	83	86	0.96	0.16204	0.00481	1.64706	0.05169	0.07372	0.00223	968.1	26.7	988.4	19.8
112	414	178	2.32	0.18251	0.00413	1.91533	0.04547	0.07611	0.00111	1080.7	22.5	1086.4	15.8
113	169	81	2.09	0.26915	0.00553	3.71176	0.06899	0.10002	0.00119	1536.5	28.1	1573.9	14.9
114	55	23	2.38	0.18390	0.00444	1.89696	0.05483	0.07481	0.00198	1088.2	24.2	1080.0	19.2
115	40	63	0.63	0.17548	0.00415	1.87333	0.05044	0.07743	0.00195	1042.2	22.8	1071.7	17.8
116	335	170	1.97	0.50105	0.01238	12.92542	0.29015	0.18710	0.00234	2618.3	53.2	2674.2	21.2
117	65	88	0.73	0.54645	0.01524	14.01691	0.35579	0.18604	0.00286	2810.4	63.5	2750.9	24.1
118	38	40	0.95	0.16404	0.00358	1.86743	0.05700	0.08256	0.00279	979.2	19.8	1069.6	20.2
119	16	13	1.22	0.24550	0.00573	3.23127	0.09580	0.09546	0.00296	1415.2	29.7	1464.7	23.0

Spot	Conc. (ppm)	[U]	[Th]	Ratios						Age						
				$^{206}\text{Pb}/^{238}\text{U}$	$^{206}\text{Pb}/^{235}\text{U}$	$\pm 2\sigma$	$^{207}\text{Pb}/^{235}\text{U}$	$\pm 2\sigma$	$^{206}\text{Pb}/^{207}\text{Pb}$	$\pm 2\sigma$	$^{207}\text{Pb}/^{235}\text{U} \pm 2\sigma$	$^{207}\text{Pb}/^{206}\text{Pb} \pm 2\sigma$				
120	132	167	0.79	0.18314	0.00451	1.93094	0.05433	0.07647	0.00135	1084.1	24.6	1091.9	18.8	1107.4	35.4	2.1
121	155	173	0.90	0.16690	0.00341	1.69633	0.03840	0.07372	0.00108	995.0	18.9	1007.1	14.5	1033.7	29.5	3.9
122	74	43	1.73	0.16435	0.00359	1.71830	0.04255	0.07583	0.00160	980.9	19.9	1015.4	15.9	1090.5	42.3	11.2
123	112	107	1.05	0.16683	0.00412	1.85948	0.05780	0.08084	0.00189	994.6	22.7	1066.8	20.5	1217.6	45.9	22.4
124	24	21	1.14	0.17406	0.00363	1.79633	0.06558	0.07485	0.00239	1034.5	19.9	1044.1	23.8	1064.4	64.1	2.9
125	29	20	1.47	0.27543	0.00869	5.16142	0.17927	0.13591	0.00262	1568.3	43.9	1846.3	29.6	2175.7	33.6	38.7
				<i>NRH-15-86 (25 μm)</i>												
1	40	57	0.71	0.33490	0.00898	5.70860	0.20613	0.12363	0.00261	1862.1	43.4	1932.7	31.2	2009.2	37.4	7.9
2	88	45	1.93	0.20881	0.00499	2.40606	0.05248	0.08357	0.00154	1222.5	26.6	1244.4	15.6	1282.5	35.9	4.9
3	247	173	1.42	0.53368	0.01309	14.25429	0.34244	0.19372	0.00286	2756.9	55.0	2766.8	22.8	2774.0	24.2	0.6
4	366	33	11.06	0.60741	0.01428	19.50676	0.46229	0.23292	0.00329	3059.6	57.3	3067.2	22.9	3072.2	22.6	0.4
5	502	226	2.22	0.33511	0.00866	5.27749	0.13048	0.114422	0.00154	1863.1	41.8	1865.2	21.1	1867.6	24.3	0.2
6	279	151	1.85	0.09087	0.00227	0.74574	0.01880	0.05952	0.00104	560.7	13.4	565.8	10.9	586.2	37.8	4.6
7	935	448	2.09	0.26546	0.00837	5.82813	0.12859	0.15923	0.00371	1517.7	42.6	1950.6	19.1	2447.5	39.5	61.3
8	48	21	2.29	0.16401	0.00431	1.66266	0.04894	0.07353	0.00164	979.0	23.8	994.4	18.7	1028.5	45.1	5.1
9	204	108	1.89	0.21549	0.00531	2.54634	0.06205	0.08570	0.00146	1258.0	28.2	1285.4	17.8	1331.4	32.9	5.8
10	206	112	1.85	0.34339	0.00955	5.40363	0.14968	0.11413	0.00156	1903.0	45.8	1885.4	23.7	1866.2	24.6	-1.9
11	284	19	15.11	0.50636	0.01238	11.84196	0.26819	0.16961	0.00249	2641.1	53.0	2592.0	21.2	2553.8	24.6	-3.3
12	553	789	0.70	0.50500	0.01192	12.92485	0.27870	0.18562	0.00258	2635.2	51.0	2674.2	20.3	2703.8	22.9	2.6
13	22	15	1.49	0.19216	0.00539	2.06861	0.05920	0.07807	0.00193	1133.1	29.1	1138.5	19.6	1148.8	49.1	1.4
14	285	173	1.64	0.18847	0.05064	2.03056	0.62243	0.07814	0.00843	1113.1	274.9	1125.8	211.6	1150.4	214.2	3.4
15	58	55	1.04	0.24052	0.06468	3.03307	0.93138	0.09146	0.00991	1389.4	336.4	1416.0	238.8	1456.2	206.1	4.8
16	69	34	2.06	0.16594	0.05504	1.70911	0.64932	0.07470	0.00979	989.7	304.5	1012.0	248.2	1060.4	263.8	7.1
17	16	0	15273.37	0.18572	0.08038	1.88890	0.94222	0.07377	0.01247	1098.1	437.7	1077.2	343.7	1035.1	341.6	-5.7
18	186	82	2.26	0.19297	0.08340	2.14014	1.06494	0.08044	0.01327	1137.4	451.4	1161.9	358.5	1207.7	324.9	6.2
19	179	176	1.02	0.55212	0.23908	15.56767	7.75933	0.20450	0.03381	2834.0	1000.9	2850.6	515.8	2862.4	268.9	1.0
20	39	23	1.71	0.16681	0.05541	1.69414	0.64386	0.07366	0.00969	994.5	306.4	1006.3	247.4	1032.2	265.9	3.8
21	55	16	3.33	0.16579	0.05501	1.71438	0.65099	0.07500	0.00984	988.9	304.4	1013.9	248.4	1068.5	263.6	8.1
22	28	21	1.31	0.17060	0.07377	1.80610	0.90000	0.07678	0.01282	1015.4	406.8	1047.7	337.6	1115.6	333.1	9.9
23	173	122	1.42	0.18891	0.06256	2.10032	0.79627	0.08064	0.01048	1115.5	339.5	1148.9	266.8	1212.6	255.7	8.7
24	263	60	4.35	0.27943	0.07510	3.81789	1.17046	0.09910	0.01063	1588.5	378.8	1596.5	251.7	1607.2	199.9	1.2
25	64	40	1.57	0.16186	0.04363	1.76602	0.54328	0.07913	0.00884	967.1	242.2	1033.1	202.1	1175.5	220.9	21.5

Spot	Conc. (ppm)	Ratios						Ages								
		[U]	[Th]	$^{206}\text{Pb}/^{238}\text{U}$	$\pm 2\sigma$	$^{207}\text{Pb}/^{235}\text{U}$	$\pm 2\sigma$	$^{207}\text{Pb}/^{206}\text{Pb}$	$\pm 2\sigma$	$^{206}\text{Pb}/^{238}\text{U} \pm 2\sigma$	$^{207}\text{Pb}/^{235}\text{U} \pm 2\sigma$	$^{207}\text{Pb}/^{206}\text{Pb} \pm 2\sigma$	% Disc			
26	100	20	4.99	0.17947	0.05923	1.87507	0.70936	0.07578	0.00987	1064.1	324.0	1072.3	255.8	1089.2	261.0	2.4
27	70	120	0.58	0.47504	0.01410	12.10656	0.36422	0.18484	0.00338	2505.6	61.6	2612.7	28.2	2696.8	30.2	7.6
28	32	16	1.96	0.17523	0.00606	1.91376	0.07115	0.07921	0.00286	1040.8	33.2	1085.9	24.8	1177.4	71.5	13.1
29	161	103	1.56	0.17898	0.00530	1.83765	0.05471	0.07447	0.00137	1061.4	29.0	1059.0	19.6	1054.1	37.0	-0.7
30	205	64	3.22	0.18716	0.00530	2.03461	0.06003	0.07884	0.00129	1106.0	28.8	1127.2	20.1	1168.2	32.5	5.6
31	109	95	1.15	0.24880	0.00641	3.34355	0.09421	0.09747	0.00176	1432.3	33.1	1491.3	22.0	1576.2	33.7	10.0
32	161	70	2.31	0.23759	0.00577	2.88164	0.08036	0.08797	0.00164	1374.2	30.1	1377.1	21.0	1381.7	35.8	0.6
33	77	37	2.07	0.16947	0.00398	1.70033	0.04580	0.07277	0.00140	1009.2	21.9	1008.7	17.2	1007.4	39.1	-0.2
34	53	24	2.15	0.17855	0.00376	1.87602	0.05274	0.07620	0.00172	1059.0	20.6	1072.7	18.6	1100.5	45.1	3.9
35	281	96	2.91	0.17943	0.00461	1.86400	0.05059	0.07535	0.00133	1063.8	25.2	1068.4	17.9	1077.7	35.5	1.3
36	29	47	0.61	0.55290	0.01468	15.65734	0.45842	0.20539	0.00453	2837.2	60.9	2856.1	28.0	2869.5	35.8	1.1
37	565	315	1.79	0.31918	0.00768	5.04762	0.13939	0.11469	0.00217	1785.7	37.5	1827.3	23.4	1875.1	34.2	5.0
38	89	45	1.97	0.16951	0.00499	1.71292	0.05667	0.07329	0.00192	1009.4	27.5	1013.4	21.2	1022.0	53.1	1.3
39	34	33	1.04	0.16611	0.00444	1.72190	0.05828	0.07518	0.00236	990.6	24.5	1016.7	21.7	1073.4	63.1	8.4
40	699	10594	0.07	0.09282	0.00288	1.00997	0.04481	0.07891	0.00245	572.2	17.0	708.9	22.6	1170.0	61.4	104.5
41	653	419	1.56	0.46136	0.01104	11.89329	0.36094	0.18696	0.00314	2445.6	48.7	2596.0	28.4	2715.6	27.7	11.0
42	44	38	1.15	0.17049	0.00396	1.74361	0.06126	0.07417	0.00221	1014.8	21.8	1024.8	22.7	1046.2	60.2	3.1
43	172	138	1.24	0.15412	0.00360	1.52100	0.04086	0.07157	0.00121	924.0	20.1	938.9	16.5	973.9	34.4	5.4
44	468	108	4.32	0.17303	0.00464	1.80322	0.05822	0.07558	0.00149	1028.8	25.5	1046.6	21.1	1084.1	39.4	5.4
45	23	45	0.52	0.53249	0.01362	14.46677	0.36766	0.19704	0.00380	2752.0	57.3	2780.8	24.1	2801.8	31.5	1.8
46	184	108	1.70	0.16518	0.00372	1.66144	0.04166	0.07295	0.00126	985.5	20.6	993.9	15.9	1012.6	35.1	2.7
47	528	404	1.31	0.22972	0.00642	3.36716	0.11526	0.10631	0.00156	1333.0	33.7	1496.8	26.8	1737.1	26.9	30.3
48	27	64	0.42	0.53268	0.01302	14.43738	0.38004	0.19657	0.00383	2752.7	54.8	2778.9	25.0	2797.9	31.9	1.6
49	518	82	6.35	0.50328	0.01233	12.58795	0.32724	0.18140	0.00245	2627.9	52.9	2649.3	24.5	2665.7	22.4	1.4
50	50	32	1.55	0.18597	0.00557	1.94579	0.06653	0.07588	0.00183	1099.5	30.3	1097.0	22.9	1092.0	48.3	-0.7
51	172	114	1.50	0.50382	0.01199	12.88865	0.32304	0.18554	0.00258	2630.2	51.4	2671.5	23.6	2703.0	23.0	2.8
52	234	341	0.69	0.46877	0.01093	11.89829	0.26054	0.18409	0.00250	2478.2	48.0	2596.4	20.5	2690.0	22.5	8.5
53	57	38	1.50	0.08822	0.00235	0.76118	0.02998	0.06258	0.00207	545.0	13.9	574.7	17.3	693.8	70.4	27.3
54	164	127	1.29	0.21867	0.00503	2.55755	0.06497	0.08483	0.00145	1274.8	26.6	1288.6	18.5	1311.6	33.2	2.9
55	24	21	1.13	0.40806	0.00993	7.42999	0.20892	0.13206	0.00229	2206.1	45.5	2164.6	25.2	2125.5	30.4	-3.7
56	69	42	1.63	0.16883	0.00415	1.76112	0.04729	0.07566	0.00159	1005.7	22.9	1031.3	17.4	1086.0	42.1	8.0

Conc. (ppm)	Ratios						Ages							
	Spot [U]	[Th]	$^{206}\text{Pb}/^{238}\text{U}$	$\pm 2\sigma$	$^{207}\text{Pb}/^{235}\text{U}$	$\pm 2\sigma$	$^{207}\text{Pb}/^{206}\text{Pb}$	$\pm 2\sigma$	$^{206}\text{Pb}/^{238}\text{U}$	$\pm 2\sigma$	$^{207}\text{Pb}/^{235}\text{U}$	$\pm 2\sigma$	$^{207}\text{Pb}/^{206}\text{Pb}$	$\pm 2\sigma$
57 29	11	2.69	0.20531	0.00599	2.41639	0.06418	0.08536	0.00225	1203.8	32.0	1247.5	19.1	1323.8	51.0
58 433	188	2.30	0.32173	0.00870	5.17563	0.13952	0.11667	0.00204	1798.2	42.4	1848.6	22.9	1905.9	31.4
59 31	24	1.30	0.35027	0.01133	6.49206	0.16774	0.13443	0.00341	1935.9	54.1	2044.8	22.7	2156.6	44.3
60 36	54	0.67	0.16675	0.00434	1.68666	0.04821	0.07336	0.00220	994.2	24.0	1003.5	18.2	1023.9	60.8
61 66	35	1.91	0.56962	0.01350	15.81899	0.40616	0.20142	0.00356	2906.3	55.4	2865.9	24.5	2837.7	28.8
62 53	29	1.81	0.19798	0.00465	2.24942	0.06546	0.08240	0.00189	1164.5	25.0	1196.6	20.5	1255.1	44.8
63 304	180	1.69	0.08996	0.00213	0.72508	0.01876	0.05846	0.00104	555.3	12.6	553.7	11.0	547.0	38.7
64 65	53	1.22	0.54183	0.01366	15.21709	0.40310	0.20369	0.00381	2791.1	57.1	2828.9	25.2	2856.0	30.4
65 386	646	0.60	0.32195	0.00772	5.08398	0.13229	0.11453	0.00181	1799.2	37.7	1833.4	22.1	1872.5	28.4
66 331	80	4.13	0.30654	0.00871	4.44767	0.12544	0.10523	0.00184	1723.7	43.0	1721.3	23.4	1718.3	32.1
67 135	31	4.36	0.22530	0.00893	2.54028	0.09899	0.08178	0.00200	1309.8	47.0	1283.7	28.4	1240.2	47.8
68 154	55	2.81	0.17707	0.00437	1.80935	0.04919	0.07411	0.00152	1050.9	23.9	1048.8	17.8	1044.5	41.5
69 60	88	0.69	0.49560	0.01264	12.52586	0.31280	0.18330	0.00353	2594.9	54.5	2644.7	23.5	2683.0	31.8
70 238	8	30.60	0.17360	0.00473	1.80197	0.05760	0.07528	0.00145	1031.9	26.0	1046.2	20.9	1076.1	38.6
71 76	532	0.14	0.48913	0.01315	11.63492	0.30222	0.17252	0.00320	2566.9	56.9	2575.5	24.3	2582.2	31.0
72 65	41	1.60	0.18021	0.00486	1.90685	0.06308	0.07674	0.00189	1068.1	26.6	1083.5	22.0	1114.5	49.1
73 71	68	1.04	0.51706	0.01305	13.27992	0.32753	0.18628	0.00348	2686.7	55.5	2699.8	23.3	2709.6	30.8
74 166	62	2.69	0.18268	0.00498	1.92267	0.05236	0.07633	0.00154	1081.6	27.1	1089.0	18.2	1103.8	40.4
75 137	127	1.08	0.24268	0.00647	2.95073	0.08076	0.08819	0.00157	1400.6	33.6	1395.0	20.8	1386.5	34.1
76 601	416	1.44	0.41934	0.01295	8.36946	0.25815	0.14475	0.00249	2257.5	58.8	2271.9	28.0	2284.8	29.6
77 119	84	1.42	0.51851	0.01553	13.16293	0.38733	0.18412	0.00375	2692.8	65.9	2691.4	27.8	2690.3	33.7
78 99	78	1.26	0.52598	0.01414	13.48732	0.34814	0.18597	0.00344	2724.5	59.7	2714.4	24.4	2706.9	30.5
79 57	35	1.63	0.22025	0.00806	2.32121	0.09055	0.07643	0.00209	1283.2	42.6	1218.8	27.7	1106.5	54.6
80 122	156	0.78	0.27462	0.00856	3.75370	0.12444	0.09913	0.00187	1564.2	43.3	1582.9	26.6	1607.9	35.1
81 248	98	2.53	0.33804	0.00833	5.37203	0.13429	0.11526	0.00194	1877.2	40.1	1880.4	21.4	1883.9	30.3
82 67	64	1.04	0.24228	0.00705	2.96827	0.08594	0.08886	0.00170	1398.5	36.6	1399.5	22.0	1401.1	36.7
83 91	42	2.17	0.53323	0.01775	13.72354	0.40456	0.18666	0.00329	2755.1	74.6	2730.8	27.9	2712.9	29.1
84 23	8	2.75	0.17662	0.00468	1.81900	0.05804	0.07469	0.00223	1048.5	25.6	1052.3	20.9	1060.3	60.0
85 89	57	1.56	0.22822	0.00591	2.69248	0.08017	0.08557	0.00159	1325.1	31.0	1326.4	22.1	1328.4	35.9
86 118	142	0.83	0.17694	0.00440	1.81025	0.05383	0.07420	0.00140	1050.2	24.1	1049.2	19.5	1047.0	38.1
87 26	13	1.97	0.19459	0.00588	2.25462	0.07210	0.08403	0.00257	1146.2	31.7	1198.2	22.5	1293.3	59.6

Conc. (ppm)	Spot [U]	[Th]	Ratios			Ages										
			$^{206}\text{Pb}/^{238}\text{U}$	$^{207}\text{Pb}/^{235}\text{U}$	$\pm 2\sigma$	$^{207}\text{Pb}/^{206}\text{Pb}$	$\pm 2\sigma$	$^{206}\text{Pb}/^{238}\text{U}$	$\pm 2\sigma$	$^{207}\text{Pb}/^{235}\text{U}$	$\pm 2\sigma$	$^{207}\text{Pb}/^{206}\text{Pb}$				
88	65	69	0.93	0.48934	0.01266	11.86759	0.33655	0.17590	0.00294	2567.8	54.8	2594.0	26.6	2614.5	27.8	1.8
89	31	14	2.26	0.17496	0.00485	1.81895	0.05751	0.07540	0.00207	1039.4	26.6	1052.3	20.7	1079.3	55.1	3.8
90	86	29	2.95	0.18746	0.00625	1.87762	0.06612	0.07264	0.00167	1107.6	33.9	1073.2	23.3	1004.0	46.6	-9.4
91	190	90	2.10	0.17800	0.00481	1.81202	0.05505	0.07383	0.00165	1056.0	26.3	1049.8	19.9	1036.9	45.2	-1.8
92	41	23	1.80	0.17130	0.00464	1.75276	0.05739	0.07421	0.00195	1019.3	25.5	1028.2	21.2	1047.2	52.9	2.7
93	251	4	65.85	0.17444	0.00391	1.78704	0.04159	0.07430	0.00147	1036.5	21.4	1040.7	15.2	1049.6	39.8	1.3
94	42	23	1.85	0.18159	0.00421	1.90811	0.05261	0.07621	0.00190	1075.6	23.0	1083.9	18.4	1100.6	49.9	2.3
95	228	158	1.44	0.53063	0.01286	13.92735	0.33364	0.19036	0.00285	2744.1	54.2	2744.8	22.7	2745.3	24.6	0.0
96	70	56	1.24	0.18632	0.00411	1.89727	0.05187	0.07385	0.00172	1101.4	22.3	1080.1	18.2	1037.5	47.0	-5.8
97	72	70	1.02	0.51332	0.01338	13.06307	0.31733	0.18457	0.00281	2670.8	57.0	2684.2	22.9	2694.4	25.2	0.9
98	23	26	0.88	0.23912	0.00571	3.16505	0.08505	0.09600	0.00241	1382.1	29.7	1448.7	20.7	1547.8	47.1	12.0
99	550	121	4.54	0.19774	0.00454	2.16248	0.05148	0.07931	0.00109	1163.2	24.5	1169.1	16.5	1180.0	27.1	1.4
100	76	39	1.94	0.57344	0.01115	18.45229	0.38460	0.23338	0.00352	2921.9	45.7	3013.6	20.1	3075.4	24.1	5.3
101	145	171	0.84	0.17120	0.00417	1.72709	0.04739	0.07317	0.00165	1018.7	23.0	1018.7	17.6	1018.6	45.5	0.0
102	87	42	2.08	0.21332	0.00539	2.44400	0.07005	0.08309	0.00222	1246.5	28.6	1255.7	20.7	1271.4	52.1	2.0
103	261	171	1.53	0.32857	0.00817	5.05528	0.12271	0.11159	0.00230	1831.4	39.6	1828.6	20.6	1825.5	37.5	-0.3
104	11	7	1.50	0.17495	0.00442	1.99581	0.08470	0.08274	0.00331	1039.3	24.3	1114.1	28.7	1263.0	78.2	21.5
105	292	181	1.61	0.28665	0.00697	3.95394	0.09396	0.10004	0.00193	1624.7	34.9	1624.8	19.3	1624.9	35.8	0.0
106	78	61	1.28	0.19812	0.00575	2.12568	0.06191	0.07782	0.00177	1165.2	30.9	1157.2	20.1	1142.2	45.3	-2.0
107	87	64	1.35	0.52012	0.01394	13.26716	0.41518	0.18500	0.00405	2699.7	59.1	2698.8	29.6	2698.2	36.2	-0.1
108	21	10	2.12	0.21703	0.00643	3.17927	0.19190	0.10625	0.00721	1266.1	34.1	1452.1	46.7	1736.0	124.4	37.1
109	78	80	0.97	0.38097	0.00857	6.94841	0.19282	0.13228	0.00302	2080.8	40.0	2104.9	24.6	2128.4	40.0	2.3
110	255	136	1.88	0.18166	0.00514	1.87291	0.05838	0.07478	0.00161	1076.0	28.0	1071.6	20.6	1062.5	43.2	-1.3
111	259	157	1.64	0.25431	0.00587	3.23766	0.08587	0.09233	0.00186	1460.7	30.2	1466.2	20.6	1474.3	38.3	0.9
112	435	226	1.93	0.25500	0.00668	3.21483	0.08841	0.09144	0.00168	1464.2	34.3	1460.7	21.3	1455.7	34.9	-0.6
113	236	323	0.73	0.33694	0.00948	5.21600	0.14638	0.11228	0.00175	1871.9	45.7	1855.2	23.9	1836.6	28.2	-1.9
114	111	53	2.09	0.18589	0.00559	3.05923	0.22571	0.11936	0.00630	1099.1	30.4	1422.5	56.5	1946.6	94.4	77.1
115	80	68	1.18	0.55504	0.01299	15.82942	0.38794	0.20684	0.00346	2846.1	53.9	2866.6	23.4	2881.0	27.1	1.2
										NPM-ID-86-2 (25 μm)						
1	59	71	0.84	0.165598	2.774	1.684139	2.972	0.075605	3.134	987.8	25.4	1002.5	18.9	1084.6	62.8	9.8
2	179	101	1.78	0.178653	1.821	1.793463	1.806	0.075367	1.985	1059.6	17.8	1043.1	11.8	1078.3	39.8	1.8

Conc. (ppm)	Ratios										Ages				
	Spot [U]	[Th]	$^{206}\text{Pb}/^{238}\text{U}$	$^{207}\text{Pb}/^{235}\text{U}$	$\pm 2\sigma$	$^{207}\text{Pb}/^{206}\text{Pb}$	$\pm 2\sigma$	$^{206}\text{Pb}/^{238}\text{U}$	$\pm 2\sigma$	$^{207}\text{Pb}/^{235}\text{U}$	$\pm 2\sigma$	$^{207}\text{Pb}/^{206}\text{Pb}$	$\pm 2\sigma$	% Disc	
3	139	162	0.86	0.233173	2.026	2.718021	2.181	0.087015	1.983	1351.1	24.7	1333.4	16.2	1360.8	38.2
4	88	66	1.34	0.180685	1.896	1.832888	2.263	0.075923	2.355	1070.7	18.7	1057.3	14.9	1093.1	47.2
5	489	37	13.17	0.183142	2.228	1.879125	3.158	0.076613	3.012	1084.1	22.2	1073.8	20.9	1111.1	60.2
6	2672	4679	0.57	0.175896	2.566	1.901147	2.804	0.081067	3.182	1044.5	24.7	1081.5	18.7	1223.1	62.5
7	48	33	1.48	0.075835	2.458	0.583241	2.152	0.056882	1.887	471.2	11.2	466.5	8.0	487.0	41.6
8	456	299	1.53	0.257403	2.277	3.257157	1.719	0.093276	1.376	1476.5	30.0	1470.9	13.4	1493.5	26.0
9	1319	900	1.47	0.383506	2.442	6.846021	1.987	0.132114	1.967	2092.6	43.6	2091.7	17.6	2126.3	34.4
10	1330	921	1.44	0.243679	2.223	2.935693	1.579	0.089013	1.610	1405.8	28.1	1391.2	12.0	1404.4	30.8
11	50	35	1.44	0.182566	2.801	1.903175	2.590	0.077385	1.885	1081.0	27.9	1082.2	17.2	1131.1	37.5
12	236	209	1.13	0.198438	2.727	2.129375	2.700	0.079713	2.660	1166.9	29.1	1158.4	18.7	1189.9	52.5
13	205	95	2.15	0.258097	2.653	3.066009	2.674	0.088375	1.952	1480.1	35.1	1424.2	20.5	1390.6	37.5
14	376	36	10.33	0.227244	2.163	2.760950	1.952	0.090023	1.747	1320.0	25.8	1345.0	14.5	1426.0	33.4
15	384	40	9.71	0.176087	2.635	1.849906	3.410	0.078843	2.611	1045.6	25.4	1063.4	22.5	1168.2	51.7
16	159	120	1.32	0.174915	2.436	1.890093	2.753	0.080502	3.009	1039.1	23.4	1077.6	18.3	1209.3	59.2
17	242	142	1.71	0.172879	2.175	1.745994	2.077	0.075288	1.899	1028.0	20.7	1025.7	13.4	1076.2	38.1
18	69	67	1.03	0.185437	2.442	1.887378	1.724	0.076123	1.484	1096.6	24.6	1076.7	11.4	1098.3	29.7
19	449	38	11.85	0.203942	2.180	2.253041	1.934	0.082223	1.736	1196.5	23.8	1197.7	13.6	1250.8	34.0
20	1310	813	1.61	0.191784	2.080	2.214132	2.101	0.085483	2.132	1131.0	21.6	1185.5	14.7	1326.5	41.3
21	1321	820	1.61	0.076505	2.106	0.596078	2.472	0.057419	2.258	475.2	9.6	474.7	9.4	507.7	49.7
22	169	128	1.32	0.215455	2.467	2.484809	2.100	0.085586	1.954	1257.8	28.2	1267.6	15.2	1328.8	37.8
23	72	119	0.61	0.447753	3.258	10.161194	2.321	0.169738	1.922	2385.3	65.0	2449.6	21.5	2555.1	32.2
24	549	464	1.18	0.329281	2.362	4.910875	1.805	0.111747	1.741	1834.9	37.7	1804.1	15.2	1828.0	31.6
25	164	134	1.23	0.501969	2.247	12.122204	1.709	0.177864	1.837	2622.3	48.4	2613.9	16.0	2633.1	30.5
26	203	89	2.29	0.434533	2.694	9.073734	2.372	0.154397	1.868	2326.1	52.6	2345.5	21.7	2395.2	31.8
27	286	166	1.72	0.097467	2.144	0.776424	3.318	0.059593	3.093	599.5	12.3	583.4	14.7	588.8	67.1
28	117	85	1.37	0.082344	1.899	0.622012	3.115	0.055765	3.177	510.1	9.3	491.1	12.1	443.0	70.7
29	378	38	10.04	0.256283	1.585	3.223042	1.994	0.092584	1.389	1470.8	20.8	1462.7	15.5	1479.4	26.3
30	412	41	9.99	0.205491	2.274	2.257290	2.538	0.082612	2.189	1204.8	25.0	1199.1	17.9	1260.1	42.8
31	1420	910	1.56	0.289352	1.585	3.827187	2.053	0.097758	1.560	1638.3	22.9	1598.5	16.5	1581.8	29.2
32	102	70	1.46	0.232912	2.542	2.856690	3.603	0.092362	3.129	1349.7	31.0	1370.6	27.1	1474.8	59.4
33	279	201	1.39	0.403597	1.958	7.690409	2.567	0.141725	2.097	2185.6	36.3	2195.5	23.1	2248.4	36.2
34	306	143	2.14	0.189652	3.212	2.051008	5.903	0.078697	6.571	1119.5	33.0	1132.6	40.3	1164.5	130.2

Spot	Conc. (ppm)	Ratios								Ages						
		[U]	[Th]	U/Th	$^{206}\text{Pb}/^{238}\text{U}$	$\pm 2\sigma$	$^{207}\text{Pb}/^{235}\text{U}$	$\pm 2\sigma$	$^{207}\text{Pb}/^{206}\text{Pb}$	$\pm 2\sigma$	$^{206}\text{Pb}/^{238}\text{U}$	$\pm 2\sigma$	$^{207}\text{Pb}/^{235}\text{U}$	$\pm 2\sigma$	$^{207}\text{Pb}/^{206}\text{Pb}$	$\pm 2\sigma$
35	129	72	1.79	0.177730	2.042	1.780537	2.417	0.074115	1.519	1054.6	19.9	1038.4	15.7	1044.6	30.7	-0.9
36	138	81	1.71	0.205069	2.606	2.273265	2.768	0.082784	2.186	1202.5	28.6	1204.0	19.5	1264.1	42.7	5.1
37	60	44	1.38	0.075129	2.192	0.584803	2.445	0.057861	1.780	467.0	9.9	467.5	9.2	524.5	39.0	12.3
38	11	7	1.69	0.258580	1.807	3.223444	2.025	0.091935	1.468	1482.6	23.9	1462.8	15.7	1466.0	27.9	-1.1
39	339	204	1.66	0.272185	1.971	3.645856	2.249	0.098594	1.787	1551.9	27.2	1559.6	17.9	1597.7	33.4	3.0
40	86	85	1.00	0.323063	1.831	4.828247	1.930	0.110928	1.453	1804.7	28.8	1789.8	16.2	1814.7	26.4	0.6
41	367	36	10.18	0.259106	1.969	3.240441	2.153	0.092948	1.672	1485.3	26.1	1466.9	16.7	1486.8	31.7	0.1
42	401	41	9.77	0.471348	2.391	11.300156	2.457	0.178107	1.862	2489.5	49.4	2548.2	22.9	2635.3	30.9	5.9
43	1429	914	1.56	0.079801	2.495	0.6335122	3.807	0.059598	3.338	494.9	11.9	499.3	15.0	589.0	72.4	19.0
44	406	227	1.79	0.074671	2.091	0.588228	3.028	0.057685	2.944	464.2	9.4	469.7	11.4	517.8	64.6	11.5
45	407	403	1.01	0.176247	1.812	1.741974	3.978	0.073361	3.544	1046.4	17.5	1024.2	25.7	1023.9	71.7	-2.2
46	323	165	1.95	0.473260	1.843	10.405661	3.631	0.162435	3.244	2497.8	38.2	2471.6	33.7	2481.2	54.7	-0.7
47	413	39	10.55	0.299401	2.612	3.712515	5.022	0.090753	4.804	1688.3	38.8	1574.1	40.2	1441.4	91.6	-14.6
48	360	87	4.13	0.188870	2.281	1.856366	4.773	0.073517	4.568	1115.3	23.4	1065.7	31.5	1028.2	92.4	-7.8
49	739	528	1.40	0.326306	2.098	4.882244	4.179	0.110843	3.809	1820.5	33.3	1799.2	35.2	1813.3	69.2	-0.4
50	286	166	1.72	0.166343	2.105	1.628729	4.274	0.072918	3.981	991.9	19.4	981.4	26.9	1011.7	80.7	2.0
51	158	47	3.35	0.524553	3.248	18.173219	4.536	0.258279	4.027	2718.5	72.0	2998.9	43.7	3236.2	63.5	19.0
52	381	39	9.71	0.217983	1.962	2.480112	4.038	0.084852	3.746	1271.2	22.6	1266.2	29.2	1312.1	72.7	3.2
53	601	409	1.47	0.312920	2.503	4.764498	5.105	0.114013	4.770	1755.1	38.5	1778.7	42.9	1864.3	86.1	6.2
54	692	504	1.37	0.152686	2.162	1.502809	4.743	0.072904	4.647	916.0	18.5	931.5	28.9	1011.3	94.2	10.4
55	25	27	0.91	0.169760	2.335	1.739287	4.913	0.076074	5.014	1010.8	21.8	1023.2	31.7	1097.0	100.3	8.5
56	52	44	1.19	0.513149	2.346	12.490121	5.488	0.183546	5.401	2670.1	51.3	2642.0	51.6	2685.2	89.3	0.6
57	587	265	2.22	0.197732	2.040	2.109978	5.570	0.078106	4.462	1163.1	21.7	1152.1	38.4	1149.6	88.6	-1.2
58	19	19	1.03	0.213607	1.922	2.378397	5.403	0.083428	4.467	1248.0	21.8	1236.1	38.6	1279.3	87.1	2.5
59	56	42	1.34	0.236998	1.931	2.773805	6.964	0.086717	4.950	1371.1	23.9	1348.5	52.0	1354.2	95.5	-1.2
60	64	42	1.52	0.204969	2.813	2.338857	10.102	0.083991	6.968	1202.0	30.8	1224.2	72.0	1292.3	135.6	7.5

Table 3 – Irish Town Formation

Conc. (ppm)	Ratios										Ages					
	Spot [U]	[Th]	$^{206}\text{Pb}/^{238}\text{U}$	$\pm 2\sigma$	$^{207}\text{Pb}/^{235}\text{U}$	$\pm 2\sigma$	$^{207}\text{Pb}/^{206}\text{Pb}$	$\pm 2\sigma$	$^{206}\text{Pb}/^{238}\text{U}$	$\pm 2\sigma$	$^{207}\text{Pb}/^{235}\text{U}$	$\pm 2\sigma$	$^{207}\text{Pb}/^{206}\text{Pb}$	$\pm 2\sigma$		
1	505	133	3.78	0.515557	0.02673	12.49334	0.60981	0.17575	0.00872	2680.4	113.7	2642.2	45.9	2613.1	82.6	-2.5
2	725	573	1.27	0.31892	0.01666	4.23752	0.20839	0.09637	0.00480	1784.4	81.4	1681.3	40.4	1554.9	93.5	-12.9
3	277	94	2.94	0.47097	0.02446	9.89286	0.49110	0.15235	0.00759	2487.8	107.2	2424.8	45.8	2372.4	85.0	-4.6
4	170	254	0.67	0.17896	0.00850	1.70524	0.08346	0.06911	0.00277	1061.3	46.5	1010.5	31.3	902.0	82.8	-15.0
5	113	50	2.25	0.51303	0.01897	12.47097	0.51327	0.17630	0.00774	2669.6	80.8	2640.5	38.7	2618.4	73.1	-1.9
6	122	81	1.51	0.53780	0.01227	11.94840	0.59485	0.16113	0.00741	2774.3	51.4	2600.4	46.7	2467.6	77.7	-11.1
7	24	21	1.14	0.17645	0.00500	1.96180	0.12736	0.08064	0.00421	1047.5	27.4	1102.5	43.7	1212.6	102.8	15.8
8	102	199	0.51	0.22101	0.00668	2.45304	0.13705	0.08050	0.00381	1287.2	35.2	1258.3	40.3	1209.3	93.2	-6.1
9	61	86	0.71	0.17102	0.00339	1.82103	0.09921	0.07723	0.00368	1017.7	18.7	1053.1	35.7	1127.1	95.0	10.7
10	171	95	1.80	0.51311	0.00973	11.86430	0.58134	0.16770	0.00770	2669.9	41.5	2593.8	45.9	2534.8	77.0	-5.1
11	746	66	11.33	0.27532	0.00620	3.42276	0.12090	0.09017	0.00284	1567.7	31.3	1509.6	27.8	1429.0	60.1	-8.8
12	12	0	561.81	0.32520	0.00763	4.45446	0.15460	0.09934	0.00276	1815.1	37.1	1722.5	28.8	1611.8	51.8	-11.2
13	29	37	0.79	0.20692	0.00656	4.65514	0.21673	0.16317	0.00746	1212.4	35.0	1759.2	38.9	2488.8	77.0	105.3
14	48	53	0.90	0.19177	0.00698	2.98197	0.19278	0.11278	0.00475	1130.9	37.8	1403.0	49.2	1844.7	76.2	63.1
15	101	39	2.59	0.19391	0.00494	2.43245	0.11387	0.09098	0.00329	1142.5	26.7	1252.2	33.7	1446.1	69.0	26.6
16	30	38	0.80	0.51573	0.01458	11.85478	0.58527	0.16671	0.00440	2681.1	62.0	2593.0	46.3	2524.9	44.3	-5.8
17	181	131	1.38	0.24111	0.00992	3.75630	0.29107	0.11299	0.00473	1392.4	51.5	1583.5	62.2	1848.1	75.7	32.7
18	101	106	0.95	0.49903	0.01357	11.26033	0.54746	0.16365	0.00418	2609.6	58.4	2544.9	45.4	2493.8	43.1	-4.4
19	42	1	71.46	0.35268	0.00966	5.06579	0.25446	0.10418	0.00290	1947.4	46.0	1830.4	42.6	1699.8	51.3	-12.7
20	113	40	2.83	0.16838	0.00575	2.30068	0.14152	0.09910	0.00368	1003.2	31.7	1212.5	43.6	1607.2	69.2	60.2
21	119	168	0.71	0.45444	0.01350	9.19846	0.58768	0.14680	0.00654	2414.9	59.8	2358.0	58.6	2309.0	76.5	-4.4
22	245	63	3.89	0.53150	0.01543	12.33167	0.78937	0.16827	0.00742	2747.8	64.9	2630.0	60.2	2540.5	73.9	-7.5
23	47	43	1.08	0.57659	0.01247	15.00601	0.72766	0.18876	0.00655	2934.8	51.0	2815.6	46.2	2731.3	57.1	-6.9
24	3948	3084	1.28	0.19151	0.00799	3.19231	0.23481	0.12089	0.00925	1129.6	43.3	1455.3	56.9	1969.5	136.4	74.4
25	182	112	1.63	0.09594	0.00377	1.20398	0.05791	0.09101	0.00193	590.6	22.2	802.4	26.7	1446.9	40.3	145.0
26	612	360	1.70	0.33552	0.00718	4.66908	0.14777	0.10093	0.00198	1865.1	34.6	1761.7	26.5	1641.3	36.4	-12.0
27	80	93	0.86	0.32435	0.00821	4.52582	0.14659	0.10120	0.00203	1810.9	40.0	1735.7	26.9	1646.2	37.2	-9.1
28	141	65	2.16	0.18229	0.00458	2.07149	0.10270	0.08242	0.00253	1079.5	25.0	1139.4	34.0	1255.4	60.1	16.3

Conc. (ppm)	Ratios						Ages						
	Spot [U]	[Th]	$^{206}\text{Pb}/^{238}\text{U}$	$\pm 2\sigma$	$^{207}\text{Pb}/^{235}\text{U}$	$\pm 2\sigma$	$^{206}\text{Pb}/^{206}\text{Pb}$	$\pm 2\sigma$	$^{207}\text{Pb}/^{235}\text{U}$	$\pm 2\sigma$	$^{207}\text{Pb}/^{206}\text{Pb}$	$\pm 2\sigma$	
29	127	111	1.15	0.50821	0.01207	11.51682	0.37044	0.116436	0.00340	2649.0	51.6	2565.9	30.1
30	137	60	2.27	0.56795	0.01375	14.60816	0.48682	0.18654	0.00349	2899.4	56.5	2790.1	31.7
31	110	134	0.82	0.54353	0.02612	12.14116	0.46681	0.16201	0.00173	2798.2	109.1	2615.4	36.1
32	85	67	1.28	0.18640	0.00891	1.94681	0.07867	0.07575	0.00137	1101.8	48.4	1097.3	27.1
33	255	192	1.32	0.52210	0.01898	11.72453	0.37514	0.16287	0.00234	2708.1	80.4	2582.7	29.9
34	188	265	0.71	0.56862	0.02026	13.80843	0.56186	0.17613	0.00305	2902.1	83.3	2736.7	38.5
35	147	49	2.99	0.34395	0.01183	5.05378	0.20114	0.10657	0.00194	1905.7	56.8	1828.4	33.7
36	91	46	1.99	0.18657	0.00696	2.22142	0.11753	0.08635	0.00233	1102.8	37.8	1187.8	37.1
37	161	235	0.68	0.42152	0.01372	7.95798	0.36475	0.13693	0.00302	2267.4	62.2	2226.3	41.4
38	133	47	2.81	0.33981	0.01176	4.92078	0.23645	0.10503	0.00197	1885.7	56.6	1805.8	40.6
39	371	132	2.82	0.17419	0.00630	1.72867	0.08951	0.07198	0.00165	1035.1	34.6	1019.3	33.3
40	111	42	2.66	0.35449	0.01245	5.26004	0.25283	0.10762	0.00198	1956.0	59.2	1862.4	41.0
41	61	42	1.47	0.13826	0.00443	2.35491	0.10226	0.12354	0.00250	834.8	25.1	1229.0	31.0
42	91	393	0.23	0.53410	0.01383	12.76341	0.39577	0.17332	0.00353	2758.7	58.1	2662.3	29.2
43	5213	2818	1.85	0.63733	0.01816	55.14299	1.85941	0.62751	0.01127	3178.5	71.5	4089.9	33.6
44	1219	492	2.48	0.06082	0.00233	0.63701	0.02712	0.07596	0.00119	380.6	14.2	500.5	16.8
45	147	70	2.11	0.40327	0.01248	8.52298	0.23872	0.15328	0.00219	2184.1	57.3	2288.4	25.5
46	2328	2061	1.13	0.12663	0.00281	1.68440	0.03459	0.09647	0.00149	768.6	16.1	1002.6	13.1
47	84	64	1.30	0.09762	0.00284	1.48231	0.05506	0.11012	0.00241	600.5	16.7	923.2	22.5
48	65	45	1.44	0.49368	0.00833	11.14418	0.19149	0.16372	0.00258	2586.6	36.0	2535.3	16.0
49	403	214	1.88	0.04508	0.00226	0.52881	0.05876	0.08507	0.00491	284.3	14.0	431.0	39.0
50	136	61	2.24	0.33814	0.00881	5.07988	0.12515	0.10896	0.00157	1877.7	42.4	1832.8	20.9
51	678	136	5.00	0.17380	0.00519	1.86924	0.05960	0.07800	0.00220	1033.0	28.5	1070.3	21.1
52	884	75	11.74	0.33266	0.00995	4.79145	0.13012	0.10447	0.00210	1851.2	48.2	1783.4	22.8
53	56	29	1.89	0.34236	0.01026	5.02839	0.13246	0.10652	0.00207	1898.0	49.3	1824.1	22.3
54	141	197	0.71	0.59426	0.01581	16.86819	0.38596	0.20587	0.00421	3006.7	63.9	2927.4	21.9
55	223	297	0.75	0.55011	0.01404	13.52461	0.32558	0.17831	0.00335	2825.6	58.4	2717.0	22.8
56	679	240	2.83	0.21366	0.01176	3.13361	0.54406	0.10637	0.01195	1248.3	62.5	1441.0	134.4
57	332	458	0.72	0.36219	0.01014	5.39817	0.13885	0.10809	0.00199	1992.6	48.0	1884.6	22.0
58	132	209	0.64	0.34981	0.00827	5.16444	0.11522	0.10708	0.00212	1933.7	39.5	1846.8	19.0
59	62	434	0.14	0.56032	0.01396	14.35705	0.33761	0.18583	0.00360	2868.0	57.7	2773.6	22.3

Conc. (ppm)	Ratios										Ages				
	Spot [U]	[Th]	$^{206}\text{Pb}/^{238}\text{U}$	$\pm 2\sigma$	$^{207}\text{Pb}/^{235}\text{U}$	$\pm 2\sigma$	$^{207}\text{Pb}/^{206}\text{Pb}$	$\pm 2\sigma$	$^{206}\text{Pb}/^{238}\text{U}$	$\pm 2\sigma$	$^{207}\text{Pb}/^{235}\text{U}$	$\pm 2\sigma$	$^{207}\text{Pb}/^{206}\text{Pb}$	$\pm 2\sigma$	
60	121	52	2.31	0.55729	0.01112	44.62247	0.65258	0.58072	0.01105	2855.4	46.0	3879.2	14.5	4460.5	27.7
61	66	29	2.24	0.34651	0.00728	5.18479	0.09288	0.10852	0.00172	1917.9	34.9	1850.1	15.3	1774.8	29.0
62	102	128	0.80	0.61272	0.01515	17.71438	0.39710	0.20968	0.00370	3080.9	60.6	2974.4	21.5	2903.1	28.6
63	651	187	3.48	0.53575	0.01374	13.41754	0.35038	0.18164	0.00311	2765.6	57.7	2709.5	24.7	2667.9	28.3
64	110	96	1.14	0.33827	0.00755	4.96064	0.11043	0.10636	0.00171	1878.3	36.4	1812.6	18.8	1737.9	29.4
65	94	37	2.57	0.30123	0.00613	4.12925	0.08523	0.09942	0.00187	1697.4	30.4	1660.1	16.9	1613.2	35.1
66	164	153	1.07	0.34625	0.00768	5.23028	0.11765	0.10955	0.00204	1916.7	36.8	1857.6	19.2	1792.0	33.9
67	3818	2486	1.54	0.34083	0.00725	5.02823	0.10572	0.10700	0.00205	1890.7	34.8	1824.1	17.8	1748.9	35.1
68	1316	628	2.10	0.09601	0.00539	1.40047	0.10659	0.10580	0.00334	591.0	31.7	889.1	45.1	1728.2	57.9
69	653	391	1.67	0.34991	0.00682	6.98576	0.15084	0.14479	0.00270	1934.2	32.6	2109.6	19.2	2285.3	32.1
70	101	39	2.59	0.33444	0.00834	4.86521	0.11631	0.10551	0.00195	1859.9	40.3	1796.3	20.1	1723.2	34.0
71	125	91	1.38	0.17638	0.00469	2.08810	0.06634	0.08586	0.00270	1047.2	25.7	1144.9	21.8	1335.1	60.7
72	100	134	0.75	0.30941	0.00791	4.36952	0.09145	0.10242	0.00222	1737.8	38.9	1706.6	17.3	1668.5	40.0
73	597	124	4.80	0.23384	0.00635	2.72078	0.06944	0.08439	0.00160	1354.6	33.2	1334.1	19.0	1301.4	36.8
74	565	581	0.97	0.46448	0.01309	10.28119	0.24581	0.16054	0.00251	2459.3	57.6	2460.4	22.1	2461.3	26.4
75	103	44	2.36	0.33298	0.00936	4.93749	0.12600	0.10755	0.00155	1852.8	45.3	1808.7	21.6	1758.2	26.4
76	67	146	0.46	0.17519	0.00471	1.83966	0.05145	0.07616	0.00155	1040.6	25.8	1059.7	18.4	1099.3	40.7
77	50	26	1.97	0.51895	0.01458	13.18947	0.33215	0.18433	0.00300	2694.7	61.9	2693.3	23.8	2692.3	26.9
78	90	126	0.71	0.20322	0.00609	2.43517	0.07148	0.08691	0.00207	1192.6	32.6	1253.1	21.1	1358.4	45.8
79	130	153	0.85	0.33245	0.00951	4.98894	0.12595	0.10884	0.00170	1850.3	46.0	1817.4	21.4	1780.0	28.4
80	107	46	2.35	0.54470	0.01415	13.50865	0.31796	0.17987	0.00242	2803.1	59.1	2715.9	22.3	2651.6	22.3
81	84	30	2.81	0.32887	0.01048	4.88184	0.12915	0.10766	0.00162	1832.9	50.8	1799.1	22.3	1760.2	27.5
82	109	68	1.60	0.20134	0.00600	2.16400	0.06057	0.07795	0.00166	1182.5	32.2	1169.6	19.4	1145.6	42.4
83	244	408	0.60	0.19711	0.00644	2.11338	0.05763	0.07776	0.00150	1159.8	34.7	1153.2	18.8	1140.8	38.5
84	1974	2617	0.75	0.52533	0.01483	12.78923	0.29226	0.17657	0.00282	2721.8	62.7	2664.3	21.5	2620.9	26.6
85	111	39	2.86	0.17132	0.00826	5.84415	0.26284	0.24740	0.00588	1019.4	45.5	1953.0	39.0	3168.2	37.7
86	402	471	0.85	0.17231	0.00654	1.77218	0.05680	0.07459	0.00179	1024.8	36.0	1035.3	20.8	1057.5	48.4
87	116	67	1.72	0.34136	0.01278	4.89910	0.13367	0.10409	0.00202	1893.2	61.4	1802.1	23.0	1698.3	35.8
88	327	147	2.22	0.54891	0.02053	14.51850	0.39258	0.19183	0.00357	2820.6	85.5	2784.2	25.7	2757.9	30.5
90	116	45	2.60	0.17013	0.00635	1.66552	0.04497	0.07100	0.00140	1012.8	35.0	995.5	17.1	957.4	40.4
91	311	219	1.42	0.34471	0.00917	5.23982	0.13475	0.11025	0.00180	1909.3	44.0	1859.1	21.9	1803.5	29.7

Conc. (ppm)	Spot [U]	[Th]	Ratios						Ages							
			$^{206}\text{Pb}/^{238}\text{U}$	$\pm 2\sigma$	$^{207}\text{Pb}/^{235}\text{U}$	$\pm 2\sigma$	$^{207}\text{Pb}/^{206}\text{Pb}$	$\pm 2\sigma$	$^{206}\text{Pb}/^{238}\text{U} \pm 2\sigma$	$^{207}\text{Pb}/^{235}\text{U} \pm 2\sigma$	$^{207}\text{Pb}/^{206}\text{Pb} \pm 2\sigma$	$^{207}\text{Pb}/^{206}\text{Pb} \pm 2\sigma$				
92	27	31	0.88	0.23723	0.00614	2.70234	0.06828	0.08262	0.00138	1372.3	32.0	1329.1	18.7	1260.2	32.5	-8.2
93	208	110	1.89	0.18134	0.00574	2.18455	0.08658	0.08737	0.00319	1074.3	31.3	1176.1	27.6	1368.7	70.2	27.4
94	98	58	1.71	0.34617	0.00879	5.17937	0.11721	0.10851	0.00151	1916.3	42.1	1849.2	19.3	1774.6	25.4	-7.4
95	145	75	1.93	0.22998	0.00576	2.63739	0.06596	0.08317	0.00164	1334.4	30.2	1311.1	18.4	1273.3	38.5	-4.6
96	91	410	0.22	0.33621	0.00667	5.06426	0.10198	0.10924	0.00185	1868.4	32.2	1830.1	17.1	1786.9	30.8	-4.4
97	98	96	1.02	0.32899	0.00733	4.93110	0.10088	0.10871	0.00183	1833.5	35.5	1807.6	17.3	1777.9	30.7	-3.0
98	280	466	0.60	0.53566	0.01097	13.54176	0.26272	0.18335	0.00316	2765.2	46.0	2718.2	18.3	2683.4	28.5	-3.0
99	80	31	2.57	0.34446	0.00755	5.08687	0.11600	0.10711	0.00186	1908.1	36.2	1833.9	19.4	1750.7	31.8	-8.2
100	173	98	1.77	0.20421	0.00509	2.20809	0.06351	0.07842	0.00188	1197.9	27.3	1183.6	20.1	1157.6	47.5	-3.4
101	513	457	1.12	0.15680	0.00414	1.57934	0.03928	0.07305	0.00164	938.9	23.1	962.1	15.5	1015.4	45.4	8.1
102	681	349	1.95	0.55184	0.01422	13.93893	0.31508	0.18320	0.00325	2832.8	59.1	2745.6	21.4	2682.0	29.3	-5.3
103	5895	5009	1.18	0.33032	0.00777	5.04296	0.11666	0.11073	0.00189	1839.9	37.7	1826.6	19.6	1811.4	31.1	-1.6
104	731	481	1.52	0.05474	0.00139	0.87136	0.03347	0.11546	0.00413	343.5	8.5	636.3	18.2	1887.0	64.4	449.3
105	167	93	1.78	0.09169	0.00248	0.72414	0.01882	0.05728	0.00105	565.5	14.7	553.1	11.1	502.2	40.2	-11.2
106	271	342	0.79	0.16995	0.00461	1.68952	0.04643	0.07210	0.00170	1011.8	25.4	1004.6	17.5	988.8	48.1	-2.3
107	298	370	0.81	0.34336	0.00875	5.21487	0.13495	0.11015	0.00223	1902.8	42.0	1855.0	22.1	1801.9	36.8	-5.3
108	289	190	1.53	0.33789	0.00890	5.04217	0.13809	0.10823	0.00215	1876.5	42.9	1826.4	23.2	1769.8	36.3	-5.7
109	52	54	0.96	0.17749	0.00506	1.76997	0.04951	0.07233	0.00158	1053.2	27.7	1034.5	18.2	995.1	44.3	-5.5
110	192	125	1.53	0.28719	0.01006	4.03600	0.14252	0.10193	0.00243	1627.5	50.4	1641.5	28.7	1659.5	44.1	2.0
111	314	402	0.78	0.35526	0.00836	5.48735	0.15305	0.11203	0.00162	1959.6	39.8	1898.6	24.0	1832.5	26.2	-6.5
112	226	506	0.45	0.18055	0.00408	1.83895	0.04984	0.07387	0.00129	1070.0	22.3	1059.5	17.8	1037.9	35.4	-3.0
113	45	49	0.92	0.34030	0.00851	5.15486	0.13653	0.10986	0.00163	1888.1	40.9	1845.2	22.5	1797.1	27.1	-4.8
114	254	208	1.22	0.37450	0.00915	6.226152	0.16311	0.12126	0.00228	2050.5	42.9	2013.1	22.8	1974.9	33.5	-3.7
115	178	111	1.59	0.34161	0.00718	5.02336	0.11839	0.10665	0.00170	1894.4	34.5	1823.3	20.0	1743.0	29.1	-8.0
116	27	34	0.80	0.50402	0.01393	12.27403	0.35597	0.17662	0.00276	2631.0	59.7	2625.6	27.2	2621.4	26.0	-0.4
117	92	61	1.50	0.18337	0.00417	2.14889	0.07140	0.08499	0.00249	1085.4	22.7	1164.7	23.0	1315.4	56.7	21.2
118	43	52	0.83	0.33915	0.00891	5.03929	0.12841	0.10776	0.00212	1882.6	42.9	1825.9	21.6	1762.0	36.0	-6.4
119	406	176	2.31	0.18591	0.00447	2.03379	0.06091	0.07934	0.00228	1099.2	24.3	1126.9	20.4	1180.7	56.8	7.4
120	154	86	1.80	0.52156	0.01189	12.58626	0.30120	0.17502	0.00276	2705.8	50.4	2649.2	22.5	2606.2	26.3	-3.7
1	146	37	4.00	0.54942	0.01518	16.38302	0.43334	0.21627	0.00281	2822.7	63.1	2899.4	25.3	2953.1	21.0	4.6

IT-2-89 (25 μm)

Conc. (ppm)	Ratios										Ages					
	Spot [U]	[Th]	$^{206}\text{Pb}/^{238}\text{U}$	$\pm 2\sigma$	$^{207}\text{Pb}/^{235}\text{U}$	$\pm 2\sigma$	$^{207}\text{Pb}/^{206}\text{Pb}$	$\pm 2\sigma$	$^{206}\text{Pb}/^{238}\text{U}$	$\pm 2\sigma$	$^{207}\text{Pb}/^{235}\text{U}$	$\pm 2\sigma$	$^{207}\text{Pb}/^{206}\text{Pb}$	$\pm 2\sigma$		
2	317	147	2.16	0.31804	0.00886	4.96673	0.14053	0.11326	0.00162	1780.2	43.4	1813.7	23.9	1852.4	25.8	4.1
3	607	237	2.56	0.32519	0.00872	5.07344	0.15290	0.11315	0.00202	1815.0	42.4	1831.7	25.6	1850.6	32.3	2.0
4	93	223	0.42	0.28628	0.00712	4.25848	0.08598	0.10788	0.00199	1622.9	35.7	1685.4	16.6	1764.0	33.7	8.7
5	501	549	0.91	0.31939	0.00821	4.97615	0.10259	0.11300	0.00174	1786.7	40.1	1815.3	17.4	1848.2	27.8	3.4
6	96	95	1.01	0.50037	0.01388	12.98793	0.25491	0.18826	0.00307	2615.4	59.6	2678.8	18.5	2727.0	26.8	4.3
7	17	10	1.78	0.16246	0.00617	1.73633	0.10250	0.07752	0.00507	970.4	34.2	1022.1	38.1	1134.5	130.2	16.9
8	132	79	1.67	0.31651	0.00893	4.82285	0.10297	0.11052	0.00229	1772.6	43.7	1788.9	18.0	1807.9	37.7	2.0
9	201	232	0.87	0.30933	0.00899	4.62842	0.08866	0.10852	0.00211	1737.4	44.3	1754.4	16.0	1774.7	35.4	2.1
10	88	128	0.69	0.46850	0.01565	11.41215	0.22537	0.17667	0.00343	2477.0	68.7	2557.4	18.4	2621.8	32.3	5.8
11	269	133	2.02	0.17139	0.00506	1.72710	0.03773	0.07309	0.00145	1019.7	27.9	1018.7	14.0	1016.4	40.1	-0.3
12	179	308	0.58	0.30632	0.01096	4.49476	0.10849	0.10642	0.00223	1722.6	54.1	1730.0	20.1	1739.0	38.5	1.0
13	233	352	0.66	0.31212	0.00967	4.79865	0.10730	0.11151	0.00203	1751.1	47.5	1784.7	18.8	1824.1	33.1	4.2
14	62	67	0.93	0.16778	0.00508	1.74237	0.04445	0.07532	0.00206	999.8	28.0	1024.3	16.5	1077.1	54.9	7.7
15	72	87	0.82	0.54874	0.01523	15.92909	0.33556	0.21054	0.00366	2819.9	63.4	2872.6	20.1	2909.7	28.2	3.2
16	305	155	1.97	0.31128	0.00725	4.71174	0.10088	0.10978	0.00193	1747.0	35.6	1769.3	17.9	1795.8	32.1	2.8
17	98	84	1.16	0.51986	0.01049	13.22487	0.19021	0.18450	0.00304	2698.6	44.5	2695.8	13.6	2693.8	27.2	-0.2
18	115	172	0.67	0.32397	0.00661	5.03470	0.09764	0.11271	0.00183	1809.1	32.2	1825.2	16.4	1843.6	29.4	1.9
19	192	188	1.02	0.31731	0.00667	4.86518	0.08906	0.11120	0.00186	1776.6	32.7	1796.2	15.4	1819.1	30.4	2.4
20	53	44	1.19	0.21557	0.00470	2.51659	0.06213	0.08467	0.00202	1258.4	24.9	1276.8	17.9	1307.9	46.3	3.9
21	186	161	1.15	0.32895	0.00751	5.18903	0.10818	0.11441	0.00184	1833.3	36.4	1850.8	17.7	1870.6	29.0	2.0
22	186	156	1.19	0.16464	0.00402	1.65124	0.04079	0.07274	0.00133	982.5	22.2	990.0	15.6	1006.7	37.1	2.5
23	91	215	0.42	0.15983	0.00314	1.63958	0.04352	0.07440	0.00171	955.9	17.5	985.6	16.7	1052.3	46.3	10.1
24	138	201	0.68	0.51633	0.00972	13.48700	0.24287	0.18945	0.00237	2683.6	41.3	2714.4	17.0	2737.4	20.6	2.0
25	160	125	1.28	0.31165	0.00662	4.80887	0.09858	0.11191	0.00171	1748.8	32.5	1786.5	17.2	1830.7	27.7	4.7
26	77	161	0.48	0.51150	0.01158	12.96345	0.27236	0.18381	0.00282	2663.0	49.4	2677.0	19.8	2687.6	25.4	0.9
27	115	153	0.75	0.08707	0.00242	0.76784	0.02555	0.06396	0.00184	538.2	14.3	578.5	14.7	740.2	60.8	37.5
28	45	30	1.49	0.16712	0.00388	1.68437	0.05109	0.07310	0.00223	996.2	21.4	1002.6	19.3	1016.7	61.7	2.1
29	46	19	2.40	0.22210	0.00501	2.67701	0.07009	0.08742	0.00215	1293.0	26.4	1322.1	19.4	1369.7	47.3	5.9
30	298	185	1.61	0.27321	0.00510	3.70202	0.06803	0.09828	0.00127	1557.1	25.8	1571.8	14.7	1591.7	24.1	2.2
31	67	48	1.39	0.52184	0.01113	13.79573	0.29019	0.19174	0.00310	2707.0	47.1	2735.8	19.9	2757.1	26.5	1.9
32	138	9	16.13	0.33634	0.00698	5.37078	0.12071	0.11581	0.00181	1869.1	33.7	1880.2	19.2	1892.5	28.1	1.3

Spot	Conc. (ppm)	Ratios						Ages						108		
		[U]	[Th]	$^{206}\text{Pb}/^{238}\text{U}$	$\pm 2\sigma$	$^{207}\text{Pb}/^{235}\text{U}$	$\pm 2\sigma$	$^{206}\text{Pb}/^{206}\text{Pb}$	$\pm 2\sigma$	$^{207}\text{Pb}/^{238}\text{U}$	$\pm 2\sigma$	$^{206}\text{Pb}/^{235}\text{U}$	$\pm 2\sigma$			
33	360	511	0.70	0.47900	0.01020	11.45274	0.26391	0.17341	0.00228	2522.9	44.5	2560.7	21.5	2590.8	21.9	2.7
34	150	172	0.87	0.52449	0.01045	13.32987	0.28797	0.18433	0.00263	2718.2	44.2	2703.3	20.4	2692.2	23.6	1.0
35	217	164	1.33	0.45959	0.00821	10.92069	0.21364	0.17234	0.00210	2437.8	36.3	2516.4	18.2	2580.5	20.3	5.9
36	494	147	3.36	0.48326	0.00966	12.05381	0.29012	0.18016	0.00227	2550.1	41.9	2608.6	22.6	2654.3	20.9	4.1
37	151	59	2.55	0.53373	0.01109	14.65732	0.37486	0.19917	0.00234	2757.1	46.6	2793.3	24.3	2819.4	19.2	2.3
38	172	120	1.43	0.28016	0.00614	3.88134	0.10742	0.10048	0.00177	1592.2	30.9	1609.8	22.3	1632.9	32.7	2.6
39	49	47	1.04	0.18543	0.00439	1.93402	0.07345	0.07565	0.00219	1096.6	23.9	1092.9	25.4	1085.7	58.0	-1.0
40	44	33	1.31	0.26302	0.00591	3.47270	0.09786	0.09576	0.00207	1505.3	30.2	1521.0	22.2	1543.0	40.6	2.5
41	348	301	1.16	0.17467	0.00373	1.79295	0.04536	0.07445	0.00130	1037.8	20.4	1042.9	16.5	1053.6	35.2	1.5
42	77	72	1.07	0.31841	0.00700	4.88308	0.12529	0.11123	0.00221	1782.0	34.2	1799.3	21.6	1819.5	36.1	2.1
43	523	127	4.11	0.52653	0.01087	13.62264	0.32431	0.18765	0.00287	2726.8	45.9	2723.8	22.5	2721.6	25.2	-0.2
44	63	65	0.97	0.51618	0.00987	13.04779	0.28668	0.18333	0.00265	2683.0	42.0	2683.1	20.7	2683.2	23.9	0.0
45	49	89	0.55	0.16266	0.00321	1.64785	0.05510	0.07348	0.00227	971.5	17.8	988.7	21.1	1027.1	62.4	5.7
46	249	100	2.49	0.34460	0.00683	5.47600	0.09278	0.11525	0.00199	1908.7	32.7	1896.8	14.5	1883.8	31.1	-1.3
47	242	275	0.88	0.19735	0.00355	2.16222	0.04033	0.07946	0.00158	1161.1	19.1	1169.0	13.0	1183.6	39.3	1.9
48	447	125	3.57	0.33736	0.00646	5.33337	0.10564	0.11466	0.00199	1874.0	31.1	1874.2	16.9	1874.5	31.3	0.0
49	253	211	1.20	0.32760	0.00589	5.06063	0.09309	0.11203	0.00220	1826.8	28.6	1829.5	15.6	1832.7	35.6	0.3
50	195	207	0.94	0.50586	0.01044	12.44036	0.24034	0.17836	0.00292	2638.9	44.7	2638.2	18.2	2637.7	27.2	0.0
51	93	93	1.00	0.27698	0.00593	3.91119	0.08330	0.10241	0.00177	1576.1	29.9	1616.0	17.2	1668.3	31.9	5.8
52	38	38	1.01	0.25741	0.00500	3.51512	0.09842	0.09904	0.00273	1476.6	25.7	1530.6	22.1	1606.1	51.4	8.8
53	43	15	2.81	0.19034	0.00484	2.01229	0.08205	0.07668	0.00240	1123.2	26.2	1119.7	27.7	1112.8	62.6	-0.9
54	118	169	0.70	0.16209	0.00524	1.68368	0.06508	0.07533	0.00234	968.4	29.0	1002.4	24.6	1077.4	62.2	11.3
55	29	28	1.02	0.17402	0.00345	1.84753	0.07508	0.07700	0.00297	1034.2	19.0	1062.5	26.8	1121.1	76.9	8.4
56	90	78	1.14	0.21970	0.00517	2.57955	0.08032	0.08516	0.00227	1280.3	27.3	1294.9	22.8	1319.1	51.6	3.0
57	532	302	1.76	0.32201	0.00556	4.96617	0.14494	0.11185	0.00310	1799.5	27.1	1813.6	24.7	1829.8	50.2	1.7
58	28	59	0.48	0.16278	0.00411	1.68486	0.07045	0.07507	0.00320	972.2	22.8	1002.8	26.6	1070.4	85.5	10.1
59	260	44	5.88	0.32542	0.00623	5.01861	0.15344	0.11185	0.00314	1816.1	30.3	1822.5	25.9	1829.7	50.9	0.7
60	258	112	2.30	0.47313	0.00757	11.05580	0.25759	0.16948	0.00370	2497.3	33.1	2527.8	21.7	2552.5	36.6	2.2
61	22	39	0.55	0.17230	0.00426	1.73093	0.08099	0.07286	0.00309	1024.8	23.4	1020.1	30.1	1010.1	86.0	-1.4
62	26	12	2.11	0.17463	0.00455	1.82177	0.08767	0.07566	0.00369	1037.6	25.0	1053.3	31.6	1086.1	97.8	4.7
63	113	69	1.64	0.21783	0.00543	2.57168	0.08432	0.08562	0.00253	1270.4	28.7	1292.6	24.0	1329.7	57.2	4.7

Spot	Conc. (ppm)	Ratios						Ages						% Disc		
		[U]	[Th]	$^{206}\text{Pb}/^{238}\text{U}$	$\pm 2\sigma$	$^{207}\text{Pb}/^{235}\text{U}$	$\pm 2\sigma$	$^{206}\text{Pb}/^{206}\text{Pb}$	$\pm 2\sigma$	$^{207}\text{Pb}/^{238}\text{U}$	$\pm 2\sigma$	$^{207}\text{Pb}/^{235}\text{U}$	$\pm 2\sigma$			
64	22	26	0.85	0.17557	0.00461	1.87009	0.08356	0.07725	0.00308	1042.7	25.3	1070.6	29.6	1127.8	79.5	8.2
65	310	287	1.08	0.47547	0.01405	12.88903	0.44686	0.19660	0.00373	2507.5	61.4	2671.6	32.7	2798.2	31.1	11.6
66	141	40	3.56	0.34668	0.00761	5.47715	0.15004	0.11459	0.00238	1918.7	36.4	1897.0	23.5	1873.4	37.4	-2.4
67	92	58	1.59	0.17102	0.00471	1.72870	0.05109	0.07331	0.00148	1017.7	25.9	1019.3	19.0	1022.5	40.8	0.5
68	576	346	1.66	0.32063	0.00850	4.82680	0.13055	0.10918	0.00135	1792.8	41.5	1789.6	22.8	1785.8	22.6	-0.4
69	98	108	0.91	0.16979	0.00446	1.67936	0.04704	0.07174	0.00139	1010.9	24.6	1000.7	17.8	978.5	39.6	-3.2
70	276	211	1.31	0.28837	0.00786	3.96862	0.11000	0.09981	0.00129	1633.4	39.3	1627.8	22.5	1620.6	24.1	-0.8
71	661	309	2.14	0.32647	0.00797	5.08163	0.11802	0.11289	0.00163	1821.3	38.7	1833.0	19.7	1846.4	26.1	1.4
72	432	312	1.38	0.31867	0.00823	4.86834	0.13368	0.11080	0.00173	1783.2	40.2	1796.8	23.1	1812.6	28.3	1.6
73	180	192	0.94	0.16859	0.00393	1.72724	0.04253	0.07431	0.00132	1004.3	21.7	1018.7	15.8	1049.8	35.8	4.5
74	93	27	3.48	0.65451	0.01403	24.14799	0.51108	0.26758	0.00308	3245.8	54.6	3274.4	20.6	3291.9	18.1	1.4
75	60	35	1.72	0.16176	0.00409	1.71809	0.04975	0.07703	0.00208	966.6	22.7	1015.3	18.6	1122.0	53.9	16.1
76	53	37	1.45	0.16489	0.00372	1.70178	0.04738	0.07485	0.00206	983.9	20.6	1009.2	17.8	1064.5	55.4	8.2
77	77	42	0.54	0.21907	0.00513	2.54721	0.07645	0.08433	0.00248	1277.0	27.1	1285.6	21.9	1300.1	57.2	1.8
78	357	135	2.65	0.16809	0.00290	1.69210	0.03392	0.07301	0.00124	1001.6	16.0	1005.6	12.8	1014.2	34.4	1.3
79	67	49	1.37	0.16445	0.00309	1.66131	0.03952	0.07327	0.00182	981.5	17.1	993.9	15.1	1021.4	50.2	4.1
80	16	29	0.53	0.27652	0.00679	3.95561	0.11666	0.10375	0.00365	1573.8	34.3	1625.1	23.9	1692.3	65.0	7.5
81	172	107	1.61	0.19185	0.00384	2.03449	0.04109	0.07691	0.00140	1113.4	20.7	1127.1	13.8	1118.9	36.4	-1.1
82	100	143	0.70	0.32074	0.00655	4.93348	0.09922	0.11156	0.00183	1793.3	32.0	1808.0	17.0	1824.9	29.7	1.8
83	43	49	0.88	0.16047	0.00378	1.71283	0.05679	0.07741	0.00263	959.4	21.0	1013.3	21.3	1131.9	67.7	18.0
84	37	22	1.70	0.17077	0.00414	1.80596	0.06542	0.07670	0.00223	1016.4	22.8	1047.6	23.7	1113.3	58.1	9.5
85	301	282	1.07	0.33280	0.00626	5.15323	0.10572	0.11231	0.00141	1851.9	30.3	1844.9	17.4	1837.1	22.8	-0.8
86	14	13	1.13	0.16769	0.00491	1.80960	0.08263	0.07827	0.00401	999.4	27.1	1048.9	29.9	1153.6	101.8	15.4
87	652	239	2.73	0.49889	0.01050	12.27946	0.27806	0.17851	0.00247	2609.0	45.2	2626.0	21.3	2639.1	23.0	1.2
88	56	70	0.80	0.16324	0.00394	1.68338	0.05113	0.07479	0.00214	974.7	21.8	1002.3	19.3	1063.0	57.7	9.0
89	74	177	0.42	0.57898	0.01240	17.53647	0.37287	0.21967	0.00327	2944.6	50.6	2964.7	20.4	2978.3	24.0	1.1
90	102	102	1.00	0.16618	0.00324	1.74194	0.04743	0.07602	0.00157	991.0	17.9	1024.2	17.6	1095.7	41.3	10.6
91	159	2	86.33	0.18215	0.00330	1.88089	0.06206	0.07489	0.00231	1078.7	18.0	1074.4	21.9	1065.5	62.0	-1.2
92	95	81	1.17	0.51500	0.01130	13.38452	0.48415	0.18849	0.00551	2677.9	48.1	2707.2	34.2	2729.1	48.1	1.9
93	177	221	0.80	0.32301	0.00654	4.90467	0.15029	0.11013	0.00287	1804.4	31.9	1803.1	25.8	1801.5	47.4	-0.2
94	371	192	1.94	0.57320	0.01031	17.24050	0.45589	0.21814	0.00457	2920.9	42.2	2948.3	25.4	2967.0	33.8	1.6

Spot	Conc. (ppm)	Ratios										Ages				
		[U]	[Th]	U/Th	$^{206}\text{Pb}/^{238}\text{U}$	$\pm 2\sigma$	$^{207}\text{Pb}/^{235}\text{U}$	$\pm 2\sigma$	$^{207}\text{Pb}/^{206}\text{Pb}$	$\pm 2\sigma$	$^{206}\text{Pb}/^{238}\text{U}$	$\pm 2\sigma$	$^{207}\text{Pb}/^{235}\text{U}$	$\pm 2\sigma$	$^{207}\text{Pb}/^{206}\text{Pb}$	$\pm 2\sigma$
95	152	181	0.84	0.24235	0.00439	3.14716	0.08654	0.09418	0.00247	1398.9	22.8	1444.3	21.2	1511.8	49.5	8.1
96	209	252	0.83	0.31125	0.00562	4.67610	0.13850	0.10896	0.00275	1746.9	27.6	1763.0	24.8	1782.1	46.1	2.0
97	247	96	2.56	0.22253	0.00436	2.65445	0.09986	0.08651	0.00273	1295.2	23.0	1315.9	27.8	1349.7	60.8	4.2
98	117	26	4.55	0.16512	0.00342	1.67562	0.06489	0.07360	0.00240	985.2	18.9	999.3	24.6	1030.5	65.8	4.6
99	287	108	2.66	0.33054	0.00656	5.18284	0.18276	0.11372	0.00318	1841.0	31.8	1849.8	30.0	1859.7	50.4	1.0
100	284	180	1.58	0.32835	0.00582	5.15984	0.15750	0.11397	0.00282	1830.4	28.3	1846.0	26.0	1863.7	44.7	1.8
101	155	298	0.52	0.31745	0.00768	4.83842	0.36909	0.11054	0.00690	1777.3	37.6	1791.6	64.3	1808.3	113.5	1.7
102	194	106	1.83	0.16613	0.00471	1.68465	0.16333	0.07355	0.00583	990.7	26.1	1002.7	61.8	1029.1	160.3	3.9
103	66	31	2.10	0.27230	0.00717	3.78242	0.29680	0.10074	0.00651	1552.5	36.3	1589.0	63.1	1637.9	120.0	5.5
104	59	81	0.73	0.21855	0.00481	2.56639	0.17071	0.08517	0.00478	1274.2	25.4	1291.1	48.6	1319.3	108.7	3.5
105	470	259	1.81	0.16969	0.00422	1.66884	0.10947	0.07133	0.00380	1010.4	23.2	996.7	41.7	966.8	108.7	4.3
106	357	310	1.15	0.32651	0.00802	5.05155	0.39410	0.11221	0.00714	1821.5	39.0	1828.0	66.2	1835.5	115.3	0.8
107	145	56	2.57	0.15964	0.00530	1.67657	0.16779	0.07617	0.00633	954.8	29.4	999.7	63.7	1099.5	166.4	15.2
108	415	471	0.88	0.33378	0.00820	5.17598	0.50078	0.11247	0.00903	1856.7	39.6	1848.7	82.5	1839.7	145.4	-0.9
109	44	25	1.75	0.57459	0.01468	17.12162	1.66156	0.21612	0.01748	2926.6	60.1	2941.7	93.4	2952.0	130.6	0.9
110	947	297	3.19	0.19516	0.00490	2.08557	0.16131	0.07751	0.00494	1149.2	26.4	1144.1	53.1	1134.3	126.9	-1.3
111	177	172	1.03	0.50383	0.01156	12.78481	0.97157	0.18404	0.01133	2630.3	49.6	2663.9	71.7	2689.6	101.8	2.3
112	370	223	1.66	0.28005	0.00567	3.83298	0.06847	0.09927	0.00168	1591.6	28.5	1599.7	14.4	1610.4	31.6	1.2
113	157	96	1.63	0.16211	0.00336	1.60813	0.03771	0.07195	0.00141	968.5	18.6	973.4	14.7	984.4	39.9	1.6
114	481	141	3.41	0.31872	0.00679	4.89678	0.10503	0.11143	0.00152	1783.5	33.2	1801.7	18.1	1822.8	24.8	2.2
115	230	317	0.72	0.50337	0.01059	12.74379	0.25155	0.18362	0.00270	2628.2	45.4	2660.9	18.6	2685.8	24.3	2.2
116	128	106	1.21	0.32783	0.00689	5.24572	0.11477	0.11605	0.00202	1827.8	33.4	1860.1	18.7	1896.3	31.3	3.7
117	200	225	0.89	0.32278	0.00781	4.89365	0.10572	0.10996	0.00163	1803.3	38.0	1801.2	18.2	1798.7	27.0	-0.3
118	327	90	3.65	0.32551	0.00787	4.97232	0.11154	0.11079	0.00147	1816.6	38.3	1814.6	19.0	1812.4	24.1	-0.2
119	140	51	2.74	0.21725	0.00463	2.55650	0.06124	0.08535	0.00154	1267.3	24.5	1288.3	17.5	1323.4	34.9	4.4
120	598	508	1.18	0.33065	0.00821	5.40354	0.12829	0.11852	0.00137	1841.5	39.8	1885.4	20.3	1934.1	20.7	5.0

Table 4 – Summerside Formation

Spot	Conc. (ppm)	[U]	[Th]	U/Th	$^{206}\text{Pb}/^{238}\text{U}$	$\pm 2\sigma$	$^{207}\text{Pb}/^{235}\text{U}$	$\pm 2\sigma$	$^{206}\text{Pb}/^{206}\text{Pb}$	$\pm 2\sigma$	$^{206}\text{Pb}/^{238}\text{U}$	$\pm 2\sigma$	$^{207}\text{Pb}/^{235}\text{U}$	$\pm 2\sigma$	Ages			
1	142	54	2.62	0.117644	0.00801	1.98638	0.08068	0.08165	0.00144	1047.5	43.9	1110.9	27.4	1237.1	34.5	18.1		
2	1706	791	2.16	0.16330	0.00731	1.77029	0.07219	0.07862	0.00116	975.1	40.5	1034.6	26.5	1162.7	29.2	19.2		
3	1717	710	2.42	0.21286	0.00944	2.52556	0.09990	0.08605	0.00143	1244.1	50.2	1279.4	28.8	1339.3	32.0	7.7		
4	134	66	2.01	0.16696	0.00616	1.74282	0.06201	0.07571	0.00120	995.3	34.1	1024.5	23.0	1087.4	31.7	9.3		
5	249	90	2.75	0.19526	0.00714	1.98849	0.06987	0.07386	0.00126	1149.8	38.5	1111.6	23.7	1037.6	34.5	-9.8		
6	94	39	2.41	0.09911	0.00475	0.93866	0.04260	0.06869	0.00188	609.2	27.9	672.2	22.3	889.3	56.7	46.0		
7	133	37	3.59	0.16330	0.00781	1.68533	0.07732	0.07485	0.00125	975.1	43.3	1003.0	29.2	1064.5	33.6	9.2		
8	249	79	3.14	0.17741	0.00833	1.87873	0.07974	0.07680	0.00103	1052.8	45.6	1073.6	28.1	1116.1	26.8	6.0		
9	441	292	1.51	0.18771	0.00894	1.99368	0.08526	0.07703	0.00098	1109.0	48.5	1113.4	28.9	1122.0	25.3	1.2		
10	44	16	2.66	0.16821	0.00803	1.92176	0.09186	0.08286	0.00202	1002.2	44.3	1088.7	31.9	1265.9	47.5	26.3		
11	211	112	1.88	0.09445	0.00364	0.83904	0.03400	0.06443	0.00132	581.8	21.5	618.6	18.8	755.7	43.4	29.9		
12	190	137	1.39	0.17228	0.00637	1.84883	0.06546	0.07783	0.00141	1024.7	35.0	1063.0	23.3	1142.6	35.9	11.5		
13	145	80	1.81	0.16242	0.00559	1.71171	0.05464	0.07643	0.00139	970.2	31.0	1012.9	20.5	1106.5	36.3	14.0		
14	236	105	2.25	0.15816	0.00540	1.65959	0.05287	0.07610	0.00123	946.5	30.0	993.2	20.2	1097.8	32.5	16.0		
15	976	551	1.77	0.24912	0.00734	3.19180	0.08544	0.09292	0.00132	1433.9	37.9	1455.2	20.7	1486.3	26.9	3.7		
17	565	244	2.32	0.18766	0.00658	2.01371	0.05764	0.07782	0.00133	1108.7	35.7	1120.1	19.4	1142.4	34.0	3.0		
18	325	153	2.12	0.16292	0.00643	1.63731	0.05652	0.07289	0.00137	973.0	35.6	984.7	21.8	1010.8	38.1	3.9		
19	114	61	1.87	0.16341	0.00598	1.73042	0.05182	0.07680	0.00156	975.7	33.1	1019.9	19.3	1116.1	40.6	14.4		
20	197	116	1.70	0.19009	0.00705	2.04156	0.06610	0.07789	0.00148	1121.9	38.2	1129.5	22.1	1144.2	37.6	2.0		
21	152	48	3.18	0.15297	0.00598	1.57928	0.05276	0.07488	0.00146	917.6	33.4	962.1	20.8	1065.2	39.2	16.1		
22	260	126	2.07	0.18464	0.00663	1.99347	0.05516	0.07831	0.00123	1092.2	36.1	1113.3	18.7	1154.6	31.2	5.7		
23	52	25	2.09	0.18327	0.00730	2.07602	0.07544	0.08216	0.00182	1084.8	39.8	1140.9	24.9	1249.2	43.3	15.2		
24	76	32	2.38	0.17427	0.00589	1.87216	0.05921	0.07792	0.00152	1035.6	32.4	1071.3	20.9	1144.7	38.7	10.5		
25	878	346	2.54	0.17162	0.00540	1.71108	0.04793	0.07231	0.00102	1021.0	29.7	1012.7	18.0	994.7	28.7	-2.6		
26	85	29	2.90	0.16635	0.00718	1.78438	0.06174	0.07780	0.00152	991.9	39.7	1039.8	22.5	1141.7	39.0	15.1		
27	394	241	1.63	0.25523	0.01067	3.17905	0.10294	0.09034	0.00119	1465.4	54.8	1452.1	25.0	1432.6	25.1	-2.2		
28	306	142	2.16	0.16964	0.00744	1.73780	0.06059	0.07430	0.00113	1010.1	41.0	1022.6	22.5	1049.6	30.5	3.9		
29	126	72	1.75	0.20288	0.00871	2.11637	0.07765	0.07566	0.00161	1190.8	46.7	1154.2	25.3	1086.0	42.7	-8.8		

Spot	Conc. (ppm)	Ratios						Ages						Ages		
		[Th]	U/Th	$^{206}\text{Pb}/^{238}\text{U}$	$\pm 2\sigma$	$^{207}\text{Pb}/^{235}\text{U}$	$\pm 2\sigma$	$^{207}\text{Pb}/^{206}\text{Pb}$	$\pm 2\sigma$	$^{206}\text{Pb}/^{238}\text{U}$	$\pm 2\sigma$	$^{207}\text{Pb}/^{235}\text{U}$	$\pm 2\sigma$			
30	83	39	2.15	0.18459	0.00777	2.04179	0.06855	0.08023	0.00161	1092.0	42.3	1129.6	22.9	1202.5	39.5	10.1
31	61	40	1.52	0.16608	0.00672	1.78899	0.06212	0.07812	0.00205	990.5	37.1	1041.5	22.6	1150.0	52.1	16.1
32	358	154	2.32	0.26207	0.01115	3.30221	0.10151	0.09139	0.00142	1500.4	57.0	1481.6	24.0	1454.7	29.6	-3.0
33	2469	129	19.16	0.17772	0.00759	1.99400	0.07978	0.08137	0.00143	1054.5	41.5	1113.5	27.1	1230.5	34.6	16.7
34	160	82	1.96	0.17004	0.00612	1.73791	0.04872	0.07413	0.00136	1012.3	33.7	1022.7	18.1	1044.9	37.1	3.2
35	252	148	1.70	0.19018	0.00673	2.04676	0.05636	0.07806	0.00129	1122.3	36.5	1131.2	18.8	1148.3	32.8	2.3
36	232	68	3.39	0.18131	0.00637	1.86366	0.06619	0.07455	0.00127	1074.1	34.7	1068.3	23.5	1056.4	34.3	-1.7
37	454	182	2.49	0.17798	0.00690	1.82201	0.06712	0.07425	0.00108	1055.9	37.8	1053.4	24.2	1048.2	29.3	-0.7
38	333	121	2.74	0.25457	0.00954	3.25371	0.11687	0.09270	0.00164	1462.0	49.0	1470.1	27.9	1481.7	33.5	1.4
39	187	120	1.56	0.21733	0.00913	2.22858	0.08931	0.07437	0.00152	1267.8	48.4	1190.1	28.1	1051.5	41.2	17.1
40	88	40	2.18	0.16823	0.00630	1.78119	0.06652	0.07679	0.00142	1002.4	34.8	1038.6	24.3	1115.7	37.0	11.3
41	561	241	2.33	0.25287	0.01006	3.22176	0.12338	0.09241	0.00192	1453.2	51.8	1462.4	29.7	1475.7	39.4	1.5
42	50	23	2.19	0.20661	0.00838	2.31710	0.10312	0.08134	0.00219	1210.7	44.8	1217.5	31.6	1229.6	52.8	1.6
43	119	43	2.75	0.17952	0.00738	1.85761	0.07542	0.07505	0.00158	1064.4	40.3	1066.1	26.8	1069.8	42.4	0.5
44	144	49	2.93	0.18812	0.00583	1.96772	0.06299	0.07586	0.00140	1111.2	31.6	1104.5	21.6	1091.4	36.8	-1.8
45	563	119	4.74	0.19127	0.00559	2.02772	0.05858	0.07689	0.00121	1128.2	30.2	1124.9	19.6	1118.3	31.5	-0.9
46	66	29	2.25	0.16059	0.00553	1.66742	0.06353	0.07531	0.00178	960.0	30.7	996.2	24.2	1076.7	47.3	12.2
47	318	186	1.71	0.09718	0.00330	0.82379	0.02943	0.06148	0.00097	597.8	19.4	610.2	16.4	656.2	33.7	9.8
48	332	304	1.09	0.18724	0.00633	1.95615	0.06466	0.07577	0.00104	1106.4	34.4	1100.6	22.2	1089.0	27.5	-1.6
49	282	142	1.98	0.18995	0.00642	2.00724	0.06620	0.07664	0.00104	1121.1	34.8	1118.0	22.4	1111.9	27.0	-0.8
50	252	118	2.14	0.18625	0.00641	1.99797	0.06849	0.07780	0.00106	1101.0	34.9	1114.8	23.2	1141.8	27.0	3.7
51	200	90	2.22	0.17351	0.00555	1.76792	0.07859	0.07390	0.00116	1031.4	30.5	1033.8	28.8	1038.7	31.6	0.7
52	107	57	1.86	0.22157	0.00800	2.39648	0.11392	0.07845	0.00148	1290.1	42.2	1241.5	34.1	1158.2	37.3	10.2
53	2067	494	4.18	0.21592	0.00572	2.40860	0.07375	0.08090	0.00105	1260.3	30.3	1245.2	22.0	1219.1	25.5	-3.3
54	40	27	1.52	0.19750	0.00623	2.29411	0.09133	0.08425	0.00275	1161.9	33.5	1210.5	28.2	1298.2	63.4	11.7
55	465	161	2.90	0.19435	0.00637	2.04604	0.07587	0.07635	0.00100	1144.9	34.4	1131.0	25.3	1104.3	26.1	-3.5
56	65	45	1.45	0.17499	0.00540	1.99209	0.07233	0.08256	0.00296	1039.6	29.6	1112.8	24.5	1258.9	70.1	21.1
57	86	51	1.68	0.19076	0.00460	2.04726	0.05118	0.07783	0.00136	1125.5	24.9	1131.4	17.1	1142.7	34.8	1.5
58	70	34	2.05	0.17655	0.00426	1.87140	0.05228	0.07688	0.00171	1048.1	23.3	1071.0	18.5	1118.1	44.5	6.7
59	75	33	2.27	0.17182	0.00414	1.77154	0.04776	0.07478	0.00142	1022.1	22.8	1035.1	17.5	1062.6	38.3	4.0
60	159	78	2.04	0.17053	0.00407	1.69864	0.04272	0.07224	0.00123	1015.0	22.4	1008.0	16.1	992.8	34.5	-2.2

Spot	Conc. (ppm)	Ratios						Ages					
		[U]	[Th]	$^{206}\text{Pb}/^{238}\text{U}$	$\pm 2\sigma$	$^{207}\text{Pb}/^{235}\text{U}$	$\pm 2\sigma$	$^{206}\text{Pb}/^{206}\text{Pb}$	$\pm 2\sigma$	$^{207}\text{Pb}/^{235}\text{U}$	$\pm 2\sigma$	$^{207}\text{Pb}/^{206}\text{Pb}$	$\pm 2\sigma$
61	107	47	2.27	0.20277	0.00842	2.17200	0.05442	0.07769	0.00197	1190.2	45.1	1172.1	17.4
62	276	161	1.72	0.18279	0.00748	1.95109	0.05250	0.07742	0.00193	1082.2	40.8	1098.8	18.1
63	272	131	2.08	0.19519	0.00549	2.11368	0.04964	0.07854	0.00152	1149.4	29.6	1153.3	16.2
64	1682	19	88.68	0.18787	0.00583	1.98269	0.04970	0.07654	0.00128	1109.8	31.6	1109.6	16.9
65	60	29	2.05	0.19263	0.00720	1.97990	0.06244	0.07455	0.00192	1135.6	38.9	1108.7	21.3
66	70	41	1.70	0.19523	0.00741	2.16991	0.07050	0.08061	0.00178	1149.6	40.0	1171.5	22.6
67	900	310	2.91	0.20324	0.00808	2.16294	0.07193	0.07719	0.00127	1192.7	43.3	1169.2	23.1
68	260	83	3.14	0.27599	0.01011	3.50145	0.10577	0.09201	0.00155	1571.2	51.1	1527.5	23.9
69	380	140	2.72	0.16954	0.00654	1.73042	0.05109	0.07402	0.00125	1009.6	36.0	1019.9	19.0
70	603	229	2.63	0.17232	0.00616	1.77244	0.05239	0.07460	0.00125	1024.9	33.9	1035.4	19.2
71	67	39	1.73	0.18436	0.00710	1.93416	0.07684	0.07609	0.00186	1090.7	38.6	1093.0	26.6
72	356	105	3.40	0.21100	0.00886	2.26261	0.08294	0.07777	0.00114	1234.1	47.2	1200.7	25.8
73	131	61	2.14	0.18872	0.00587	1.94831	0.06100	0.07487	0.00134	1114.5	31.8	1097.9	21.0
74	85	31	2.74	0.26686	0.00810	4.11910	0.12884	0.11195	0.00208	1524.8	41.2	1658.1	25.6
75	445	195	2.28	0.25304	0.00698	3.23664	0.08247	0.09277	0.00117	1454.1	35.9	1466.0	19.8
76	261	156	1.67	0.19106	0.00462	2.08491	0.04376	0.07914	0.00152	1127.1	25.0	1143.9	14.4
77	1044	124	8.39	0.20245	0.00568	2.01322	0.04835	0.07212	0.00135	1188.4	30.4	1120.0	16.3
78	1049	270	3.88	0.17053	0.00488	1.73008	0.04192	0.07358	0.00120	1015.0	26.9	1019.8	15.6
79	75	43	1.74	0.19684	0.00584	2.32593	0.10835	0.08570	0.00332	1158.3	31.5	1220.2	33.1
80	236	73	3.24	0.16892	0.00413	1.74728	0.03634	0.07502	0.00136	1006.1	22.8	1026.2	13.4
81	97	96	1.00	0.18863	0.00592	2.08221	0.06099	0.08006	0.00175	1113.9	32.1	1143.0	20.1
82	78	43	1.84	0.17350	0.00577	1.78264	0.05307	0.07452	0.00147	1031.4	31.7	1039.1	19.4
83	106	42	2.50	0.18558	0.00581	2.03555	0.06275	0.07955	0.00142	1097.4	31.6	1127.5	21.0
84	827	169	4.88	0.19500	0.00570	2.11767	0.06380	0.07876	0.00128	1148.4	30.8	1154.6	20.8
85	82	44	1.87	0.19346	0.00605	2.15845	0.06337	0.08092	0.00183	1140.1	32.7	1167.8	20.4
86	158	165	0.96	0.19909	0.00779	2.00727	0.06765	0.07312	0.00120	1170.5	41.9	1118.0	22.8
87	194	56	3.46	0.17122	0.00649	1.75254	0.05921	0.07423	0.00132	1018.8	35.7	1028.1	21.8
88	269	111	2.42	0.20181	0.00769	2.15386	0.06944	0.07741	0.00124	1185.0	41.3	1166.3	22.4
89	108	83	1.30	0.18778	0.00696	2.03798	0.06549	0.07871	0.00137	1109.4	37.8	1128.3	21.9
90	129	35	3.65	0.18092	0.00662	1.84794	0.05572	0.07408	0.00141	1072.0	36.1	1062.7	19.9
91	170	106	1.60	0.16836	0.00493	1.72668	0.05180	0.07438	0.00113	1003.1	27.2	1018.5	19.3

Spot	Conc. (ppm)	Ratios										Ages				
		[Th]	U/Th	$^{206}\text{Pb}/^{238}\text{U}$	$\pm 2\sigma$	$^{207}\text{Pb}/^{235}\text{U}$	$\pm 2\sigma$	$^{207}\text{Pb}/^{206}\text{Pb}$	$\pm 2\sigma$	$^{206}\text{Pb}/^{238}\text{U}$	$\pm 2\sigma$	$^{207}\text{Pb}/^{235}\text{U}$	$\pm 2\sigma$	$^{207}\text{Pb}/^{206}\text{Pb}$	$\pm 2\sigma$	% Disc
92	260	97	2.67	0.20304	0.00581	2.15438	0.06285	0.07696	0.00101	1191.6	31.2	1166.5	20.2	1120.0	26.1	-6.0
93	297	61	4.86	0.18068	0.00808	1.85124	0.08286	0.07431	0.00111	1070.7	44.1	1063.9	29.5	1049.9	30.0	-1.9
94	272	131	2.07	0.19042	0.00478	2.02913	0.05113	0.07729	0.00122	1123.6	25.9	1125.3	17.1	1128.6	31.4	0.4
95	318	142	2.24	0.20144	0.00576	2.16275	0.05763	0.07787	0.00121	1183.1	30.9	1169.2	18.5	1143.5	30.8	-3.3
96	84	40	2.07	0.16373	0.00427	1.72120	0.04821	0.07624	0.00158	977.5	23.7	1016.5	18.0	1101.5	41.4	12.7
97	280	301	0.93	0.16638	0.00444	1.71164	0.03969	0.07461	0.00125	992.1	24.5	1012.9	14.9	1058.1	33.8	6.6
98	548	111	4.93	0.16318	0.00421	1.64628	0.03772	0.07317	0.00112	974.4	23.3	988.1	14.5	1018.7	30.9	4.5
99	470	110	4.29	0.18914	0.00558	2.01909	0.05527	0.07742	0.00127	1116.7	30.2	1122.0	18.6	1132.1	32.7	1.4
100	143	77	1.85	0.16301	0.00398	1.66762	0.04742	0.07420	0.00135	973.5	22.1	996.3	18.1	1046.9	36.6	7.5
101	426	460	0.93	0.33427	0.00883	5.14575	0.11439	0.11165	0.00149	1859.1	42.7	1843.7	18.9	1826.4	24.2	-1.8
102	281	121	2.32	0.18500	0.00485	1.94958	0.04192	0.07643	0.00112	1094.2	26.4	1098.3	14.4	1106.4	29.4	1.1
103	166	48	3.46	0.16766	0.00367	1.70082	0.03278	0.07357	0.00124	999.2	20.2	1008.8	12.3	1029.8	34.1	3.1
104	85	44	1.93	0.18585	0.00498	2.02004	0.05440	0.07883	0.00141	1098.8	27.1	1122.3	18.3	1167.9	35.4	6.3
105	212	204	1.04	0.18202	0.00386	1.91187	0.03602	0.07618	0.00124	1078.0	21.0	1085.2	12.6	1099.8	32.5	2.0
106	84	23	3.70	0.17077	0.00441	1.74093	0.04418	0.07394	0.00132	1016.4	24.3	1023.8	16.4	1039.8	36.0	2.3
107	742	215	3.45	0.24743	0.00626	3.14697	0.06481	0.09224	0.00113	1425.2	32.4	1444.3	15.9	1472.4	23.2	3.3
108	227	86	2.65	0.16813	0.00372	1.73588	0.03421	0.07488	0.00116	1001.8	20.5	1021.9	12.7	1065.3	31.2	6.3
109	143	50	2.85	0.21219	0.00610	2.28108	0.06312	0.07797	0.00138	1240.5	32.4	1206.5	19.5	1146.0	35.2	-7.6
110	204	115	1.77	0.19745	0.00435	2.11948	0.03630	0.07785	0.00113	1161.6	23.4	1155.2	11.8	1143.1	28.9	-1.6
111	190	74	2.57	0.17772	0.00350	1.91717	0.04756	0.07824	0.00154	1054.5	19.2	1087.1	16.6	1152.9	39.0	9.3
112	134	88	1.53	0.17315	0.00453	1.80195	0.05386	0.07548	0.00159	1029.4	24.9	1046.2	19.5	1081.3	42.4	5.0
113	334	110	3.03	0.17056	0.00401	1.75602	0.04950	0.07467	0.00134	1015.2	22.1	1029.4	18.2	1059.7	36.2	4.4
114	218	89	2.45	0.25264	0.00591	3.23563	0.08015	0.09289	0.00146	1452.1	30.4	1465.7	19.2	1485.6	29.8	2.3
115	207	171	1.22	0.18976	0.00391	2.02109	0.04501	0.07725	0.00129	1120.1	21.2	1122.6	15.1	1127.6	33.2	0.7
116	268	119	2.26	0.17100	0.00472	1.74995	0.05374	0.07422	0.00145	1017.6	26.0	1027.1	19.8	1047.4	39.5	2.9
117	1833	209	8.78	0.16815	0.00445	1.86621	0.05549	0.08050	0.00146	1001.9	24.6	1069.2	19.7	1209.1	35.8	20.7
118	137	33	4.21	0.16416	0.00432	1.68915	0.05527	0.07463	0.00175	979.9	23.9	1004.4	20.9	1058.4	47.3	8.0
119	279	86	3.26	0.18720	0.00578	2.00347	0.06664	0.07762	0.00163	1106.2	31.4	1116.7	22.5	1137.2	41.7	2.8
120	247	75	3.29	0.15303	0.00387	1.55337	0.04541	0.07362	0.00152	917.9	21.7	951.8	18.1	1031.1	41.9	12.3
1	166	80	2.07	0.16586	0.00344	1.70647	0.03772	0.07462	0.00100	989.2	19.0	1011.0	14.2	1058.3	27.0	7.0

SS-4-89 (25 μm)

Spot	Conc. (ppm)	Ratios						Ages								
		[Th]	U/Th	$^{206}\text{Pb}/^{238}\text{U}$	$\pm 2\sigma$	$^{207}\text{Pb}/^{235}\text{U}$	$\pm 2\sigma$	$^{206}\text{Pb}/^{208}\text{Pb}$	$\pm 2\sigma$	$^{207}\text{Pb}/^{238}\text{U}$	$\pm 2\sigma$	$^{207}\text{Pb}/^{235}\text{U}$	$\pm 2\sigma$	$^{207}\text{Pb}/^{206}\text{Pb}$	$\pm 2\sigma$	
2	389	178	2.18	0.18517	0.00478	1.98949	0.05261	0.07793	0.00118	1095.1	26.0	1111.9	17.9	1145.0	30.1	4.6
3	171	60	2.86	0.17649	0.00436	1.87009	0.04716	0.07685	0.00125	1047.8	23.9	1070.6	16.7	1117.3	32.4	6.6
4	225	70	3.23	0.17921	0.00356	1.90994	0.03888	0.07730	0.00117	1062.7	19.5	1084.6	13.6	1128.8	30.1	6.2
5	167	133	1.26	0.17174	0.00384	1.77029	0.04596	0.07476	0.00139	1021.7	21.1	1034.6	16.8	1062.1	37.3	4.0
6	215	73	2.94	0.16390	0.00335	1.71389	0.03319	0.07584	0.00126	978.4	18.5	1013.7	12.4	1090.9	33.4	11.5
7	73	41	1.80	0.15917	0.00379	1.69885	0.04679	0.07741	0.00168	952.1	21.1	1008.1	17.6	1131.8	43.2	18.9
8	139	48	2.87	0.16434	0.00368	1.92657	0.07856	0.08502	0.00273	980.9	20.4	1090.4	27.3	1316.1	62.3	34.2
9	62	24	2.57	0.16060	0.00387	1.65967	0.04774	0.07495	0.00163	960.1	21.5	993.2	18.2	1067.2	43.6	11.2
10	4324	784	5.52	0.15246	0.00815	1.62537	0.06913	0.07732	0.00214	914.7	45.6	980.1	26.7	1129.5	55.0	23.5
11	108	52	2.08	0.15842	0.00342	1.60759	0.03979	0.07360	0.00136	948.0	19.0	973.2	15.5	1030.5	37.3	8.7
12	137	31	4.43	0.15886	0.00362	1.61069	0.04110	0.07354	0.00160	950.4	20.1	974.4	16.0	1028.8	43.9	8.2
13	295	106	2.78	0.16630	0.00390	1.69620	0.04267	0.07397	0.00125	991.7	21.6	1007.1	16.1	1040.8	34.1	5.0
14	111	33	3.38	0.16444	0.00383	1.68813	0.04407	0.07446	0.00127	981.4	21.2	1004.1	16.6	1053.9	34.4	7.4
15	509	145	3.51	0.18624	0.00413	2.01526	0.05056	0.07848	0.00133	1101.0	22.4	1120.7	17.0	1159.1	33.5	5.3
16	63	30	2.09	0.18414	0.00512	1.99025	0.05992	0.07839	0.00177	1089.5	27.9	1112.2	20.3	1156.8	44.7	6.2
17	84	37	2.29	0.18509	0.00522	2.01806	0.05536	0.07908	0.00182	1094.7	28.4	1121.6	18.6	1174.1	45.5	7.3
18	188	72	2.59	0.16081	0.00419	1.62742	0.03924	0.07340	0.00148	961.3	23.3	980.9	15.2	1025.0	40.7	6.6
19	1366	483	2.83	0.19801	0.00492	2.20289	0.04895	0.08069	0.00136	1164.6	26.5	1182.0	15.5	1213.8	33.1	4.2
20	128	59	2.15	0.18115	0.00479	1.99137	0.05487	0.07973	0.00172	1073.3	26.1	1112.6	18.6	1190.3	42.6	10.9
21	42	14	3.00	0.18380	0.00442	2.01560	0.05812	0.07954	0.00198	1087.7	24.1	1120.8	19.6	1185.5	49.2	9.0
22	200	61	3.26	0.17764	0.00461	1.94155	0.04993	0.07927	0.00171	1054.1	25.3	1095.5	17.2	1178.9	42.8	11.8
23	314	131	2.40	0.18132	0.00426	1.99426	0.05069	0.07977	0.00163	1074.2	23.3	1113.6	17.2	1191.3	40.3	10.9
24	142	54	2.63	0.16714	0.00392	1.72305	0.04678	0.07477	0.00176	996.3	21.7	1017.2	17.4	1062.3	47.4	6.6
25	266	118	2.26	0.17481	0.00417	1.86794	0.04395	0.07750	0.00162	1038.5	22.9	1069.8	15.6	1134.1	41.7	9.2
26	1181	398	2.97	0.18788	0.00487	2.02759	0.05021	0.07827	0.00156	1109.9	26.4	1124.8	16.8	1153.8	39.7	4.0
27	322	122	2.63	0.18649	0.00469	2.00639	0.04815	0.07803	0.00175	1102.3	25.5	1117.7	16.3	1147.7	44.5	4.1
28	1323	511	2.59	0.16056	0.00395	1.64518	0.03974	0.07432	0.00148	959.9	21.9	987.7	15.3	1050.1	40.0	9.4
29	1327	274	4.84	0.20229	0.00569	2.17594	0.06045	0.07801	0.00159	1187.6	30.5	1173.4	19.3	1147.2	40.5	-3.4
30	121	31	3.87	0.17216	0.00444	1.84087	0.06044	0.07755	0.00177	1024.0	24.4	1060.2	21.6	1135.4	45.4	10.9
31	75	36	2.08	0.09869	0.00262	0.81709	0.03567	0.06005	0.00222	606.7	15.3	606.4	19.9	605.4	80.0	-0.2
32	289	110	2.62	0.09599	0.00270	0.80665	0.03256	0.06095	0.00154	590.9	15.9	600.6	18.3	637.4	54.2	7.9

Spot	Conc. (ppm)	Ratios						Ages						116	
		[U]	[Th]	$^{206}\text{Pb}/^{238}\text{U}$	$\pm 2\sigma$	$^{207}\text{Pb}/^{235}\text{U}$	$\pm 2\sigma$	$^{206}\text{Pb}/^{208}\text{Pb}$	$\pm 2\sigma$	$^{207}\text{Pb}/^{238}\text{U}$	$\pm 2\sigma$	$^{207}\text{Pb}/^{235}\text{U}$	$\pm 2\sigma$		
33	183	101	1.81	0.10850	0.00362	1.58043	0.09478	0.10565	0.00555	664.0	21.0	962.5	37.3	1725.6	96.5
34	113	45	2.49	0.16250	0.00455	1.90073	0.10207	0.08483	0.00294	970.7	25.2	1081.3	35.7	1311.7	67.3
35	2684	400	6.71	0.14617	0.00523	1.74108	0.06809	0.08639	0.00236	879.5	29.4	1023.9	25.2	1346.9	52.8
36	90	46	1.97	0.17993	0.00511	1.95953	0.07203	0.07898	0.00187	1066.6	27.9	1101.7	24.7	1171.7	46.9
37	580	324	1.79	0.18960	0.00907	2.04372	0.11402	0.07818	0.00208	1119.2	49.2	1130.2	38.1	1151.4	52.9
38	376	163	2.30	0.24737	0.00821	3.21818	0.12969	0.09435	0.00174	1424.9	42.4	1461.5	31.2	1515.2	34.9
39	69	30	2.30	0.17793	0.00516	1.93118	0.07420	0.07872	0.00185	1055.7	28.2	1091.9	25.7	1165.0	46.7
40	42	25	1.65	0.15548	0.00415	1.63104	0.06238	0.07608	0.00217	931.6	23.1	982.3	24.1	1097.2	57.2
42	220	211	1.04	0.16698	0.00439	1.86495	0.05685	0.08100	0.00191	995.5	24.2	1068.7	20.2	1221.5	46.3
43	149	53	2.81	0.24420	0.00649	3.13496	0.08854	0.09311	0.00194	1408.5	33.6	1441.3	21.7	1490.1	39.5
44	132	61	2.16	0.17525	0.00401	1.88577	0.05563	0.07804	0.00169	1041.0	22.0	1076.1	19.6	1148.0	43.0
45	77	29	2.64	0.15935	0.00408	1.65359	0.04732	0.07526	0.00176	953.2	22.7	990.9	18.1	1075.5	46.9
46	186	92	2.03	0.21836	0.00470	2.71330	0.06594	0.09012	0.00178	1273.2	24.8	1332.1	18.0	1428.1	37.8
47	723	218	3.32	0.16694	0.00432	1.73752	0.04507	0.07549	0.00141	995.2	23.9	1022.5	16.7	1081.5	37.4
48	234	92	2.55	0.16776	0.00415	1.72136	0.04537	0.07442	0.00163	999.7	22.9	1016.5	16.9	1052.9	44.1
49	358	108	3.30	0.17879	0.00514	1.92607	0.05021	0.07813	0.00164	1060.4	28.1	1090.2	17.4	1150.2	41.6
50	194	109	1.78	0.16285	0.00476	1.72696	0.04752	0.07691	0.00181	972.6	26.4	1018.6	17.7	1118.9	47.0
51	573	198	2.89	0.15876	0.00437	1.64714	0.04706	0.07525	0.00175	949.9	24.3	988.5	18.1	1075.2	46.7
52	132	63	2.11	0.16194	0.00501	1.70241	0.05347	0.07624	0.00200	967.5	27.8	1009.4	20.1	1101.5	52.4
53	106	44	2.40	0.18046	0.00719	2.62682	0.28640	0.10557	0.00801	1069.5	39.3	1308.2	80.3	1724.3	139.3
54	141	42	3.37	0.16658	0.00517	1.70906	0.05674	0.07441	0.00166	993.2	28.6	1011.9	21.3	1052.6	45.0
55	125	75	1.66	0.19705	0.00649	2.14822	0.07143	0.07907	0.00177	1159.5	35.0	1164.5	23.0	1173.8	44.4
56	15	13	1.12	0.15943	0.00586	1.68279	0.07929	0.07655	0.00400	953.6	32.6	1002.0	30.0	1109.5	104.4
57	30	8	3.60	0.15738	0.00435	1.68905	0.05755	0.07784	0.00279	942.2	24.3	1004.4	21.7	1142.7	71.3
58	450	114	3.95	0.16631	0.00514	1.69595	0.05443	0.07396	0.00172	991.7	28.4	1007.0	20.5	1040.4	46.9
59	178	77	2.33	0.15988	0.00389	1.71199	0.05028	0.07766	0.00186	956.1	21.6	1013.0	18.8	1138.2	47.6
60	110	58	1.89	0.15405	0.00357	1.59136	0.04473	0.07492	0.00151	923.6	19.9	966.8	17.5	1066.4	40.6
61	82	34	2.45	0.15585	0.00510	1.60279	0.05689	0.07459	0.00200	933.6	28.4	971.3	22.2	1057.5	54.0
62	67	30	2.19	0.15559	0.00510	1.63128	0.05859	0.07604	0.00218	932.2	28.4	982.4	22.6	1096.1	57.4
63	304	114	2.68	0.22494	0.00739	2.91596	0.10881	0.09402	0.00205	1307.9	38.9	1386.1	28.2	1508.5	41.1
64	117	43	2.72	0.15603	0.00539	1.65288	0.06006	0.07683	0.00193	934.7	30.0	990.7	23.0	1116.8	50.1

Spot	Conc. (ppm)	Ratios						Ages						117		
		[U]	[Th]	$^{206}\text{Pb}/^{238}\text{U}$	$\pm 2\sigma$	$^{207}\text{Pb}/^{235}\text{U}$	$\pm 2\sigma$	$^{207}\text{Pb}/^{206}\text{Pb}$	$\pm 2\sigma$	$^{206}\text{Pb}/^{238}\text{U}$	$\pm 2\sigma$	$^{207}\text{Pb}/^{235}\text{U}$	$\pm 2\sigma$			
65	91	65	1.41	0.17878	0.00504	1.97084	0.06240	0.07995	0.00192	1060.3	27.6	1105.6	21.3	1195.8	47.4	12.8
66	1266	408	3.11	0.17538	0.00607	1.91762	0.06742	0.07930	0.00184	1041.7	33.3	1087.2	23.5	1179.6	45.8	13.2
67	169	79	2.12	0.16264	0.00632	1.93656	0.08635	0.08636	0.00252	971.4	35.1	1093.8	29.9	1346.2	56.3	38.6
68	290	68	4.25	0.20791	0.00758	2.65123	0.09157	0.09249	0.00215	1217.7	40.5	1315.0	25.5	1477.4	44.2	21.3
69	368	188	1.96	0.15257	0.00486	1.56582	0.05582	0.07444	0.00177	915.3	27.2	956.8	22.1	1053.3	48.0	15.1
70	236	165	1.43	0.17249	0.00576	1.86612	0.07127	0.07847	0.00181	1025.8	31.7	1069.2	25.3	1158.7	45.6	13.0
71	347	31	11.04	0.16822	0.00788	1.81232	0.08707	0.07814	0.00186	1002.3	43.5	1049.9	31.4	1150.3	47.3	14.8
72	149	58	2.58	0.17402	0.00522	1.90264	0.05972	0.07930	0.00178	1034.2	28.7	1082.0	20.9	1179.6	44.4	14.1
73	470	169	2.79	0.17763	0.00554	1.90044	0.06466	0.07760	0.00163	1054.0	30.3	1081.2	22.6	1136.6	41.8	7.8
74	418	1358	0.31	0.09249	0.00299	0.77875	0.02778	0.06106	0.00159	570.3	17.7	584.8	15.9	641.5	56.0	12.5
75	154	74	2.07	0.16221	0.00475	1.69313	0.06419	0.07570	0.00205	969.1	26.4	1005.9	24.2	1087.2	54.3	12.2
76	186	65	2.87	0.17614	0.00590	1.89894	0.06782	0.07819	0.00195	1045.9	32.3	1080.7	23.8	1151.7	49.6	10.1
77	57	26	2.14	0.16153	0.00535	1.71103	0.06535	0.07682	0.00228	965.3	29.7	1012.7	24.5	1116.6	59.2	15.7
78	219	74	2.98	0.16156	0.00545	1.68578	0.06220	0.07568	0.00211	965.4	30.2	1003.2	23.5	1086.6	56.0	12.5
79	55	23	2.43	0.16165	0.00457	1.69834	0.06518	0.07620	0.00262	966.0	25.4	1007.9	24.5	1100.3	68.9	13.9
80	70	23	3.10	0.15674	0.00431	1.62308	0.06177	0.07511	0.00236	938.6	24.0	979.2	23.9	1071.3	63.2	14.1
81	80	39	2.04	0.16242	0.00390	1.68236	0.06035	0.07512	0.00176	970.2	21.6	1001.9	22.8	1071.8	47.2	10.5
82	121	125	0.97	0.16051	0.00449	1.89126	0.05178	0.08546	0.00254	959.6	24.9	1078.0	18.2	1325.9	57.6	38.2
83	84	29	2.91	0.15987	0.00435	1.65118	0.04886	0.07491	0.00185	956.1	24.2	990.0	18.7	1066.0	49.8	11.5
84	123	63	1.95	0.16097	0.00451	1.67672	0.05434	0.07554	0.00205	962.2	25.0	999.7	20.6	1083.0	54.3	12.6
85	605	165	3.67	0.16353	0.00424	1.72413	0.05296	0.07646	0.00166	976.4	23.5	1017.6	19.7	1107.3	43.3	13.4
86	288	105	2.75	0.18072	0.00436	1.96276	0.05971	0.07877	0.00179	1070.9	23.8	1102.8	20.5	1166.4	45.0	8.9
87	168	120	1.40	0.17965	0.00442	1.95380	0.06841	0.07888	0.00189	1065.1	24.2	1099.8	23.5	1169.0	47.4	9.8
88	112	45	2.48	0.16169	0.00346	1.65634	0.04767	0.07430	0.00185	966.2	19.2	992.0	18.2	1049.5	50.2	8.6
89	362	45	8.07	0.15634	0.00420	1.62850	0.05574	0.07555	0.00173	936.4	23.4	981.3	21.5	1083.1	46.0	15.7
90	137	68	2.01	0.17346	0.00426	1.84327	0.05321	0.07707	0.00190	1031.2	23.4	1061.0	19.0	1123.0	49.1	8.9
91	171	79	2.16	0.16869	0.00357	2.22472	0.15635	0.09565	0.00543	1004.9	19.7	1188.9	49.3	1540.9	106.7	53.3
92	179	75	2.40	0.18207	0.00440	2.00657	0.06717	0.07993	0.00192	1078.3	24.0	1117.7	22.7	1195.2	47.4	10.8
93	180	75	2.41	0.17357	0.00374	1.83824	0.04712	0.07681	0.00150	1031.8	20.6	1059.2	16.9	1116.3	38.9	8.2
94	1512	253	5.97	0.20104	0.00657	2.58520	0.11292	0.09326	0.00195	1180.9	35.3	1296.5	32.0	1493.2	39.6	26.4
95	401	350	1.15	0.18352	0.00354	2.04616	0.04535	0.08086	0.00155	1086.2	19.3	1131.0	15.1	1218.1	37.6	12.1

Spot	Conc. (ppm)	Ratios						Ages						%		
		[U]	[Th]	U/Th	$^{206}\text{Pb}/^{238}\text{U}$	$\pm 2\sigma$	$^{207}\text{Pb}/^{235}\text{U}$	$\pm 2\sigma$	$^{207}\text{Pb}/^{206}\text{Pb}$	$\pm 2\sigma$	$^{206}\text{Pb}/^{238}\text{U}$	$\pm 2\sigma$	$^{207}\text{Pb}/^{235}\text{U} \pm 2\sigma$	$^{207}\text{Pb}/^{206}\text{Pb} \pm 2\sigma$	Disc	
96	90	29	3.15	0.16836	0.00388	1.75980	0.04495	0.07581	0.00178	1003.1	21.4	1030.8	16.5	1090.0	47.1	8.7
97	283	121	2.34	0.16853	0.00379	1.72890	0.04333	0.07440	0.00167	1004.0	20.9	1019.3	16.1	1052.5	45.3	4.8
98	262	136	1.93	0.17630	0.00355	1.89067	0.04030	0.07778	0.00173	1046.7	19.5	1077.8	14.2	1141.2	44.2	9.0
99	247	35	6.98	0.17521	0.00436	1.89472	0.04557	0.07843	0.00158	1040.8	23.9	1079.2	16.0	1157.8	39.9	11.2
100	45	26	1.72	0.18109	0.00489	2.01544	0.08932	0.08072	0.00334	1072.9	26.7	1120.7	30.1	1214.6	81.4	13.2
101	200	68	2.93	0.17169	0.00405	1.81476	0.04714	0.07666	0.00150	1021.4	22.3	1050.8	17.0	1112.4	39.0	8.9
102	495	162	3.06	0.19501	0.00518	2.10711	0.05097	0.07836	0.00115	1148.5	27.9	1151.1	16.7	1156.1	29.1	0.7
103	103	53	1.96	0.17928	0.00566	1.90300	0.06297	0.07698	0.00158	1063.1	30.9	1082.1	22.0	1120.8	40.9	5.4
105	793	225	3.53	0.17107	0.00576	1.83806	0.06335	0.07793	0.00172	1018.0	31.7	1059.2	22.7	1145.0	43.9	12.5
106	621	197	3.15	0.23972	0.00756	3.14448	0.09598	0.09514	0.00193	1385.2	39.3	1443.6	23.5	1530.8	38.2	10.5
107	413	180	2.29	0.16718	0.00552	1.80975	0.06609	0.07851	0.00153	996.6	30.5	1049.0	23.9	1159.8	38.6	16.4
108	262	123	2.13	0.16091	0.00454	1.69997	0.05316	0.07662	0.00181	961.8	25.2	1008.5	20.0	1111.4	47.2	15.6
109	386	236	1.64	0.15223	0.00484	1.58399	0.04796	0.07547	0.00175	913.5	27.1	963.9	18.8	1080.9	46.5	18.3
110	132	42	3.15	0.15692	0.00461	1.65073	0.05908	0.07630	0.00203	939.6	25.7	989.8	22.6	1102.8	53.2	17.4
111	142	50	2.81	0.16860	0.00511	1.82945	0.06091	0.07870	0.00190	1004.4	28.2	1056.1	21.9	1164.5	47.7	15.9
112	715	161	4.45	0.16069	0.00537	1.67031	0.05234	0.07539	0.00168	960.6	29.8	997.3	19.9	1078.9	44.7	12.3
113	107	65	1.63	0.15368	0.00434	1.63363	0.05261	0.07710	0.00199	921.6	24.2	983.3	20.3	1123.7	51.6	21.9
114	318	159	2.00	0.17273	0.00543	1.87040	0.06310	0.07853	0.00167	1027.2	29.8	1070.7	22.3	1160.4	42.2	13.0
115	369	119	3.10	0.14654	0.00368	1.55718	0.04508	0.07707	0.00178	881.5	20.7	953.3	17.9	1123.0	46.0	27.4
116	92	72	1.27	0.15204	0.00417	1.55585	0.04963	0.07422	0.00190	912.4	23.4	952.8	19.7	1047.4	51.7	14.8
117	343	124	2.76	0.16275	0.00465	1.69261	0.05932	0.07543	0.00177	972.1	25.8	1005.7	22.4	1079.9	47.0	11.1
118	517	180	2.88	0.24672	0.00799	3.34207	0.11024	0.09824	0.00224	1421.5	41.3	1490.9	25.8	1591.1	42.6	11.9
119	158	96	1.65	0.09210	0.00256	1.07269	0.10197	0.08447	0.00611	567.9	15.1	740.1	50.0	1303.5	140.4	129.5
120	138	42	3.26	0.17564	0.00522	1.91509	0.06402	0.07908	0.00190	1043.1	28.6	1086.4	22.3	1174.1	47.6	12.6

Table 5 – Blow Me Down Brook Formation

Spot	Conc. (ppm)	[U]	[Th]	$^{206}\text{Pb}/^{238}\text{U}$	$^{207}\text{Pb}/^{235}\text{U}$	$\pm 2\sigma$	Ratios			Ages			% Disc
							$^{207}\text{Pb}/^{206}\text{Pb}$	$\pm 2\sigma$	$^{206}\text{Pb}/^{238}\text{U}$	$\pm 2\sigma$	$^{207}\text{Pb}/^{235}\text{U}$	$\pm 2\sigma$	
BW-1-88 (25 μm)													
1	168	59	2.84	0.21831	0.00940	2.23424	0.08910	0.07422	0.00142	1273.0	49.7	1191.8	28.0
2	66	44	1.50	0.16343	0.00725	2.01594	0.09008	0.08947	0.00229	975.8	40.2	1120.9	30.3
3	396	380	1.04	0.16495	0.00577	1.69613	0.05518	0.07458	0.00110	984.2	31.9	1007.1	20.8
4	88	62	1.42	0.19727	0.00703	2.28684	0.17711	0.08407	0.00464	1160.7	37.8	1208.2	54.8
5	55	49	1.13	0.18575	0.00684	2.20794	0.09385	0.08621	0.00197	1098.3	37.2	1183.6	29.7
6	2787	561	4.96	0.14949	0.00327	1.45955	0.02976	0.07081	0.00093	898.1	18.3	913.8	12.3
7	175	71	2.45	0.18219	0.00459	1.88134	0.04792	0.07489	0.00123	1078.9	25.0	1074.5	16.9
8	248	105	2.35	0.18041	0.00452	1.83538	0.04399	0.07378	0.00126	1069.2	24.7	1058.2	15.8
9	88	94	0.94	0.17902	0.00454	2.01102	0.05531	0.08147	0.00160	1061.6	24.8	1119.2	18.7
10	229	79	2.89	0.16982	0.00428	1.72344	0.04186	0.07360	0.00118	1011.1	23.6	1017.3	15.6
11	76	81	0.94	0.18784	0.00537	2.05490	0.08418	0.07934	0.00178	1109.7	29.1	1133.9	28.0
12	367	206	1.78	0.18412	0.00431	1.86498	0.05332	0.07346	0.00102	1089.4	23.5	1068.8	18.9
13	39	1.02	0.20153	0.00568	2.62850	0.13495	0.09459	0.00399	1183.5	30.5	1308.6	37.8	
14	600	161	3.73	0.21168	0.00619	2.51005	0.06380	0.08600	0.00147	1237.8	32.9	1274.9	18.5
15	284	169	1.68	0.17109	0.00449	1.76971	0.04822	0.07502	0.00109	1018.1	24.7	1034.4	17.7
16	161	72	2.23	0.17323	0.00430	1.79116	0.04822	0.07499	0.00135	1029.9	23.6	1042.2	17.5
17	161	71	2.27	0.18481	0.00428	1.92459	0.04708	0.07553	0.00114	1093.2	23.3	1089.7	16.3
18	19	24	0.78	0.19383	0.00498	2.61260	0.10701	0.09776	0.00356	1142.1	26.9	1304.2	30.1
19	189	85	2.21	0.16958	0.00484	1.73634	0.04921	0.07426	0.00143	1009.8	26.7	1022.1	18.3
20	146	60	2.42	0.18021	0.00452	1.89272	0.05534	0.07617	0.00126	1068.1	24.7	1078.5	19.4
21	226	102	2.21	0.17753	0.00553	1.83571	0.05861	0.07500	0.00093	1053.5	30.3	1058.3	21.0
22	356	113	3.14	0.20271	0.00688	2.08686	0.06795	0.07467	0.00087	1189.8	36.9	1144.5	22.4
23	172	57	3.02	0.17865	0.00450	1.87585	0.05344	0.07615	0.00106	1059.6	24.6	1072.6	18.9
24	102	38	2.66	0.18193	0.00519	1.94887	0.06190	0.07769	0.00132	1077.5	28.3	1098.1	21.3
25	51	36	1.43	0.17803	0.00532	2.14111	0.07541	0.08723	0.00204	1056.2	29.1	1162.2	24.4
26	35	24	1.42	0.19087	0.00749	2.49097	0.11398	0.09465	0.00266	1126.1	40.5	1269.4	33.2
27	105	32	3.24	0.16853	0.00534	1.88104	0.06657	0.08095	0.00148	1004.0	29.5	1074.4	23.5
28	84	55	1.52	0.18267	0.00642	2.08757	0.07963	0.08289	0.00162	1081.5	35.0	1144.7	26.2

Conc. (ppm)	Ratios										Ages					
	Spot	[U]	[Th]	U/Th	$^{206}\text{Pb}/^{238}\text{U}$	$\pm 2\sigma$	$^{207}\text{Pb}/^{235}\text{U}$	$\pm 2\sigma$	$^{207}\text{Pb}/^{206}\text{Pb}$	$\pm 2\sigma$	$^{206}\text{Pb}/^{238}\text{U}$	$\pm 2\sigma$	$^{207}\text{Pb}/^{235}\text{U}$	$\pm 2\sigma$	$^{207}\text{Pb}/^{206}\text{Pb}$	$\pm 2\sigma$
29	316	163	1.93	0.18176	0.00638	1.85927	0.06444	0.07419	0.00109	1076.6	34.8	1066.7	22.9	1046.6	29.7	-2.8
30	241	97	2.50	0.17718	0.00566	1.86998	0.05820	0.07655	0.00105	1051.5	31.0	1070.5	20.6	1109.4	27.5	5.5
31	138	56	2.48	0.19062	0.00614	2.11539	0.05453	0.08048	0.00184	1124.8	33.3	1153.8	17.8	1208.9	45.0	7.5
32	273	156	1.75	0.17420	0.00588	1.80817	0.04603	0.07528	0.00165	1035.2	32.3	1048.4	16.6	1076.1	44.1	4.0
33	763	264	2.89	0.17588	0.00620	1.78088	0.05309	0.07344	0.00126	1044.4	34.0	1038.5	19.4	1026.0	34.6	-1.8
34	113	63	1.77	0.18954	0.00672	1.99020	0.06389	0.07615	0.00174	1118.9	36.4	1112.2	21.7	1099.1	45.7	-1.8
35	192	64	3.02	0.19635	0.00604	2.12044	0.05835	0.07832	0.00152	1155.7	32.6	1155.5	19.0	1155.1	38.5	0.0
36	146	43	3.40	0.17538	0.00573	1.83976	0.05773	0.07608	0.00162	1041.7	31.4	1059.8	20.6	1097.2	42.6	5.3
37	143	143	1.00	0.17957	0.00577	1.93290	0.06358	0.07807	0.00160	1064.6	31.6	1092.5	22.0	1148.6	40.8	7.9
38	149	57	2.61	0.18406	0.00518	2.02471	0.05669	0.07978	0.00163	1089.1	28.2	1123.8	19.0	1191.6	40.2	9.4
39	275	81	3.41	0.17031	0.00489	1.73914	0.04482	0.07406	0.00140	1013.8	26.9	1023.1	16.6	1043.2	38.1	2.9
40	140	54	2.61	0.16641	0.00471	1.77015	0.05107	0.07715	0.00162	992.3	26.1	1034.6	18.7	1125.0	41.8	13.4
41	717	339	2.12	0.18194	0.00439	1.83755	0.05804	0.07325	0.00110	1077.6	24.0	1059.0	20.8	1020.8	30.4	-5.3
42	117	29	3.99	0.16342	0.00382	1.77123	0.05314	0.07861	0.00143	975.7	21.2	1035.0	19.5	1162.3	36.0	19.1
43	71	42	1.70	0.18061	0.00454	1.97848	0.06209	0.07945	0.00186	1070.3	24.8	1108.2	21.2	1183.3	46.2	10.6
44	484	85	5.67	0.16921	0.00430	1.70675	0.04156	0.07315	0.00110	1007.8	23.7	1011.1	15.6	1018.2	30.4	1.0
45	123	68	1.82	0.16948	0.00405	1.81689	0.04889	0.07775	0.00126	1009.2	22.3	1051.6	17.6	1140.6	32.3	13.0
46	288	242	1.19	0.16627	0.00474	1.72071	0.03948	0.07506	0.00126	991.5	26.2	1016.3	14.7	1070.1	33.6	7.9
47	84	51	1.63	0.17034	0.00437	1.86151	0.05368	0.07926	0.00165	1014.0	24.0	1067.5	19.1	1178.6	41.2	16.2
48	357	155	2.30	0.17603	0.00578	1.86402	0.05681	0.07680	0.00149	1045.2	31.7	1068.4	20.1	1116.0	38.8	6.8
49	325	210	1.55	0.16847	0.00423	1.71205	0.03914	0.07370	0.00107	1003.7	23.3	1013.1	14.7	1033.4	29.5	3.0
50	219	255	0.86	0.17285	0.00467	1.81863	0.04117	0.07631	0.00123	1027.8	25.7	1052.2	14.8	1103.1	32.3	7.3
51	259	111	2.34	0.20583	0.00700	2.42289	0.09375	0.08537	0.00148	1206.6	37.4	1249.4	27.8	1324.0	33.5	9.7
52	168	52	3.25	0.16513	0.00439	1.71570	0.04230	0.07535	0.00133	985.2	24.3	1014.4	15.8	1078.0	35.5	9.4
53	238	103	2.31	0.16239	0.00418	1.64975	0.04196	0.07368	0.00130	970.0	23.2	989.5	16.1	1032.7	35.7	6.5
54	279	161	1.73	0.17362	0.00432	1.81004	0.04866	0.07561	0.00127	1032.0	23.7	1049.1	17.6	1084.8	33.5	5.1
55	103	64	1.60	0.16566	0.00353	1.76947	0.03860	0.07747	0.00142	988.1	19.5	1034.3	14.2	1133.3	36.5	14.7
56	247	182	1.36	0.24812	0.00708	3.20071	0.07318	0.09356	0.00166	1428.8	36.6	1457.3	17.7	1499.2	33.5	4.9
57	187	49	3.81	0.16058	0.00448	1.63986	0.03529	0.07407	0.00139	960.0	24.9	985.7	13.6	1043.3	38.0	8.7
58	143	81	1.77	0.17914	0.00557	1.86187	0.04975	0.07538	0.00140	1062.3	30.5	1067.7	17.7	1078.6	37.3	1.5
59	110	83	1.33	0.16600	0.00487	1.77207	0.04460	0.07742	0.00166	990.0	26.9	1035.3	16.3	1132.1	42.8	14.4

Spot	Conc. (ppm)	Ratios						Ages						121		
		[Th]	U/Th	$^{206}\text{Pb}/^{238}\text{U}$	$\pm 2\sigma$	$^{207}\text{Pb}/^{235}\text{U}$	$\pm 2\sigma$	$^{207}\text{Pb}/^{206}\text{Pb}$	$\pm 2\sigma$	$^{206}\text{Pb}/^{238}\text{U}$	$\pm 2\sigma$	$^{207}\text{Pb}/^{235}\text{U}$	$\pm 2\sigma$			
60	187	114	1.64	0.15327	0.00437	1.56700	0.04006	0.07415	0.00171	919.3	24.4	957.2	15.8	1045.6	46.6	13.7
61	162	75	2.16	0.15905	0.00307	1.64408	0.04032	0.07497	0.00160	951.5	17.1	987.3	15.5	1067.7	43.0	12.2
62	169	102	1.66	0.21740	0.00462	2.57218	0.05087	0.08581	0.00155	1268.1	24.5	1292.8	14.5	1333.9	35.0	5.2
63	255	90	2.82	0.22300	0.00780	2.92583	0.10305	0.09516	0.00174	1297.7	41.1	1388.6	26.7	1531.2	34.4	18.0
64	60	24	2.46	0.17707	0.00478	2.01400	0.06068	0.08249	0.00197	1050.9	26.2	1120.2	20.4	1257.3	46.7	19.6
65	168	57	2.97	0.15804	0.00418	1.64018	0.04645	0.07527	0.00122	945.9	23.3	985.8	17.9	1075.8	32.5	13.7
66	82	33	2.47	0.18051	0.00528	1.98846	0.06715	0.07989	0.00176	1069.8	28.8	1111.6	22.8	1194.3	43.5	11.6
67	102	47	2.16	0.16746	0.00472	1.78740	0.05969	0.07741	0.00156	998.1	26.1	1040.9	21.7	1131.8	40.1	13.4
68	115	55	2.09	0.16344	0.00478	1.74755	0.05452	0.07755	0.00165	975.9	26.5	1026.3	20.1	1135.3	42.3	16.3
69	90	27	3.30	0.16722	0.00499	1.79379	0.06440	0.07780	0.00182	996.8	27.6	1043.2	23.4	1141.8	46.4	14.6
70	89	50	1.78	0.17494	0.00529	1.80411	0.06255	0.07479	0.00192	1039.3	29.0	1046.9	22.7	1062.9	51.6	2.3
71	150	32	4.66	0.17675	0.00598	2.40007	0.11482	0.09848	0.00336	1049.2	32.8	1242.6	34.3	1595.6	63.8	52.1
72	121	41	2.98	0.15492	0.00511	1.59074	0.05451	0.07447	0.00170	928.5	28.5	966.6	21.4	1054.3	46.0	13.6
73	144	56	2.57	0.15898	0.00487	1.66060	0.05128	0.07576	0.00150	951.1	27.1	993.6	19.6	1088.7	39.7	14.5
74	392	181	2.17	0.19948	0.00535	2.28009	0.06445	0.08290	0.00155	1172.5	28.7	1206.1	20.0	1266.9	36.5	8.0
75	161	99	1.63	0.16408	0.00461	1.67040	0.04631	0.07383	0.00155	979.4	25.5	997.3	17.6	1036.9	42.5	5.9
76	220	30	7.43	0.16675	0.00371	1.71374	0.04325	0.07454	0.00132	994.2	20.5	1013.7	16.2	1056.1	35.6	6.2
77	181	70	2.59	0.16396	0.00386	1.66763	0.03799	0.07377	0.00167	978.7	21.4	996.3	14.5	1035.1	45.8	5.8
78	651	153	4.24	0.18035	0.00471	1.92868	0.04734	0.07756	0.00136	1068.9	25.7	1091.1	16.4	1135.7	34.8	6.2
79	59	60	0.98	0.16505	0.00378	1.75073	0.04999	0.07693	0.00207	984.8	20.9	1027.4	18.5	1119.4	53.6	13.7
80	223	78	2.84	0.15998	0.00358	1.62147	0.03510	0.07351	0.00147	956.7	19.9	978.6	13.6	1028.0	40.5	7.5
81	46	35	1.29	0.15769	0.00541	1.71520	0.06437	0.07889	0.00260	943.9	30.1	1014.2	24.1	1169.3	65.2	23.9
82	51	39	1.29	0.17589	0.00631	1.86985	0.06709	0.07710	0.00238	1044.5	34.6	1070.5	23.7	1123.9	61.4	7.6
83	65	22	2.96	0.16739	0.00484	1.73134	0.05220	0.07502	0.00185	997.7	26.7	1020.2	19.4	1068.9	49.7	7.1
84	60	63	0.94	0.16102	0.00439	1.69246	0.04541	0.07623	0.00186	962.4	24.4	1005.7	17.1	1101.2	48.9	14.4
85	112	34	3.30	0.16575	0.00512	1.66231	0.04686	0.07274	0.00165	988.6	28.3	994.3	17.9	1006.7	46.0	1.8
86	496	153	3.26	0.19291	0.00822	2.12703	0.09605	0.07997	0.00181	1137.1	44.4	1157.6	31.2	1196.2	44.6	5.2
87	50	24	2.13	0.17330	0.00585	1.81477	0.05486	0.07595	0.00207	1030.2	32.2	1050.8	19.8	1093.8	54.6	6.2
88	38	29	1.30	0.17800	0.00620	2.32049	0.12372	0.09455	0.00463	1056.0	33.9	1218.6	37.9	1519.1	92.3	43.9
89	130	44	2.93	0.19065	0.00656	2.04498	0.06013	0.07780	0.00164	1124.9	35.5	1130.6	20.1	1141.6	42.0	1.5
90	111	49	2.26	0.16749	0.00594	1.76165	0.05661	0.07628	0.00192	998.2	32.8	1031.5	20.8	1102.6	50.4	10.4

Spot	Conc. (ppm)	Ratios										% Disc				
		[Th]	U/Th	$^{206}\text{Pb}/^{238}\text{U}$	$\pm 2\sigma$	$^{207}\text{Pb}/^{235}\text{U}$	$\pm 2\sigma$	$^{207}\text{Pb}/^{206}\text{Pb}$	$\pm 2\sigma$	$^{206}\text{Pb}/^{238}\text{U}$	$\pm 2\sigma$					
91	141	54	2.58	0.18560	0.00380	1.99804	0.04428	0.07808	0.00153	1097.5	20.7	1114.9	15.0	1148.8	39.0	4.7
92	466	149	3.13	0.17262	0.00378	1.73989	0.02783	0.07310	0.00120	1026.5	20.8	1023.4	10.3	1016.8	33.2	-1.0
93	193	97	1.99	0.16685	0.00358	1.69938	0.03276	0.07387	0.00133	994.7	19.8	1008.3	12.3	1037.9	36.4	4.3
94	134	42	3.20	0.16094	0.00348	1.65661	0.03352	0.07465	0.00163	962.0	19.3	992.1	12.8	1059.2	43.8	10.1
95	268	108	2.47	0.18634	0.00438	1.99236	0.03914	0.07754	0.00120	1101.5	23.8	1112.9	13.3	1135.2	30.8	3.1
96	137	48	2.87	0.18042	0.00415	1.81797	0.04619	0.07308	0.00161	1069.3	22.7	1052.0	16.6	1016.2	44.6	-5.0
97	153	93	1.64	0.19448	0.00417	2.17356	0.04738	0.08106	0.00129	1145.6	22.5	1172.6	15.2	1222.8	31.2	6.7
98	222	194	1.14	0.17733	0.00423	1.79963	0.04479	0.07361	0.00115	1052.4	23.1	1045.3	16.2	1030.7	31.6	-2.1
100	54	26	2.05	0.17349	0.00385	1.84992	0.05552	0.07733	0.00200	1031.3	21.2	1063.4	19.8	1129.8	51.5	9.5
101	206	172	1.20	0.17412	0.00409	1.77067	0.04210	0.07375	0.00103	1034.8	22.5	1034.8	15.4	1034.7	28.3	0.0
102	705	375	1.88	0.17673	0.00379	1.76824	0.03777	0.07257	0.00088	1049.1	20.8	1033.9	13.9	1001.9	24.7	-4.5
103	249	86	2.88	0.18001	0.00382	1.80486	0.04425	0.07272	0.00105	1067.0	20.8	1047.2	16.0	1006.2	29.2	-5.7
104	234	102	2.29	0.20714	0.00507	2.19732	0.05539	0.07694	0.00102	1213.5	27.1	1180.2	17.6	1119.6	26.5	-7.7
105	167	99	1.68	0.17281	0.00297	1.80347	0.03556	0.07569	0.00123	1027.6	16.3	1046.7	12.9	1086.9	32.6	5.8
106	97	73	1.34	0.15680	0.00405	1.62556	0.04933	0.07519	0.00177	939.0	22.6	980.1	19.1	1073.5	47.2	14.3
107	542	222	2.44	0.18677	0.00545	1.92596	0.05352	0.07479	0.00096	1103.8	29.6	1090.1	18.6	1062.9	25.8	-3.7
108	151	140	1.08	0.16807	0.00520	1.72254	0.05022	0.07433	0.00153	1001.5	28.7	1017.0	18.7	1050.5	41.5	4.9
109	157	51	3.11	0.17510	0.00462	1.80921	0.04753	0.07494	0.00134	1040.2	25.3	1048.8	17.2	1066.8	35.9	2.6
111	78	30	2.62	0.17289	0.00312	1.80104	0.04366	0.07555	0.00157	1028.0	17.1	1045.8	15.8	1083.2	41.6	5.4
112	337	149	2.26	0.18335	0.00465	1.86100	0.04278	0.07361	0.00115	1085.3	25.3	1067.3	15.2	1030.9	31.6	-5.0
113	124	39	3.18	0.16925	0.00416	1.75523	0.03909	0.07521	0.00137	1008.0	22.9	1029.1	14.4	1074.2	36.5	6.6
114	137	74	1.86	0.19076	0.00472	2.05073	0.05186	0.07797	0.00135	1125.5	25.5	1132.5	17.3	1146.1	34.3	1.8
115	51	44	1.16	0.17905	0.00480	1.86148	0.04734	0.07540	0.00176	1061.8	26.2	1067.5	16.8	1079.3	46.9	1.6
116	49	44	1.11	0.17918	0.00449	1.87156	0.04602	0.07576	0.00200	1062.5	24.5	1071.1	16.3	1088.6	52.8	2.5
117	321	111	2.90	0.17764	0.00506	1.82238	0.04159	0.07440	0.00140	1054.1	27.7	1053.5	15.0	1052.4	38.0	-0.2
118	68	71	0.95	0.17220	0.00412	1.78197	0.04276	0.07505	0.00175	1024.2	22.7	1038.9	15.6	1069.9	46.9	4.5
119	293	137	2.13	0.17823	0.00436	1.82978	0.03436	0.07446	0.00126	1057.3	23.9	1056.2	12.3	1053.9	34.1	-0.3
120	132	41	3.18	0.16474	0.00451	1.68108	0.04456	0.07401	0.00143	983.1	25.0	1001.4	16.9	1041.8	38.9	6.0

Table 6 – Bradore Formation

Spot	Conc. (ppm)	Ratios										Ages				
		[U]	[Th]	U/Th	$^{206}\text{Pb}/^{238}\text{U}$	$\pm 2\sigma$	$^{207}\text{Pb}/^{235}\text{U}$	$\pm 2\sigma$	$^{207}\text{Pb}/^{206}\text{Pb}$	$\pm 2\sigma$	$^{206}\text{Pb}/^{238}\text{U}$	$\pm 2\sigma$	$^{207}\text{Pb}/^{235}\text{U}$	$\pm 2\sigma$	$^{207}\text{Pb}/^{206}\text{Pb}$	$\pm 2\sigma$
LAB-5C-88 (25 μm)																
1	298	125	2.39	0.17332	0.00411	1.75760	0.04445	0.07355	0.00131	1030.4	22.6	1030.0	16.4	1029.1	36.1	-0.1
2	299	364	0.82	0.17230	0.00362	1.76481	0.04157	0.07429	0.00137	1024.8	19.9	1032.6	15.3	1049.3	37.2	2.4
3	95	109	0.87	0.09379	0.00252	0.75691	0.02686	0.05853	0.00174	577.9	14.9	572.2	15.5	549.6	64.8	-4.9
4	162	80	2.04	0.16806	0.00401	1.70906	0.04459	0.07376	0.00167	1001.4	22.1	1011.9	16.7	1034.8	45.8	3.3
5	95	94	1.01	0.17013	0.00448	1.64389	0.04934	0.07008	0.00174	1012.8	24.7	987.2	18.9	930.7	51.1	-8.1
6	64	39	1.63	0.16871	0.00419	1.72374	0.05103	0.07410	0.00214	1005.0	23.1	1017.4	19.0	1044.3	58.2	3.9
7	252	44	5.74	0.17037	0.00514	1.71018	0.04795	0.07280	0.00162	1014.1	28.3	1012.4	18.0	1008.5	45.2	-0.6
8	407	292	1.40	0.09718	0.00273	0.79711	0.02189	0.05949	0.00138	597.9	16.1	595.2	12.4	584.9	50.5	-2.2
9	130	70	1.86	0.16375	0.00479	1.66442	0.05034	0.07372	0.00182	977.6	26.5	995.1	19.2	1033.8	49.8	5.7
10	79	33	2.40	0.18998	0.00539	2.09880	0.06732	0.08012	0.00204	1121.3	29.2	1148.4	22.1	1200.1	50.2	7.0
11	38	22	1.73	0.16736	0.00493	1.76900	0.06637	0.07666	0.00266	997.5	27.2	1034.2	24.3	1112.4	69.4	11.5
12	282	351	0.80	0.18253	0.00480	1.86487	0.05000	0.07410	0.00154	1080.8	26.2	1068.7	17.7	1044.1	41.9	-3.4
13	103	77	1.33	0.17840	0.00474	1.85322	0.05120	0.07534	0.00156	1058.2	25.9	1064.6	18.2	1077.6	41.6	1.8
14	176	82	2.13	0.16933	0.00431	1.71771	0.04428	0.07357	0.00174	1008.4	23.8	1015.2	16.5	1029.8	47.8	2.1
15	710	4035	0.18	0.09160	0.00262	0.82422	0.02267	0.06526	0.00141	565.0	15.5	610.4	12.6	782.7	45.3	38.5
16	407	218	1.87	0.17637	0.00441	1.79745	0.04219	0.07391	0.00155	1047.1	24.1	1044.5	15.3	1039.1	42.3	-0.8
17	24	17	1.44	0.16850	0.00487	1.79304	0.08083	0.07718	0.00333	1003.8	26.8	1042.9	29.4	1125.8	86.0	12.1
18	137	42	3.28	0.17517	0.00434	1.75325	0.04936	0.07259	0.00168	1040.5	23.8	1028.4	18.2	1002.5	47.0	-3.7
19	226	72	3.13	0.25529	0.00626	3.29248	0.07247	0.09354	0.00203	1465.7	32.1	1479.3	17.1	1498.8	41.1	2.3
20	254	125	2.04	0.17360	0.00512	1.78688	0.05266	0.07465	0.00169	1031.9	28.1	1040.7	19.2	1059.1	45.5	2.6
21	115	123	0.93	0.17715	0.00545	1.78748	0.05861	0.07318	0.00178	1051.4	29.9	1040.9	21.4	1018.9	49.3	-3.1
22	81	90	0.90	0.17197	0.00602	1.76806	0.05832	0.07457	0.00209	1023.0	33.1	1033.8	21.4	1056.8	56.4	3.3
23	49	33	1.50	0.17560	0.00570	1.81669	0.05351	0.07503	0.00222	1042.9	31.3	1051.5	19.3	1069.4	59.4	2.5
24	39	26	1.50	0.10191	0.00388	0.87118	0.05590	0.06200	0.00356	625.6	22.7	636.2	30.3	674.2	122.7	7.8
25	132	75	1.76	0.10100	0.00333	0.84075	0.03022	0.06037	0.00199	620.3	19.5	619.6	16.7	617.0	71.1	-0.5
26	95	38	2.52	0.17596	0.00544	1.78584	0.05548	0.07361	0.00180	1044.8	29.8	1040.3	20.2	1030.8	49.5	-1.3
27	114	61	1.85	0.09546	0.00377	0.80581	0.03150	0.06122	0.00194	587.8	22.2	600.1	17.7	647.0	68.0	10.1
28	640	494	1.30	0.17561	0.00641	1.75782	0.05689	0.07260	0.00117	1043.0	35.1	1030.0	21.0	1002.7	32.8	-3.9

Spot	Conc. (ppm)	Ratios										Ages				
		[U]	[Th]	U/Th	$^{206}\text{Pb}/^{238}\text{U}$	$\pm 2\sigma$	$^{207}\text{Pb}/^{235}\text{U}$	$\pm 2\sigma$	$^{207}\text{Pb}/^{206}\text{Pb}$	$\pm 2\sigma$	$^{206}\text{Pb}/^{238}\text{U}$	$\pm 2\sigma$	$^{207}\text{Pb}/^{235}\text{U}$	$\pm 2\sigma$	$^{207}\text{Pb}/^{206}\text{Pb}$	$\pm 2\sigma$
29	93	78	1.20	0.09839	0.00378	0.87977	0.03813	0.06485	0.00220	605.0	22.2	640.9	20.6	769.5	71.6	27.2
30	111	92	1.21	0.09745	0.00372	0.80342	0.03264	0.05980	0.00178	599.4	21.8	598.8	18.4	596.2	64.6	-0.5
31	295	146	2.02	0.17528	0.00597	1.91343	0.05873	0.07917	0.00194	1041.1	32.8	1085.8	20.5	1176.5	48.5	13.0
32	71	46	1.55	0.08922	0.00313	0.75334	0.03292	0.06124	0.00224	550.9	18.5	570.2	19.1	647.7	78.7	17.6
33	40	30	1.35	0.16359	0.00484	1.73919	0.06522	0.07711	0.00268	976.7	26.8	1023.2	24.2	1123.9	69.2	15.1
34	68	24	2.81	0.16381	0.00438	1.69182	0.05648	0.07490	0.00211	977.9	24.3	1005.4	21.3	1065.9	56.8	9.0
35	80	80	1.00	0.16566	0.00445	1.72501	0.05375	0.07552	0.00189	988.2	24.6	1017.9	20.0	1082.4	50.1	9.5
36	444	220	2.02	0.09396	0.00262	0.78153	0.02258	0.06032	0.00151	578.9	15.4	586.4	12.9	615.2	54.1	6.3
37	3070	451	6.80	0.04225	0.00391	0.52322	0.04378	0.08981	0.00155	266.8	24.2	427.3	29.2	1421.6	32.9	432.9
38	103	93	1.11	0.17104	0.00515	1.75947	0.04944	0.07461	0.00213	1017.8	28.4	1030.7	18.2	1058.0	57.4	3.9
39	117	57	2.05	0.16025	0.00428	1.62856	0.04312	0.07371	0.00183	958.2	23.8	981.3	16.7	1033.4	50.3	7.9
40	352	156	2.26	0.16235	0.00508	1.62155	0.04283	0.07244	0.00139	969.8	28.2	978.6	16.6	998.3	39.0	2.9
41	434	132	3.28	0.17011	0.00551	1.71099	0.04969	0.07295	0.00142	1012.7	30.4	1012.7	18.6	1012.5	39.4	0.0
42	175	98	1.78	0.16118	0.00566	1.62285	0.05215	0.07302	0.00178	963.3	31.4	979.1	20.2	1014.6	49.5	5.3
43	37	16	2.35	0.08808	0.00304	0.78375	0.03592	0.06454	0.00273	544.1	18.0	587.6	20.4	759.3	89.2	39.5
44	136	47	2.90	0.17003	0.00568	1.71514	0.05218	0.07316	0.00200	1012.3	31.3	1014.2	19.5	1018.4	55.4	0.6
45	489	367	1.33	0.16798	0.00511	1.68397	0.05168	0.07271	0.00141	1000.9	28.2	1002.5	19.6	1005.8	39.3	0.5
46	495	318	1.56	0.17130	0.00520	1.76963	0.04666	0.07493	0.00155	1019.2	28.6	1034.4	17.1	1066.5	41.7	4.6
47	241	170	1.41	0.16737	0.00484	1.73721	0.05614	0.07528	0.00199	997.6	26.7	1022.4	20.8	1075.9	53.0	7.9
48	294	194	1.51	0.09372	0.00260	0.78535	0.02125	0.06078	0.00164	577.5	15.3	588.5	12.1	631.3	58.1	9.3
49	200	115	1.74	0.16305	0.00367	1.67714	0.04199	0.07460	0.00189	973.7	20.3	999.9	15.9	1057.8	50.9	8.6
50	72	47	1.56	0.17605	0.00490	1.84944	0.05324	0.07619	0.00213	1045.3	26.9	1063.2	19.0	1100.1	55.8	5.2
51	209	104	2.00	0.19707	0.00424	2.16964	0.05329	0.07985	0.00153	1159.6	22.8	1171.4	17.1	1193.2	37.9	2.9
52	46	55	0.84	0.09422	0.00290	0.81539	0.03569	0.06276	0.00273	580.5	17.1	605.5	20.0	700.2	92.7	20.6
53	371	337	1.10	0.17060	0.00473	1.74535	0.04930	0.07420	0.00135	1015.4	26.1	1025.4	18.2	1046.9	36.8	3.1
54	21	12	1.74	0.16917	0.00540	1.70997	0.07898	0.07331	0.00325	1007.5	29.8	1012.3	29.6	1022.6	89.6	1.5
55	165	20	8.32	0.17172	0.00471	1.77084	0.05132	0.07479	0.00145	1021.6	25.9	1034.8	18.8	1063.0	39.1	4.1
56	62	60	1.02	0.17895	0.00526	1.86774	0.06548	0.07570	0.00224	1061.3	28.8	1069.7	23.2	1087.1	59.2	2.4
57	31	25	1.25	0.16504	0.00523	1.75491	0.07444	0.07712	0.00267	984.7	28.9	1029.0	27.4	1124.3	68.9	14.2
58	42	15	2.71	0.16742	0.00499	1.70246	0.06838	0.07375	0.00213	997.9	27.6	1009.5	25.7	1034.6	58.3	3.7
59	276	144	1.91	0.17116	0.00462	1.75351	0.05291	0.07430	0.00126	1018.5	25.5	1028.5	19.5	1049.7	34.3	3.1

Spot	Conc. (ppm)	Ratios						Ages						
		[U]	[Th]	$^{206}\text{Pb}/^{238}\text{U}$	$\pm 2\sigma$	$^{207}\text{Pb}/^{235}\text{U}$	$\pm 2\sigma$	$^{206}\text{Pb}/^{208}\text{Pb}$	$\pm 2\sigma$	$^{207}\text{Pb}/^{235}\text{U}$	$\pm 2\sigma$	$^{207}\text{Pb}/^{206}\text{Pb}$	$\pm 2\sigma$	
60	79	54	1.45	0.09427	0.00267	0.80908	0.03291	0.06225	0.00224	580.7	15.8	601.9	18.5	
61	1024	641	1.60	0.17309	0.00642	1.80631	0.05405	0.07569	0.00140	1029.1	35.3	1047.7	19.6	
62	1064	476	2.23	0.18748	0.00566	1.95510	0.05762	0.07563	0.00147	1107.7	30.7	1100.2	19.8	
63	1179	582	2.03	0.16160	0.00465	1.74242	0.05047	0.07820	0.00163	965.7	25.8	1024.4	18.7	
64	128	66	1.93	0.15976	0.00465	1.65910	0.04721	0.07532	0.00180	955.4	25.9	993.0	18.0	
65	154	95	1.61	0.16516	0.00511	1.67599	0.05100	0.07360	0.00164	985.4	28.3	999.5	19.4	
66	75	47	1.58	0.09424	0.00280	0.79499	0.03181	0.06118	0.00204	580.5	16.5	594.0	18.0	
67	505	293	1.73	0.17576	0.00500	1.82188	0.04960	0.07518	0.00144	1043.8	27.4	1053.4	17.8	
69	186	68	2.71	0.17170	0.00525	1.71464	0.04794	0.07243	0.00154	1021.4	28.9	1014.0	17.9	
70	100	39	2.56	0.09210	0.00282	0.76411	0.02777	0.06017	0.00222	567.9	16.6	576.4	16.0	
71	82	27	3.01	0.16341	0.00524	1.67682	0.06255	0.07442	0.00192	975.7	29.0	999.8	23.7	
72	342	202	1.70	0.16342	0.00581	1.63660	0.05735	0.07263	0.00126	975.7	32.2	984.4	22.1	
73	250	232	1.08	0.09326	0.00293	0.77930	0.03097	0.06060	0.00174	574.8	17.3	585.1	17.7	
74	74	408	611	0.67	0.17146	0.00528	1.75896	0.05400	0.07440	0.00139	1020.2	29.1	1030.5	19.9
75	1052	1531	0.69	0.09188	0.00267	3.00184	0.08707	0.23697	0.00450	566.6	15.8	1408.1	22.1	
76	739	205	3.61	0.17989	0.00596	1.82256	0.06116	0.07348	0.00146	1066.4	32.6	1053.6	22.0	
77	80	55	1.45	0.09638	0.00334	0.80428	0.03532	0.06052	0.00208	593.2	19.6	599.2	19.9	
78	22	20	1.10	0.17297	0.00649	1.93978	0.09600	0.08134	0.00363	1028.4	35.7	1094.9	33.2	
79	72	46	1.58	0.17395	0.00639	1.77374	0.06931	0.07395	0.00191	1033.8	35.1	1035.9	25.4	
80	174	58	3.00	0.17027	0.00524	1.73434	0.05530	0.07387	0.00155	1013.6	28.9	1021.4	20.5	
81	72	96	0.75	0.09947	0.00319	0.84683	0.03449	0.06175	0.00199	611.3	18.7	622.9	19.0	
82	61	42	1.44	0.18095	0.00459	1.89124	0.05956	0.07580	0.00215	1072.2	25.1	1078.0	20.9	
83	546	488	1.12	0.21059	0.00612	2.21174	0.05940	0.07617	0.00137	1231.9	32.6	1184.8	18.8	
84	138	83	1.67	0.17493	0.00430	1.77816	0.05688	0.07373	0.00176	1039.2	23.6	1037.5	20.8	
85	320	111	2.89	0.17923	0.00494	1.80404	0.04585	0.07300	0.00147	1062.8	27.0	1046.9	16.6	
86	26	22	1.19	0.16962	0.00508	1.72578	0.06577	0.07379	0.00287	1010.0	28.0	1018.2	24.5	
87	716	307	2.33	0.09607	0.00283	0.84884	0.03523	0.06408	0.00179	591.3	16.6	624.0	19.4	
88	326	187	1.74	0.18938	0.00488	1.94814	0.05698	0.07461	0.00160	1118.0	26.4	1097.8	19.6	
89	77	44	1.73	0.17876	0.00597	1.81615	0.06499	0.07369	0.00200	1060.2	32.7	1051.3	23.4	
90	150	86	1.75	0.09764	0.00260	0.82694	0.02578	0.06143	0.00179	600.6	15.3	611.9	14.3	
91	392	192	2.04	0.10142	0.00250	0.83654	0.02116	0.05982	0.00129	622.7	14.6	617.2	11.7	

Spot	Conc. (ppm)	Ratios										Ages				
		[U]	[Th]	U/Th	$^{206}\text{Pb}/^{238}\text{U}$	$\pm 2\sigma$	$^{207}\text{Pb}/^{235}\text{U}$	$\pm 2\sigma$	$^{207}\text{Pb}/^{206}\text{Pb}$	$\pm 2\sigma$	$^{206}\text{Pb}/^{238}\text{U}$	$\pm 2\sigma$	$^{207}\text{Pb}/^{235}\text{U}$	$\pm 2\sigma$	$^{207}\text{Pb}/^{206}\text{Pb}$	$\pm 2\sigma$
92	82	40	2.07	0.17467	0.00509	1.76206	0.05655	0.07316	0.00180	1037.8	28.0	1031.6	20.8	1018.5	49.9	-1.9
93	328	177	1.85	0.09589	0.00273	0.80222	0.02459	0.06067	0.00129	590.3	16.1	598.1	13.9	627.7	46.0	6.3
94	80	72	1.12	0.17896	0.00462	1.85607	0.05973	0.07522	0.00189	1061.3	25.3	1065.6	21.2	1074.3	50.5	1.2
95	125	295	0.42	0.10058	0.00284	0.84474	0.02831	0.06091	0.00175	617.8	16.7	621.8	15.6	636.1	61.9	3.0
96	650	605	1.07	0.18826	0.00572	1.94743	0.05417	0.07502	0.00125	1111.9	31.0	1097.6	18.7	1069.2	33.6	-3.8
97	75	47	1.58	0.20947	0.00518	2.31395	0.07189	0.08012	0.00191	1226.0	27.6	1216.6	22.0	1199.9	46.9	-2.1
98	371	331	1.12	0.17697	0.00423	1.81772	0.04806	0.07450	0.00132	1050.4	23.2	1051.9	17.3	1054.9	35.8	0.4
99	88	33	2.64	0.18131	0.00522	1.81993	0.05870	0.07280	0.00206	1074.1	28.5	1052.7	21.1	1008.4	57.3	-6.1
100	181	83	2.19	0.18106	0.00432	1.90505	0.04998	0.07631	0.00151	1072.8	23.6	1082.9	17.5	1103.2	39.7	2.8
101	216	81	2.67	0.16841	0.00521	1.68127	0.05417	0.07241	0.00167	1003.3	28.7	1001.5	20.5	997.4	46.9	-0.6
102	125	99	1.26	0.17300	0.00489	1.73842	0.05376	0.07288	0.00170	1028.6	26.9	1022.9	19.9	1010.6	47.3	-1.8
103	65	85	0.77	0.10243	0.00331	0.84527	0.03686	0.05985	0.00237	628.6	19.3	622.0	20.3	598.2	85.9	-4.8
104	181	106	1.70	0.18014	0.00509	1.81980	0.05517	0.07327	0.00142	1067.7	27.8	1052.6	19.9	1021.4	39.3	-4.3
105	166	55	2.99	0.16878	0.00445	1.68427	0.04669	0.07238	0.00156	1005.4	24.6	1002.6	17.7	996.5	43.8	-0.9
106	109	150	0.73	0.17446	0.00515	1.81191	0.05833	0.07532	0.00180	1036.7	28.3	1049.8	21.1	1077.1	48.0	3.9
107	256	57	4.47	0.23336	0.00557	2.76581	0.07135	0.08596	0.00178	1352.1	29.1	1346.4	19.2	1337.3	40.1	-1.1
108	535	215	2.48	0.18542	0.00515	1.90473	0.05510	0.07450	0.00152	1096.5	28.0	1082.7	19.3	1055.1	41.2	-3.8
109	373	261	1.43	0.20906	0.00567	2.29570	0.06538	0.07964	0.00148	1223.8	30.2	1211.0	20.1	1188.2	36.8	-2.9
110	292	154	1.89	0.17694	0.00616	1.83165	0.07322	0.07508	0.00256	1050.2	33.7	1056.9	26.3	1070.6	68.4	1.9
111	82	47	1.75	0.17897	0.00547	1.83418	0.07008	0.07433	0.00266	1061.3	29.9	1057.8	25.1	1050.4	72.1	-1.0
112	62	47	1.32	0.09967	0.00345	0.86272	0.04052	0.06278	0.00310	612.5	20.2	631.6	22.1	700.6	105.0	14.4
113	744	124	5.99	0.17243	0.00570	1.70427	0.06628	0.07168	0.00226	1025.5	31.3	1010.1	24.9	977.0	64.2	-4.7
114	104	45	2.28	0.17487	0.00467	1.80142	0.06663	0.07471	0.00220	1038.9	25.6	1046.0	24.2	1060.8	59.2	2.1
115	195	37	5.23	0.17847	0.00501	1.77537	0.06219	0.07215	0.00212	1058.6	27.4	1036.5	22.8	990.1	59.8	-6.5
116	650	388	1.68	0.10118	0.00264	0.85048	0.03329	0.06096	0.00200	621.3	15.5	624.9	18.3	638.0	70.6	2.7
117	150	144	1.04	0.18501	0.00473	1.89639	0.08435	0.07434	0.00266	1094.3	25.7	1079.8	29.6	1050.7	72.0	-4.0
118	608	584	1.04	0.18230	0.00496	1.87915	0.08459	0.07476	0.00267	1079.5	27.1	1073.8	29.8	1062.1	71.9	-1.6
119	45	36	1.25	0.10525	0.00283	0.91100	0.05138	0.06278	0.00310	645.1	16.5	657.6	27.3	700.7	105.0	8.6
120	63	28	2.20	0.20963	0.00757	2.16315	0.11922	0.07484	0.00318	1226.8	40.3	1169.3	38.3	1064.2	85.4	-13.3
										LAB-7B-88 (50 μm)						
1	91	61	1.49	0.17000	0.00488	1.68923	0.04798	0.07207	0.00150	1012.1	26.9	1004.5	18.1	987.8	42.2	2.40

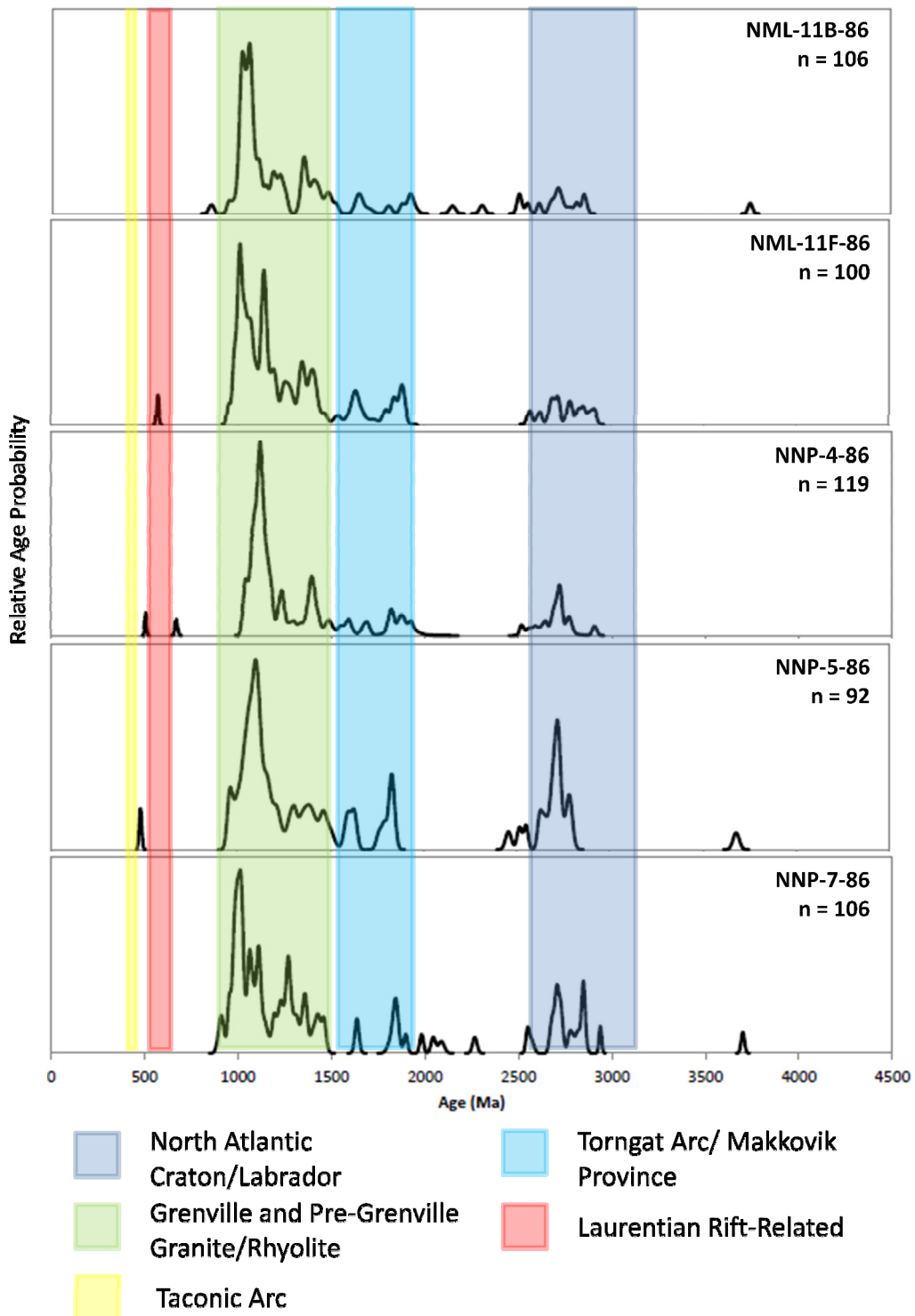
Spot	Conc. (ppm)	Ratios						Ages						% Disc		
		[U]	[Th]	$^{206}\text{Pb}/^{238}\text{U}$	$^{207}\text{Pb}/^{235}\text{U}$	$\pm 2\sigma$	$^{207}\text{Pb}/^{206}\text{Pb}$	$\pm 2\sigma$	$^{206}\text{Pb}/^{238}\text{U}$	$\pm 2\sigma$	$^{207}\text{Pb}/^{235}\text{U}$	$\pm 2\sigma$	$^{207}\text{Pb}/^{206}\text{Pb}$			
2	103	47	2.18	0.17129	0.00490	1.71721	0.04868	0.07271	0.00150	1019.2	27.0	1015.0	18.2	1005.9	41.6	1.30
3	75	29	2.61	0.17070	0.00490	1.72098	0.04920	0.07312	0.00154	1016.0	27.0	1016.4	18.4	1017.4	42.3	0.14
4	105	130	0.81	0.17218	0.00494	1.81206	0.05118	0.07633	0.00156	1024.1	27.1	1049.8	18.5	1103.8	40.7	7.78
5	148	145	1.02	0.16767	0.00480	1.66667	0.04670	0.07210	0.00146	999.3	26.5	995.9	17.8	988.6	40.7	1.07
6	18	23	0.78	0.09913	0.00298	0.84686	0.03108	0.06196	0.00200	609.3	17.5	622.9	17.1	672.9	68.2	10.44
7	91	91	1.01	0.09780	0.00282	0.80829	0.02366	0.05994	0.00132	601.5	16.5	601.5	13.3	601.5	47.4	0.00
8	11	14	0.78	0.09735	0.00302	0.82454	0.03574	0.06143	0.00248	598.8	17.8	610.6	19.9	654.5	85.5	9.30
9	41	55	0.76	0.09609	0.00280	0.79127	0.02514	0.05973	0.00154	591.5	16.5	591.9	14.3	593.8	55.1	0.39
10	31	35	0.89	0.09564	0.00282	0.79940	0.02624	0.06063	0.00164	588.8	16.6	596.5	14.8	626.0	58.1	6.32
11	47	65	0.73	0.16858	0.00486	1.71768	0.05018	0.07391	0.00162	1004.3	26.8	1015.2	18.7	1038.9	44.2	3.45
12	797	2646	0.30	0.09082	0.00260	0.73932	0.02056	0.05904	0.00116	560.4	15.3	562.0	12.0	568.7	42.7	1.48
13	33	30	1.10	0.09625	0.00282	0.79625	0.02566	0.06000	0.00158	592.4	16.6	594.7	14.5	603.6	56.5	1.89
14	62	44	1.42	0.17208	0.00496	1.82546	0.05248	0.07694	0.00164	1023.6	27.2	1054.7	18.9	1119.7	42.2	9.39
15	58	79	0.73	0.09757	0.00282	0.80959	0.02450	0.06018	0.00142	600.2	16.6	602.2	13.8	610.1	50.5	1.65
16	60	92	0.65	0.15357	0.00442	1.59305	0.04602	0.07524	0.00162	921.0	24.7	967.5	18.0	1074.9	42.9	16.71
17	141	50	2.81	0.16866	0.00482	1.68887	0.04750	0.07263	0.00148	1004.7	26.6	1004.3	17.9	1003.6	40.9	0.11
18	1410	2750	0.51	0.12095	0.00344	1.65574	0.04582	0.09929	0.00194	736.1	19.8	991.7	17.5	1610.8	36.2	118.83
19	47	47	1.00	0.09709	0.00282	0.82357	0.02522	0.06153	0.00148	597.3	16.6	610.0	14.0	657.7	51.3	10.11
20	54	61	0.88	0.16804	0.00484	1.71971	0.04956	0.07423	0.00158	1001.3	26.7	1015.9	18.5	1047.7	42.9	4.63
21	504	156	3.23	0.16508	0.00470	1.62868	0.04516	0.07156	0.00140	985.0	26.0	981.3	17.4	973.4	39.8	1.18
22	345	241	1.43	0.09769	0.00280	0.80429	0.02254	0.05972	0.00120	600.9	16.4	599.2	12.7	593.5	42.8	1.23
23	23	30	0.78	0.09844	0.00294	0.82112	0.02870	0.06050	0.00182	605.2	17.2	608.7	16.0	621.6	64.2	2.71
24	105	69	1.51	0.17937	0.00514	1.88170	0.05320	0.07609	0.00156	1063.5	28.1	1074.7	18.7	1097.4	40.8	3.19
25	165	180	0.92	0.09481	0.00272	0.77406	0.02214	0.05922	0.00124	583.9	16.0	582.1	12.7	575.1	45.4	1.51
26	90	48	1.90	0.09518	0.00274	0.78087	0.02306	0.05951	0.00134	586.1	16.2	586.0	13.2	585.7	48.4	0.07
27	176	79	2.23	0.16997	0.00486	1.70933	0.04778	0.07294	0.00146	1011.9	26.8	1012.0	17.9	1012.4	40.3	0.05
28	117	70	1.67	0.09561	0.00276	0.78574	0.02286	0.05960	0.00130	588.7	16.2	588.8	13.0	589.2	47.0	0.08
29	34	23	1.48	0.09808	0.00292	0.82579	0.02828	0.06107	0.00178	603.1	17.1	611.3	15.7	641.7	62.2	6.40
30	40	20	1.95	0.09247	0.00270	0.76744	0.02446	0.06020	0.00156	570.1	16.0	578.3	14.0	610.7	55.4	7.12
31	296	186	1.59	0.09438	0.00270	0.77639	0.02186	0.05967	0.00122	581.4	15.9	583.4	12.5	591.5	43.7	1.74
32	155	49	3.18	0.18384	0.00526	1.90210	0.05324	0.07505	0.00150	1087.9	28.6	1081.8	18.6	1069.7	40.1	1.67

Conc. (ppm)	Spot [U]	[Th]	Ratios						Ages						
			$^{206}\text{Pb}/^{238}\text{U}$	$\pm 2\sigma$	$^{207}\text{Pb}/^{235}\text{U}$	$\pm 2\sigma$	$^{207}\text{Pb}/^{206}\text{Pb}$	$\pm 2\sigma$	$^{206}\text{Pb}/^{238}\text{U}$	$\pm 2\sigma$	$^{207}\text{Pb}/^{235}\text{U}$	$\pm 2\sigma$	$^{207}\text{Pb}/^{206}\text{Pb}$	$\pm 2\sigma$	
33	67	32	2.09	0.16582	0.00476	1.67500	0.04806	0.07327	0.00156	989.1	26.4	999.1	18.2	1021.3	42.7
34	226	126	1.79	0.09440	0.00270	0.79049	0.02238	0.06074	0.00124	581.5	15.9	591.5	12.7	630.0	44.0
35	518	296	1.75	0.09403	0.00268	0.80162	0.02240	0.06184	0.00124	579.3	15.8	597.7	12.6	668.5	42.5
36	497	236	2.10	0.16821	0.00480	1.67879	0.04658	0.07239	0.00142	1002.2	26.5	1000.5	17.7	996.9	39.7
37	167	61	2.72	0.16836	0.00482	1.69234	0.04740	0.07291	0.00146	1003.0	26.6	1005.6	17.9	1011.4	40.5
38	37	21	1.76	0.09910	0.00292	0.83357	0.02692	0.06101	0.00162	609.1	17.1	615.6	14.9	639.7	56.5
39	53	47	1.12	0.09535	0.00276	0.78331	0.02406	0.05958	0.00144	587.1	16.3	587.4	13.7	588.5	52.1
40	60	78	0.77	0.16863	0.00486	1.69473	0.04892	0.07289	0.00156	1004.6	26.8	1006.5	18.4	1011.0	43.3
41	182	136	1.34	0.19214	0.00550	2.05255	0.05738	0.07748	0.00154	1132.9	29.7	1133.1	19.1	1133.8	39.2
42	147	97	1.51	0.17709	0.00506	1.81271	0.05096	0.07424	0.00150	1051.1	27.7	1050.1	18.4	1048.1	40.6
43	114	62	1.84	0.09582	0.00276	0.78497	0.02278	0.05942	0.00128	589.8	16.2	588.3	13.0	582.6	46.8
44	78	83	0.94	0.17383	0.00498	1.76787	0.05038	0.07377	0.00154	1033.2	27.4	1033.7	18.5	1035.1	41.4
45	262	234	1.12	0.09236	0.00264	0.75244	0.02126	0.05909	0.00122	569.5	15.6	569.6	12.3	570.3	45.3
46	52	50	1.05	0.09557	0.00278	0.79536	0.02444	0.06036	0.00146	588.4	16.3	594.2	13.8	616.5	52.0
47	20	17	1.13	0.16448	0.00484	1.68940	0.05360	0.07450	0.00192	981.6	26.8	1004.5	20.2	1054.7	52.1
48	62	48	1.31	0.09400	0.00272	0.75596	0.02314	0.05833	0.00140	579.2	16.1	571.7	13.4	541.5	53.5
49	177	63	2.82	0.09359	0.00268	0.78964	0.02264	0.06120	0.00130	576.7	15.8	591.0	12.8	646.2	45.1
50	61	78	0.78	0.17325	0.00498	1.78896	0.05154	0.07489	0.00160	1030.0	27.4	1041.4	18.8	1065.7	42.8
51	87	54	1.61	0.09243	0.00268	0.76170	0.02332	0.05977	0.00144	569.9	15.8	575.0	13.4	594.9	52.6
52	83	70	1.18	0.09429	0.00272	0.76946	0.02284	0.05919	0.00134	580.9	16.0	579.5	13.1	574.0	48.9
53	55	46	1.19	0.09362	0.00272	0.77027	0.02396	0.05967	0.00148	576.9	16.1	579.9	13.7	591.8	53.3
54	154	70	2.21	0.16842	0.00482	1.71971	0.04836	0.07406	0.00150	1003.4	26.6	1015.9	18.1	1043.1	40.7
55	91	70	1.31	0.16336	0.00468	1.64750	0.04696	0.07315	0.00152	975.4	26.0	988.6	18.0	1018.1	42.1
56	137	141	0.97	0.16167	0.00462	1.61440	0.04546	0.07243	0.00148	966.1	25.7	975.8	17.7	998.0	41.0
57	189	86	2.21	0.16481	0.00472	1.66335	0.04666	0.07320	0.00148	983.4	26.1	994.7	17.8	1019.6	40.6
58	124	85	1.46	0.16986	0.00486	1.74029	0.04912	0.07431	0.00152	1011.4	26.8	1023.6	18.2	1049.9	41.0
59	319	144	2.21	0.15973	0.00456	1.59078	0.04428	0.07223	0.00144	955.3	25.3	966.6	17.4	992.5	40.0
60	113	75	1.52	0.09232	0.00266	0.76446	0.02230	0.06006	0.00132	569.2	15.7	576.6	12.8	605.8	47.1
61	51	55	0.92	0.13213	0.00384	1.35476	0.04072	0.07437	0.00174	800.0	21.9	869.6	17.6	1051.4	46.7
62	265	193	1.37	0.16588	0.00474	1.71461	0.04778	0.07497	0.00148	989.4	26.2	1014.0	17.9	1067.7	39.7
63	728	365	2.00	0.09381	0.00268	0.77498	0.02156	0.05992	0.00118	578.0	15.8	582.6	12.3	600.8	42.5

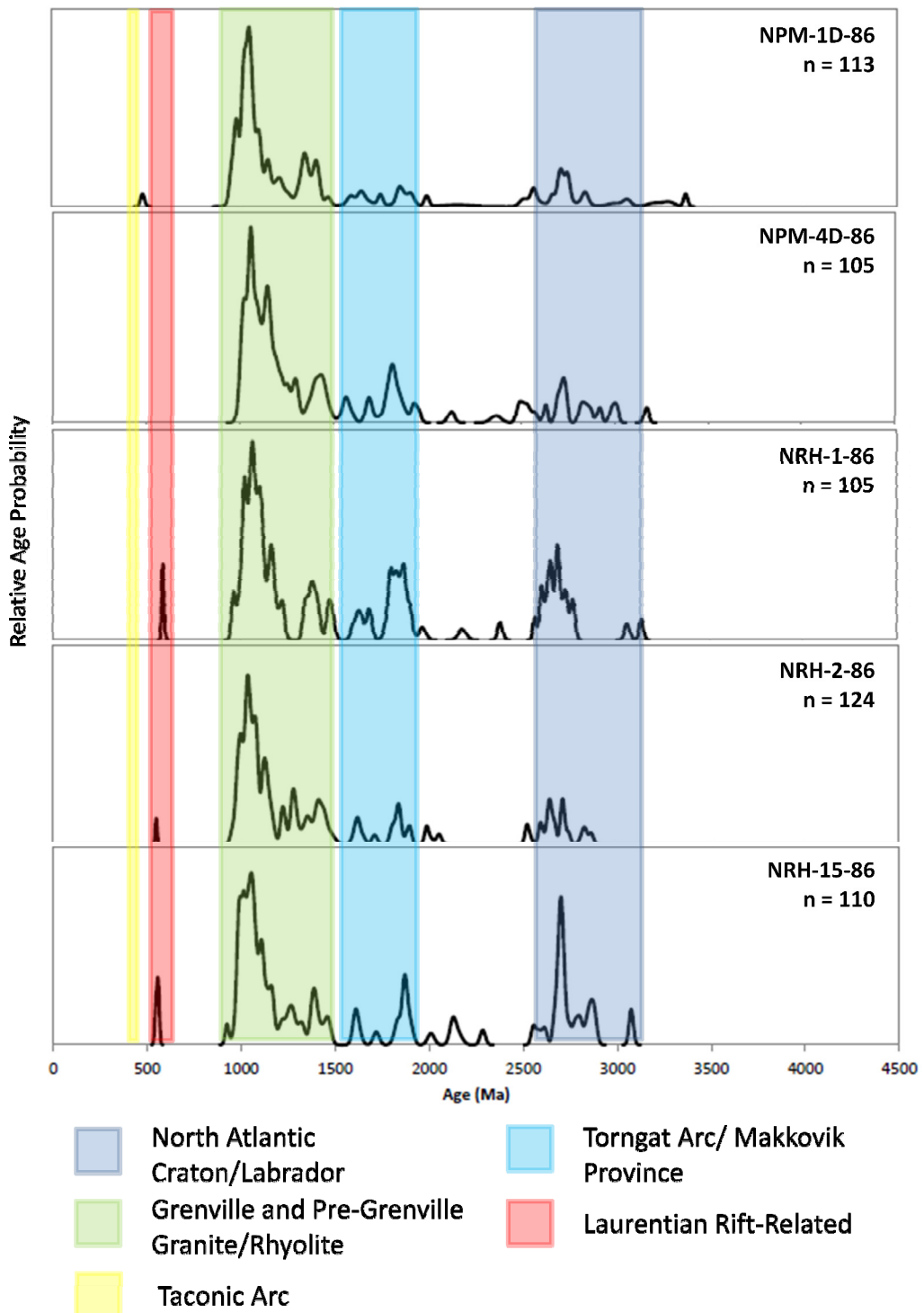
Conc. (ppm)	Spot	[U]	[Th]	Ratios						Ages			
				$^{206}\text{Pb}/^{238}\text{U}$	$\pm 2\sigma$	$^{207}\text{Pb}/^{235}\text{U}$	$\pm 2\sigma$	$^{207}\text{Pb}/^{206}\text{Pb}$	$\pm 2\sigma$	$^{206}\text{Pb}/^{238}\text{U}$	$\pm 2\sigma$	$^{207}\text{Pb}/^{235}\text{U}$	$\pm 2\sigma$
64	722	339	2.13	0.09519	0.00272	0.78693	0.02188	0.05996	0.001118	586.1	16.0	589.4	12.4
65	85	73	1.16	0.09798	0.00284	1.59007	0.04576	0.11770	0.00254	602.6	16.6	966.3	17.9
66	131	104	1.27	0.09332	0.00268	0.77910	0.02240	0.06056	0.00128	575.1	15.8	585.0	12.8
67	20	4	4.60	0.17036	0.00502	1.74919	0.05582	0.07447	0.00194	1014.1	27.7	1026.9	20.6
68	12	17	0.74	0.09805	0.00304	0.83898	0.03450	0.06206	0.00236	603.0	17.9	618.6	19.0
69	182	249	0.73	0.16862	0.00482	1.71083	0.04790	0.07359	0.00148	1004.5	26.6	1012.6	17.9
70	119	121	0.98	0.08285	0.00238	0.69477	0.02030	0.06082	0.00134	513.1	14.2	535.7	12.2
71	74	58	1.27	0.16481	0.00474	1.63955	0.04710	0.07216	0.00154	983.4	26.2	985.5	18.1
72	54	73	0.73	0.16310	0.00472	1.65105	0.04834	0.07342	0.00162	974.0	26.1	990.0	18.5

Appendix 2 – Relative Age Distribution Plots for Individual Samples

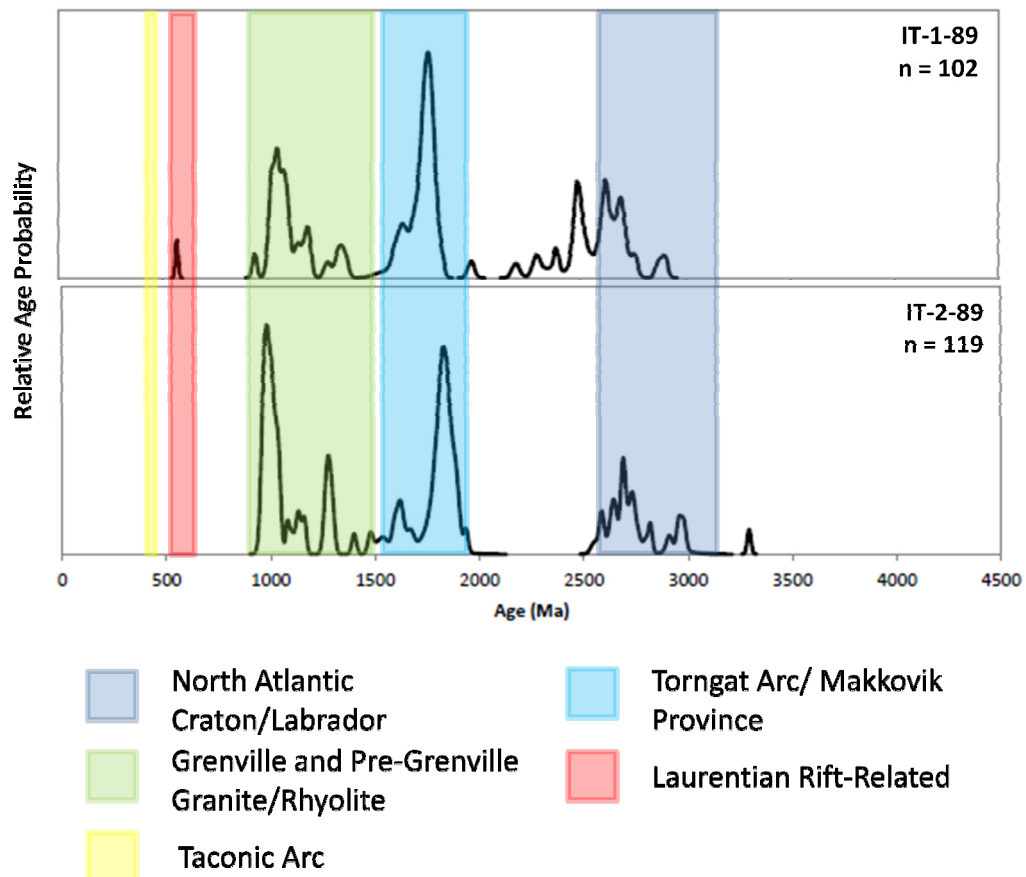
Supplementary Figure 1: Goose Tickle Formation



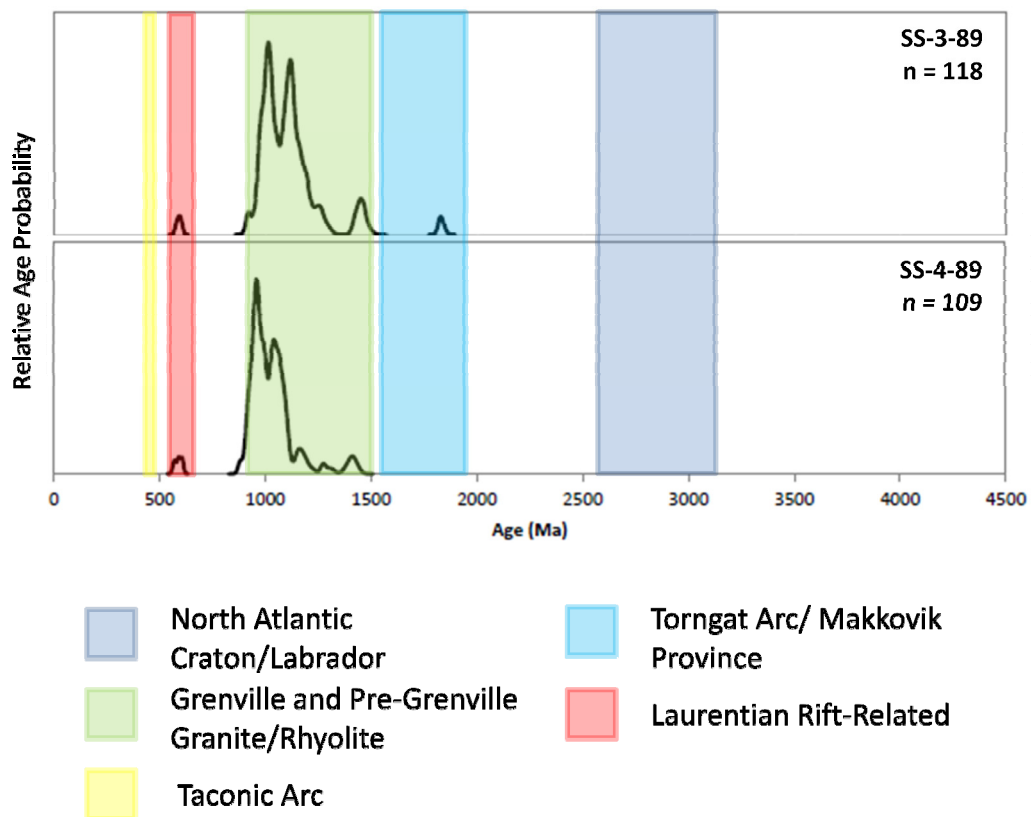
Supplementary Figure 2: Lower Head Formation



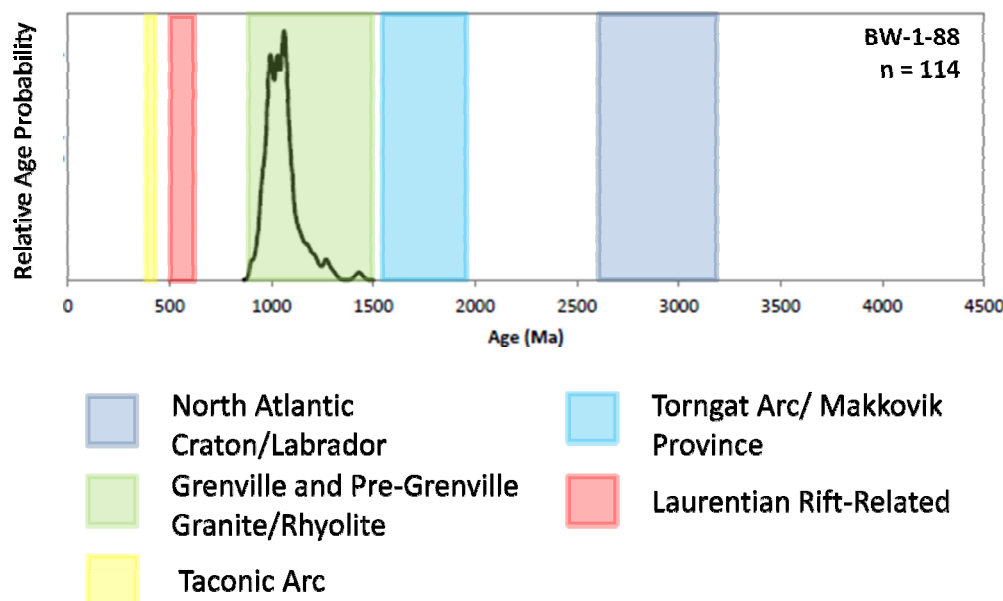
Supplementary Figure 3: Irishtown Formation



Supplementary Figure 4: Summerside Formation



Supplementary Figure 5: Blow Me Down Brook Formation



Supplementary Figure 6: Bradore Formation

